UNCLASSIFIED

| AD NUMBER |
|---|
| AD383737 |
| CLASSIFICATION CHANGES |
| TO: unclassified |
| FROM: confidential |
| LIMITATION CHANGES |
| TO:<br>Approved for public release, distribution unlimited |
| FROM:<br>Distribution authorized to U.S. Gov't. agencies and their contractors; Administrative/Operational Use; AUG 1967. Other requests shall be referred to Air Force Rocket Propulsion Lab., Edwards AFB, CA. |
| AUTHORITY |
| 31 Aug 1979, DoDD 5200.10; AFRL ltr, 5 Feb 1986 |

THIS PAGE IS UNCLASSIFIED

# SECURITY

# MARKING

**The classified or limited status of this report applies to each page, unless otherwise marked.**
**Separate page printouts MUST be marked accordingly.**

THIS DOCUMENT CONTAINS INFORMATION AFFECTING THE NATIONAL DEFENSE OF THE UNITED STATES WITHIN THE MEANING OF THE ESPIONAGE LAWS, TITLE 18, U.S.C., SECTIONS 793 AND 794. THE TRANSMISSION OR THE REVELATION OF ITS CONTENTS IN ANY MANNER TO AN UNAUTHORIZED PERSON IS PROHIBITED BY LAW.

NOTICE: When government or other drawings, specifications or other data are used f any purpose other than in connection with a definitely related ernment procurement operation, the U. S. Government thereby incurs no responsibility, nor any obligation whatsoever; and the fact that the Government may have formulated, furnished, or in any way supplied the said drawings, specifications, or other data is not to be regarded by implication or otherwise as in any manner licensing the holder or any other person or corporation, or conveying any rights or permission to manufacture, use or sell any patented invention that may in any way be related thereto.

CONFIDENTIAL

AD383737

AFRPL-TR-67-75 August 1967

(TITLE UNCLASSIFIED)

# ADVANCED ROCKET ENGINE--STORABLE
# PHASE I INTERIM FINAL REPORT

Part 1 of three parts

Sections I through IV

Prepared by

AEROJET-GENERAL CORPORATION
ADVANCED STORABLE ENGINE PROGRAM DIVISION
LIQUID ROCKET OPERATIONS
SACRAMENTO, CALIFORNIA

Prepared for

AIR FORCE ROCKET PROPULSION LABORATORY
RESEARCH AND TECHNOLOGY DIVISION
AIR FORCE SYSTEMS COMMAND
UNITED STATES AIR FORCE
EDWARDS, CALIFORNIA

0947

CONFIDENTIAL

Report 10830-F-1, Phase I

LEGAL NOTICE

"When U.S. Government drawings, specifications, or other data are used for any purpose other than a definitely related Government procurement operation, the Government thereby incurs no responsibility nor any obligation whatsoever, and the fact that the Government may have formulated, furnished, or in any way supplied the said drawings, specifications, or other data, is not to be regarded by implication or otherwise, or in any manner licensing the holder or any other person or corporation, or conveying any rights or permission to manufacture, use, or sell any patented invention that may in any way be related thereto."

Best
Available
Copy

AFRPL-TR-67-75 August 1967

(TITLE UNCLASSIFIED)

# ADVANCED ROCKET ENGINE--STORABLE
# PHASE I INTERIM FINAL REPORT

Part 1 of three parts
Sections I through IV

Prepared by
AEROJET-GENERAL CORPORATION
ADVANCED STORABLE ENGINE PROGRAM DIVISION
LIQUID ROCKET OPERATIONS
SACRAMENTO, CALIFORNIA

Prepared for
AIR FORCE ROCKET PROPULSION LABORATORY
RESEARCH AND TECHNOLOGY DIVISION
AIR FORCE SYSTEMS COMMAND
UNITED STATES AIR FORCE
EDWARDS, CALIFORNIA

GROUP 4
DOWNGRADED AT 3 YEAR INTERVALS; DECLASSIFIED AFTER 12 YEARS

"THIS DOCUMENT CONTAINS INFORMATION AFFECTING THE NATIONAL DEFENSE OF THE UNITED STATES WITHIN THE MEANING OF THE ESPIONAGE LAWS, TITLE 18, U.S.C., SECTIONS 793 AND 794. ITS TRANSMISSION OR THE REVELATION OF ITS CONTENTS IN ANY MANNER TO AN UNAUTHORIZED PERSON IS PROHIBITED BY LAW."

6798T

**AEROJET-GENERAL CORPORATION**
A SUBSIDIARY OF THE GENERAL TIRE & RUBBER COMPANY

# FOREWORD

This report reviews the technical accomplishments of the ARES Advanced Development Program, Contract AF 04(611)-10830, from 1 July 1965 through 27 January 1967. The work during this period was directed primarily toward demonstrating the feasibility of advanced components and subsystems considered critical to the integrated engine module design. Analysis, design, fabrication, and test activities are summarized.

All work was performanced by Liquid Rocket Operations of Aerojet-General Corporation for the Air Force Rocket Propulsion Laboratory at Edwards Air Force Base, California. Mr. R. Beichel is the Aerojet Program Manager, and Mr. C. W. Hawk is the Air Force Program Manager.

This report has been divided into three separate parts for ease of handling.

This technical report has been reviewed and is approved.

C. W. Hawk
USAF Program Manager

Report 10830-F-1, Phase I

## UNCLASSIFIED ABSTRACT

(U) This report summarizes the Phase I work on Contract AF 04(611)-10830 through 27 January 1967.

(U) The objective of the program was to demonstrate in two phases the engineering practicality and performance characteristics of a high chamber pressure, staged combustion engine module. Before the complete engine can be assembled and tested in Phase II, a Phase I effort must demonstrate the feasibility of several features considered critical to the engine design.

(U) The Phase I program to date has accomplished the following:

a. Established master layouts for both an advanced engine design and for a relatively more conservative back-up version of the engine.

b. Established a master layout for a very large thrust propulsion system utilizing 20 engine modules in a cluster, with all modules exhausting into a single large forced deflection nozzle.

c. Detail designed all the engine components.

d. Demonstrated a successful primary injector and combustion chamber for production of the turbine drive gas.

e. Demonstrated transpiration cooled chambers that can apparently meet contractual performance goals when a suitable secondary injector is evolved.

f. Demonstrated the feasibility of lubricating turbopump bearings with the storable propellants used in the engine.

UNCLASSIFIED ABSTRACT (cont.)

g. Demonstrated pump wear ring designs that permit operation at very close clearance with little or no explosion hazard from pump rub.

h. Demonstrated the suitability of high pressure multiple purpose housings for the turbopump and primary combustion chamber assembly.

i. Developed and demonstrated satisfactory propellant flow control components for the full-scale engine.

j. Completed several supporting studies that provide additional design criteria in such areas as nozzle Aerodynamics, low frequency stability, fluid flow characteristic of propellant and turbine drive-gas passage, and design changes required for conversion to advanced storable propellants.

(U) Remaining Phase I technical goals are conclusion of 60 sec of simulated engine operation with the hydrostatic combustion seal, and three 20-sec firings of a cooled combustion chamber at contractually required specific impulse or higher. The current effort to achieve a high performance, streak free secondary injector must be completed before the cooled thrust chamber demonstration can take place.

Report 10830-F-1, Phase I

## TABLE OF CONTENTS

### Part 1

Page

I. Introduction I-1

II. Summary II-1

- A. Engine and Propulsion System Design II-1
- B. Turbopump Assembly II-1
- C. Thrust Chamber Assembly II-8
- D. Controls II-16
- E. Supporting Studies II-18

III. Module III-1

- A. Objective and Approach III-1
- B. Propulsion System III-5
- C. Engine Module, Advanced Turbopump III-8
- D. Engine Module, Conservative Turbopump III-15

IV. Turbopump Assembly IV-1

- A. Summary IV-1
- B. T-Design Turbopump IV-7
- C. Engine Housing, T-Configuration IV-41
- D. Backup Turbopump IV-79
- E. Engine Housing, Inline Configuration IV-112
- F. Boost Pump IV-124
- G. Propellant-Lubricated Bearings IV-136
- H. Pump Wear Rings IV-158
- I. Combustion Seal IV-183
- J. Purge Seal IV-204

### Part 2

V. Primary Combustor Assembly V-1

- A. Objective V-1
- B. Summary V-1
- C. Component Design V-2
- D. Development Testing V-7

## TABLE OF CONTENTS (cont.)

### Part 2 (cont.)

| | | Page |
|---|---|---|
| VI. | Secondary Combustion Program | VI-1 |
| | A. ICP Residual Hardware Program | VI-1 |
| | B. Modular Secondary Injector Program | VI-25 |
| | C. Modular-Cooled Chamber Program | VI-52 |
| | D. Uncooled Two-Dimensional Nozzle Program | VI-116 |
| VII. | Controls | VII-1 |
| | A. Introduction | VII-1 |
| | B. Suction Valve | VII-2 |
| | C. Fuel Controls | VII-15 |
| | D. Suction and Feed Lines | VII-29 |
| | E. Conclusions | VII-31 |
| VIII. | Supporting Studies | VIII-1 |
| | A. Module Fluid Dynamic Testing | VIII-1 |
| | B. Subscale Nozzle Program | VIII-11 |
| | C. Advanced Propellants | VIII-29 |
| | D. Analytical Models | VIII-32 |
| | E. Reliability | VIII-47 |

### Part 3 (APPENDIXES)

| | Appendix |
|---|---|
| ARES Engine Handbook | I |
| Suction Valve Storage Seal and Cutter Development | II |
| Advanced Propellants | III |

## TABLE LIST

| | Table |
|---|---|
| Test Requirements and Results of the Suction Valve | VII-1 |

## FIGURE LIST

| | Figure |
|---|---|
| Propulsion System, 20-Module Forced Deflection Nozzle | III-1 |
| Advanced Storable Engine--Demonstrator | III-2 |
| ARES Module Subassembly | III-3 |
| ARES Module, External View | III-4 |
| ARES System Staged Combustion Cycle | III-5 |
| "C" Design TPA Layout | IV-1 |
| Oxidizer Pump Design Data | IV-2 |
| Fuel Pump Design Data | IV-3 |
| TPA Water Test Sequence | IV-4 |
| Turbine Design Data | IV-5 |
| Air Test Turbine Photos | IV-6 |
| Turbine Mod. I and Mod. II Configurations | IV-7 |
| Air Test Setup | IV-8 |
| Turbine Weight Flow & Effeciency vs Pressure Ratio | IV-9 |
| Turbine Efficiency vs Pressure Ratio and Speed | IV-10 |
| Mod. I Rotor Discharge Survey | IV-11 |
| Ball Bearing Life vs Load | IV-12 |
| Bearing Thrust Load vs Time - Engine Start Transient | IV-13 |
| Roller Bearing Life vs Misalignment | IV-14 |
| TPA Filter Pressure Drop Data | IV-15 |
| Metal Model I | IV-16a |
| Metal Model II | IV-16b |
| Metal Model Bearing Axial Displacement | IV-16c |
| Metal Model Diametral Expansion | IV-16d |
| Metal Model I Test Results | IV-17 |
| Photo Elastic Model Longitudinal and Lateral Section Stresses (Four Views) | IV-18 |

FIGURE LIST (cont.)

| | Figure |
|---|---|
| Housing A | IV-19 |
| Housing A Rib Pattern | IV-20 |
| Housing A Hydrotest Pressure Zones | IV-21 |
| Housing A Hydrotest Assembly | IV-22a |
| Stress at Test, View 1; Pressure Test, View 2 | IV-22b |
| Housing A Pressure and Thrust Proof Test Results | IV-23 |
| Vibration Test Results | IV-24a |
| Vibration Test Results | IV-24b |
| Two Walled Housing | IV-25 |
| Housing B | IV-26 |
| Oxidizer Dome Parameter vs Displacement | IV-27 |
| Housing C Rib Pattern | IV-28 |
| Configuration Survey | IV-29 |
| Pump Efficiency vs Specific Speed | IV-30 |
| Turbine Efficiency vs Design Speed | IV-31 |
| Inline TPA Weight vs Design Speed | IV-32 |
| Inline TPA Cross Section | IV-33 |
| Turbine Cross Section | IV-34 |
| Inline Turbopump (Two Views) | IV-35 |
| Inline Turbopump Housing | IV-36 |
| Inline Turbopump Housing Hydrotest Assembly | IV-37 |
| Inline Turbopump Housing (Pressure Zones and Test Setup) | IV-38 |
| Location of Displacement of Inline Turbopump Housing Bearing, (Pressure Diagram and Pressure and Thrust Proof Curves) | IV-39 |
| Inline Turbopump Housing Vibration Test Results | IV-40 |

## FIGURE LIST (cont.)

| | Figure |
|---|---|
| Boost Pump Operation Requirements | IV-41 |
| Oxidizer Boost Pump Layout | IV-42 |
| Fuel Boost Pump Layout | IV-43 |
| Oxidizer Boost Pump Axial Thrust | IV-44 |
| 25,000 rpm Posttest Bearings Cages - $N_2O_4$ Lubricated | IV-45 |
| Summary of 25,000 rpm Bearing Tests in $N_2O_4$ | IV-46 |
| 40,000 rpm Bearing Tester | IV-47 |
| Ball Bearing Cage Designs | IV-48 |
| Roller Bearing Cage Designs | IV-49 |
| Summary of 40,000 and 31,250 rpm Bearing Tests in $N_2O_4$ | IV-50 |
| 31,250 rpm Posttest Bearings - $N_2O_4$ Lubricated | IV-51 |
| Summary of 40,000 and 31,250 rpm Bearing Tests in AeroZINE 50 | IV-52 |
| 31,250 rpm Posttest Bearings - AeroZINE 50 Lubricated | IV-53 |
| Test Data Plot - 40,000 rpm $N_2O_4$ Lubricated Bearing Test 1.2-03-WAW-006B | IV-54 |
| 40,000 rpm Posttest Bearings - $N_2O_4$ Lubricated | IV-55 |
| 40,000 rpm Posttest Bearings - AeroZINE 50 Lubricated | IV-56 |
| Wear-Ring Configurations Selected for Propellant Testing | IV-57 |
| Oxidizer-Pump Efficiency Loss as a Function of Wear-Ring Radial Clearance | IV-58 |
| Retention Mechanisms for Straight-Labyrinth Inert Inserts | IV-59 |
| Design Parameters of the Hydrostatic Face Wear-Ring Seal | IV-60 |
| Design Parameters of the Hydrostatic Journal Wear-Ring Seal | IV-61 |
| Wear-Ring Tester | IV-62 |
| Typical Wear-Ring Test Installation and Nomenclature | IV-63 |
| $N_2O_4$ Wear-Ring Test Summary -- Hydrostatic Face Seal and Vespel SP-21 Labyrinth Insert | IV-64 |
| AeroZINE 50 Wear-Ring Test Summary-Kynar and Kel-F Labyrinth Inserts | IV-65 |
| Water-Flow Data from Nonrotating and Rotating Straight-Labyrinth Tests | IV-66 |
| Stepped-Labyrinth Water-Flow Data | IV-67 |
| Water and $N_2O_4$ Flow Data for Hydrostatic Face Seal with Correlation with Estimated Flows | IV-68 |

## FIGURE LIST (cont.)

Figure

Post-Test Photograph of Hydrostatic Journal Seal and Water-Test Data IV-69

Water-Flow Data for Hydrostatic Journal Seal Correlated with Estimated Flows IV-70

Stiffness and Clearance of Hydrostatic Face Seal as a Function of Impeller Angular Deflections IV-71

Combustion Concept of Seal IV-72

Bellow Stresses Under Operative Condition IV-73

2-D Seal Tester and Flow Diagram IV-74a

2-D Test Segment IV-74b

2-D Test Summary IV-75

2-D Test Data — Test 030 IV-76

Flow Diagram, Hot Tests IV-77

Cold Rotating Test Summary IV-78

Start Transient Simulation IV-79

Data Plots Test 14 IV-80

Hydrostatic Combustion Seal in Tester IV-81

Hot Testing Test Summary IV-82

Post-Test Photograph of Seal Test 14 IV-83

Purge Seal in ARES TPA IV-84

ARES Purge Seal Flowrate & Temperature Rise vs Viscosity (changed) IV-85

Purge Fluid Viscosity vs Pressure IV-86

Purge Seal in Tester IV-87

Flow Diagram IV-88

Test Summary IV-89

Purge Seal Test Data (added) IV-90

Final Configuration of the Primary Combustor V-1

Work Statement Requirement and Experimental Test Results V-2

Primary Combustor Components V-3

Full-flow and Quadlet Injectors V-4

Pentad Injector V-5

Primary Combustor Housing and Combustion Chamber Liner V-6

## FIGURE LIST (cont.)

| | Figure |
|---|---|
| Primary Combustor Burnoff Stack Duct and Injector | V-7 |
| Test Configuration and Data Summary | V-8 |
| Primary Combustor Test Setup | V-9 |
| Typical Oscillograph, Start Transient and Steady State | V-10 |
| Quadlet Injector and Liner Vane Assembly Posttest 1.2-04-WAG-006 | V-11 |
| Turbulator Ring, Vane Assembly Pretest 1.2-04-WAG-008 | V-12 |
| Chamber Pressure Oscillation Characteristic 1.2-03-WAG-007, -008, -009, -010 | V-13 |
| Injector and Turbulator Vane Assembly Posttest 1.2-04-WAG-010 | V-14 |
| Quadlet Injector Posttest 1.2-04-WAG-012 | V-15 |
| Canted Blade Turbulators | V-16 |
| Full Flow Injector-Turbulator Vane Assembly Posttest 1.2-04-WAG-017 | V-17 |
| Quadlet Injector Posttest 1.2-04-WAG-018 | V-18 |
| Turbulator-Solid Triangular Inner Ring, Notched Triangular Outer Ring | V-19 |
| Combustion Loss Versus Chamber L* | VI-1 |
| Film Cooling Performance Degradation Versus Film Coolant Flow | VI-2 |
| Mark 32 Secondary Injector | VI-3 |
| Mark 125 Secondary Injector | VI-4 |
| Mark 20 Primary Injector | VI-5 |
| Uncooled Ablative Chambers, 20 and 45 L* | VI-6 |
| Photograph of Regenerative Chamber Installed on Test Stand H-2 | VI-7 |
| Capillary Tube Chamber | VI-8 |
| Hydraulic Test of Regenerative Chamber SN R-6 | VI-9 |
| Multiple Orifice Film Coolant Ring | VI-10 |
| Multiple Tube Film Coolant Ring | VI-11 |
| Pump-Feed Staged-Combustion Test Engine | VI-12 |
| Intensifier System Schematic with Sector Engine | VI-13 |
| ICP Residual Hardware Program Performance Summary | VI-14 |

FIGURE LIST (cont.)

Figure

Postfire Condition Mark 32 Injector VI-15

Postfire Condition Mark 125 Injector VI-16

Injector Chamber Configuration L* Evaluation Series VI-17

Prefire Photograph of Film Coolant Ring - Looking Upstream Through the Nozzle Throat VI-18

Postfire Photographs of SN4 Regenerative Test VI-19

Thermocouple Data from ICP Film-Cooled, Ablative Chamber Tests (Test Series 1.2-07-WAM) VI-20

Test Parameters for ICP Chamber Tests VI-21

Chamber Wall Temperatures for Test 1.2-07-WAM-009 VI-22

Chamber Wall Temperatures for Test 1.2-07-WAM-010 VI-23

Chamber Wall Temperatures for Test 1.2-07-WAM-011 VI-24

Regenerative Coolant Bulk Temperature, Test 1.2-08-WAM-002 VI-25

Regenerative Coolant Bulk Temperature, Test 1.2-08-WAM-003 VI-26

Modular Configuration--Mark 125 Injector VI-27

Turbopump-Injector-Cooled Chamber Interface VI-28

Fuel Swirl Rake Injector VI-29

Uncooled Ablative Thrust Chambers of Different L*'s VI-30

Uncooled Instrumented Thrust Chamber Schematic VI-31

Test Stand Adapter VI-32

Modular Secondary Injector Performance Summary VI-33

Typical Oscillograph, Secondary Injector Test VI-34

Injector-Chamber Interface Development VI-35

Mixture Ratio Distribution Effects VI-36

Effect of Characteristic Length on Combustion Loss VI-37

Mark 125 Injector Vanes VI-38

Mark 125 Secondary Injector Performance Certification VI-39

Effects of Oxidizer Film Coolant on the Performance of the ARES Thrust Chamber VI-40

Modified Rake Injector VI-41

Thermocouple Data for Test No. 1.2-11-WAM-018 VI-42

Thermocouple Data for Test No. 1.2-11-WAM-019 VI-43

FIGURE LIST (cont.)

| | Figure |
|---|---|
| Film Temperatures for Test No. 1.2-11-WAM-018 | VI-44 |
| Cooled Chamber Predicted Temperatures | VI-45 |
| Regeneratively Cooled Combustion Chamber | VI-46 |
| Regeneratively Cooled Combustion Chamber | VI-47 |
| Flow Characteristics of Capillary Regenerative Chambers | VI-48 |
| Flow Characteristics of Noncapillary Regenerative Chambers | VI-49 |
| Capillary Tube Installation | VI-50 |
| Total Pressure Distribution for ARES Regenerative Chambers | VI-51 |
| Regenerative Coolant Capability | VI-52 |
| ARES Chamber Heat Load | VI-53 |
| ARES Chamber Wall Temperatures | VI-54 |
| Film Cooling Requirements for ARES Chambers | VI-55 |
| Performance Potential in ARES Chambers | VI-56 |
| Uncoated 0.040-in. Capillary Tube Heat Flux Capability | VI-57 |
| Uncoated 0.045-in. Capillary Tube Heat Flux Capability | VI-58 |
| Uncoated 0.050-in. Capillary Tube Heat Flux Capability | VI-59 |
| Typical Inconel 718 Tubing Defect | VI-60 |
| Typical Inconel 718 Tubing Defect | VI-61 |
| Selection of Transpiration Chamber Wall Material | VI-62 |
| Transpiration Cooled Combustion Chamber | VI-63 |
| Transpiration Cooled Combustion Chamber | VI-64 |
| Layout of Transpiration Cooled Chamber | VI-65 |
| Sectional Washer Pairs for Transpiration Chambers | VI-66 |
| Summary of ARES Transpiration Cooled Chamber Assembly (Flow Rates, Supply Pressure and Wall Temperatures) | VI-67 |
| Advanced Thermal Model | VI-68 |
| Transpiration Coolant Flow Rates vs Axial Distance (1500°F Wall) | VI-69 |
| Throat Wall and Coolant Temperatures vs Transpiration Coolant Flow Rates | VI-70 |
| Transpiration Coolant Flow Rates vs Axial Distance (1900°F Wall) | VI-71 |

FIGURE LIST (cont.)

| | Figure |
|---|---|
| Transpiration Chamber Wall Temperatures vs Coolant Flow Rate (Compartment 1-4) | VI-72 |
| Transpiration Chamber Wall Temperatures vs Coolant Flow Rate (Compartment 5-7) | VI-73 |
| Transpiration Chamber Wall Temperatures vs Coolant Flow Rate (Compartment 8-10) | VI-74 |
| Transpiration Chamber Wall Temperatures vs Coolant Flow Rate (Compartment 11 and 12) | VI-75 |
| Radial Wall Temperature Distribution in ARES Transpiration Cooled Chamber | VI-76 |
| Radial Wall Temperature Distribution in ARES Transpiration Cooled Chamber | VI-77 |
| Transpiration Chamber Flow Data Summary (Chamber SN 001) | VI-78 |
| Transpiration Chamber Flow Data Summary (Chamber SN 002) | VI-79 |
| Transpiration Chamber Test Data and Performance Summary | VI-80 |
| Transpiration Cooled Chamber Intensifier Fed Test Schematic | VI-81 |
| Transpiration Chamber Postfire Conditions (Test 1.2-12-WAM-002) | VI-82 |
| Transpiration Chamber Postfire Conditions (Test 1.2-12-WAM-012) | VI-83 |
| Transpiration Chamber Postfire Conditions (Test 1.2-12-WAM-024) | VI-84 |
| Transpiration Chamber Postfire Conditions (Test 1.2-12-WAM-030) | VI-85 |
| Regenerative Chamber Postfire Conditions (Test 1.2-14-WAM-002) | VI-86 |
| Regenerative Chamber Postfire Conditions (Test 1.2-14-WAM-005) | VI-87 |
| Predicted ARES Performance | VI-88 |
| Percent Film Coolant Loss vs Percent Coolant Flow (Test Series 1.2-12-WAM) | VI-89 |
| Injector-Chamber Configuration for Transpiration Chamber SN-001 (Test Series 1.2-12-WAM) | VI-90 |
| Injector-Chamber Configuration for Transpiration Chamber SN-002 (Test Series 1.2-12-WAM) | VI-91 |
| Regenerative Chamber Test Data and Performance Summary | VI-92 |
| Transpiration Chamber SN 001 Temperature Summary | VI-93 |
| Transpiration Chamber SN 002 Temperature Summary | VI-94 |
| Transpiration Chamber SN 002 Surface Temperatures (Tests 1.2-12-WAM-016 to 018) | VI-95 |

## FIGURE LIST (cont.)

Figure

Measured and Predicted Temperatures for Test 1.2-12-WAM-016 VI-96
Measured and Predicted Temperatures for Test 1.2-12-WAM-017 VI-97
Measured and Predicted Temperatures for Test 1.2-12-WAM-018 VI-98
Plasma Thermal Shock/Oxidation Test Results VI-99
Shroud Types VI-100
Brazed Bonded Laminated Tungsten Cermet Thermal Barrier VI-101
Brazed Bonding Microstructure VI-102
Transpiration Laboratory Program, Subscale Washers VI-103
Photograph of Transparent Scale Model Simulating Diffusion Area VI-104
Two-Dimensional Nozzle Design VI-105
Two-Dimensional Nozzle Assembly VI-106
Chamber-Nozzle Instrumentation Schematic VI-107
Test Data Summary VI-108
Condition of Nozzle after Test 1.2-11-WAM-025 VI-109
Nozzle Temperature Data, Test 1.2-11-WAM-023 VI-110
Nozzle Temperature Data, Test 1.2-11-WAM-025 VI-111
Suction Valve Configuration VII-1
Electron Beam Welding Parameters VII-2
PCFCV Flow Characteristics VII-3
PCFCV Control Port Configurations VII-4
SCFCV Flow Characteristics VII-5
SCFCV Exploded View VII-6
Suction Valve Selective Control Circuit VII-7
Fuel Valve Servo Controller (schematic) VII-8
Air Test Facility Schematic VIII-1
Oxidizer Discharge Model VIII-2
Oxidizer Discharge Housing Rib Pattern VIII-3
Pressure Drop Parameter vs Hole Number VIII-4
Flow Distribution Parameter vs Hole Number VIII-5
Oxidizer Return Housing Rib Pattern VIII-6

FIGURE LIST (cont.)

| | Figure |
|---|---|
| Pressure Drop Parameter vs Inlet Hole Number | VIII-7 |
| Flow Distribution Parameter vs Injector Hole Number | VIII-8 |
| Turbine Inlet Model | VIII-9 |
| Instrumentation Planes | VIII-10 |
| Turbine Inlet Passage | VIII-11 |
| Flow Pitch Angle at Turbine Inlet | VIII-12 |
| Total Pressure Distribution at Turbine Inlet | VIII-13 |
| Turbine Exhaust Model | VIII-14 |
| Flow Distribution Concepts | VIII-15 |
| Flow Distribution | VIII-16 |
| Nozzle Performance Program Summary | VIII-17 |
| Nozzle Design Parameters | VIII-18 |
| Nozzle Performance Models | VIII-19 |
| Subscale Nozzle Performance | VIII-20 |
| Full-scale Nozzle Performance | VIII-21 |
| Ambient Base Bleed Effects | VIII-22 |
| IES Area Ratio Effects | VIII-23 |
| Module Skirt Merging Angle Effects | VIII-24 |
| Skirt Length Effects | VIII-25 |
| Module Cant Angle Effects | VIII-26 |
| Module-Out Effects on Performance | VIII-27 |
| Module-Out Effects on Thrust Vector Angle | VIII-28 |
| Engine Throttling by Module Shutdown | VIII-29 |
| Model 2-D | VIII-30 |
| Heat Transfer Test Conditions | VIII-31 |
| Model 2-D Shadowgraphs | VIII-32 |
| Model 2-D Heat Transfer Coefficients | VIII-33 |
| Heat Transfer Model 1a, Skirt | VIII-34 |
| Heat Transfer Model 1a, Heat Shield | VIII-35 |
| Heat Transfer Model 2 | VIII-36 |

## FIGURE LIST (cont.)

| | Figure |
|---|---|
| Time from Initial Valve Motion to Partial Outflow from Injector Manifold | VIII-37 |
| Engine Model Flow Chart | VIII-38 |

# I.

# INTRODUCTION

# I. INTRODUCTION

(U) This report summarizes the technical accomplishments of the first 19 months of Contract AF 04(611)-10830, extending from 1 July 1965 through 27 January 1967.

(U) The objectives of the program were to demonstrate within a two-phase effort the engineering practicality and performance characteristics of a high chamber pressure, staged combustion engine module. These demonstration firings will be accomplished during the second phase with high-performance 20-sec firings of a complete, full-scale engine module. However, before the complete engine work can be initiated, Aerojet-General Corporation must demonstrate in Phase I the feasibility of several features which are considered critical to the proposed engine design. The principal items in this category are the integrated turbopump housing, the propellant-lubricated bearings, the hydrostatic seals, and high-performance 20-sec firings with a cooled thrust chamber. In addition, the Phase I effort includes analysis, design, and test activity on several other aspects of the overall engine and of its unique components.

(U) All of the work summarized in this report was accomplished for the Phase I objectives.

# II.

# SUMMARY

# II.

# SUMMARY

## A. ENGINE AND PROPULSION SYSTEM DESIGN

(C) The ARES engine module master layout and operating specifications were prepared and continuously updated during the report period. The basic engine module layout (Figure III-2) is for a 100,000-lb-thrust, turbopump-fed, regeneratively cooled engine with a nozzle expansion ratio of 20:1 and a dry weight of 675 lb. The engine burns $N_2O_4$ and 0.5 $N_2H_4$/0.5 UDMH in a staged combustion cycle in which all of the oxidizer and approximately 18% of the fuel are used to produce the turbine drive gas. After turning the single-shaft turbopump at 40,000 rpm, the drive gas is then united in the main combustion chamber with the balance of fuel and is burned at 2800 psia chamber pressure with a minimum specific impulse (sea level) of 285 lb/sec. Detailed engine operating specifications are listed in Appendix I.

(U) The individual module design has been used to prepare a master layout of a 2-million-lb-thrust propulsion system with 20 individual modules exhausting into a common forced-deflection nozzle (Figure III-1).

(U) An engine module layout was also prepared using a relatively more conservative backup turbopump that operates at 30,000 rpm and is equipped with a purge seal (Figure I-9.1.1-2, Appendix I).

## B. TURBOPUMP ASSEMBLY

### 1. General

(C) The turbopump is designed to provide high pressure fuel and oxidizer for the ARES staged combustion cycle with minimum weight, size and complexity. The $N_2O_4$ is provided at 6000 psi for thrust chamber coolant and

II, B, Turbopump Assembly (cont.)

for the primary combustor. Fuel is supplied at 5750 psia to the primary injector and 3750 psia to the secondary injector.

(C) The advanced turbopump consists of a two-stage fuel pump and a single-stage oxidizer pump at opposite ends of a common shaft, driven by one single-stage turbine located between the pumps. The turbine is driven by oxidizer-rich gas provided by an annular primary combustor located between the oxidizer pump and the turbine. The bearings are lubricated by the storable propellants. Separation of fuel and oxidizer along the shaft is attained by a unique hydrostatic combustion seal which deliberately leaks a metered amount of fuel into the turbine exhaust. The entire package of rotating machinery and primary combustion chamber is enclosed in a high-pressure housing, which also acts as a thrust takeout member and as the propellant distribution medium from the pumps. The turbopump cutaway is shown in Figure IV-1.

(C) The Phase I effort consists of several design and component feasibility demonstration tasks. In addition to the overall TPA design effort, Aerojet is required in Phase I to:

(a) Demonstrate the feasibility of lubricating rolling contact bearings at 40,000 rpm (DN of 1.6 million) in both of the propellants.

(b) Demonstrate the structural integrity of the turbopump housing under various imposed structural and vibrational loads.

(c) Demonstrate successful operation of the hydrostatic combustion seal in simulated engine operating conditions.

(d) Develop pump wear rings that will provide adequate pump efficiency by operating at very close clearances, but with minimum explosion hazard from pump rubbing.

II, B, Turbopump Assembly (cont.)

(e) Design and test a purge seal to be utilized if the hydrostatic combustion seal is found not feasible.

(f) Design a relatively more conservative backup turbopump to be utilized if the advanced design is not practical.

### 2. Advanced and Backup Turbopump Assembly Designs

(U) Design layouts were completed for both the advanced "T"-engine, and the backup, "in-line" engine. Detail designs of the "T"-engine turbopump were also completed. The T-engine cutaway is shown in Figure IV-1; the backup design is shown in Figure IV-33. Detail designs were also prepared for fuel and oxidizer boost pumps which are suitable for either turbopump.

### 3. Turbopump Housing Development

(C) Integrated turbopump and primary combustor housings were designed and tested for both the advanced "T" and the backup "in-line" turbopumps. The contract requires that the housings not weigh more than 350 lb, that they have a permanent axial deflection less than 0.020 in., and that the radial misalignment be less than 0.008 in. at 1.4 times nominal design pressure and thrust, applied simultaneously. Also, the housing cannot have a critical vibration mode in any axis of 667 ± 10% cps, either without internal pressure or when pressurized to 1.2 times design pressure under an exciting force of 1-g input. It is also important that the housing have a low-pressure drop across the propellant distribution passages, that it adequately cool itself with the propellant flow, and that it permit easy insertion and removal of the turbopump and primary combustor components.

II, B, Turbopump Assembly (cont.)

(U) Analytical stress methods are not adequate to treat the three-wall structure used for the "T" configuration advanced turbopump. Consequently, single-wall, double-wall, and photoelastic models were built and tested to obtain necessary design data for the full-scale three-wall structure. This work indicated the actual stresses that would be encountered--generally lower than predicted by stress analytical models--and suggested design changes to optimize the configuration.

(C) One of the two full-scale models was electron-beam welded and one was plug welded. Manufacturing difficulties were experienced with both housings but refined welding and heat treat methods solved these problems. Pressure testing was accomplished with (1) Internal pressures simulating actual engine operating conditions, (2) with 50% design thrust load and no internal pressure, and (3) with combined thrust loads and internal pressures, both at 1.4 times nominal design values (140,000 lb of thrust and 8400 psi internal pressure).

(U) These tests and the subsequent vibration tests demonstrated the ability of the design to meet contractual requirements, and also indicated several desirable improvements that will be incorporated into the housing design carried on into Phase II of the program. This housing will make greater use of castings and will have modified propellant passage design to improve cooling. Figure IV-1 shows the "C" housing design with these improvements.

(U) A simpler test program was conducted on the "in-line" turbopump housing with equally successful results.

### 4. Propellant-Lubricated Bearings

(C) The program has demonstrated the feasibility of eliminating conventional lubrication systems for the turbopump bearings. Both ball and roller bearings were successfully lubricated for at least 12 minutes of operation with $N_2O_4$ and with AeroZINE 50 at rotating speeds of 40,000 rpm (DN of 1,600,000). During the 40,000 rpm tests, the tandem ball bearings were subjected to an axial load of 2,500 lb for 8 sec, and to 1500 lb for the remainder of the run. Roller bearings were subjected to 1000-lb radial load for 8 sec and to 500 lb for the remainder of the run.

(C) The fuel (AeroZINE 50) generally proved to be a more severe environment for the bearings, cages, and races than was the oxidizer ($N_2O_4$). All rollers, for example, experienced definite end wear in A-50, but only burnishing in $N_2O_4$; however, the amount of wear in A-50 was not excessive for TPA life requirements. Ball bearings with titanium and tungsten carbide balls (designated K5H by Kenemetal) in 440C races proved to be the best design for AeroZINE 50 operation. Use of 440C for both the rollers and for the races was satisfactory for the radial bearings. A 25% glass-filled Teflon shrouded with stainless steel provided the best cages.

(U) The ball bearings were also successfully tested up to 4400 lb for 8 sec at a lower rpm (31,250), with 2200 lb for the remainder of the run.

### 5. Pump Wear Rings

(U) A wear-ring development program was conducted to limit internal leakage in the pump to a value consistent with the turbopump efficiency and thrust-balance requirements, and to do this safely and reliably in spite of intermittent rubbing in both $N_2O_4$ and AeroZINE 50. Secondary objectives were to establish insert materials for other close-running components, such as shaft labyrinths, inducers, and boost pumps.

(U) One approach allowed intermittent rubbing of the impeller wear ring on compatible inserts; straight labyrinth seals were designed and tested with various combinations of insert materials and pressure retention mechanisms.

(U) The second approach allowed low-speed transient rubbing, but prevented high-speed contact by maintaining a fluid film between the impeller rubbing surfaces and the seal itself. Hydrostatic face and journal seals, based upon this concept, were designed and tested.

(U) For oxidizer pump application, both the hydrostatic face seal and the straight labyrinth with Vespel SP-21 inserts limited flow through the wear ring to very low values at the required 4000-psi pressure differential. Both withstood intentional attempts at rubbing at 40,000 rpm without causing fire or explosion and were in reusable condition.

(U) The fuel pump is designed integrally with the thrust balancer in a manner that requires a straight labyrinth seal at the outside diameter of the fuel-pump impeller. The optimum design of this labyrinth seal requires operation at a clearance of 0.007 in. Two inert inserts of Kynar and Kel-F were satisfactorily designed and tested under simulated conditions. This included repeatable flow rate before and after rubbing at high speed and pressure differentials of 2250 psi. Kynar was selected for the fuel pump application on the basis of its slightly better properties after exposures to AeroZINE 50 in laboratory tests.

(U) On the basis of this program and analysis of the turbopump requirements, hydrostatic face seals were selected for the oxidizer-pump wear ring and straight labyrinths with pressure relieved Kynar inserts were selected for the fuel-pump wear ring. These designs are shown for the advanced turbopump in Figure IV-1 and the backup turbopump in Figure IV-33.

### 6. Hydrostatic Combustion Seal

(U) The ARES engine requires a rotating shaft seal between the fuel pump and the oxidizer-rich turbine exhaust gas. A hydrostatic seal was adopted because the operating speed of 40,000 rpm imposes an excessive surface velocity of 600 ft/sec on rubbing contact seals. The seal maintains separation of the nonrotating seal face from the running ring with a fluid film of fuel, leaking from the pump and exhausting into the oxidizer-rich turbine exhaust. The seal and its adjacent parts are cooled by streams of oxidizer flowing through holes on each side of the seal. The cross section of the seal is shown in Figure IV-72.

(U) The hydrostatic combustion seal is one of the concepts critical to the advanced engine design. The Phase I program requires a 60-sec demonstration of the seal under simulated engine operating conditions.

(U) Several tests were conducted in a two-dimensional tester to determine surface temperatures, feasible operating clearances and optimum design configurations. The data from this program was then incorporated into full scale seals which were initially tested without combustion in the separate propellants, both with and without shaft rotation. After solving some initial sequence problems, the seal operated successfully at design rpm with operating clearances of 0.001 in. and less. The seal demonstrated its ability to tolerate axial wobble several times larger than the nominal operating clearance.

II, B, Turbopump Assembly (cont.)

(U) Several hot rotating tests with actual propellants were then conducted for a total testing time with combustion of over 80 sec. The same seal was used for four of these tests, establishing that the seal is capable of restarts. The required 60 sec of problem-free operation was not attained because of various difficulties with the shield downstream of the seal face and with operation of the tester itself. Additional testing is now underway with modified designs that take advantage of the test experience to date.

### 7. Purge Seal

(U) A purge seal design was developed as an alternative approach in event the hydrostatic combustion seal proved impractical. The purge seal operates on the hydrostatic principle to avoid high rubbing contact velocities, but it uses an inert purge fluid instead of controlled fuel leakage, as in the primary design. Figure IV-84 shows the design utilized.

(U) Initial cold rotating tests attained 40,000 rpm at less than design purge fluid flow, causing slight rubbing contact. Hot testing was then initiated with increased purge-fluid flow. Although as high as 55 sec of testing at 40,000 rpm was attained, problem free operation was not achieved. Further development was not continued because of the favorable progress attained with the hydrostatic combustion seal.

## C. THRUST CHAMBER ASSEMBLY

### 1. General

(U) The ARES thrust chamber assembly consists of two main engine subsystems: the primary combustor assembly and the secondary combustor assembly. The primary combustor assembly produces the oxidizer-rich turbine drive gas and consists of an injector and combustion chamber. The secondary combustor assembly consists of a gas-liquid secondary injector, which unites the turbine drive gas with the balance of the fuel, and a cooled secondary combustion chamber. When ARES engine modules are used in clusters to provide a high-thrust engine, the expansion nozzle of the secondary combustion chamber can be designed as a two-dimensional configuration to provide additional performance improvement. Evaluation of an uncooled two-dimensional nozzle to determine nozzle heat-transfer conditions was included as part of the Phase I program.

### 2. Primary Combustor Assembly

(U) The objective of the primary combustor program was to evaluate primary combustor injectors, define performance characteristics, and obtain temperature profiles along the chamber wall and across the gas stream. Injector testing was to be conducted at off-design conditions to define the minimum injector pressure drop, the sensitivity to off-design mixture ratio operation, and finally to define inherent stability of the combustor by shocking it with a pulse gun. The goal of the program was to develop one injector configuration to the point where it could be used in conjunction with the modular turbopump housing for early Phase II testing.

(U) The success criteria for the primary combustor effort was that the temperature of the primary combustor exhaust gas, as measured by three thermocouples at the entrance to the turbine nozzle ring, could not exceed 1650°F, with the variation between each thermocouple not exceeding 400°F. Also, chamber pressure oscillations must not exceed ± 5% of the average chamber pressure value and must not be divergent with time when measured during the steady-state portion of the test firings. Compliance with these conditions was to be demonstrated in three tests, each having a minimum duration of 1-sec steady state. The primary combustor must be in a refirable condition following the demonstration series.

(U) Three injector concepts were test evaluated during the program, designated the pentad, quadlet, and full-flow configurations. These injectors were evaluated in a heavyweight workhorse housing which was designed to have the same interface dimensions and gas-passage configurations as the flightweight modular TPA housing. This housing included extensive instrumentation to facilitate the evaluation of injector performance and operating characteristics.

(U) The test program consisted of 31 hot-fire tests. Development problems encountered during the test program included low-frequency feed system coupled instability, and minor erosion of the injectors and combustion chamber. Incorporation of five axial vanes to inhibit the instability together with two turbulators to provide mechanical mixing of the propellants solved both problems. The pentad injector proved to be the best injector.

(C) The primary combustor configuration developed during the test program met or exceeded all requirements. The average temperature obtained on the three required successful tests was 1340°F; the average chamber pressure was 4650 psia; the chamber pressure oscillations at steady state averaged ± 1.27%. The average mixture ratio during these tests was 11.63. The final injector and combustor chamber configuration which ultimately satisfied all contract work statement requirements is shown in Section V, Figures V-1 and V-2.

### 3. Secondary Combustor Assembly

#### a. Testing with Residual Hardware from Contract AF 04(611)-8548, Integrated Components Program (ICP)

(U) Significant amounts of untested hardware were residual from a contract which preceded the current program. Initial secondary

II, C, Thrust Chamber Assembly (cont.)

combustor testing on the current program was conducted with this hardware to obtain early design data for modular-configuration secondary injectors and cooled combustion chambers. The residual hardware included two new secondary injectors and two single-pass regeneratively cooled chambers.

(C) The test program consisted of 13 valid hot firing tests, of which nine were for injector evaluation and four were for cooled chamber evaluation. The two injectors, designated the Mark 32 and the Mark 125, both delivered specific impulse efficiencies of 86.4% and 86.7%, respectively. The computed combustion loss efficiencies for these injectors, which is the parameter indication of inherent injector performance, were 97.5% and 97.6%, respectively. The Mark 32 injector, however, sustained erosion on the trailing edge of its vanes while the Mark 125 experienced no erosion. Based upon these results, the Mark 125 concept was selected for test evaluation in the ARES modular configuration hardware. Additional tests were conducted with the Mark 125 injector to determine performance as a function of chamber characteristic length (L*) and to determine the performance loss attendant with various amounts of supplementary film cooling. Using this data, the optimum L* was determined to be 40 in., which was the value used in the subsequent ARES modular cooled-chamber design.

(U) Two tests were conducted on each of the two regeneratively cooled chambers. The first chamber was designed for single-point film-cooling injection. During testing of this chamber, part of its protective thermal barrier coating was lost, which resulted in pin-hole leaks in the throat area. The second chamber was designed for two-point film-cooling injection; one at the injector face and one in the convergent section of the nozzle. The first test conducted with the chamber produced good data and no hardware damage was incurred. Unfortunately, the chamber was lost during the second test because of a ruptured oxidizer supply hose which caused a fuel-rich mixture ratio excursion and subsequent chamber destruction, thus ending this test phase.

(U) The residual hardware testing established a foundation for the subsequent design and development of new injectors and chambers. Heat transfer, engine stability, and other analytical models were verified and/or refined.

### b. Modular Secondary Injector Development

(U) Two basic injector patterns were evaluated during this program, including the Mark 125 design and a new alternative design designated the fuel swirl rake. Both injectors were designed in a flight-weight configuration to match the ARES modular TPA interface. All testing was performed with uncooled ablative-lined combustion chambers; test objectives were to establish injector performance, stability characteristics, and structural integrity.

(C) Initial testing of both injectors revealed that performance was significantly below that obtained in the residual hardware test program with the Mark 125 injector. Analysis showed that excessive oxidizer was escaping into the combustion chamber around the periphery of the injector, preventing adequate mixing and combustion with the fuel. A circular shroud was therefore installed around the injector to contain the oxidizer gas within the fuel injection envelope. In this configuration, the Mark 125 and fuel-swirl-rake injectors delivered specific impulse efficiencies of 93.5 and 91.1%, respectively, at area ratio 11; this corresponds to 96.4 and 94.6%, respectively, when corrected to the ARES chamber design point of 40 in. L* and 20:1 area ratio. Stability characteristics and structural integrity were satisfactory with both injectors. On the basis of higher performance, the Mark 125 injector was selected for testing with cooled thrust chambers.

(U) The subsequent transpiration-cooled chamber test series revealed an unforeseen compatibility problem between the injector and the cooled thrust chamber. After transpiration coolant was reduced, a streaking became evident on the chamber wall in line with the injector vanes. This condition caused the loss of two transpiration-cooled chambers. At the end of the report period, two solutions were being pursued to solve the injector and chamber compatibility problem. The first was to modify the Mark 125 injector at its periphery to give a finer fuel injection pattern and to eliminate any fuel impingement onto the chamber wall by ensuring that all of the outer fuel was directed axially from the injector. The second solution was to design and test new injector patterns which will maintain high performance and be compatible with cooled thrust chamber operation. This effort is now underway.

### c. Modular Cooled Thrust Chamber Development

(C) The objective of this task is demonstration of a cooled thrust chamber and secondary injector combination delivering a minimum sea-level specific impulse of 280 sec during three 20-sec duration firings. The hardware must be refirable at the end of the third test.

(U) Two basic concepts were evaluated during the reporting period: (1) regenerative cooling, supplemented with film cooling and a thermal barrier coating, and (2) transpiration cooling.

(U) Based on the residual hardware test program, a new flight-weight regeneratively cooled thrust chamber design was evolved and tested. The new design had a 10.5-in. internal diameter, a two-pass $N_2O_4$ cooling circuit, and a high-temperature thermal-barrier coating on the inside tube wall to reduce the amount of supplemental film coolant. Four of these chambers were fabricated, but experienced considerable delay because of fabrication problems associated with use of Inconel 718 thin-walled tubes.

II, C, Thrust Chamber Assembly (cont.)

(U) A heavy-weight transpiration-cooled chamber was designed which permitted $N_2O_4$ transpiration-coolant flow to be varied over wide ranges in various portions of the chamber. The workhorse chamber (Figure VI-63 and -64) is composed of 12 individually fed compartments, each compartment being composed of a stack of "washer pairs" (Figure VI-66). Each washer pair, in turn, consists of a 0.001-in.-thick flow-control washer and a 0.010- or 0.020-in.-thick-flow-diffusion washer, with the thickness depending on location in the chamber. Three of these chambers were fabricated.

(U) The test program consisted of five tests on three regeneratively cooled chambers and 30 tests on two transpiration-cooled chambers. The initial tests demonstrated structural integrity and basic operation of each design while using a maximum amount of film or transpiration coolant. The coolant was then decreased incrementally to give progressively higher performance. When contractually required performance was obtained, test duration was to be extended in steps to meet the three 20-sec duration tests required by the terms of the contract.

(C) Attainment of the required performance and duration was not demonstrated during the report period because of the incompatibility problem with the Mark 125 injector; however, the basic feasibility of the transpiration-cooled chamber design was demonstrated. Structural integrity, stability, heat transfer and performance-trend data all indicate that this chamber concept can meet ARES engine requirements when a non-streaking injector is developed. Insufficient testing has been performed to date with the regeneratively cooled chamber to firmly establish its feasibility. Based on data obtained to date, it is predicted that the regeneratively cooled chamber will meet Phase I requirements with about 29 lb/sec film coolant and that the transpiration-cooled chamber will meet requirements with 25 lb/sec of coolant with an injector delivering 93.5% $I_s$ or better in the uncooled condition.

II, C, Thrust Chamber Assembly (cont.)

Coolant has already been successfully reduced from over 50 lb/sec to about 35 lb/sec with the transpiration cooled chamber.

### d. Uncooled Two-Dimensional Nozzle Evaluation

(U) The ARES engine module can be used singly or in clusters to provide thrust in multiples of 100,000 lb. Approximately eight or more engines can be arranged to discharge through a common nozzle to increase effective area ratio. A possible design improvement to the basic engine, when used in such an application, involves use of a two-dimensional, nonaxisymmetric nozzle which is flared and flattened to distribute the gases evenly into the forced deflection or plug nozzle.

(U) The Phase I effort included a task to determine the temperature distribution in a two-dimensional nozzle using both uniform and tailored film coolant injection. A two-dimensional nozzle with an area ratio of 5:1 was fabricated and tested twice. The chamber consisted of an ablative liner enclosed in a heavy steel case. Thermocouples penetrated the chamber wall in axial rows along both the curved and the flat sides. The chamber configuration is shown in Figures VI-105 and VI-106.

(U) The first test with uniform film coolant injection confirmed that temperature distribution was uneven, with the higher temperatures occurring on the flat side of the nozzle. The second test then tailored the film coolant at its injection point in the main chamber to provide relatively greater amounts of coolant on the flat side of the nozzle. The thermocouple data indicated that this was an effective way to equalize the temperature distribution around the nozzle.

II, Summary (cont.)

D. CONTROLS

1. General

(U) The principal goal of this portion of the program was to develop the fuel and oxidizer valves which will be used in the complete full-scale engine module testing. In addition, it was necessary to size the propellant suction lines between the boost pumps and the suction valves and to establish satisfactory interface designs for the suction lines at those points.

2. Suction Valve

(U) A multiple purpose suction valve suitable for both propellants was designed and demonstrated. The valve was designed to act as both a long-term storage seal and as a positive-shutoff operational seal. It is required to have a response capability to open or close in less than 0.400 sec, and to give unobstructed flow from the propellant line through the valve to the pump. The valve must also have low operating torque, low weight, and a diameter not greatly in excess of the propellant line.

(U) The configuration that eventually met all work statement requirements is a unique design in which a segmented ball gate lifts from the operational seal, and then rotates entirely out of the flow path. A metal foilseal which acts as a long-term storage seal is sheared during the initial lifting motion. In the reverse motion, the segmented ball gate rotates into the flow path and is then pushed linearly against a spring-loaded lip seal. This design, with its cam operating mechanism, is shown in Figure VII-1.

II, D, Controls (cont.)

(U) The operation of the valve after endurance cycling with both water and propellants met or exceeded contract requirements; there was no discernible internal or external leakage of either propellant.

### 3. Fuel Controls

(U) Separate fuel control valves were developed for both the primary and secondary injectors. The primary fuel control valve must accurately control the fuel flow rate to the primary combustor over a flow range of 25:1, and be able to repeat the flow for any preselected position. It must also have the capability to shut off 6,000 psi flow from any position in less than 0.025 sec.

(U) The rotary sleeve valve configuration selected to meet this requirement is shown in Figure I-7.1.1-1 of Appendix I. Two of these valves were fabricated and tested. The tests verified the structural integrity of the design, and demonstrated that all of the design criteria were met or exceeded. The flow constant (Kw) actually attained was 2.1, against a requirement of only 1.45. Thus, the valve gives more flow for a given ΔP than originally demanded, giving it the ability to accommodate lower inlet pressures than originally contemplated. The control range demonstrated was 80:1, versus a required range of 25:1.

(U) The secondary injector fuel control valve is similar in concept to the primary control valve: it must handle approximately four times the flow, but must have a maximum operating pressure of only 4,000 psi. The valve configuration is shown in Figure I-7.1.2-2 of Appendix I. This valve also met or exceeded all contractual requirements and gave a control range of 75:1, versus a requirement of 25:1.

II, Summary (cont.)

## E. SUPPORTING STUDIES

### 1. General

(U) Several studies and laboratory testing efforts were conducted to provide specialized design data, or to investigate matters relating to application and growth of the ARES engine concept. These are summarized below:

### 2. Fluid Dynamic Testing

(U) Analytical techniques cannot accurately predict pressure drop and flow distribution for some of the flow passages on the integrated ARES engine. Consequently, a program was undertaken to experimentally determine this information with air flow test models. Four full-scale models were built and tested to predict performance of the passages in the "T" configuration advanced turbopump from the:

a. Oxidizer pump discharge down to the thrust chamber flange.
b. Thrust chamber flange up to the primary injector face.
c. Primary injector to the turbine inlet.
d. Turbine exhaust to the secondary injector face.

(U) The results of the air-flow testing gave sufficient information to confidently design all of the flow passages with the exception of the turbine exhaust to injector face passage. Additional effort is needed to optimize the design of this passage for uniform flow to the secondary injector.

### 3. Subscale Nozzle Program

(U) When the ARES engine module is clustered into large single nozzles, discontinuities occur where the individual modules exhaust onto the common skirt. Also, in the forced-deflection nozzle, a base heat shield is needed to prevent base recirculation from damaging the bottom of the vehicle. In regions of flow discontinuities, experimental data were needed to optimize performance and determine heat transfer rates. Therefore, a subscale program was conducted to obtain design criteria for a 2-million-lb thrust engine employing twenty 100K modules exhausting into a single forced deflection nozzle skirt. The engine was designed for a vehicle approximately 18 ft in diameter. The first part of the program was to determine the performance potential of the nozzle and to evaluate the effect of various design parameters on the performance (see Section VIII,B,2). The second part was to obtain heat transfer data in regions of the nozzle where flow conditions are such that purely analytical techniques would not be expected to apply (see Section VIII,B,3).

(U) The resulting test program revealed a great amount of useful design information on the 20 module ARES configuration. Some of the significant conclusions are:

a. Forced-deflection and plug nozzles using 20 modules perform better with axisymmetric internal expansion sections (IES) than with contoured-wedge "two dimensional" IES's.

(C) b. Ambient base bleed offers between 2.5% and 3.5% performance improvement over nonvented performance within the atmosphere.

(C) c. Throttling by module shutdown results in a performance ($I_s$) loss of only 0.5% down to 20% thrust under vacuum conditions for forced deflection nozzles employing either axisymmetric IES's or contoured-wedge IES's.

(U) d. The heat transfer coefficient in the region where the IES's flow onto the skirt is higher than would be predicted for a continuous wall with no discontinuities. The magnitude of the increase is strongly dependent on the IES geometry and spacing.

(C) e. Axisymmetric IES's result in the lowest heat-transfer rate of the cases tested.

(U) f. The heat transfer rate on the base heat shield at sea-level atmospheric conditions is approximately four times as high as at vacuum.

(U) g. The heat transfer rate inside the nozzle of a shutdown module is approximately the same as on the base heat shield.

### 4. Advanced Propellants

(U) A program was conducted to determine the changes necessary for the engine to be suitable for use with several advanced propellants--peroxide/Alumizine, Compound A/Hydrazine and $N_2O_4$/Alumizine.

(U) The results of this study showed that conversion of the ARES module to the use of advanced propellants changes the flow schedule of the module significantly. However, boost pumps, suction lines, suction valves, and the primary combustor fuel valve can be used with no component design changes. The existing turbopump oxidizer housing is adequate for $N_2O_4$/Alumizine and for $H_2O_2$/Alumizine but not for Compound A/$N_2H_4$. It can be made acceptable for Compound A/Alumizine if shaft speed is increased, or operating pressure of the secondary combustor is reduced, or if capability to accommodate a large-diameter pump impeller is provided.

(U) The oxidizer impeller and the second-stage fuel impeller can be reworked from the ARES configuration to accommodate a specific propellant.

II, E, Supporting Studies (cont.)

(U) Other major components are not acceptable because of the increased fluid flow to the secondary combustor. These components will have to be resized.

(U) Greater convertibility could be achieved by using an $N_2O_4$/AeroZINE 50 cycle based on a fuel-rich rather than an oxidizer-rich primary combustor. However, conversion to this cycle would demand the development of a high-temperature turbine as well as new primary and secondary combustors. Therefore, the fuel-rich primary combustor cycle with $N_2O_4$/AeroZINE 50 is not recommended in the current program.

### 5. Analytical Models

(U) Several analytical models were developed to establish the engine steady-state and transient operation and to define its stability characteristics. To accomplish this, three engine simulation computer programs were developed:

(U) a. A steady-state program to establish the engine operating point, and the ability of the engine to regain the design point when perturbed.

(U) b. A transient program including water hammer effects to show the behavior of the engine during start, steady-state and shutdown operations.

(U) c. A low-frequency analysis program for studying the system stability characteristics of the engine during steady-state operation.

(U) Similar models were prepared for use with the component test hardware. These used basically the same equations, but their boundary conditions were varied to suit the particular test setup.

II, E, Supporting Studies (cont.)

### 6. Reliability

(U) A reliability effort was conducted to assure that the engine will have high operational reliability. Most effort was concentrated in the areas of failure-mode analysis and design review, with limited effort devoted to such tasks as maintainability and reliability prediction.

(U) An initial task was to obtain applicable failure data from related programs. This task provided essential inputs for the failure mode analyses, maintainability reviews, reliability predictions, and various comparison studies. Data was obtained from the Titan II, Titan III, and Gemini programs on component failure modes, frequency of experienced failures, and the reliability of each component.

(U) Each component of the ARES engine was analyzed to identify the potential failure modes, the causes of those failures, and the anticipated effects of those failures on the engine. It is concluded that, even though effort must be directed toward the solution of some remaining design problems, greater emphasis must be placed in such nondesign areas as fabrication, assembly, inspection, transportation, checkout, cleaning, and testing. There are cases in which trapped propellants pose a potential safety hazard. The use of inert materials such as Kynar and Kel-F for inserts in the wear-rings removed all significant explosion hazards from main-stage or boost pump rub.

# III.

# MODULE

# III.

# MODULE

## A. OBJECTIVE AND APPROACH

### 1. Propulsion System Objective

(U) The Phase I objective of the propulsion system design and analysis effort was to establish the master layout for a propulsion system with twenty 100,000-lbf-thrust engine modules clustered within a forced deflection nozzle to define the engine-module envelope constraints and interface conditions.

### 2. Engine Module, Advanced Turbopump, Phase I Objectives

(C) The Phase I objectives of the engine module, advanced turbopump, design and analysis effort was to establish a layout design for an engine module to operate to the target design point tabulated below.

| | Target Design Point | Phase II Demonstration Range |
|---|---|---|
| Thrust, Sea Level, lbf | 100,000 | 100,000 ± 5000 |
| Chamber Pressure, psia | 2800 | 2800 ± 140 |
| Specific Impulse, sec | 285 | 283 (minimum) |
| Propellants | $N_2O_4$/A-50* | $N_2O_4$/A-50* |
| Mixture Ratio, Injector | 2.2:1 Nominal | 2.2:1 Nominal |
| Area Ratio, Nozzle (80% Optimum Bell contour) | 20:1 | 20:1 |
| NPSH, Fuel, ft | 43.0 | 43.0 |
| NPSH, Oxidizer, ft | 30.0 | 30.0 |
| Dry Weight (including boost pump) | 675 | 850 (maximum) |

*A-50, Aerojet-General Corporation Trade Name for 0.5 Hydrazine, 0.5 UDMH fuel blend

III, A, Objective and Approach (cont.)

From this layout design, working designs of the engine module assembly and its component parts were to be established. These designs will be tested in Phase II of this program within the demonstration range tabulated above.

### 3. Engine Module, Conservative Turbopump, Phase I Objective

(U) The Phase I objective of the engine module, conservative turbopump, design and analysis effort was to establish a layout design for an engine module incorporating a turbopump assembly of conservative design.

### 4. Approach

(U) The module envelope constraints were defined by the requirements to fit into the 20-module propulsion system.

(U) Specifications were developed early in the program so component designs could be initiated. From the component designs there was a feedback of predicted performance and size and envelope requirements. The steady state operating point was revised to reflect the latest component design changes and, conversely, there were component design changes necessitated by changes in the operating point. Thus, an iterative process was used to refine both the engine and component designs.

(U) To analyze the engine module it was necessary to determine the pressure values throughout the system based on pressure drops required by the injectors, the turbine and the fluid passages. Component functional requirements such as TPA speed and pump pressure rises were defined and preliminary component designs evolved.

III, A, Objective and Approach (cont.)

(U) Separate supporting efforts were performed to assist in the design of the propulsion system, engine module, and the engine components. These efforts included (1) fluid dynamic testing of the module, (2) aerodynamic testing of the propulsion system nozzle, (3) advanced propellants, (4) mathematical models, and (5) reliability. The results of these efforts are discussed in Section VIII of this report. In summary, these studies supported and contributed to the design program as follows:

a. Module Fluid Dynamic Testing

(U) Air-flow testing of the interior flow passages of the engine module was performed and aided in developing fluid passages with pressure drop and flow distribution characteristics sufficient to satisfy design requirements.

b. Propulsion System Nozzle Aerodynamic Testing

(U) Testing of a 20-module propulsion system forced deflection subscale nozzle models provided performance and heat transfer data.

c. Advanced Propellants

(U) An advanced propellants study was performed to consider the changes that could be incorporated into the engine design to make the engine more suitable for use with advanced propellants. The results of this study were considered in selection of materials in component designs.

III, A, Objective and Approach (cont.)

d. Mathematical Models

(U) Mathematical models of the ARES engine cycle were programed for computer evaluation of the engine steady state, start and shutdown (including water hammer effects), and low frequency stability characteristics. These programs were used to define the engine operating characteristics.

e. Reliability

(U) A reliability analysis was performed aimed at achieving an engine design with maximum reliability potential. Potential modes of failure were identified and design approaches to eliminate or reduce these potential problems were established.

## 5. Engine Handbook

(U) Concurrent with the engine and component design efforts, an Engine Handbook was established and kept up to date by periodic revisions. This handbook was a part of the documentation contractual requirements and was also a technical part of the design effort in that it provided a vehicle for the documentation and coordination of the module and component designs.

(U) The Engine Handbook, Revision No. 18, is included as Appendix I of this report. This revision of the handbook documents the working design of the engine module with advanced (T configuration) turbopump and the layout of the engine module with the conservative (backup or inline configuration) turbopump. This handbook revision includes the latest module and component data and supersedes previous issues and changes.

III, Module (cont.)

## B. PROPULSION SYSTEM

### 1. Objective

(U) The objective of this effort was to establish the master layout of a propulsion system which incorporates twenty 100,000-lbf-thrust engine modules clustered within a forced deflection nozzle, and to define the engine module envelope constraints and interface conditions.

### 2. Description

(U) The propulsion system shown in Figure III-1 consists of 20 engine modules, including boost pumps, arranged in a circular pattern within a forced deflection (FD) nozzle. The axis of the engine modules are canted at an angle of 22.4 degrees from the propulsion system centerline. Each of the 20 module nozzles serves as an inner expansion section with an expansion ratio of 14:1. The circular nozzles discharge into a single skirt, an ablative forced deflection nozzle, resulting in an overall expansion ratio of 70:1.

(U) The entire assembly of 20 engine modules and the forced deflection nozzle are held together by an upper thrust ring which takes the thrust from the engines, and by a heat shield across the forced deflection nozzle inlet that ties the engine module nozzles to the FD nozzle. Structural cans surrounding the module nozzles take the thrust from the FD nozzle to the upper flange of the module thrust chamber. The engine-module boost pumps are mounted on the vehicle and connected to the bottom of their respective tanks. Flexible lines connect the boost pumps and the engine intakes.

III, B, Propulsion System (cont.)

### 3. Thrust Vector Control

(U) The propulsion system achieves thrust vector control by pivoting the integrated module forced-deflection nozzle assembly. The assembly is pivoted by two wedge rings between the thrust ring of the propulsion system and a fixed thrust ring at the bottom of the vehicle. The wedge rings can be individually rotated to any position to achieve the desired TVC angle up to the maximum angle (6 degrees) of the wedge ring system. The thrust is transmitted through the thrust bearing rollers between the upper and lower wedge rings. Thrust ring clamps are provided to take tensile loads during shipping or handling.

### 4. Module Envelope Constraints

(U) The engine module configuration is constrained by the envelope allocation for the individual modules in the propulsion system. The configuration shown in Figure III-1 is a minimum configuration for the circular arrangement of modules. The module envelope was monitored continuously during the program to assure that the module and its components will fit in the allocated space. Adequate space was allocated for available off-the-shelf type actuators which are to be used for the engine module Phase II demonstration engine tests. By orienting these actuators as shown in Figure III-1, the actuators will fit within the allocated engine envelope.

### 5. Program Accomplishments

(U) The propulsion system layout design was completed during February 1966 and was subsequently reviewed with regard to nozzle performance considerations and established to be satisfactory on the basis of the extrapolated results of the subscale 20-module nozzle aerodynamic test program.

III, B, Propulsion System (cont.)

The engine module interfaces as established by the layout design have been incorporated in the engine module and component designs.

## C. ENGINE MODULE, ADVANCED TURBOPUMP

### 1. Objectives

(U) The objective was to establish a layout design for an engine module which has the sea level target operating characteristics as tabulated in Section III,A,2.

From this layout design a working design of the engine module and component parts was to be established. This design would be tested in Phase II of this program.

### 2. Description

#### a. Design

(U) The ARES demonstration engine module with the advanced (T-design) turbopump including boost pumps is shown in Figure III-2, an updated version of Aerojet Drawing 1120394 referred to in the contract work statement. The engine module subassembly cross-section layout, Figure III-3, shows the engine without boost pump and engine feed lines. High performance is achieved by improvements in both specific impulse and specific weight over those of engines currently in use. A higher specific impulse is attained by using high chamber pressure and the staged-combustion engine cycle. Lower specific weight is achieved through an integrated design and by using high-strength materials for pressure-containing components.

(U) The ARES demonstration engine module consists of a 40,000 rpm turbopump assembly, a 20:1 area ratio regeneratively cooled thrust chamber assembly, fuel and oxidizer suction valves, and boost pumps. The turbopump housing accommodates the pumps, turbine, primary combustor, and control valves and forms the main structural component of the engine. The general configuration of the housing is that of a T-pipe. The pumps are located at opposite ends of the 13 in. dia cylindrical portion, with the thrust chamber attached to the lower end of the vertical branch. The engine uses a single-stage oxidizer pump and a two-stage fuel pump. The module subassembly external view with envelope dimensions defined is shown in Figure III-4.

### b. Cycle

(U) The staged combustion cycle of the ARES demonstration engine is shown schematically by Figure III-5. In this cycle the propellants enter the module from the propellant tanks then flow through the suction boost pumps where the pressure is raised to a safe suction pressure to suppress cavitation in the main stage, high speed pumps. The propellants enter the main stage pumps through eyelid type suction valves located at the main pump inlets.

(U) The bulk of the oxidizer from the main oxidizer pump flows through the secondary combustor coolant tubes and then is injected into the primary combustor.

(U) The bulk of the fuel from the first-stage fuel pump flows through the secondary combustor fuel control valve to the secondary combustor. Approximately 18% of the fuel is pumped to a higher pressure by the second-stage fuel pump and then flows through the primary fuel control valve to the primary combustor. The propellants are burned in the primary combustor to generate an oxidizer rich, moderate temperature (1200°F) gas. This gas passes through the turbine nozzle and rotor to power the pumps. The turbine exhaust passes through the secondary combustor injector where it mixes and burns with the main fuel flow in the secondary combustor to generate the rated thrust. Boost pumps are driven by hydraulic turbines powered by high pressure propellant from the main propellant pumps. Thrust chamber film cooling is supplied from the discharge of the main oxidizer pump.

### c. Operation

#### (1) Design Point Operation

(U) The predicted operating point of the engine module for target specific impulse is given in Table I-2.7-1, Appendix I. This operating point is based on predicted component performances, on allocated pressure drops or passage friction loss characteristics throughout the system, and on the required film coolant flow rate. The steady state mathematical model of the engine was used to calculate this operating point. The two fuel control valves would be adjusted to attain the operating point shown. Predicted operating point flow values for all flow circuits of the engine module are shown in Figure I-2.6-1, Appendix I.

(U) The target operating point in relation to the operating region specified in the work statement for the engine module is shown in Figures I-2.7-5 and I-2.7-6, Appendix I.

#### (2) Start-Shutdown

(U) The engine module start and shutdown transients have been analytically defined using the transient mathematical model and

III, C, Engine Module, Advanced Turbopump (cont.)

predicted component performance characteristics. These predicted start and shutdown transients are shown in Figures I-2.4.3-1 and I-2.4.4-1, Appendix I, respectively. A detailed discussion of the transient mathematical model is given in Section VIII of this report for both the start and shutdown operations.

(U) The engine operating sequence to accomplish the predicted start transient is as follows.

(a) Pressurize propellant tanks to 60 psia.

(b) Open oxidizer suction valve.

(c) Open fuel suction valve approximately 1/2 sec later.

(d) Open primary combustor fuel control valve (PCFCV) to preset amount (5% operating point $K_w$ value) which causes fuel to flow to the primary combustor.

(e) Open secondary combustor fuel control valve (SCFCV) to its full operating position.

(f) Continue opening PCFCV at a preset rate from its step to the steady state operating point.

The shutdown operation is the reverse of the startup operation and ends with all engine module valves closed.

### (3) Off-Design Operation

(U) The Phase-I ARES engine module was designed to achieve specified performance at full thrust. Off design operation can be obtained by varying the PCFCV and the SCFCV positions. Figures I-2.4.1-1 through I-2.4.1-7 inclusive, Appendix I, show the operational maps for this off-design operation. The predicted relationships of engine thrust and engine specific impulse to control valve position are shown in Figure I-2.4.1-1, Appendix I and indicates that the engine can be throttled to approximately 80% of rated thrust while maintaining constant engine mixture ratio. To reduce the thrust to this 80% point while holding the engine mixture ratio constant, the PCFCV is partially closed while the SCFCV is fully opened. The engine can be throttled further by continuing to close the PCFCV; however, the engine mixture ratio will increase for this off-design operation because the SCFCV is already fully open.

### d. Influence Coefficients

(U) The effects of component performance deviations from allocated design values were calculated to establish their criticality to the engine system. It was established from this analysis that the two fuel control valves of the system have more than adequate control capability to achieve target engine thrust and mixture ratio for anticipated variations in component performance due to manufacturing tolerances. Predicted effects of turbopump component efficiency deviations from nominal operating values on engine performance and on turbine inlet temperature are shown in Figures I-2.7-2 and I-2.7-3, Appendix I, respectively.

### e. Weight

(U) Engine weight, broken down by component, has been estimated. These weight values are tabulated in Table I-11.1-1, Appendix I, AD 383 737

AUTHORITY:
AFRPL ltr 5 Feb 86

along with the allocated weight values. The chargeable dry weight of the engine module assembly is currently estimated to be 743 lb.

### f. Materials

(U) The materials to be used in the components of the engine module have been selected based on their environmental and operational requirements. A list of materials for the engine components is shown in Table I-12.1-1, Appendix I. Included in this table are component temperature and operating environments.

## 3. Design Criteria

(U) Engine and component design criteria were defined and revised as required to establish the specification as documented in Appendix I. The engine module performance specifications are documented in Appendix I, Section 2.3, which defines the performance, envelope and weight requirements. The engine design pressure schedule is given in Table I-2.6-1, Appendix I. This table gives the propellant and gas design pressures at major flow stations throughout the module. The module flow passage design requirements are given in Table I-2.6-2, Appendix I.

(U) Component design criteria have been established from the engine module pressure and flow schedule mentioned above. These component design requirements are documented under their respective component headings in Appendix I.

(U) Physical dimensions of all components and the interfaces between components were defined. This was done by means of interface drawings that defined both sides of each interface in detail, including dimensions, tolerances, surface finishes, sealing, and bolting requirements. A list of the interface drawings is given in Table I-13.1-1, Appendix I.

## 4. Program Accomplishments

(U) In establishing the engine design, three variations of the configurations were evolved. The initial engine design variation incorporated the Model A turbopump which in turn was used for the turbopump housing structural testing. Section IV,C, of this report discusses the results of turbopump housing structural testing. A second engine design variation incorporating a Model B turbopump was prepared. A plastic model of the engine fluid passages with the B configuration turbopump housing was evaluated by air flow testing. Data from this testing indicated that both flow distribution and pressure drop were unsatisfactory in the oxidizer pump housing. The pump housing passages were developed to achieve satisfactory flow characteristics and the improved passages were incorporated in the Model C turbopump housing. Section VIII,A, of this report presents results of the module air flow development program. The third engine design variation was then prepared incorporating the Model C turbopump; this engine design was presented in Figure III-3.

## D. ENGINE MODULE, CONSERVATIVE TURBOPUMP

### 1. Objective

(U) The objective was to establish a layout design for an engine module incorporating a turbopump assembly of conservative design which has the same engine sea level operating characteristics as the demonstration module with advanced turbopump as tabulated in Section III,A,2, of this report.

### 2. Description

#### a. Design

(U) A layout design was made of an engine modul incorporating a conservative design turbopump which meets the basic operation requirements of the engine module. This module design is shown in Figures I-9.1.1-2, Appendix I.

(U) This conservative turbopump is of inline configuration with the turbopump shaft on the same center line as the thrust chamber. This results in the turbine exhaust discharging directly to the thrust chamber injector. The turbopump design is discussed further in Section IV,D, of this report.

(U) The same thrust chamber assembly, suction valves, PCFCV and SCFCV are used in this engine subassembly as are used in the engine with the advanced turbopump. Also, the same design boost pumps, propellant suction lines, and hydraulic turbine feed lines would be used. The turbopump speed is 30,000 rpm in this design compared to 40,000 rpm in the advanced design. Also, there is a purge seal between the propellant pumps compared to a burn-off seal in the advanced turbopump housing.

b. Cycle

(U) The engine cycle for the backup design is shown in Figure I-9.1.1-1, Appendix I. This cycle is basically the same as for the advanced design, but the component arrangment is shown to correspond to the inline turbopump configuration.

c. Operation

(U) The predicted operating point of the backup engine module for the target specific impulse is given in Table I-9.1.3-1, Appendix I. This operating point is based on predicted component performances and on allocated pressure throughout the system and film coolant flow rate.

(U) The same steady state mathematical model of the engine was used to define this operating point as was used for the engine module with the advanced turbopump. The predicted performance of the components, however, was adjusted to reflect those of this engine. In general, the components are similar to those of the advanced turbopump design with the major difference being in the turbopump assembly.

### 3. Design Criteria

(U) The engine performance specification for the backup engine are the same as those for the demonstration engine module and are documented in Appendix I, Section 2.3. The engine design specification is given in Table I-9.1.2-1, Appendix I.

III, D, Engine Module, Conservative Turbopump (cont.)

### 4. Program Accomplishments

(U) Two configurations layouts of the engine module with conservative turbopump were prepared. The initial configuration was based on the turbopump configurations used for turbopump housing structural tests. The second layout, Figure I-9.1.1-2, Appendix I, has an improved but similar configuration turbopump with an improved thrust chamber design.

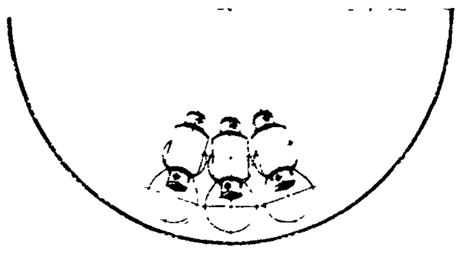

MODULE ARRANGEMENT
- TOP VIEW -

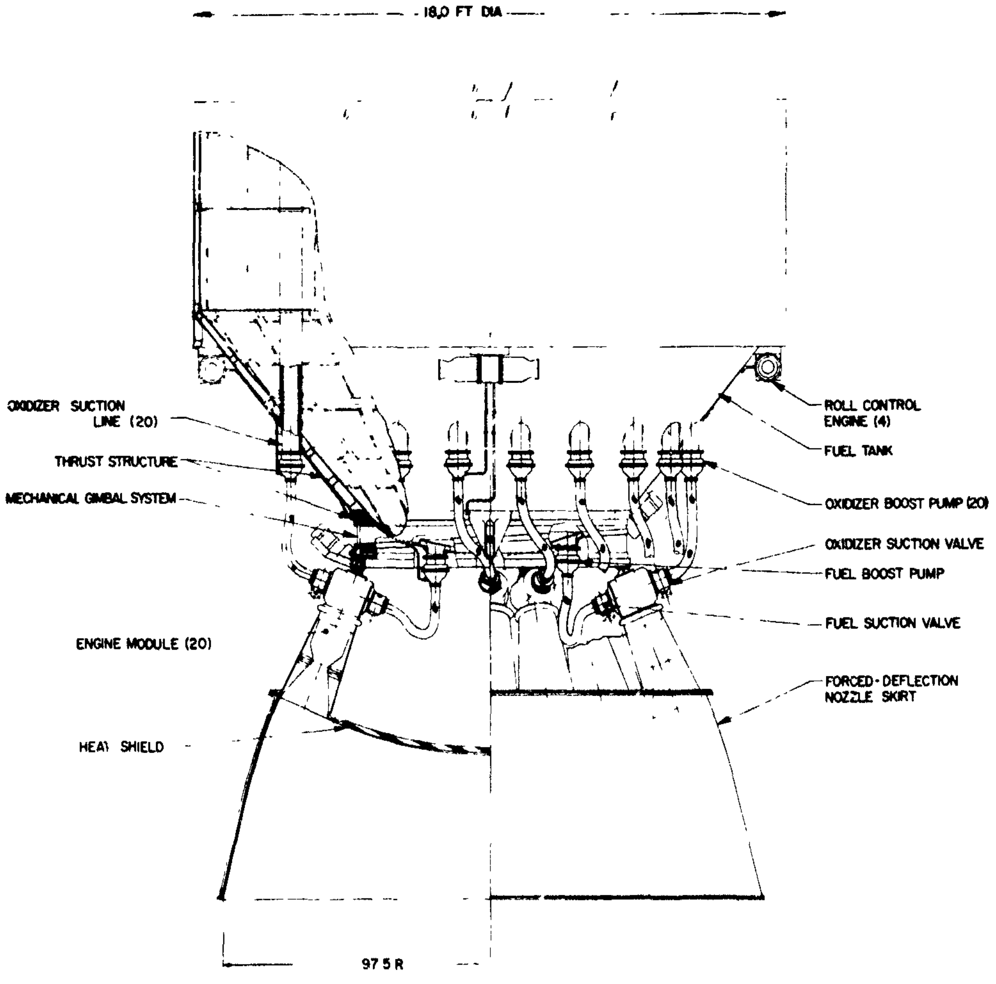
18.0 FT DIA
OXIDIZER SUCTION LINE (20)
THRUST STRUCTURE
MECHANICAL GIMBAL SYSTEM
ENGINE MODULE (20)
HEAT SHIELD
ROLL CONTROL ENGINE (4)
FUEL TANK
OXIDIZER BOOST PUMP (20)
OXIDIZER SUCTION VALVE
FUEL BOOST PUMP
FUEL SUCTION VALVE
FORCED-DEFLECTION NOZZLE SKIRT
97.5 R

Propulsion System, 20-Module Forced Deflection Nozzle

Figure III-1

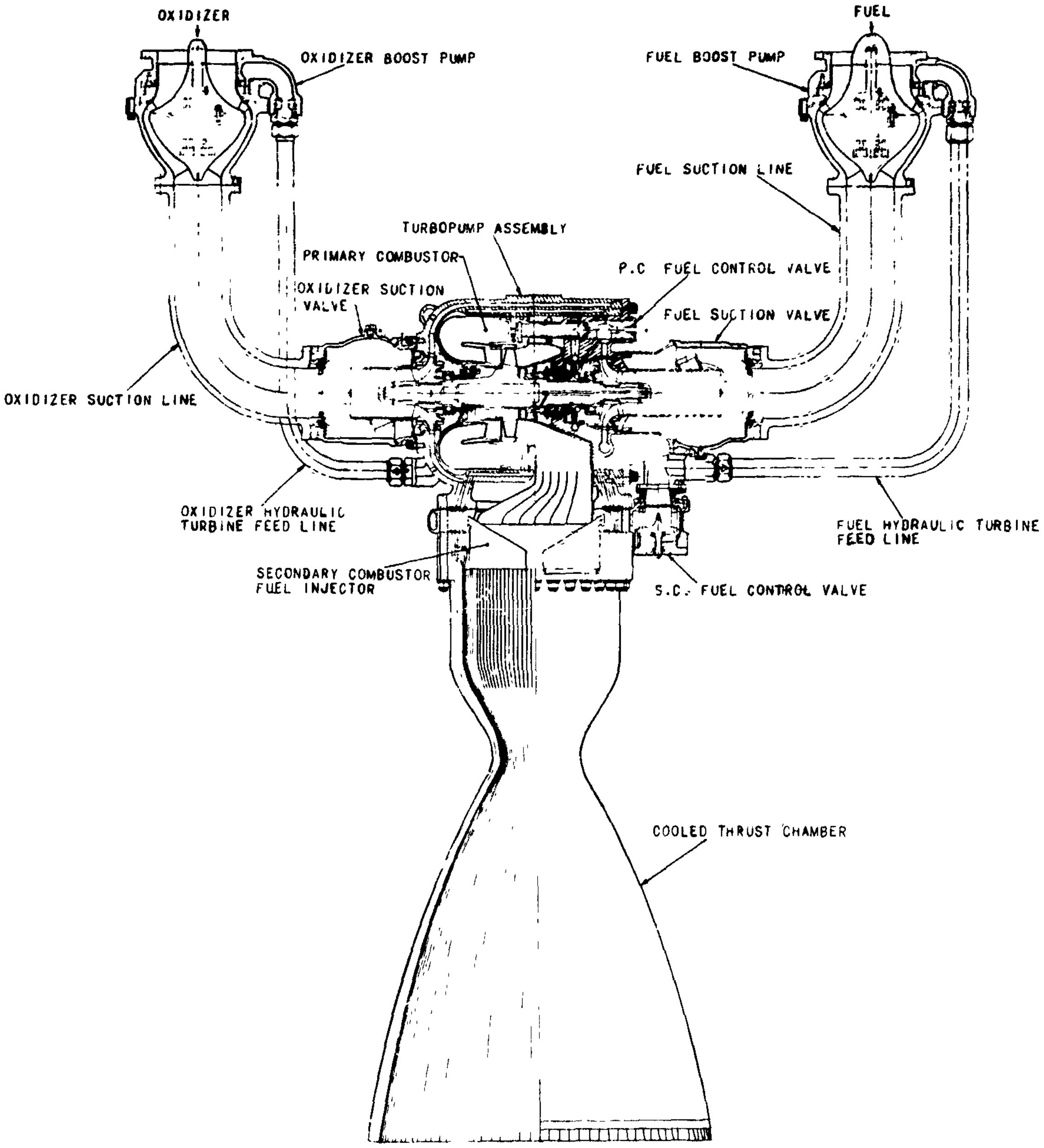
OXIDIZER
OXIDIZER BOOST PUMP
FUEL
FUEL BOOST PUMP
FUEL SUCTION LINE
TURBOPUMP ASSEMBLY
PRIMARY COMBUSTOR
OXIDIZER SUCTION VALVE
P.C FUEL CONTROL VALVE
FUEL SUCTION VALVE
OXIDIZER SUCTION LINE
OXIDIZER HYDRAULIC TURBINE FEED LINE
FUEL HYDRAULIC TURBINE FEED LINE
SECONDARY COMBUSTOR FUEL INJECTOR
S.C. FUEL CONTROL VALVE
COOLED THRUST CHAMBER

Advanced Storable Engine—Demonstrator (u)

Figure III-2

CONFIDENTIAL

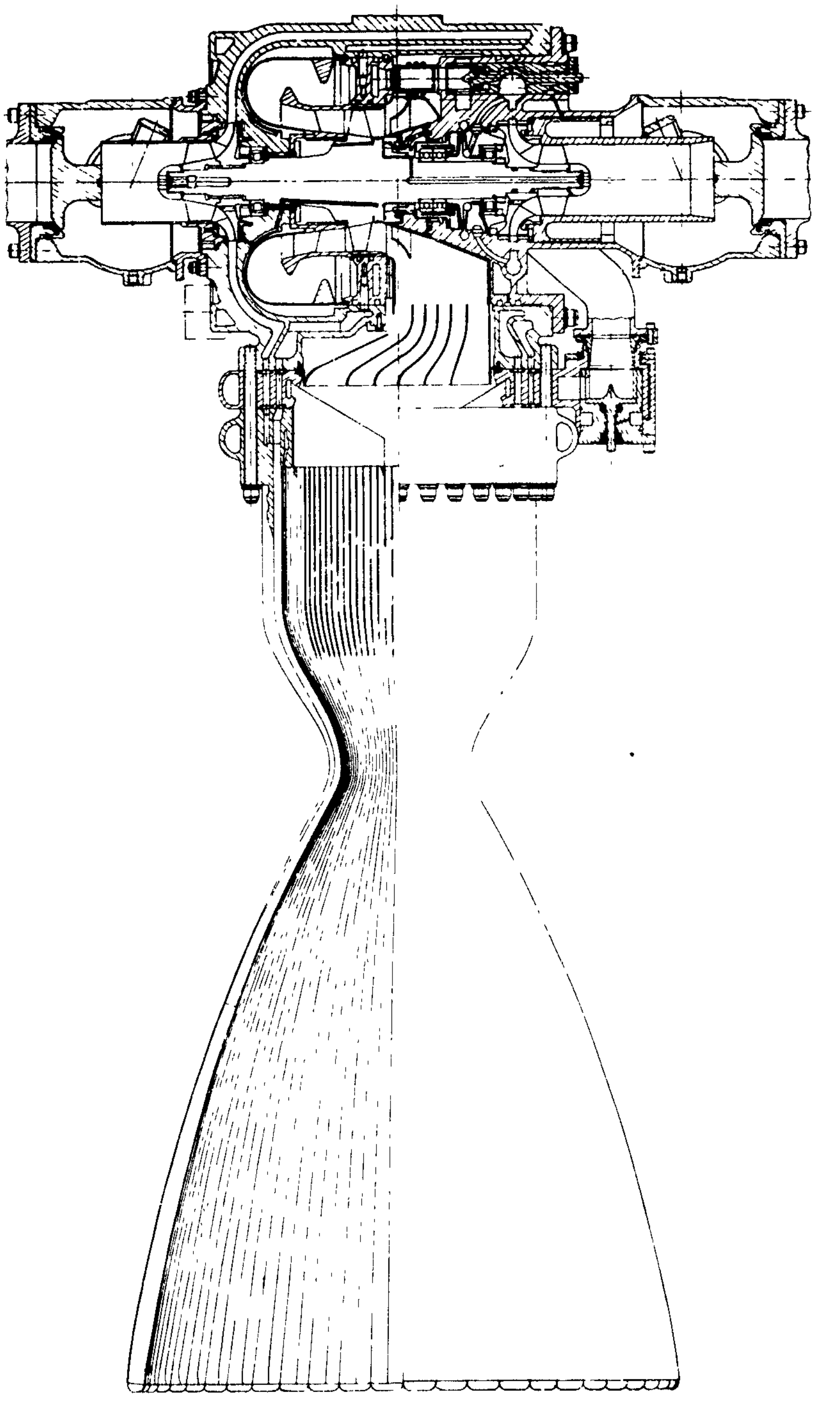

ARES Module Subassembly (u)

Figure III-3

CONFIDENTIAL

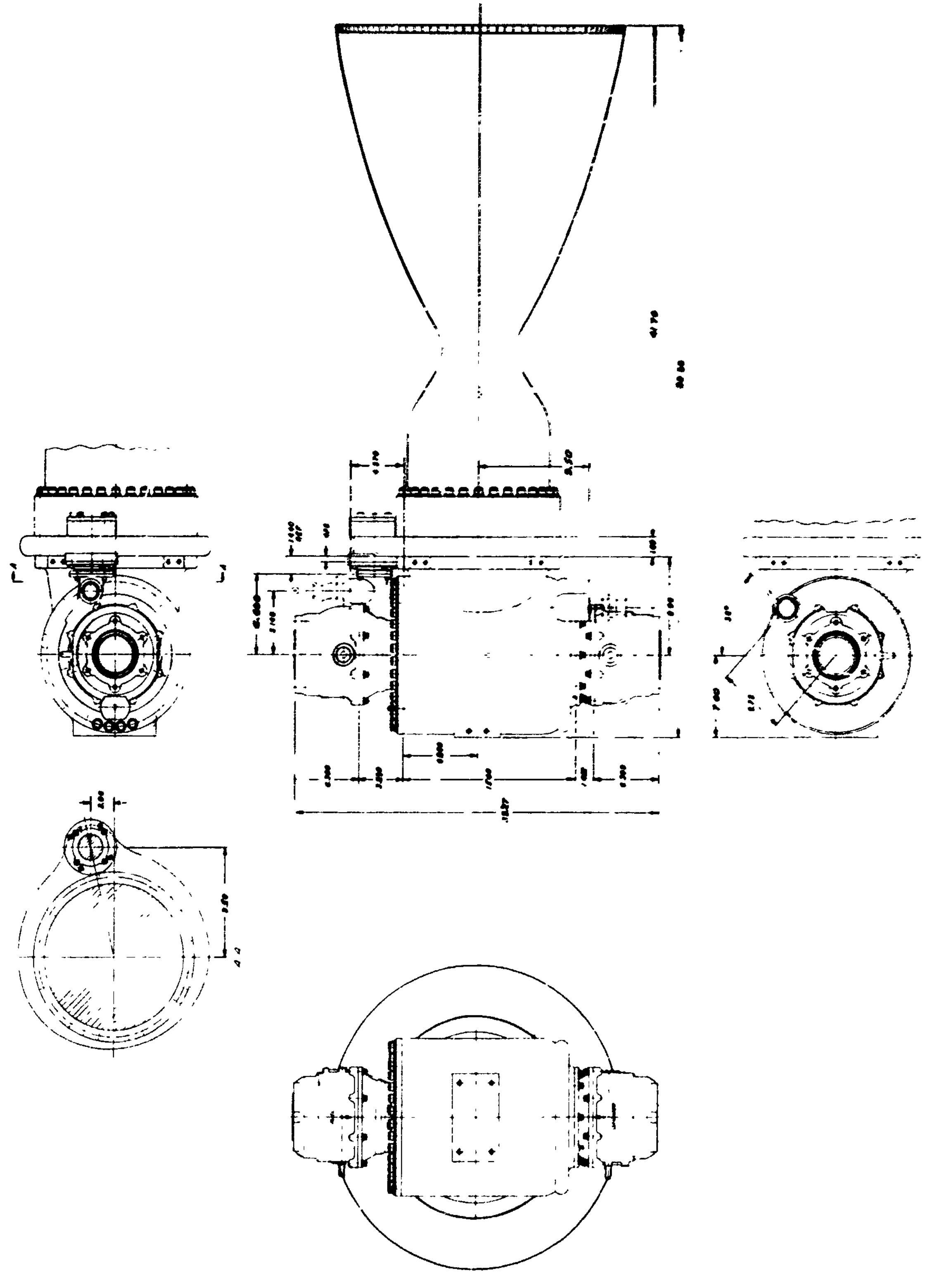

Figure III-4

**CONFIDENTIAL**
(This page is Unclassified)

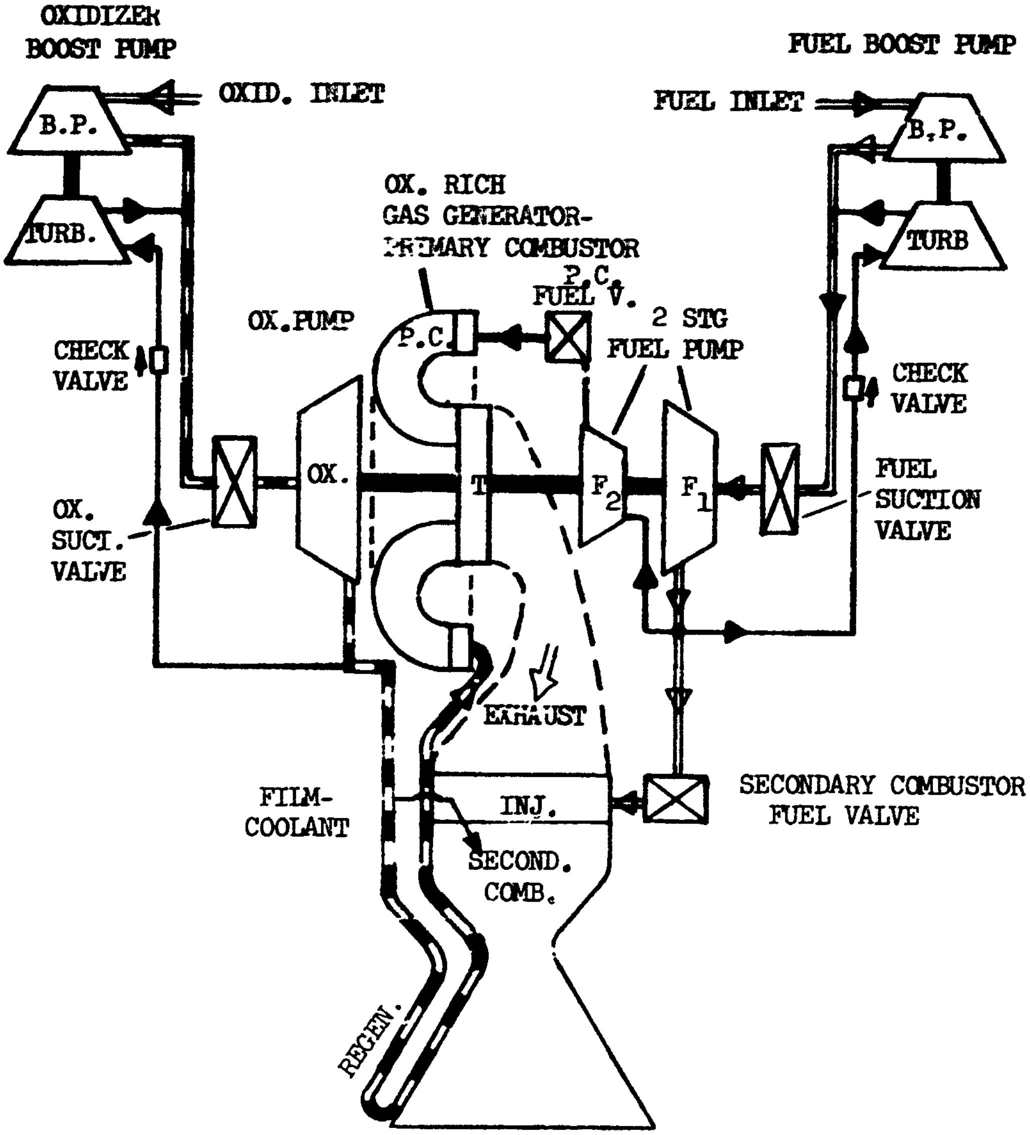
OXIDIZER BOOST PUMP
B.P.
OXID. INLET
TURB.
CHECK VALVE
OX. SUCT. VALVE
OX. PUMP
OX.
OX. RICH GAS GENERATOR-PRIMARY COMBUSTOR
P.C.
P.C. FUEL V.
T
2 STG FUEL PUMP
$F_2$
$F_1$
FUEL BOOST PUMP
FUEL INLET
B.P.
TURB
CHECK VALVE
FUEL SUCTION VALVE
EXHAUST
FILM-COOLANT
INJ.
SECOND. COMB.
SECONDARY COMBUSTOR FUEL VALVE
REGEN.

ARES System Staged Combustion Cycle (u)

Figure III-5

# IV.

# TURBOPUMP ASSEMBLY

# IV.

# TURBOPUMP ASSEMBLY

## A. SUMMARY

### 1. Objectives

#### a. Program Objectives

(C) The basic objective of the ARES turbopump program is to provide a reliable flight weight feed system for a 100,000 lb thrust engine utilizing high pressure storable propellants in the staged combustion or topping cycle. The ARES engine program objectives--high performance, light weight, high reliability, low initial cost, ease of maintenance, and versatility of engine module application--created stringent design objectives for the turbopump. These objectives and resulting design concepts for the ARES turbopump include:

(U) (1) An integrated design of the pumps, turbine, and primary combustor which is capable of distributing the fluids from the pumps to the primary and secondary combustors and the turbine at low pressure drop, with an absolute minimum of external high-pressure seals. The design should provide for multifunctions, such as thrust takeout and pressure containment without objectionable distortions.

(U) (2) Elimination of all redundant lubrication cooling, circulation and storage requirements by the utilization of propellant-lubricated bearings.

(U) (3) Simplification of the rotating shaft seal to eliminate all purges, vents, loose parts, and wearing surfaces.

(U) (4) Use of a single turbine to drive both pumps so that a minimum number of parts will be required, which will also result in higher turbine efficiency because of the more favorable blade heights when all of the gas passes through a single turbine.

(U) (5) Avoidance of gears and their auxiliary systems and the attendant complexity.

(U) (6) Use of boost pumps to permit optimized shaft speed for the main pumps and turbine to suit the engine requirement for 20 ft NPSH for universality of application.

(U) (7) Improved design of pump wear rings which can safely operate at close clearances so that adequate pump efficiency at the extreme head rise of these pumps can be achieved with minimum explosion hazard from rubbing.

### b. Phase I Objectives

(U) The advanced turbopump concept was to be designed in detail. Of the four items of the ARES engine design which were considered to be critical during Phase I, three were in the advanced turbopump. These were the integrated engine housing, the propellant-lubricated bearings which operate at $1.6 \times 10^6$ DN, and the hydrostatic combustion shaft seal. The demonstration of the feasibility of these items was established as criteria of success for continuing with the advanced or T-engine turbopump. A backup turbopump was also to be designed. The backup turbopump feasibility demonstration did not require a seal demonstration but it did require demonstrations of the semi-integrated housing and operation of the propellant-lubricated bearings at lower DN values ($1.25 \times 10^6$), but higher loads.

IV, A, Summary (cont.)

(U) In addition to the critical items, a number of additional items had to be designed and the feasibility of several items verified by test. This included the design of oxidizer and fuel boost pumps for both turbopumps, design and test of improved pump wear rings, turbine air tests to verify the predicted efficiency, finalization of the design of the turbopumps for Phase II selection and testing, and design of the schedule pacing portions of test fixtures for Phase II testing.

## 2. Approach

(U) To achieve the objectives, the advanced or T-engine turbopump was designed. This turbopump operates at 40,000 rpm, which is the optimum speed. It features unrestricted pump inlets at both ends of the shaft; a single, central drive turbine of very high efficiency, propellant lubricated bearings; separate hydraulically driven boost pumps to achieve 20 ft NPSH; a hydrostatic combustion seal that avoids vents and operating purges; a fully integrated housing with a minimum of external lines and seals; an integrated engine thrust takeout structure; improved pump wear rings; and a simple-shaft thrust balancer to ensure maximum thrust-bearing life. This design is shown in Figure IV-1 and is described in detail in Section IV,B.

(U) In addition, a more conventional and conservative turbopump was designed as a backup TPA in the event that the advanced concepts were not feasible. This turbopump, which operates at 30,000 rpm, was renamed the "in-line turbopump" to reflect its shaft configuration which is in-line with the axis of the thrust chamber. The design met almost all of the objectives, specified for the "T" configuration advanced turbopump. The inline turbopump is shown in Figure IV-29 and is described in detail in Section IV,D. The design features a semi-integrated housing; a slightly lower than optimum operating speed to achieve more conventional bearing DN value and seal surface

IV, A, Summary (cont.)

speed, at a moderate sacrifice in pump and turbine efficiency; a more direct flow path to the secondary injector; and a purged seal rather than a combustion seal.

3. Accomplishments

(U) All design objectives of the T-engine turbopump have been achieved and are described in Section IV,B. The detail drawings of pacing hardware for the turbopump and boost pumps (described in Section IV,F) are ready to order. Test objectives on the housing, bearing, pump wear ring, and turbine met all work statement requirements. The only item not fully completed is the seal work.

(U) The unique hydrostatic combustion shaft seal, which avoids the use of auxiliary purge systems, was demonstrated for short duration. Hydrostatic seal operation at 40,000 rpm, on a 0.001-in.-thick film of AeroZINE 50 leaking to 3000 psi $GN_2$ has been demonstrated for 60 sec. Combustion seal tests, on static subscale hardware and full-scale rotating seals with AeroZINE 50 leaking to oxidizer rich gas under full operating conditions, have also been conducted. Several restarts on the same seal with the aid of startup purges were also accomplished during testing. Tests of increased duration will continue during the Phase I extension. The combustion seal testing is described in Section IV,I. An alternative hydrostatic purge seal has also been designed and tested with limited success for a duration of 60 sec at 40,000 rpm with a turbine exhaust condition of 3400 psia and 1050°F. This work is described in Section IV,J.

(U) The flight-weight housing is the key item to integrating the engine module. Two of these housings for the regeneratively cooled thrust chamber arrangement were fabricated. The first housing tested met the structural and vibrational criteria for success. An improved housing, incorporating modifications derived from results of the air tests of the

IV, A, Summary (cont.)

flow passages, was completed. It is expected that radial distortion between bearings will be less than 0.004 in. Economical fabrication methods for the improved housing were also investigated. Firm quotations and delivery schedules were received on the castings required. Estimates of welding and machining required were based on knowledge obtained by the fabrication of the two flightweight housings. A relative cost comparison between three housing designs is shown in Section IV,C,4,d. The advanced turbopump housing effort is shown in Section IV,C.

(U) The satisfactory operation of the 40-mm bearings at 40,000 rpm ($1.6 \times 10^6$ DN) was also essential to the integrated engine concept. Feasibility of the ball and roller bearing operation was demonstrated in $N_2O_4$ and AeroZINE 50 at the specified loads for more than 12-min require duration. The bearing effort is described in Section IV,G.

(U) Three improved types of pump wear rings were designed and successfully tested in water. The two best designs (a face hydrostatic seal and a labyrinth with inert inserts) were then successfully demonstrated in $N_2O_4$. This demonstration included simulated operation at design pressure differentials of over 4000 psi and 40,000 rpm, plus purposely induced rubbing, without explosion. The face type of hydrostatic seal was selected for the oxidizer pump on the basis of its more reliable operation and lower leakage rate. The labyrinth type of wear ring was selected for the fuel pump on the basis of the combined wear ring and shaft thrust-balancer design. Therefore, only the labyrinth with inert inserts was demonstrated in AeroZINE 50. Purposely induced rubbing tests were also satisfactorily conducted at operating pressure and high rotational speed. This work is described in detail in Section IV,H.

IV, A, Summary (cont.)

(U) Two single-stage turbines were designed and tested to evaluate the value of twisted blade profiles versus straight blade profiles. The air test results of the twisted blade design showed a total to static efficiency of 86%. This design was selected over the straight blade design because its efficiency was 7 to 12 points higher at various operating conditions.

(U) The inline engine turbopump was designed through the layout and detail calculation stages. In view of the successful completion of the majority of the advanced turbopump Phase I objectives, detail drawings were not prepared for the backup approach. A detailed description of this design activity is presented in Section IV,D. This arrangement is competitive with the advanced turbopump.

(U) One housing for the inline configuration was fabricated and tested and met the structural and vibrational test requirements of the work statement. The ball and roller bearing tests at $1.25 \times 10^6$ DN values in $N_2O_4$ and AeroZINE 50 were conducted in two steps. The first step was to demonstrate 50-mm bearings at 25,000 rpm; the second step was to demonstrate 40-mm bearings at 31,250 rpm. All work statement objectives were met or exceeded.

## B. T-DESIGN TURBOPUMP

### 1. Objectives and Approach

(U) The T-engine turbopump (Figure IV-1) was designed to meet the requirements of the new generation of high-pressure staged combustion engines utilizing storable propellants, $N_2O_4$ and AeroZINE 50. If required, the concept could be adapted to other propellants. The design utilizes advancement in the state of the art such as: integration of the pumps, turbine, primary combustor and controls into a single housing; a minimum number of static and rotating shaft seals, including a simple hydrostatic combustion seal; propellant lubricated bearings; improved pump wear rings; high efficiency turbopump components; ultra-low NPSH requirements resulting from the use of separate low-speed hydraulic turbine-driven boost pumps, and a direct approach to the development and integration of the ultimate flight-weight components early in the program.

(U) The experience gained on previous high-pressure programs dictated that a minimum number of engine parts of high reliability should be used to achieve a low initial cost and minimum maintenance engine. This led to the high degree of component integration, which eliminates unnecessary high-pressure flange joints and external plumbing, and utilizes the pump housing to perform many functions. It also led to the use of propellant-lubricated bearings so that auxiliary inert fluid systems and their controls are no longer required. A hydrostatic combustion shaft seal with no-rubbing elements, purges, or vents was incorporated to replace the conventional high-rubbing-velocity shaft seals.

(U) The minimum turbopump size and weight consistent with high turbine efficiency and the required primary combustor volume set the selected operating speed of 40,000 rpm. A further increase in speed does not significantly reduce the turbopump weight since the primary combustor and turbine exhaust volume requirements limit any further reduction in housing size.

(U) The selection of separate hydraulic-driven low-speed (8000 rpm) boost pumps mounted between the propellant tanks and turbopump inlet permits the engine to operate at ultra-low tank pressures, minimizes engine weight, and provides the engine with a much broader application.

(U) This section describes the advanced or T-engine turbopump design in detail. It also describes air test results of the turbine efficiency. Separate sections describe the detailed design of the boost pumps and the design and test results of the housing, bearings, seals, and wear rings.

## 2. Design and Analysis

### a. Description

(C) The T-turbopump (Figure IV-1) features unrestricted pump inlets at opposite ends of the shaft which operates at 40,000 rpm. The first-stage fuel pump supplies approximately 80% of the AeroZINE 50 fuel at 3750 psia to the secondary injector, 20% of the fuel to the second-stage pump, and also supplies the fuel boost pump hydraulic turbine requirements which is a recirculating flow loop in the pumping system. The second-stage fuel pump supplies 20% of the fuel at 5750 psia to the primary injector.

(C) The oxidizer pump supplies all of the $N_2O_4$ at 6000 psia for turbopump housing and thrust-chamber cooling before it enters the primary injector, plus the recirculating boost pump flow.

(U) The oxidizer housing is the major structural component of the engine. The housing encloses the primary combustor, turbine, hydrostatic seal, bearings, and fuel housing, and also serves as a structural member which transmits the engine thrust to the thrust takeout pad.

(U) The pumps are driven by a single 10,070-hp turbine. The turbine is a subsonic single-stage axial flow design operating with oxidizer-rich gas at a pressure ratio of 1.5 and an inlet temperature of approximately 1241°F.

(U) The power transmission assembly consists of one 40-mm roller bearing on the oxidizer side and a 40-mm roller and duplex mounted ball bearing set on the fuel side. The ball bearings act with the dual-acting thrust balancer piston to compensate for variations in axial thrust. The fuel impeller is used as the balance piston and has flow restriction lands on the front and back side of the impeller shrouds to compensate for variations in thrust loads. The roller bearings are mounted in a spherical seat to compensate for housing distortions. Since propellant leakage on the oxidizer side of the TPA flows into an oxidizer-rich gas, positive seals are not required and labyrinths are used to reduce the leakage to low, acceptable values. On the fuel pump side of the shaft a hydrostatic seal controls the small amount of fuel flow into the oxidizer rich gas where combustion takes place. An alternative hydrostatic purge seal utilizing an inert fluid purge can be used interchangeably with the combustion seal if required.

(U) Boost pumps are incorporated to satisfy the engine low tank pressure requirements and supply the necessary NPSH for the main stage pumps. A discussion of the boost pump is included in Section IV,F. The use of the boost pump allows the main turbopump to operate with relatively high pump suction pressures which allow high turbopump speed and resultant small size and light weight.

b. Engine Requirements

(C) The ARES engine is a 100K high-pressure gas-liquid staged combustion cycle engine using $N_2O_4$ and AeroZINE 50 as the oxidizer and fuel propellants, respectively. A schematic of the engine using the T-design turbopump is shown in Section III,C.

(U) The turbopump starts with tankhead pressure only. The unit will accelerate gradually as the propellant valves are properly sequenced and primary combustor ignition occurs, causing excess turbine torque and subsequent rapid acceleration to the operating speed. A maximum acceleration rate of 80,000 rpm/sec was established to avoid bearing skidding problems under light loads during the engine start transient phase.

(U) The turbopump hydraulic and aerodynamic design specifications were derived from engine steady-state and transient computer analysis based on predicted component pressure drops and component performance characteristics which are referenced in Appendix I, ARES Engine Handbook, Sections 1 and 3.

(U) The mechanical design requirements were investigated for the most severe steady-state engine operating condition anticipated, and these were found to be less than 105% overspeed conditions. To allow for component performance variations, a 110% overspeed criterion was used and this results in maximum operating pressures equal to 121% times the nominal design value.

(U) The A-design turbopump noted in the weight summary below is the initial Phase I design used to build hardware for housing, bearing and seal testing. Phase I final design incorporates improvements in the design on the basis of the test results. Both designs have been based on the

IV, B, T-Design Turbopump (cont.)

regeneratively cooled thrust-chamber requirements. It can also be used for a transpiration-cooled chamber but a simpler design would be preferable.

(C) The estimated weight of the turbopump components with their allocated target values are listed below. The target weights can be defined as the component weights consistent with the nominal engine target weight of 675 lb.

| | Target | A-Design | Phase I Final Design |
|---|---|---|---|
| Oxidizer housing | 189 | 228 | 196 |
| Fuel housing | 60 | 82 | 58 |
| Primary injector and liner | 30 | 36 | 25 |
| Rotor, shaft, impellers, and inducers | 19 | 22 | 24 |
| Inducer housings | 19 | 17 | 13 |
| Bearings | 3 | 3 | 4 |
| Combustion seal and flange | 1 | 7 | 7 |
| Turbine nozzle | 3 | 3 | 10 |
| Turbine exhaust duct | 3 | 3 | 3 |
| Miscellaneous nuts, labyrinths, and wear rings | 7 | 7 | 7 |
| | 334 | 409 | 347 |

### c. Pump Design

#### (1) Requirements and Design Considerations

(U) The main-stage pumps are conventional high-speed centrifugal designs with backward swept vanes operating at tip speeds of approximately 800 ft/sec. The designs incorporate separate high-speed inducers to meet the low suction pressures available to the pump. The inducers were sized for a maximum suction specific speed of 30,000; however, they operate at a nominal value of 18,000 suction specific speed. This design margin was provided to be conservative to minimize potential operational problems that are associated with pumps operating at high suction specific speeds such as pump discharge pressure oscillations, large pump head rise changes due to cavitation and cavitation damage. Another factor that influenced the inducer sizing was the vane root stresses. At tip speeds of 600 ft/sec and with high-density propellants such as $N_2O_4$, the inducer vane stresses also limit the maximum suction specific speed operation to approximately 30,000 when utilizing high-strength steel materials such as AM-355 selected for this design.

(U) Both main-stage pumps incorporate vaned diffuser type housings. Vaned diffusers were selected over free-vortex type housing to reduce bearing radial loads in the single discharge fuel housing and to provide structural support to the discharge oxidizer housing. Provisions for orificing the oxidizer housing flow passages are included in the design (housing-thrust chamber interface) to ensure a constant pressure drop in all passages and thus provide an equal pressure upstream and downstream of the thrust chamber coolant tubes. Design data show that the radial loads caused by impeller discharge circumferential static pressure variations can be reduced by a factor of 6 with diffuser vanes for single discharge housings similar to the fuel pump design.

### (2) Inducers

#### (a) Hydraulic Design

(U) The main-stage inducers were designed for a maximum suction specific speed of 30,000. The flat-plate high solidity type inducer was selected because of its demonstrated high suction specific speed capability. The inlet eye diameter was determined by the accepted criteria where the inlet velocity head of the fluid is approximately one-third of the net positive suction head (NPSH). The resulting diameters are 3.31 and 3.00 in. for the oxidizer and fuel inducers, respectively. The blade inlet tip angle for the fuel was set for an incidence to vane angle ratio of 0.425. This empirical ratio has been shown by tests to be near optimum for maximum cavitation performance and efficiency. The oxidizer inducer deviates slightly from a flat-plate design and has 2 degrees of camber. This modification was incoporated to reduce the leading edge vane loading by lowering the fluid incidence to vane angle ratio from 0.425 to 0.325. The added camber of 2 degrees provides the same fluid turning as a flat-plate design with $i/\beta = 0.425$. Significant inducer design parameters are summarized as follows:

Inducer Design Parameter

| | Oxidizer | Fuel |
|---|---|---|
| Inlet flow coefficient | 0.118 | 0.103 |
| Head coefficient | 0.16 | 0.16 |
| Inlet vane angle (tip), degrees | 10.5 | 10.3 |
| Discharge vane angle (tip), degrees | 12.81 | 10.3 |
| Number of vanes | 4 | 3 |
| Solidity (tip) | 1.93 | 2.01 |
| Hub/tip diameter ratio (inlet) | 0.45 | 0.45 |
| $NPSH/U^2_{Tip}/2g$ (5% head loss) | 0.0385 | 0.0327 |

(b) Mechanical Design

(U) he highest stress in flat-plate inducers occurs at the root of the vane near the inlet region. The stress results from a combination of fluid bending and centrifugal loads. Because of the high tip speeds of the inducers and the high density of the propellants, the stresses exceeded the strength properties of aluminum alloys. In selecting higher strength materials, titanium 6Al-4V was chosen for the fuel and AM-355 for the oxidizer inducers. The use of heavier AM-355 steel material for the oxidizer inducers is not desirable from critical speed considerations; however, titanium is incompatible with $N_2O_4$. The use of these heavier materials did not reduce the critical speed below the design requirements of 48,000 rpm. The maximum stress for the oxidizer inducer is 42,000 psi versus an allowable stress of 105,000 psi. The maximum stress for the fuel inducer is 49,000 psi versus an allowable stress of 70,000 psi

### (3) Impellers and Diffusers

#### (a) Hydraulic Design

(U) The main-stage impellers were sized to deliver the engine module flow, the boost pump hydraulic turbine flow, wear-ring leakage flows and bearing plus other miscellaneous flows. Impellers with 28-degree discharge angle were selected for both main-stage impellers as a compromise between high efficiency (low vane angle) and small diameter (high vane angles). The discharge flow coefficients of 0.12 for the fuel and 0.15 for the oxidizer are recommended values for high efficiency at the corresponding specific speeds of 1250 and 1500. These values are slightly higher than those normally used in the past by Aerojet-General where some efficiency was sacrificed for a reduction in impeller and pump size. Shrouded impellers were selected over the unshrouded designs to minimize the potential pump rubbing problems and resulting explosion hazard. A detailed discussion on impeller wear rings is given in Section IV,E. The shrouded oxidizer impeller also permits larger pump housing axial displacements during operation without affecting pump performance. Discharge diameters of 4.70 and 5.03 in. for the fuel and oxidizer pumps, respectively, were obtained using Stodola's slip criteria which give the best correlation of Aerojet-General's pump data. Both impellers have three inlet vanes and six partial vanes.

(U) The two-stage fuel pump concept was selected over a single-stage design because it reduces the turbine power requirements by approximately 1000 hp and also provides more flexibility if higher primary fuel pressures are required without increasing turbine power requirements significantly. The second-stage impeller has seven single curvature vanes with 22-degree discharge angle. Since the second-stage fuel impeller is located adjacent to the thrust bearing assembly, an unshrouded impeller is used. At this location, shaft and housing axial movements are small.

(U) Both main-stage pumps have diffuser vanes for mechanical as well as hydraulic considerations that were noted previously. Systematic tests have confirmed that the basic quantity that determines the optimum efficiency of a pump is the inlet area of the diffuser throat. The magnitude of the inlet vane angle, the number of vanes and their profile have little effect in this respect. The diffuser areas were sized on the basis of these tests which agree with experience at Aerojet-General. The inlet vane angles were based upon the fluid following a logarithmic spiral from impeller discharge to the diffuser throat. This angle was then corrected for vane blockage and set with 3 or 4 degrees of incidence. The diffuser exits were sized for approximately 1.6 times the throat area and the diffuser length is 4 times the height, which corresponds to a divergence angle of 8.5 degrees.

(U) A summary of significant pump design parameters is given in Figures IV-2 and IV-3 for the oxidizer and fuel, respectively.

### (b) Mechanical Design

(U) The stress distribution and magnitude of shrouded impeller designs were determined by a finite-element axisymmetric computer program. Several cross-sections of the impeller were investigated to obtain the section with the highest stresses. The results of the stress analysis indicated that cast aluminum alloys would have marginal strength properties. As a result, cast 17-4 PH steel was selected for both the fuel and oxidizer impeller. The heavier fuel impeller does not significantly affect the TPA critical speed and was not a problem. However, the heavier oxidizer impeller reduces the critical speed by approximately 4000 rpm, which was unacceptable. To correct this problem, the oxidizer impeller and inducer lengths were reduced slightly. This permitted a reduction in the distance between the oxidizer bearing and the inducer-impeller center of gravity. On the basis of the critical speed analysis, these modifications will cancel the critical speed reduction because of the heavier oxidizer impeller.

(U) A summary of the pump impeller stresses is given in Figures IV-2 and IV-3 for the oxidizer and fuel pump, respectively.

### (4) Performance

(U) Predicted pump performance curves are referenced in Appendix I, Section 3. The characteristic shape of head versus flow curve is based on existing Aerojet pumps of similar design. The first-stage fuel and oxidizer pump characteristics are similar to Aerojet's Titan IIA oxidizer pump. This pump has a specific speed of 1500 rpm and incorporates diffuser vanes. The second-stage fuel pump H-Q characteristics were based on the Titan I first-stage fuel pump. This pump has a specific speed of 900 rpm, a free vortex type housing, and the impeller has a 22-degree discharge angle.

(U) The pump cavitation performance characteristic of percent head loss versus suction specific speed are based on the M-1 oxidizer inducer performance which was designed for a suction specific speed of 35,000 rpm.

IV, B, T-Design Turbopump (cont.)

#### (5) Component Tests

(U) Performance testing of the pumps will be conducted during Phase II in several steps at AGC's electric-motor-driven pump water test facilities. Test fixtures have been designed for these tests as shown in Figure IV-4. The first series of tests (Figure IV-4, view 1) will evaluate the cavitating and noncavitating performance of the inducers from 0 to 120% of design flow and at design speed. The second series (Figure IV-4, view 3) will evaluate the pump impeller performance without inducers at 25,000 rpm. The reduced speed is set by the test facility speed limitation. The third series (Figure IV-4 view 3) of tests will combine the inducer and impeller and evaluate the overall pump performance. This test series will determine if proper inducer and impeller matching was achieved and it will provide data to correct any performance deficiencies. The boost pumps and hydraulic turbine will then be tested (Figure IV-4, view 2 and 4). The final series will consist of boot-strap tests where the main-stage pump and boost pump operate together. These tests will simulate engine operation and will provide interaction effects and overall performance of the pumping system.

### d. Turbine Design

#### (1) Requirements and Design Considerations

(C) The 10,070-hp turbine (Figure IV-5) is a single-stage axial flow design with a mean blade-gas spouting velocity ratio of 0.606. The turbine was designed for 1241°F inlet total tmeprature, 4650-psia inlet total pressure, and a total to static pressure ratio of 1.5. At this design temperature, the engine power balance used a turbine efficiency of 77%. Mechanically, the turbine is designed for 13,450 hp at 1400°F inlet temperatures.

IV, B, T-Design Turbopump (cont.)

(U) Based on optimization studies, a 6-in. OD was selected and made constant through the turbine. This cylindrical shape makes the tip clearance independent of axial movement of the rotor relative to the casing. The blades are designed for free vortex flow and simple radial equilibrium in front of and behind the blade rows. As a result, the rotor blades are highly twisted and are slightly more difficult to fabricate than a less optimum constant section blade. The uncertainty in the performance loss of the simpler constant section blade led to the decision of air testing the turbine with both types of blading rather than with blading of high twist only. The results of the air tests, discussed in Section IV,B,2,d,(4), Performance Tests, show that the twisted blade design exceeded the required efficiency of 77% by at least 3% after considering additional turbine losses not simulated in the air tests. The predicted turbine aerodynamic efficiency was 83% and the measured value is 86.5%. This higher efficiency reduces the turbine inlet temperature requirements by 35°F.

### (2) Aerodynamic Design

(C) The aerodynamic design and current nominal operating point of the turbine is given below:

| | Aerodynamic Design | Current Nominal Operating | Mechanical Design |
|---|---|---|---|
| Minimum output, hp | 10,070 | 10,192 | 13,450 |
| Weight, flow, lb/sec | 233.3 | 230.2 | |
| Inlet total temperature, °F | 1241 | 1218 | 1400 |
| Inlet total pressure, psia | 4650 | 4556 | 5630 |
| Outlet static pressure, psia | 3100 | 3037 | 3265 |
| Rotative speed, rpm | 40,000 | 40,000 | 44,000 |
| Efficiency (total to static) | 0.77 | 0.80 | |
| Mixture ratio | 11.30 | 11.55 | |
| Gas constant, lb/°F | 46.617 | 46.226 | |
| Specific heat ratio | 1.2572 | 1.256 | |

IV, B, T-Design Turbopump (cont.)

(U) Optimization studies showed that a maximum efficiency would be obtained with a stator outlet gas angle of approximately 73 degrees (measured from the axial direction) and about 40% reaction at the mean blade height. These values were used in the design and this results in 10% reaction at the blade root which is sufficient for good performance. The Mach numbers are low throughout the turbine (maximum at stator and rotor outlet 0.754 and 0.632, respectively). The absolute outlet Mach number is 0.178, which results in low turbine exhaust losses. Below are listed significant design parameters:

| | |
|---|---|
| Rotational speed at mean, ft/sec | 853 |
| Isentropic velocity, ft/sec | 1409 |
| Velocity ratio, Um/Co | 0.606 |
| Number of stator blades | 13 |
| Number of rotor blades | 22 |
| Blade height stator, in. | 0.95 |
| Blade height rotor, in. | 1.12 |
| Stator chord length (mean), in. | 1.720 |
| Rotor chord length (mean), in. | 1.026 |
| Stator pitch/chord ratio (mean) | 0.700 |
| Rotor pitch/chord ratio (mean) | 0.695 |

### (3) Mechanical Design

(U) Since the turbine rotor, shaft, and combustion seal face are integrated into a single unit, the thermal gradients, stresses, and resulting growth of the turbine rotor must be kept to a minimum to prevent seal face distortion. The most severe case occurs during the engine start transient when the turbine shaft, initially at ambient temperature, is exposed to the hot gas at the maximum design temperature of 1400°F and results in extreme temperature gradients.

IV, B, T-Design Turbopump (cont.)

(U) Heat-transfer and stress analyses of various designs indicate that the solid shaft has less distortion at the combustion seal rubbing face than a hollow shaft design. With the solid shaft design, the seal face distortion due to the thermal gradient and stress was reduced to an acceptable value of 0.0005 in. displacement between the inner and outer rim. The combustion seal operates with a clearance of 0.001 in. The maximum stresses, along with the corresponding temperature gradient which occurs during the start transient, are shown in Figure IV-5. The shaft material is Waspalloy.

(U) The rotor blade stresses were determined at design and at the 110% overspeed condition. The stress analysis consists of calculating the loads and stress due to gas and centrifugal forces. The variable stress is assumed to be one-third the gas bending stress, and the mean stress is equal to the gas bending plus the centrifugal stresses. Stress concentrations and stress amplification factors due to blade natural frequencies are included. At design speed, the mean stress is 59,500 psi, the variable stress is 23,400 psi, and the allowable mean stress is 71,000 psi for stress concentration factor of 1.33 and an amplification factor of 2.37. At the 110% overspeed condition, the mean stress is 66,000 psi, the variable stress is 32,700 psi, and the allowable mean stress is 66,000 psi for the same stress concentration factor noted above and with an amplification factor of 3.32. These values are shown on a Goodman diagram in Figure IV-5. The allowable stresses are based on the 10-hr stress rupture properties of Waspalloy at the maximum relative total gas temperature of 1300°F. This corresponds to a total gas inlet temperature of 1400°F. On the basis of the above stress values, the strength properties of Waspalloy are adequate for the design.

(U) Heat-transfer and stress analyses of the turbine stator indicate that the highest stresses occur at the stator support flange and the leading edge of the stator. At the maximum design inlet temperature of 1400°F, the primary stress margins of safety for cast Udimet-700 are greater than zero while the primary plus secondary stress (thermal stress) margins of safety show local yielding will occur. However, based on the low cycle fatigue properties of the material, the component can withstand approximately 100 restarts before failure and this number greatly exceeds the number of restarts anticipated at the maximum inlet temperatures of 1400°F.

### (4) Performance Tests

#### (a) Introduction

(U) Extensive air tests were performed on two models of the ARES turbine (Figure IV-6) by Dr. M. H. Vavra. Both test turbines (called Mod I and Mod II, respectively) were 1.65 x full size aluminum models.

(U) Scaling was required to fit the test facility. Mod I is a model of the ARES turbine. The turbine was designed with highly twisted rotor blades to obtain high efficiency. In addition, the blades were of tapered thickness from root to tip to reduce centrifugal stresses. The Mod II turbine was designed as a modification of Mod I for constant section blades with no twist. Both models have the same stator and rotor throat areas, but different blade shapes and annulus shapes (Figure IV-7). The purpose of the tests was to:

Establish the efficiency and weight flow at design point.

Generate an off-design performance map.

Determine the effect of tip clearance on efficiency.

Determine the locked-rotor torque as a function of pressure ratio.

**IV, B, T-Design Turbopump (cont.)**

**Formulate design changes to improve performance where necessary.**

**Compare Mod I and Mod II performance.**

### (b) Comparison of Mod I and Mod II Design

(U) Design quantities for both designs are compared below:

| | | Mod I | | Mod II | |
|---|---|---|---|---|---|
| | | Stator | Rotor | Stator | Rotor |
| Throat area, in.$^2$ | | 4.7 | 5.8 | 4.7 | 5.8 |
| Number of blades | | 13 | 22 | 19 | 18 |
| Degree of reaction | Root | | 0.11 | | 0.09 |
| | Tip | | 0.57 | | 0.48 |
| Maximum thickness/chord | Root | 0.226 | 0.310 | 0.284 | 0.367 |
| | Mean | 0.174 | 0.222 | | |
| | Tip | 0.147 | 0.114 | | |
| Chord, in. | | 1.72 | 1.026 | 1.30 | 1.19 |
| Pitch/chord at mean blade height leading edge radius, in. | Root | 0.060 | 0.030 | 0.140 | 0.178 |
| | Mean | | 0.025 | | |
| | Tip | | 0.020 | | |
| Trailing edge radius, in. | | 0.013 | 0.010 | 0.0145 | 0.0145 |
| Average blade height, in. | | 0.95 | 1.12 | 0.88 | 0.99 |
| Aspect ratio (h/c) | | 0.552 | 1.09 | 0.677 | 0.83 |
| Twist, root to tip, degree | | 0 | 44 | 0 | 0 |
| Stator-rotor overlap, in. | | 0.016 | | 0.059 | |
| Step at rotor outlet, in. | | 0 | | 0.400 | |

### (c) Description of Test Facility and Instrumentation

(U) Figure IV-8 is a sketch of the test facility. Air from a compressor enters at A, flows through B, C and D, through the test turbine to atmosphere.

(U) The weight flow, $\dot{w}$, is measured with a flow nozzle. The turbine power is absorbed by a "Vortex" air dynamometer (E). The torque, M, is measured with strain gages. The exit static pressure is ambient, $P_a$. Six Kiel probes and two thermocouples measure the inlet total pressure, $P_{T1}$, and inlet total temperature, $T_{T1}$, respectively. The rotational speed, N, is measured with an electronic counter. This instrumentation constitutes the minimum necessary to measure the overall turbine efficiency, $\eta$.

$$\eta = \frac{\frac{MN}{5252}}{1.415\,\dot{w}\,c_p T_{T1}\left[1 - \left(\frac{P_a}{P_{T1}}\right)^{\frac{\gamma-1}{\gamma}}\right]}$$

For one test point, traversing probes were used to measure the temperature, swirl angle, and total pressure profiles at turbine outlet. The bearing losses were considered small enough to be ignored. In general, the turbine efficiency is estimated to be accurate to within ±0.005, i.e., 0.800 to 0.810.

### (d) Tests Performed

#### 1 Mod I

(U) The Mod I design was tested with radial tip clearance of 0.020 and 0.033 in. (The larger clearance was obtained by increasing the inner diameter of the rotor shroud.) For each of these radial tip clearances, the axial clearance was varied from 0.090 to 0.410 in. The pressure ratio was varied from 1.2 to 1.55, and the speed was varied from approximately 14,000 to 16,000 rpm. The locked rotor torque was measured for pressure ratios varying from 1.2 to 1.55.

#### 2 Mod II

(U) The Mod II radial tip clearances tested were 0.033, 0.024, and 0.015 in. The axial clearance was not changed but kept at 0.410 in. The speed was varied from approximately 14,000 to 16,000 rpm, and the pressure ratio was varied from 1.3 to 1.55.

### (e) Overall Test Results

#### 1 Mod I

(U) The variation of axial clearance had no effect on turbine efficiency. The radial tip clearance had a pronounced effect on efficiency. Increasing the tip clearance from 0.020 to 0.033 in. decreased the efficiency by 0.005 to 0.020 for pressure ratios between 1.4 and 1.5, respectively, and the average decrement was 0.0135%. Figure IV-9 shows the variation of weight flow with pressure ratio and speed for a tip clearance of 0.033 in. At the equivalent design point, the measured weight flow is 1.2% higher than the design value. Figure IV-10 presents the turbine efficiency as a function of pressure ratio and speed for 0.033-in. tip clearance. The aerodynamic efficiency at the equivalent design point is $\eta = 0.865$. This is over three points higher than predicted.

IV, B, T-Design Turbopump (cont.)

### 2 Mod II

(U) The variation of efficiency with tip clearance was more erratic than for the Mod I model. Increasing the tip clearance from 0.014 in. to 0.024 and 0.033 in. decreased the design point efficiency from 0.850 to 0.836 and 0.803, respectively. The efficiency at the equivalent design point is 0.803. Figure IV-9 shows the variation of weight flow with pressure ratio for 0.033-in. tip clearance and equivalent design speed. Figure IV-10 presents the turbine efficiency as a function of pressure ratio and speed for 0.033-in. tip clearance. The efficiencies of the models are compared in Figure IV-9.

### (f) Turbine Exit Traverses for Mod I

(U) The results of a radial traverse at turbine outlet measuring total pressure, temperature, and swirl angle at approximate design point conditions are presented in Figure IV-11.

(U) The total pressure profile has the usual dip near the tip showing again that the efficiency is lowest in the tip region due to clearance effects. The temperature profile indicates that a three-element thermocouple rake would measure an efficiency of 0.863, whereas the dynamometer efficiency for this point is 0.858. The difference of 0.005 indicates an excellent agreement between the two methods of efficiency measurements, and justifies a high level of confidence in the overall test results.

### (g) Discussion of Test Results

(U) The variation of axial clearance within practical limits has very little, if any, effect on turbine performance.

IV, B, T-Design Turbopump (cont.)

The measured variation of efficiency with tip clearance is very pronounced, especially for the Mod II. No explanation is available yet for the unexpected large effect of pressure ratio on tip clearance losses and for the larger degradation of efficiency versus increased tip clearance of the Mod II model.

(U) For the Mod I, the favorable difference between measured and design efficiency indicates that the blade loss assumptions used for the efficiency estimation are conservative.

(U) The difference in design point efficiency of the two models is 6.3 points. This difference has a significant effect on the turbine inlet temperature required for an engine power balance.

(U) The small difference (1.2%) between the design weight flow and its measurement indicates satisfactory design procedures for throat sizing.

(U) The differences between Mod I and Mod II design and their estimated effect on efficiency are shown in the following table.

| | | Mod I | Mod II |
|---|---|---|---|
| 1. | Rotor and stator throat areas are identical | 0 | 0 |
| 2. | Degree of reaction at root is substantially the same | 0 | 0 |
| 3. | Maximum thickness/chord ratio is higher for Design II | 0 | -0.2 |
| 4. | Stator leading edge radius is larger for Mod II | 0 | 0 |
| 5. | Rotor leading edge radius is larger for Mod II | 0 | -0.2 |
| 6. | Pitch/chord ratio of stator II is less than optimum | 0 | -0.1 |
| 7. | Rotor trailing edge radius is larger for Mod II | 0 | 0 |

IV, B, T-Design Turbopump (cont.)

| | | Mod I | Mod II |
|---|---|---|---|
| 8. | Stator aspect ratio is larger for Mod II | 0 | 0 |
| 9. | Rotor aspect ratio is larger for Mod I | 0 | -0.2 |
| 10. | Rotor twist is 44 degrees for Mod I and 0 degree for Mod II | 0 | -5.0 |
| 11. | Stator-rotor overlap is larger for Mod II | 0 | -0.2 |
| 12. | Mod II has step behind rotor | 0 | -0.4 |
| | | 0.0 | -6.3 |

(U) The discrepancy between the measured Mod I and Mod II efficiencies can be attributed mainly to the fact that the Mod II rotor blade is designed with zero twist; a contributing factor is the blunt profile.

### (h) Significance of Test Results for Engine Performance

(U) The aerodynamic design of the ARES turbine assumed a 0.020-in. hot running tip clearance; however, the housing increases 0.018 in. more than the rotor tip between start and design point operation. If the cold clearance is maintained at 0.020 in., the clearance at design point conditions is 0.038 in. On the basis of the component test data, this would incur an extra tip clearance penalty of 0.031 for the Mod I and 0.097 for the Mod II turbine. The latter figure seems unbelievably high based on standard design practice for predicting tip clearance losses.

(U) An additional loss is due to coolant injection in front of the rotor, not accounted for in the air test data, and the amount of this loss is not well known. Therefore, a loss of 0.034 was assumed for both turbines. The estimated engine turbine efficiencies with these added losses are listed below.

IV, B, T-Design Turbopump (cont.)

| | Mod I | Mod II |
|---|---|---|
| Model test | 0.865 | 0.802 |
| Tip clearance correction to 0.038 in. | -0.031 | -0.031 |
| Coolant entrance correction | -0.034 | -0.034 |
| | 0.800 | 0.737 |

(U) If the Mod II turbine efficiency of 0.737% is used for the engine power balance, the inlet temperature is 70 degrees higher than that for the Mod I based on the engine power balance study. Therefore, the Mod I turbine was selected in order to maintain lower gas temperature requirements for the present design and to provide greater growth potential in future applications.

### e. Housing Requirements and Design Considerations

(U) The T-housing concept is unique in the liquid rocket engine industry because this concept of performing many functions with a single housing was never attempted. The advantage of using this concept is that it reduces the engine into a single, lightweight, compact package. The oxidizer housing performs the following: (1) collects and diffuses oxidizer pump flow, (2) delivers and distributes the flow to the thrust-chamber coolant tube flange, (3) collects and distributes the flow to the primary combustor and acts as a cooled primary combustor housing, (4) directs and distributes the turbine hot-gas flow, (5) transmits the engine thrust to the gimbal, and (6) supports, along with the fuel housing, the turbopump rotating shaft assembly.

(U) To perform these many tasks, several housing designs were considered. These included two- and three-walled designs with welded and unwelded flow passage ribs. After an extensive investigation, the decision was reached that the three-walled housing with welded ribs would be the most reliable and least costly to the program for a 100% regeneratively cooled thrust chamber. However, for 100% transpiration-cooled or 20% regeneratively cooled thrust chamber designs, the two-walled welded rib housing appears less costly while maintaining the same reliability. The latter condition results when the housing does not deliver a major portion of the oxidizer flow to the thrust chamber for cooling. Hence, the latter two thrust-chamber cooling concepts reduce the number of tasks the oxidizer housing must perform and, therefore, simplify the design. A detailed discussion of the housing design, fabrication, and testing is given in Section IV,C.

### f. Power Transmission

#### (1) Requirements and Design Considerations

(U) The ARES power transmission requirements are: (1) the first lateral resonant frequency of the shaft must be 20% above the design speed of 40,000 rpm, (2) the AeroZINE 50 lubricated ball bearing and thrust balancer combination must have the capability to support the transient and steady-state axial loads, (3) the AeroZINE 50 and $N_2O_4$ lubricated roller bearings must have the capacity to support the transient and steady-state radial load, (4) the oxidizer pump wear rings must limit the internal leakage consistent to engine cycle efficiency requirements as well as minimize transient and steady-state potential rubbing conditions without impeller damage or catastrophic failure (explosion), (5) the fuel pump labyrinths must reliably control the flow to the thrust balance piston (integral with the first-stage fuel pump), and (6) effective sealing must be accomplished between the turbine oxidizer-rich hot gas and the fuel pump either by controlled fuel leakage and controlled local combustion or by complete separation (utilizing a high pressure inert buffer fluid).

(U) To ensure that these requirements were met, extensive analyses were performed and test evaluation programs were conducted as discussed in the following paragraphs.

### (2) Critical Speed

(U) An extensive critical speed analysis was performed; the results are referenced in Appendix I, Section 3. This analysis included a parametric study of design variables such as rotating component weights, impeller overhang, roller bearing span, and bearing sizes (shaft size). These cases, summarized in the engine handbook, illustrate that changes in the oxidizer pump side greatly influence the critical speed, whereas changes on the fuel side have a much smaller effect. The final design critical speed, including the combined influence of housing and thrust-chamber weights, was above the requirement of 48,000 rpm.

### (3) Axial Thrust Balancer

(U) The axial forces acting on the turbopump rotating assembly are very large (approximately 200,000 lb in each direction), and each 1% error in predicting axial thrust results in a 2000-lb axial force. A steady-state operating thrust balance can theoretically be obtained by the proper location of impeller wear rings and the proper sizing of flow restrictors. A mathematical model of the rotating system pressure areas and pertinent flow networks was constructed and programed for computer analysis. From this analysis, the design for steady-state thrust balance was determined as well as the effects of varying significant parameters. It was concluded that, with load summations of such large magnitudes, normal manufacturing tolerances and pressure-caused deflections could result in unbalance loads higher than desirable for ball bearing life requirements. Considering these possible high loads as well as the loads from normal off-design transient operation, it was concluded that a thrust balance device should be included in the design.

(U) To compensate for variable axial loads, it is necessary to have a thrust balancing system that is sensitive to axial motion.

The balancing system designed for the ARES turbopump consists of a double-acting balance piston integral with the first-stage fuel impeller as shown in the turbopump layout (Figure IV-1) and in greater detail in Appendix I, Section 3. Pressure cavities (areas) on both sides of the piston provide the forces for thrust compensation. These cavities are supplied from the impeller discharge through labyrinth wear rings of a fixed radial clearance (0.007 in.) and vented by variable radial slots located at the impeller inlet eye outer diameter. Axial clearance of these slots (lands) at the null or zero load position is 0.010 in. Figure 3.1.2-2 of Appendix I, Section 3, shows the load capacity (±15,000 lb) and the flow requirements (140 gal/min at null) of the balance piston as a function of axial travel.

(U) A thrust ball bearing package consisting of a duplex "DB" pair mounted in a radial and axial flexible housing is used to support the axial loads during start and stop transients and as an axial stop in extreme rotating assembly axial movements. The principle used here is two ball bearings lightly preloaded back-to-back in a retainer that is supported in the axial direction by a relatively stiff diaphragm (spring rate = 57,000 lb/in.), which is controlled by axial stops in the turbopump housing, and is very flexible in the radial direction (Figure IV-12). Axial movements of the rotating assembly are thus controlled by the stops which are set at ±0.007 in. and prevent axial contact of the thrust piston which has ±0.010-in. clearance. The stiff axial diaphragm also centers the rotating assembly in the static or nonrotating, nonpressurized position.

(U) Figure IV-13 is a plot of a typical start-transient unbalance force and rotating assembly axial displacement from the computer mathematical model. The maximum deflection occurs toward the oxidizer pump at approximately 1.7 sec when the pressure levels are relatively low. The maximum ball bearing load is 370 lb, and the thrust balancer load is 645 lb toward the oxidizer pump. As the pressure levels throughout the turbopump rise, the thrust reverses, as do the deflections. The ball bearing load and thrust balancer load (which has achieved a larger capacity at this time and rpm) are 370 and 3000 lb, respectively, in the direction of the fuel pump. Note that for this case as steady-state conditions are reached, the axial deflection does not return to zero. A return to zero could be accomplished by slight changes in wear ring or shaft labyrinth geometry. However, this steady-state condition of 0.0038-in. axial displacement and 2100-lb unbalance would be acceptable and would be within the expected allowable variation resulting from production tolerances.

### (4) Bearings

(U) The ARES turbopump shaft is radially supported by two 108-size antifriction roller bearings and axially supported by a combined system of a hydrostatic thrust balancer and an antifriction 108-size ball bearing duplex "DB" set. As discussed in the thrust balance section above, the main purpose of the ball bearings is to support the axial loads during start and stop transients. One roller bearing is lubricated by $N_2O_4$ and the other by AeroZINE 50. The ball bearing "DB" set is lubricated with AeroZINE 50. Design speed is 40,000 rpm or $1.6 \times 10^6$ DN for 108, 40-mm bore, size bearings. Roller bearing steady-state and transient load design requirements were 500 and 1000 lb, respectively. The ball bearing duplex "DB" set has a design axial preload of 50 lb and, in turn, is not expected to support transient axial loads larger than ±1000 lb. The thrust balancer will support steady-state and high transient axial loads. Figure IV-12 illustrates the load versus life relationship of the ARES design ball bearing for both high and low loads. The original turbopump design (without thrust balancer) and consequently the work statement requirement for the ball bearing steady-state and transient loads were 1000 and 2500 lb, respectively. As can be seen from these life versus load curves, the use of the thrust balancer to support the high loads and thereby maintaining low ball bearing loads increases the ball bearing probable life approximately 100 to 1.

IV, B, T-Design Turbopump (cont.)

(U) The maximum turbopump housing deflections from combined pressure and temperature changes were estimated to be 0.030 in. axial and 0.012 in. radial. Axial movements of this magnitude are no problem to the roller bearings. However, as shown in Figure IV-14, bearing life decreases rapidly with radial misalignment. For the expected steady-state load of 500 lb, life of the 108-size roller bearing, as designed, decreases from 1550 hr (aligned) to 35 hr at 0.012-in. misalignment. To maintain bearing alignment and thus a higher life, the roller bearings were designed with spherical mounting seats on the outer race outer diameter as shown in Figure IV-14. If the housing distortion proves to be as low as now anticipated, the spherical seats could be eliminated.

(U) A test program was conducted to evaluate the ball and roller bearing designs in simulated turbopump operating conditions. All work statement requirements were met. Detail bearing designs and test results are discussed in Section IV,G.

### (5) Wear Rings and Shaft Labyrinth

(U) Designs of the wear rings and shaft labyrinths for the turbopump were based upon three basic requirements: (1) to limit internal leakages consistent with efficiency requirements and, as in the case of shaft labyrinths, consistent with bearing cooling requirements, (2) to operate safely and reliably at close clearances without hardware damage or catastrophic failure (explosion), and (3) to provide a repeatable axial thrust balance by proper radial location and the maintaining of constant running clearances.

(U) A test program was conducted to evaluate four basic wear-ring designs: (1) straight labyrinth, (2) stepped labyrinth, (3) hydrostatic face seal, and (4) hydrostatic journal seal. All work statement requirements were met. Detail designs and test results are discussed in Section IV,H.

Designs selected for the turbopump were based upon the results of this test program. These designs are incorporated in the turbopump layout (Figure IV-1) and are shown in greater detail in Appendix I, Section 3. Figure 3.3.1-1 of Appendix I shows the oxidizer impeller and the hydrostatic face wear-ring seals selected for that location. Figure 3.4.1-1 of Appendix I shows the fuel impeller and the pressure-relieved (balanced) Kynar* labyrinth wear-ring inserts selected for that location. The three shaft labyrinths on the oxidizer pump side (see the turbopump layout in Figure IV-1) incorporate Vespel SP-21** rubbing inserts and the two shaft labyrinths on the fuel pump side incorporate Kynar* rubbing inserts.

### (6) Oxidizer-Rich Gas-Fuel Shaft Seal

(C) The turbopump design requires sealing AeroZINE 50 in the fuel pump bearing cavity from turbine exhaust oxidizer-rich gases at 3000 psig and 1100°F. This requirement with the 40,000-rpm rotational speed is beyond conventional sealing technology. The AeroZINE 50 pressure at the inside diameter of the seal was a design variable set at 3000 psig to minimize the pressure differential to be sealed. Since any uncontrolled leakage of either fluid into the other could result in a catastrophic failure, only two approaches were considered as feasible. These were a controlled combustion seal and a seal incorporating a higher pressure inert buffer fluid. Obviously, the complication and weight of a third fluid system is undesirable. Consequently, the primary approach was the controlled combustion seal and the secondary approach was the buffer fluid or purge seal. Hydrostatic sealing principles were selected for both seal concepts to prevent surface contact at the high rotational speed.

---

*Kynar is a polymer of vinylidene fluoride manufactured by the Pennsalt Chemicals Corp. of Philadelphia, Pa.

**Vespel SP-21 is a graphite-filled aromatic polyimide resin manufactured by E. I. duPont De Nemours & Co. of Wilmington, Delaware.

IV, B, T-Design Turbopump (cont.)

(C) Detail designs were made, hardware was fabricated for both concepts, and test evaluation programs were conducted.

(a) Combustion Seal

(U) The combustion seal design is an orifice-compensated hydrostatic seal operating on a fluid film of AeroZINE 50. Leakage of AeroZINE 50 to the oxidizer-rich hot gas is constant and repeatable. Mixture ratio, and thus local temperature, is controlled by the addition of oxidizer coolant flows upstream and downstream of the fuel injection. Feasibility of this seal, including restart, has been demonstrated in short-duration tests; however, the program duration of 60 seconds operation has not been achieved. Detail design and test results are discussed in Section IV,I.

(b) Purge Seal

(U) The purge seal design is an orifice-compensated hydrostatic seal operating on a fluid film of inert liquid. This inert liquid provides a higher pressure barrier between the AeroZINE 50 and oxidizer-rich gas. Detail design and test results are discussed in Section IV,J.

g. Turbopump Integration

(1) Interfaces

(U) The high degree of integration in the T-turbopump design introduces interface requirements that can significantly affect the design or performance of each component. Consequently, critical turbopump interface dimensions were established early in Phase I and are included in the TPA layouts, Appendix I, Section 3. Thrust-chamber, primary combustor, and valve interface dimensions were made on released drawings and this effort was coordinated by the Engine Department.

(U) The high degree of component integration also introduces many interactions between the various major components and these include load sharing, cold and hot running operating clearances, heat generation, and flow distribution. The effect of these interactions was considered in the design of each component.

### (2) Clearances

(U) The turbopump stackup and shimming requirements are given in Appendix I, Section 3, TPA Layout Drawings. In addition, a summary of critical pump buildup and operating clearances that result from housing growth and distortions caused by operating temperatures and pressures is presented in the following table:

| | Critical Clearances, in. | | | |
|---|---|---|---|---|
| | Axial | | Radial | |
| | Build-Up | Hot Running | Build-Up | Hot Running |
| Oxidizer housing-bearing fit | | | 0.0001 | 0.00018*<br>0.0007** |
| Fuel housing-bearing fit | | | 0.0001 | 0.00049*<br>0.00030** |
| Fuel impeller wear ring-housing | | | 0.009 | 0.007 (nom)<br>0.004 (min) |
| Oxidizer impeller | 0.050 | 0.028*<br>0.040** | | |
| Fuel impeller balance piston land | 0.010 | 0.003-0.017 | | |
| Primary combustor-oxidizer housing | | | 0.0055 | 0.0016 (nom) |
| Turbine rotor tip-shroud | | | 0.020 | 0.038 (nom) |
| Turbine stator shroud-primary combustor | | | 0.040 | 0.010 (nom) |
| Turbine stator-rotor | 0.090 | 0.085 | | |

---

*Start transient condition
**Steady-state condition
NOTE: Conditions considered include housing temperature (400°F maximum on inner surface on oxidizer side and 250°F on fuel side), housing growth and misalignment, shaft deflections (critical speed and unbalanced loads), 0.0015 radial runout, and impeller growth.

### (3) Filters

(U) Because of the small internal clearance of the shaft bearings (0.001 in.), and the small operating clearance of the combustion seal (0.001 in. or less), filters are incorporated in the turbopump design at three locations (Figure IV-1) to filter the propellants flows to these components. A 2-micron filter is located at the second-stage fuel pump discharge upstream of the combustion seal where approximately 8 gal/min is filtered. Filters of 10 microns are located at the second-stage fuel pump inlet and at the oxidizer back wear-ring location. All bearing and shaft labyrinth flows are supplied from these two sources. To verify calculated pressure drops in the design, sample filters were tested in water and the results are shown in Figure IV-15. The most critical filter, regarding pressure drop and plugging, is the second-stage fuel inlet design because of the high flow rate (180 gal/min). The design pressure drop for this filter was 100 psi and the actual value is 25 psi. This margin is adequate to allow for plugging.

### (4) Instrumentation

(U) Because of the high degree of component integration, provisions for a major portion of the engine instrumentation must be included in the oxidizer and fuel pump housings. The inaccessibility in some areas limited the number of instrumentation probes; however, sufficient instrumentation is included to measure the performance or operating behavior of each component.

(U) A layout of the instrumentation type and location is shown in Appendix I, Section 3. The instrumentation measurements include: (1) TPA speed pickup on fuel impeller shroud; (2) pump suction and discharge pressure; (3) primary combustor fuel valve inlet and exit pressures; (4) primary combustor propellant inlet pressures and hot-gas exit pressure and temperature; (5) turbine inlet and exit temperatures and pressures; (6) inducer and impeller discharge static pressures; (7) bearing outer race temperature and bearing cavity pressure; (8) fuel impeller (balance piston) axial position; (9) thrust bearing axial load, and (10) boost pump hydraulic turbine feed pressure. In some cases, where accessibility permits and the measurement is considered critical to the component performance analysis, the instrumentation is redundant.

### 3. Conclusions and Recommendations

(U) a. The ARES high-pressure T-engine turbopump design has been completed. This design includes modifications to incorporate information learned from the Phase I turbopump test programs. This turbopump will provide simplified concepts with high-efficiency components at a weight of 347 lb for the turbopump and primary combustor. Boost pumps, which weigh 35 lb, have been designed for low NPSH applications. Higher NPSH requirements would allow lighter-weight boost pumps.

(U) b. The critical features of the T-engine turbopump have been demonstrated except the hydrostatic combustion seal which requires tests of longer duration. The demonstrations have shown:

(1) The T-engine housing has been demonstrated to be structurally sound. A high degree of confidence has been developed in the analysis of the T-housing. An improved housing has been designed which will further minimize deflections and is estimated to reduce the weight to 254 lb. If a transpiration-cooled thrust chamber is selected for Phase II, further design simplification, weight reduction, and cost reductions could be achieved.

IV, B, T-Design Turbopump (cont.)

(2) Ball and roller bearing operation in both propellants has been demonstrated at DN values of $1.6 \times 10^6$. Additional bearing testing is recommended to establish bearing storage life capability in AeroZINE 50 and $N_2O_4$ propellants.

(3) Single-stage turbine efficiencies of 80+%, including parasitic flow losses, have been demonstrated in cold flow testing at the 1.5 pressure ratio of the staged combustion cycle.

(4) Hydrostatic seal pump wear rings have been demonstrated in $N_2O_4$ with pressure drops in excess of 4000 psi. Inert plastic wear rings have been demonstrated in AeroZINE 50 with pressure drops in excess of 2500 psi.

## C. ENGINE HOUSING, T-CONFIGURATION

### 1. Objectives and Approach

(C) The primary objectives of Phase I of the advanced turbopump-housing program were to design and demonstrate a housing that would contain the required fluid and gas pressures, transmit the fluids from station to station with minimum pressure drops, provide a stable base for the rotating components, and transmit the thrust load developed by the thrust chamber to the missile frame. The housing had to be suitable for either the regeneratively cooled or the transpiration-cooled thrust chamber.

(C) The criteria for success were defined as follows: a housing weighing not more than 350 lb and having a permanent axial deflection of less than 0.020 in. and a radial misalignment of less than 0.008 in. between roller-bearing locations when loads of 1.4 times nominal design pressures and 1.4 times nominal design thrust were applied simultaneously. In addition, the housing could not have a critical mode of vibration in the X, Y or Z axis in the range of 667 ± 10% cps without pressure or with the cavities pressurized to 1.2 times nominal design pressure when an exciting force of 1g input acceleration amplitude was applied.

(C) The secondary objectives of the program were to design a final housing which would have a nominal oxidizer-fluid pressure drop from the oxidizer-pump discharge to the thrust-chamber flange and from the thrust-chamber flange to the primary injector of 250 psi or less. The housing walls had to be kept cool to minimize thermal stresses and deflections. The cost of the housing was to be minimized while maintaining high reliability. The internal rotating parts and the primary injector were to be removable during development testing in Phase II.

(U) The T-configuration was selected for its minimum package size and adaptability to removal of internal parts. To minimize external piping and manifolding and provide maximum resistance to the thrust loads imposed with minimum housing weight, the T-turbopump oxidizer housing was designed as a three-walled unit. The three walls were structurally fastened together by flow-guidance ribs which also formed two discrete passages for oxidizer-discharge flow to the thrust-chamber cooling tubes and the oxidizer-return flow from the cooling tubes to the primary injector. In addition, the oxidizer flow cooled the inner wall, which was exposed to the hot gases from the primary combustor and turbine.

(U) The fuel housing was made as a separate unit which was pressed into the oxidizer housing and bolted in place. This configuration allowed sufficient access to remove the primary injector and hot-gas shields for examination and replacement during Phase II testing. The fuel housing contained the two fuel-pump volutes, and the primary fuel-control valve, and transmitted fuel between pumps, to the secondary injector, to the primary injector, and to the combustion seal.

(U) The integrated, three-walled T-configuration presented a difficult fabrication and analytical problem for stresses and deflections. The literature studies revealed that limited information was available on intersecting cylinders (References 1 through 6). This information was restricted to single-walled units and was either highly empirical or applicable only to special cases. To augment this information, five tasks were performed to obtain the required structural design criteria.

IV, C, Engine Housing, T-Configuration (cont.)

(U) The first task was to build and test a full-scale, single-walled housing of similar T-configuration to determine the stress-concentration factors at the intersection of the T-section with the main cylinder and preliminary deflection characteristics of the basic shape under pressure.

(U) The second task was to build and test a full-scale, two-walled housing of the T-configuration to determine the effect of internal ribs on stress concentrations at the T-intersection and deflection characteristics with and without external ribs under pressure and thrust loads.

(U) The third task was to build two half-scale photoelastic models with wall thicknesses simulating the tensile rigidity of the three-walled housing. One model was pressurized and stress-frozen. The second model was pressurized with thrust load applied and stress-frozen. The photoelastic slices cut from the model provided stress patterns as well as additional information on the stress-concentration areas.

(U) The fourth task was to revise and check the present finite-element-analysis computer program (Reference 7) to make it applicable to the intersection of two cylinders.

(U) The fifth task was to build two full-scale, three-walled housings to determine the fabrication techniques and quality control required for manufacturing. One of these structural prototypes was used to determine the deflections and stresses during pressure and thrust loading and the vibration characteristics of the housing in order to meet the work statement requirements. The full-scale prototype contained all critical structural features of the final housing design.

(U) In addition, heat-transfer and flow data were obtained to evaluate the housing design. Air-test models were constructed to determine the passage pressure drops and mass-flow distributions with various internal rib patterns and passage heights as described in Section VIII A.

(U) These activities culminated in the design of a housing for Phase II turbopump and engine tests.

## 2. Model Testing

### a. Metal Model I

#### (1) Objectives and Description

(U) The stress-concentration factors and deflections of the T-housing are influenced by the pressure loading and the thrust loading. The objectives of Metal Model I were to determine stress concentration factors and deflections under pressure loading only. The full-scale housing was a single-walled unit without reinforcing ribs at the T-intersection. This minimized interpretation complexity when the test data were used to confirm stress and deflection hypotheses. The housing was designed on the basis of structural shape and wall stiffness similarities to the three-walled prototype.

#### (2) Fabrication

(U) Metal Model I was fabricated from normalized SAE 4130 steel rather than Inconel 718 material used for the three-walled prototype to speed fabrication and reduce costs. The fuel housing was held in position by a bolted flange. The main cylinder and T-section of the oxidizer housing were fabricated from 0.5-in. wall thickness pipe. The oxidizer dome and fuel housing were machined from forgings. The oxidizer dome was welded to one end of the main cylinder and an internal ring was welded on the inside of the T-section cylinder to form the thrust chamber flange and provide a closure attachment surface.

### (3) Test

(U) Two tests were conducted on metal Model I (Figure IV-16-a). The pressure used was based on the ratio of yield strengths between Inconel 718 and SAE 4130 materials times the highest internal gas proof pressure of the three-walled structural prototype. The SAE 4130 material had a yield strength of 50% of the yield strength of the Inconel 718.

### (a) Test 1

(U) Test I was the internal pressurization of the model in 50-psi increments to 1200 psig with a brittle lacquer coating applied to the outer surface. This test was used to determine from cracks in the brittle coating the approximate magnitude, location and direction of the principal stresses and the stress gradients on the external surface. This information was used to locate strain gages for the next test phase and to obtain a preliminary evaluation of structural response.

### (b) Test 2

(U) Test 2 was the internal pressurization of the model in 250-psig increments to 2500 psig with internal and external strain gages, and axial and radial deflection transducers to determine the magnitude and direction of the internal and external surface stresses, the bending stresses, the radial expansions of the main cylinder and the T-section, the relative axial displacement and the relative rotation of the simulated bearing housings at each end of the main cylinder.

### (4) Test Results

(U) The results of Metal Model 1 testing are shown in Figures IV-16 and -17. The comparison of the stress concentrations, deflections and rotations of Metal Model I to the three-walled prototype are given in Figure IV-17. The model test indicated that the bearing angular rotation to be expected in the three-walled prototype would be less than 1 minute. The maximum stress level expected in the three-walled prototype would be 106,000 psi at 1.2 x design operating pressure including a stress concentration factor of 1.7. The deflection characteristics of the basic housing shape are shown in Figures IV-16-c and -d. Figures IV-16-c and -d show the linear deflections of the bearing housings and the sides of the housing with increasing pressure. The deflection of the oxidizer end was 86% of the total deflection at maximum pressure. This indicated that special care must be taken in the design of the oxidizer dome to minimize axial deflection under pressure.

## b. Metal Model II

### (1) Objectives and Description

(U) The objectives of the Metal Model II testing were to determine the effect of the two-walled structure with internal rib construction on the T-shaped turbopump housing stress concentration factors and deflection characteristics under internal pressure and thrust loadings. In addition, the effectivity of external ribs and the efficiency of a single externally threaded ring closure to retain the fuel housing were determined. The housing was designed and tested on the basis of structural shape and wall stiffness similarities to the three-walled prototype.

**IV, C, Engine Housing, T-Configuration (cont.)**

### (2) Fabrication

(U) **Metal Model II (Figure IV-16-b) was fabricated from normalized SAE 4130 steel. The outer and inner walls of the oxidizer housing were 0.30 and 0.25 in. thick, respectively, and the internal passage was 0.575 in. high. The outer wall was plug-welded through 0.375-in.-dia holes, spaced 0.75 in. apart, to the 0.25-in.-wide ribs which had been welded to the outer surface of the inner cylinder. The ribs were spaced 1.5 in. apart circumferentially in the cylindrical portion of the main cylinder and in the T-section. The oxidizer dome end was machined from forgings in two pieces.** The outer portion was welded to the outer cylinder and the inner portion was welded to the inner cylinder and the outer dome. The fuel end of the main cylinder of the oxidizer housing consisted of a large ring machined and welded internally and externally to the inner and outer walls, respectively. The inner cylinder of the T-section was welded in place and the two halves of the outer cylinder of the T-section were plug-welded to the ribs of the inner cylinder, the main cylinder, and the thrust-chamber flange. The thrust pad and the five external 0.25-in.-wide ribs, which tapered from 0.75 in. at the thrust pad to 0.25 in. at the T-section, were welded in place. The fuel housing was machined from a single forging.

### (3) Testing

(U) Three tests were conducted on Metal Model II (Figure IV-16-b). The pressures used were again based on the 50% ratio of yield strengths between SAE 4130 and Inconel 718. The model inner pressure was based on 1.4 x nominal design fluid pressure of the return passage of the three-walled prototype and the pressure between the model walls was based on 1.4 x nominal design oxidizer discharge pressure of the three-walled prototype.

IV, C, Engine Housing, T-Configuration (cont.)

(C) The first test consisted of pressurization to 1520 psig in the internal chamber, 2000 psig in the external chamber, and 30,400 lb thrust load in various load increments with the outside surface coated with a brittle lacquer coating. This test was used to determine from cracks in the coating the approximate magnitude, location, and direction of the principal stresses and stress gradients on the outer surface. This information was used to locate strain gages and extensiometers for the next tests.

(C) The second test consisted of incremental pressurization and thrust loading to 110% of the specified levels. The specified levels were 3300 psig in the internal chamber, 4350 psig in the external chamber, and 70,000 lb thrust. Readings from strain gages applied in critical locations and extensiometers located to measure bearing location axial and radial deflections as well as external deflections at several locations around the outside of the housing were recorded continuously during testing.

(C) The third test consisted of removal of the external ribs to within 0.050 in. from the outside surface above the housing centerline and 0.250 in. below the housing center line and repeating the pressurization, thrust loading, and measurements of Test 2 to 3000 psig in the internal chamber, 4000 psig in the external chamber, and 60,000 lb thrust. Two additional extensiometers were added to determine the relative movements of the large retaining nut with respect to the oxidizer housing.

(4) Test Results

(U) The results of the first test indicated maximum surface stresses of 36,000 psi at the intersection of the T-section and the main cylinder on the fuel side and at the main cylinder center line on the fuel end. The theoretical stresses at these points were 32,000 and 35,000 psi, respectively.

IV, C, Engine Housing, T-Configuration (cont.)

(C) The second test showed a maximum stress of 68,700 psi on the center rib at 110% of specified levels. The maximum hoop stress on the outer surface of the shell next to the center rib was 58,000 psi and the corresponding inside surface hoop stress was 12,650 psi. Therefore, the bending stress in the hoop direction was 22,765 psi and the membrane stress was 35,325 psi. The calculated hoop membrane stress at this point was 78,200 psi under these loading conditions. The meridional outer surface stress at this point was 34,000 psi with a 15,000-psi stress on the inside surface. This equates to a 9450 meridional bending stress and a 24,550-psi meridional membrane stress. The axial deflection of the bearing locations is shown in Figure IV-16-c. The recorded curve indicates a slippage of approximately 0.006 in. between the 50 and 60% load levels. Test 3 indicated that the large retaining nut deflected linearly to a maximum of 0.008 in. at 100% of the specified load levels. Therefore, the actual deflection at 4000-psi external chamber pressure should be 0.038, 0.008, 0.006, or 0.024 in. as shown by the corrected curve. The deflection at the center line of the main cylinder is shown in Figure IV-16-d. Due to the retaining nut movement, the bearing location rotations were invalid.

(C) The third test produced a maximum stress of 59,450 psi on the center rib at the maximum load. The surface hoop stress next to the center rib was 48,000 psi but the inside hoop strain gage was not functioning. The calculated stress for this load point was 78,500 psi, maximum. The meridional outer surface stress at the same point was 42,170 psi and the inner surface stress was 20,400 psi. This equates to a bending stress of 10,885 psi with a meridional membrane stress of 31,285 psi. The recorded curve of axial deflections of the bearing locations is shown in Figure IV-16-c. The fuel housing retaining nut moved linearly under load with respect to the oxidizer housing to 0.008 in. at 100% of the specified load levels. The axial deflection recorded at 4000-psi external chamber pressure was 0.0275 in.

IV, C, Engine Housing, T-Configuration (cont.)

However, by correcting for retaining nut slippage, the deflection at 4000 psi would be 0.0195 in. The corrected curve is shown in Figure IV-16-c. The deflection at the center line of the main cylinder is shown in Figure IV-16-d. The bearing location rotations were invalid due to the large amount of retaining nut movement.

(U) The results of Metal Model testing show (Figures IV-16-c and -d) that the multi-wall construction reduces bearing location axial deflection and main cylinder center line deflections. The height of the reinforcing ribs is critical and ribs above the main cylinder center line are not needed. The calculated stress levels were 60% higher than the minimum rib design measured stress levels and 35% higher than the full rib design measured stress levels. The retaining ring closure design is not adequate for this application.

### c. Photoelastic Model

#### (1) Objectives and Description

(U) The photoelastic model test program had four functions:

(a) Establish an upper limit on stress experienced by the prototype.

(b) Delineate highly stressed locations in the prototype.

(c) Permit estimates of the actual prototype stress by correcting for differences in bending rigidity.

IV, C, Engine Housing, T-Configuration (cont.)

(d) Provide accurate data for evaluating new computation method.

(U) Due to the complexity of the prototype structure, an exact duplication in a photoelastic model could not be attempted at reasonable cost. It was considered necessary to simplify the model structure. The major simplification consisted of eliminating the three-wall construction and replacing it by a single wall of equivalent thickness. The half-scale model wall thickness was calculated on the basis that its circumferential tension rigidity must be equal to that in the three combined walls of the prototype, taking into consideration the scale factor. This equal rigidity criterion served to ensure that the model would closely approximate the resistance to membrane loading of the three-walled prototype.

(2) Fabrication

(U) The casting method was selected for preparation of the model housing since the machining of casting molds and cores did not pose the serious problems that would have been encountered in machining the model. The casting mold was machined from solid cylinders of cast acrylic resin. The cores were turned from similar acrylic stock. The molds and cores were given a light coating of silicone mold release and assembled for casting. The casting was poured, cured, and cooled.

(U) The model was removed by first withdrawing the cylindrical cores, then splitting the molds along the bonded vertical plane. After removal of the model, excess stock was machined from the aft closure end and the exit cylinder flange.

(U) A second model was prepared by the same process, rebonding the mold and repeating the casting procedure.

IV, C, Engine Housing, T-Configuration (cont.)

(3) Testing

(U) Prior to the photoelastic tests, measurements of model dimensions were taken to be compared later with the corresponding dimensions in the "frozen-stressed" elastically deformed model. Measurements included lateral diameter of the chamber along the length of its cylindrical portion, the exit flange diameter, the flange surface slope, and the inclination of the bearing housing axes with the axis of symmetry of the chamber. The models were then assembled for testing by the stress-freezing process.

(U) The stress-freezing process in photoelastic models is based on the dual-phase nature of the molecular structure. At room temperature, the material is given its rigid, glassy character by numerous molecular bonds which, however, do not exist at an elevated temperature. At the higher temperature, only a smaller number of molecular bonds of a different type exist. These give the material the relatively flexible characteristic of firm elastic rubber. When the model is strained under load at the elevated temperature, a photoelastic response (birefringence) is induced. If these forces are maintained while the model is cooled to room temperature, the other set of molecular bonds reform and the material returns again to the hard, glassy state. Furthermore, these rigid bonds form a network around the stretched rubbery bonds in the material, holding the latter in the strained configuration. When load is removed at room temperature, the internal forces are easily carried by the glassy bond structure, and there is only a barely perceptible relief of strain and birefringence. Thus, the stress pattern imposed at the higher temperature is "frozen" on a molecular scale, and sawcuts completely severing the model will not alter this frozen stress and strain distribution.

(C) Two model tests were performed. Model Test 1 was performed with the internal pressure p = 2.92 psig and the thrust pad load F = 0. Model Test 2 was performed with p = 2.50 psig and F = 13.85 lb, corresponding to the prototype with internal pressure of 4500 psi and thrust pad forces of 100,000 lb. A simple tension calibration specimen accompanied the model throughout the stress-freezing cycle to establish the stress-fringe value, f, the constant of proportionality between stress and photoelastic fringe order. After cooling to room temperature, the loads on the model were removed and the dimensional measurements were repeated. The models were then sliced and examined under polarized light.

### (4) Test Results

(U) The test results are summarized in Figure IV-18. Figures IV-18-a and -b show the longitudinal section stresses. The maximum stress occurs at the intersection of the main cylinder with the T-section. This can be reduced by a larger fillet radius. The thrust load produces a local bending condition at the thrust pad which is compensated for by the section modulus of the three-walled prototype. The lateral section stresses are shown in Figures IV-18-c and d and indicate the need for a large section modulus at the main cylinder center line. The bending stresses near the thrust pad can be reduced by local fairing to reduce the abrupt change of section. The thrust load tends to decrease the stress levels. A local increase in wall cross section in this area would be sufficient to reduce stresses. The maximum stress concentration factor determined for the T-intersection was 1.85. The actual prototype stress levels can be determined by multiplying the stress factors given in Figures IV-18-a, b, and c by the internal pressure differential of the three-walled prototype. The maximum membrane stress was determined as 75,000 psi at the T-section to main cylinder intersection. An examination of the longitudinal section with the fuel housing in place showed a gap between the oxidizer housing and the fuel housing. This can be remedied in the final turbopump housing by placing a seal on the outer diameter at the internal end of the fuel housing or by stiffening the cylindrical section between the main body of the fuel housing and the closure flange. Both revisions were made in the final housing design.

### 3. Structural Test Housing

#### a. Design

(U) The structural test turbopump housing (Figure IV-19) was a three-walled prototype. The ribs between the oxidizer housing walls were straight and in either a longitudinal or hoop direction as can be seen in the partially fabricated housing (Figure IV-20). Two fabrication methods were used for attaching the ribs to the intermediate and outer shells of the oxidizer housing. One method used plug-welded slots 1 in. long and 0.25 in. wide on 2-in. centers along each rib. The other method used three 0.080-in.-wide passes of continuous electron-beam welding along each rib.

(U) The fuel housing contained a single torus with simulated diffuser vanes and a simulated fuel valve cavity. The oxidizer bearing housing was made as a separate piece which was bolted to the inside of the oxidizer housing. The primary injector was held in the axial position by two 120-degree curved plates which hooked into slots in the fuel housing and in the primary injector. The fuel tube between the fuel housing and the primary injector was welded in place on assembly.

IV, C, Engine Housing, T-Configuration (cont.)

### (1) Stress Analysis

### (a) Loads

(U) The design yield and ultimate loads were defined as:

Design yield load = 1.44 x nominal design operating load

Design ultimate load = 1.92 x nominal design operating load. Proof test loads were almost equal to design yield values.

(U) Total stresses and deflections in the structural prototype housing design were treated in a linear manner; i.e., as the superimposed effect of the following five loading types; turbine gas pressure, thrust load, propellant pressure, thermal, and mechanical.

(C) The turbine gas pressures were the gas pressures in the primary combustion and turbine exhaust regions. They comprised the major volume of pressure-loading on the housing and thereby governed the gross deflections due to pressure as well as the stresses of major geometric discontinuities. Nominal operating values were 4775 psi in the combustor and 3100 psi in the turbine exhaust region.

(U) An evaluation of the thrust balance on the housing showed that 92% of the altitude thrust must be transmitted through the housing wall from the TCA-TPA interface to the thrust pad. This thrust loading tended to deform the main cylinder out-of-round and produce high local-bending stresses in the region of the T-intersection.

IV, C, Engine Housing, T-Configuration (cont.)

(C) The propellant pressures were the coolant passage pressures (oxidizer and fuel pump pressures). These contributed local discontinuity stresses in the housing walls and fuel tori and were also the main consideration in the design of ribs, local fillets, and weld joints. Nominal design operating pressures in the housing wall were 6200 psi for the oxidizer passage between the oxidizer pump and thrust chamber and 5300 psi for the oxidizer passage between the thrust chamber and the primary combustor.

(U) Steady-state thermal stresses and deflections induced in the basic housing wall as a result of the hot-turbine gases were not severe because of the coolant flow, thinness, and shielding of the walls.

(U) The mechanical loads included actuator forces, line loads, inertia, and vibration loads. The gimbal developed for the 624A second-stage engine was considered for the ARES module. Actuator loads were 15,000-lb maximum attainable force for each actuator. These loads were considered even though no testing would be performed to demonstrate this aspect during Phase I.

(b) Analyses

(U) Preliminary effects of gas and coolant pressure loads were determined in the basic housing walls by computer stress analysis based on the finite element method (Reference 7). In this method, plane or axisymmetric structures are divided into finite triangular or quadrilateral elements and the equilibrium and compatibility equations are solved as a large matrix. Various rib paths existed in the housing wall design; therefore, several axisymmetric and plane cross-sections were analyzed to approximate the critical regions of stress. The resulting stresses were used as a basis for design revisions. Where ribs ran predominantly in the circumferential direction, their true spacings were used and the axisymmetric solution yielded realistic local stresses and deflections. Where ribs were mainly longitudinal, a fictitious spacing was used to approximate the radial connection between walls. The local bending stresses in these regions were not realistic but the gross radial and axial deflection behavior was a good approximation. Plane sections through stations where ribs ran longitudinally were analyzed to determine the critical local hoop-bending stresses.

(U) In the vicinity of the T-intersection discontinuity the above analyses did not apply and experimental data were used. A survey was conducted of existing test results on pressurized cylinder intersections and results of the first Metal Model test of the ARES housing configuration. A concentration factor of 3.17 from Metal Model I at Point A (Figure IV-17) compares well with the 3.36 obtained by Hardenberg (Reference 1).

(U) The finite element approach (Reference 7) is primarily designed for use with axisymmetric structures. The analysis of the T-intersection was an approximate solution based on stress concentration factors from test results of similar configurations. This type of analysis was sufficient for the structural test housing, but the flight-weight version must be analyzed by more exact methods. A new finite element approach for obtaining an exact solution for the T-intersection (Reference 30) was developed and the results were checked against the photoelastic model data with good correlation.

(U) In addition to the main housing body, stress analyses were conducted on the primary injector, fuel torus housing, fuel end closure nut, and the TCA-TPA bolted joint. The finite element approach was used extensively in these analyses.

IV, C, Engine Housing, T-Configuration (cont.)

### (2) Fluid Dynamics

(U) The fluid dynamic analysis for the structural test housing consisted primarily in determining the rib pattern and passage height compatible with the flow required. The air test program described in Section VIII,A, of this report gives the details of later passage configuration and test results.

### (3) Materials

(U) The structural test housing materials were selected on the basis of strength, elongation, corrosion resistance, weldability, and machinability. The primary alloys analyzed were Inconel 718, Titanium, AM350, Haynes Alloy 25, Hastelloy B, Hastelloy C, 17-4PH, 17-7PH and AISI 347. Inconel 718 material was selected for the oxidizer housing because of its excellent properties plus the large amount of experience gained from the AF 04(611)-8548 and M-1 contracts. AISI 347 was selected for the fuel housing because of its high elongation, machinability, and weldability features. Because the calculated stress levels were low in the fuel housing, the low strength level did not appear to be a problem.

### (4) Welding and Brazing Studies

(U) The joining of the ribs to the shells presented a unique processing problem. The joining could be accomplished by diffusion bonding, brazing, electron-beam welding, or by plug welding. The plug welding method was proved by the Metal Model II tests. The diffusion bonding technique was relatively expensive. Several flat weld and brazing samples were made that typified the rib construction joining problems and also formed a container which could be pressurized for testing.

THIS REPORT HAS BEEN DELIMITED
AND CLEARED FOR PUBLIC RELEASE
UNDER DOD DIRECTIVE 5200.20 AND
NO RESTRICTIONS ARE IMPOSED UPON
ITS USE AND DISCLOSURE.

DISTRIBUTION STATEMENT A

APPROVED FOR PUBLIC RELEASE;
DISTRIBUTION UNLIMITED.

IV, C, Engine Housing, T-Configuration (cont.)

(U) The braze sample tested was bonded with 12.5% nickel and 87.5% gold braze. The required joint strength was 30,000 psi and the sample broke at 15,950 psi. A metallurgical examination of the braze material revealed 50% bonding and poor amalgamation of the nickel and gold. This could be improved by increasing the intersurface pressure at the braze joint but appeared to be a marginal joining method.

(U) The electron-beam weld sample was welded with three 0.080-in.-wide passes along the sample rib pattern. The originally flat sample warped approximately 0.050 in. in the center. This caused poor alignment on the two final weld passes. The joint strength from pressure testing was 21,000 psi. The metallurgical examination revealed that the welds on the second and third passes had not penetrated the joint and were ineffective. It was determined that the electron-beam welding method would be adequate on a cylindrical surface where warpage was minimized. It was further determined that the alignment was critical and that weld samples must be made on the same material prior to welding on the work piece to ensure proper penetration and weld width at the joint.

### b. Fabrication

(U) Two three-walled prototype turbopump housings were fabricated. The oxidizer bearing housings and the fuel housings were identical. The fuel housing was a weldment with various parts machined from forgings. The oxidizer bearing housing was a machined forging with a single, formed sheet welded in place. The oxidizer housings were initially of the same configuration but one had the rib-to-shell joints plug-welded and the other had the rib-to-shell joints electron-beam welded.

IV, C, Engine Housing, T-Configuration (cont.)

### (1) Oxidizer Housing A-1

(U) The plug-welded oxidizer housing was fabricated from forgings and plate stock. No serious problems were encountered until after the stress relief and heat treatment prior to final machining. At this point, several hairline cracks in the outer surface of the main cylinders were found by the dye-penetrant inspection. The unit was stress-relieved and heat-treated a second time after the cracks were repaired by welding. This aggravated the surface condition and produced several large cracks. An investigation revealed that the stress-relief and heat-treatment cycles were being performed improperly for the three-walled construction. The heating and cooling rates were reduced and the heat treatment and inspection following repair of the housing were satisfactory.

### (2) Oxidizer Housing A-2

(U) The electron-beam welded oxidizer housing was fabricated from forgings and plate stock. No serious problems were encountered until a routine interpassage leakage test was performed and gross leakage was observed. A detailed X-ray examination with a 2,000,000-volt Betatron machine revealed a wall separation of 0.030 in. between the outer wall and mid wall on the fuel side at the T-intersection at the bottom of the main cylinder. An attempt was made to electron-beam weld through the T-section to close the gap but this was impossible. The T-section was removed and a detailed examination of the welding revealed that the original electron-beam welds had not penetrated because of poor weld technique. The area between passages was prepared and welded by fusion welding. The T-section was changed to two concentric cylinders with eloxed holes the full length to meet the main cylinder passages. The length of the holes made the eloxing and removal of the internal cores very difficult.

IV, C, Engine Housing, T-Configuration (cont.)

c. Test

(C) The testing of the three-walled prototype consisted of three basic tests: pressurization of the four selected zones (Figure IV-21) to nominal design pressure without thrust; thrust loading to 50% of nominal thrust without internal pressurization; and pressurization to 1.4 x nominal design pressure while applying 1.4 x nominal thrust load simultaneously. The nominal design pressure for Zone 1 was 6025 psi. The nominal design pressure used for Zone 2 was 4850 psi, an average between the oxidizer return passage pressure, 5125 psi, and the primary injector pressure, 4575 psi. The Zone 3 pressure used was the first-stage fuel pump discharge nominal design pressure, 3750 psi, and the Zone 4 pressure was the turbine discharge nominal design pressure, 3050 psi. The nominal design thrust was 100,000 lb.

(1) Preliminary Tests

(U) The preliminary tests consisted of the brittle lacquer coating test and three low pressure (without thrust) load tests, a thrust-only test, and two oxidizer bearing housing tests. The three-walled prototype housing was assembled as shown in Drawing No. 1120346 (Figure IV-22-a). The fuel housing (Item 4) was assembled with the partially machined primary injector (Item 7) by inserting the two retaining shells (Item 5). The unit was then checked for concentricity between the fuel housing and primary injector and the retaining shells were tack welded on the eight corners. The fuel tube (Item 6) was then welded to the fuel housing and the misalignment gage pressed into the fuel housing bore. The oxidizer bearing housing (Item 3) was installed into the oxidizer housing (Item 1), and the turbine nozzle simulator (Item 9) was installed on the oxidizer bearing housing. The fuel housing cartridge assembly was then assembled in the oxidizer housing, the center piston (Item 10) inserted, closure plug (Item 8) attached to the oxidizer inlet flange, and the center piston nut (Item 13) installed. The mounting stand (Item 11) was then installed and the unit filled with hydraulic test fluid. The unit was then installed in a universal test fixture, which applied internal pressure loads and thrust loads.

(U) A leak test of the instrumented housing (with internal strain gages in place) revealed a leakage area of 0.007 sq in. between the oxidizer-pump discharge passage and the oxidizer return passage. Leakage apparently occurred at an internal joint around the circumference of the thrust-chamber flange connection where a shrink fit was relied upon to seal the joint. The leakage area would allow 15 gal/min of oxidizer flow to bypass the thrust-chamber coolant tubes, which would be entirely acceptable for an operational turbopump. However, the flow capacity of the structural-test system permits a leakage rate of only 0.01 gal/min, which made it impossible to maintain the required pressure differential between the two pressure zones. Therefore, various means of sealing the leakage were investigated.

(U) The outside of the housing was stress-coated (Figure IV-22-b, view 1) and the housing tested to ascertain the severity of the setup problems and to determine the need for additional external strain gages. The oxidizer discharge passage was pressurized to the same value as the return passage. The results were highly satisfactory, with stresses at predicted levels (within $^{+5}_{-10\%}$) at the nominal design operating conditions. The internal strain gages were functioning properly and showed a linear rise in strain.

(U) After the stress-coat test, the unit was cleaned and a coating of soft rubber-like material (RTV-11) applied to the surface of the oxidizer-pump discharge passage. This material sealed the leak, and the unit was again set up for test. However, since the internal strain gages had

IV, C, Engine Housing, T-Configuration (cont.)

been lost during cleaning, it was decided to perform the pressure-only and the thrust-only tests without internal strain gages in an attempt to determine if any setup or structural irregularities existed. The housing was set up, instrumented with deflection indicators and strain gages, and tested to nominal design operating pressure. On completion of the pressure test, the thrust-load test was made without internal pressurization. The test data showed that the stresses and deflections at a thrust load of 50,000 lb were satisfactory. During testing to nominal design pressure, the oxidizer bearing housing moved 0.0207 in. toward the fuel housing (predicted deflection, 0.0078 in. outward) and the fuel housing deflected outward 0.0347 in. (predicted: 0.0098 in. outward). An examination of the test data indicated that the pressure in the oxidizer discharge passage (Zone 1), Figure IV-21, and the oxidizer return passage (Zone 2) had equalized above 57% of nominal design pressure at Zone 1 pressure. This higher pressure in Zone 2 increased the differential pressure across the primary injector, which increased the load transmitted through the connecting support shells to the fuel housing and, consequently, produced excessive fuel housing deflections.

(U) To check the data, a second test to 57% nominal design pressure was made with an additional deflection transducer on the oxidizer flange and visual indicators on the deflection-transducer rod for the oxidizer end. This test indicated that the oxidizer-dome end flange was expanding outward 0.007 in. and that the oxidizer bearing housing was expanding toward the fuel housing 0.0115 in. A third test to 86% nominal design pressure was performed at rapid pressurization to determine if pressure equalization was due to the rate of pressurization. Equalization occurred again at about 57% of nominal design pressure.

IV, C, Engine Housing, T-Configuration (cont.)

(U) An axial mechanical load was applied to the oxidizer bearing housing before the bearing housing was removed from the oxidizer housing. The deflections, measured on the outside flange, on the inner shell flange, and on the oxidizer bearing housing showed that the outer wall and the internal ribs were separating 0.0085 in.

(U) A spare bearing housing was subsequently assembled in a loading fixture and tested twice at an axial mechanical load of 50,000 lb with bolts torqued to design value and twice the design value, respectively. The deflection pattern remained relatively unchanged.

(U) Housing A-1 was returned for repair. Further investigation revealed that the ribs between shells on the oxidizer-dome end under the oxidizer-end flange were not properly attached. Originally, the weld joint between the outer wall and the internal ribs had been made by electron-beam welding. However, a special X-ray examination revealed that, during pressurization, the outer wall separated from the internal ribs. Plug-welding slots were machined in the outer shell over the ribs. An examination of the rib surface revealed very poor penetration of the electron-beam weld. This weld was subsequently repaired by TIG welding and by peening after each pass to stress-relieve the weld area.

(U) The unit was set up and tested at 1000 psi in Zone 1 to ensure that the rubber coating in Zone 1 had not been damaged during repair operations. No leakage occurred in 10 min.

### (2) Design Pressure Test

(U) The design pressure test requirements were to pressurize the four turbopump housing pressure zones to the nominal design pressure for each zone with no thrust load. To accomplish this, the repaired housing was reinstrumented and set up for testing.

IV, C, Engine Housing, T-Configuration (cont.)

(a) Test Procedure

(U) The four pressure zones of the housing were pressurized by a 5000-psi pump supplying a load maintainer which was precalibrated to supply the correct differential pressures to the intensifying cylinders. The intensifying cylinders boosted the pressure to the required zone pressures. The strain gage, pressure transducers and extensiometers continuously recorded the strains, pressures, and deflections during the pressurization.

(U) The housing was pressurized to nominal design pressure in 10% increments. Although the stress and deflection data were excellent, pressure Zones 1 and 2 had equalized, nullifying the test.

(U) A leak rate was determined by pressurizing to 43 and 57% of nominal design pressure in all zones and then increasing Zone 1 pressure to 1000 psi over Zone 2 pressure. Zone 2 was bled to keep the pressure uniform, and the oil discharge was measured over a 5-min interval. The leakage rate varied from 0.46 to 0.68 cu in./min. Because these leakage rates were small in comparison to the 40-cu-in. capacity of the pressurized intensifying cylinder, the test to nominal design pressure was completed using a bleed system to maintain the proper pressure in Zone 2. The pressure was maintained for 240 sec.

(b) Test Results

(U) Under nominal design pressure without thrust load the housing oxidizer dome end deflected 0.0055 in., the oxidizer bearing location 0.0136 in. and the main cylinder diameter at the center rib 0.0204 in. The maximum recorded stresses were 78,000 psi at the top of the main cylinder halfway between the thrust pad and the oxidizer dome, and 84,000 psi at the inside juncture of the T-section to the bottom of the main cylinder on the oxidizer end as predicted by the photoelastic model tests. The radial misalignment of the bearing housings under nominal design pressure was 0.0083 in. The housing surface hoop and meridional stresses on the wall near the center rib were 37,100 and 36,600 psi, respectively. The corresponding internal surface stresses in the hoop and meridional direction were 14,200 and 36,300 psi, respectively. This indicates relatively no bending in the meridional direction, a bending stress of 11,450 psi in the hoop direction, and a membrane stress of 25,650 psi in the hoop direction.

### (3) Thrust Test

(C) The objectives of the thrust test were to apply 50% of the nominal design thrust to the turbopump housing with no internal pressures and to determine the deflection and stress characteristics of the turbopump housing under this condition.

#### (a) Test Procedure

(U) The thrust load was applied by a loading cylinder which was pressurized by the same method as described in paragraph IV,C,3,c,(2),(a). The strain, load and deflection gages and transducers were recorded continuously during the test. The thrust load was applied in 20% increments to 50,000 lb. The test was accomplished twice. The first test was held erroneously for 110 sec and this required a repeat test which was held for 195 sec to meet a work statement requirement of 180 sec minimum.

#### (b) Test Results

(U) The axial deflection of the bearing locations was less than 0.0001 in. The diametral deflection at the main cylinder center line was 0.033 in. The maximum surface stress of -10,130 psi occurred on the shell near the thrust pad which corresponds to the -8000 psi predicted by photoelastic testing. The stress levels were very low and no structural damage occurred during the test.

### (4) Pressure and Thrust Proof Tests

(U) The objectives of the pressure and thrust proof tests were to determine the deflection and stress characteristics of the T-turbopump housing under loads of 1.4 times nominal design pressures and 1.4 times nominal design thrust. The contract requirements were such that the testing had to be performed twice with a minimum of seven days between tests. In addition, the bearing location axial deflection and radial misalignment could not exceed a permanent deformation of 0.020 and 0.008 in., respectively.

### (a) Test Procedure

(U) The pressure and thrust proof tests were accomplished in two test series The test requirements were the same for each series except that test series 2 had to be accomplished a minimum of seven days after completion of test series 1.

### 1 Test Series 1

(U) Test series 1 was completed after two tests. On the first test, the 1.4 times nominal design pressure and 1.4 times nominal thrust loads were applied for 50 sec when a thrust-chamber flange O-ring failed. The O-ring design was changed to self-energizing omniseals which required a seal groove modification to the test stand. A leakage check between pressure Zones 1 and 2 revealed that the coating had failed. The housing was disassembled, cleaned, and a new coating of RTV-11 was applied to Zone 1 cavity. The test data revealed that the fuel housing had yielded

.0173 in. To increase strength, four 0.375-in.-wide shear plates were welded to the inlet tube, the outside wall of the fuel volute, and the outer cylinder. The unit was reassembled for the next test (Figure IV-22-b, view 2).

(U) On the second test the required loads were held for 110 sec when the sealant between Zones 1 and 2 began to fail. The Zone 1 pressure slowly dropped until it equalized at Zone 2 pressure after an accumulated time of 190 sec. The deflection data were within the required limits and, due to only small changes in data with the reduced zone pressure, the test was accepted.

### 2 Test Series 2

(U) Because of the response times for pressure control and the difficulties in obtaining the leakage makeup volume, a new pressure system and controller were installed. This system supplied 4.5 gal/min of hydraulic oil at 10,000 psi to a load maintainer which integrated and distributed the correct pressure to each zone.

(U) The first test in this series was aborted after 40 sec at full pressure load when the RTV-11 sealant failed.

(U) The second test followed later in the day when it was decided to attempt to stabilize the pressure in Zone 2 by bleeding Zone 2 manually. This test resulted in overpressurization of all zones except Zone 4 to as much as 150% of nominal design pressures. The seal between Zones 2 and 4 failed and the fuel housing flange and bolts were yielded. The housing was dismantled and inspected. A dye penetrant inspection showed that the ribs had cracked in the welds at the fuel housing flange. No repair welding was performed. The fuel housing flange was distorted and was remachined. The oxidizer housing was cleaned and a new application of RTV-11 was applied to the Zone 1 cavity. Upon reassembly, the metal C-ring between the fuel flange and the oxidizer housing was replaced with a rubber O-ring. No internal strain gages were applied and only those external strain gages required at maximum stress points were used. All deflection transducers were replaced.

(U) The third test was held at 140% nominal design pressure and thrust loads for 40 sec when the O-ring in the fuel housing to oxidizer housing flange failed. The O-ring was replaced with a larger size and the fuel end instrumentation was replaced.

(U) The fourth test was accomplished successfully at 140% of nominal design pressure and thrust loads for 195 sec. The Zone 2 pressure was slightly high due to leakage from Zone 1. This completed the proof testing of the three-walled structural prototype.

### (b) Test Results

### 1 Test Series 1

(U) The axial deflections of the bearing housing locations for the second test are shown in Figures IV-23. The maximum fuel end deflection was 0.0258 in. and the oxidizer end deflection was 0.0047 in. for a total of 0.0305 in. at 140% of nominal design pressure. The permanent set was [illegible]087 in. in the fuel housing and less than 0.001 in. in the oxidizer housing. The radial misalignment was a maximum of 0.010 in. at 140% of nominal design pressure with a permanent set of 0.0043 in. Because of the difficulty in obtaining the radial misalignment values caused by limited space and high pressure, the values obtained were approximate. The maximum diametral growth of the housing at the center rib and center line of the main cylinder was 0.0377 in. at 140% of nominal design pressure. The maximum recorded stress was 110,000 psi at the oxidizer end juncture of the T-section to the bottom of the main cylinder in accordance with the photoelastic results. The maximum surface stress on the main cylinder wall next to the center rib was 59,000 psi in the meridional direction and 50,920 psi in the hoop direction. The internal stresses at the same point were 45,840 psi in the meridional direction and 46,550 psi in the hoop direction. The center rib stress at this point was 47,400 psi in the hoop direction.

### 2 Test Series 2

(U) The measurements of the housings before and after testing showed that the actual permanent set was an average of 0.0155 in. The radial misalignment measured was 0.0124 in. but the gage was inoperative on return to 0. The diametral deflection of the main cylinder center line at the center rib was 0.0452 in. The maximum stress at this point was 75,600 psi. The maximum outer surface stresses, 103, 700 psi in the hoop direction and 62,350 psi in the meridional direction, occurred between the thrust pad and the oxidizer dome on the top surface of the main cylinder.

(U) X-rays of the oxidizer housing diffuser vanes to outer wall welds showed no indication of cracking or separation. A dye penetrant inspection of the housings reveal no cracks or damage to the oxidizer housing. The weld cracks in the ribs on the fuel housing had propagated approximately 0.060 in. beyond the point documented prior to the final test. This was conclusive proof that a stronger material was required for the fuel housing and that ribs were required between the first-stage fuel volute and the oxidizer housing attachment flange. Both of these improvements were incorporated in the Housing C design.

IV, C, Engine Housing, T-Configuration (cont.)

### (5) Vibration Tests

(U) On completion of the pressure and thrust proof tests, the turbopump housing was tested for vibrational characteristics with and without internal pressurization to determine the lowest natural frequency of the housing. The objectives were to determine that no critical vibrational modes existed in any of the major areas of the housing between 667 ± 10% cps with a 1g acceleration amplitude input.

#### (a) Test Procedure

(U) The turbopump housing was tested in three series: empty and unpressurized, filled with hydraulic oil and unpressurized, and filled with hydraulic oil and pressurized to 1.2 x nominal design pressures. Zone 1 was pressurized to Zone 2 pressure due to the interpassage leakage. The turbopump housing was suspended so that the vibration excitation could be applied in each of three axes, X, Y, and Z. The X axis was along the main cylinder center line. The Y axis was along the thrust-chamber center line, and the Z axis was perpendicular to the main cylinder center line at the thrust-chamber center line.

#### 1 Test Series 1

(U) A preliminary survey of the housing along the Y axis was performed with six external and six internal accelerometers without the support stand or shaft attached to the housing. This was repeated with the support stand attached and finally with support stand and shaft attached. The surveys were recorded on an oscillograph which made oscillograms of each of the 12 accelerometers while sweeping from 100 to 5000 cps.

(U) The turbopump housing with support stand and shaft in place was reoriented and the vibration excitation was applied in the direction of the X axis. The 12 accelerometer readings were recorded from 100 to 5000 cps. The final test in this series was in the X axis (Figure IV-24-a) and was performed in the same manner as the Z axis survey.

### 2 Test Series 2

(U) The turbopump housing support stand was removed to allow removal of the internal accelerometers, replaced, and the unit was then filled with hydraulic oil. The unit was suspended with the acceleration input in the Y axis direction. A frequency sweep from 100 to 5000 cps was made while readings of the six external accelerometers were recorded. This test was repeated with the housing pressurized to 1.2 times nominal design pressure and the output accelerations were recorded. This procedure was repeated for the X and Z axes.

### (b) Test Results

(U) The results (Figure IV-24-b) of the three phases of testing show that there was no critical mode of vibration in the housing between 100 and 1000 cps in any axis. There were no significant shifts in response frequency when the housing was pressurized. This indicates that the housing stiffness was much higher than the stiffness added by pressurization. When the housing was filled with oil, the response acceleration amplitude was considerably reduced because of the damping effect of the oil.

### 4. Final Housing

(U) Three detailed versions of the final turbopump housing were studied. The first version was a two-walled unwelded rib design. The second version was a three-wall design similar to the three-wall prototype and the third version was a modified three-wall design adapted to casting.

#### a. Two-Wall Oxidizer Housing

(U) The objectives of the two-wall oxidizer housing version (Figure IV-25) were to design a structurally stable housing that was easier to fabricate and had improved flow passage design and lower cost.

(U) The basic shape of the two-wall housing remained the same as the three-wall structural prototype. The main cylinder was shortened 2 in. and the T-section center line was moved 1 in. toward the oxidizer end. The return passage was replaced by a manifold in the T-section which fed a manifold on the primary injector. The ribs in the main cylinder oxidizer discharge flow passage were replaced by thin fins (to guide the flow) which were only attached to the outer diameter of the inner cylinder. The T-section oxidizer discharge and return passages consisted of drilled holes. The oxidizer dome end had plug-welded diffuser vanes and guide vanes. The design could be fabricated rapidly and at a relatively low cost with a minimum of weld reliability problems.

(U) Because the thin guide vanes between walls were not attached to the outer wall, the thicknesses of the inner and outer walls were increased to provide the additional hoop, meridional, and bending strength required. This caused a decrease in weight when compared to the three-wall structural prototype but an increase of 10 lb over the weight of the three-wall housing described in the next section. When compared to the photoelastic results, the bending stresses in the region of the thrust pad would be excessive due to an 80% reduction in the bending moment of inertia. This was later confirmed by the bending stress levels observed during the testing of the three-wall prototype. This design was abandoned for the engine design using a regeneratively cooled thrust chamber, because of the structural deficiency when the walls were not attached.

### b. Three-Wall Housing B

(U) The objectives of the housing B design effort were to optimize the flow passages, finalize the internal dimensions and fits, reduce weight, and ensure a housing capable of being used for turbopump development testing and a second round of structural testing if the three-wall structural prototype failed.

(U) The basic shape of the Inconel 718 oxidizer housing of Housing B (Figure IV-26) was the same as the three-wall structural prototype. The main cylinder was shortened approximately 2 in. and the T-section center line moved approximately 1 in. toward the oxidizer dome. The three walls were separated by two sets of 1/4-sq-in. continuous ribs which tied the walls together and formed discrete flow passages. The walls were attached to the ribs by plug welding. The ribs were curved and spaced to provide minimum pressure loss in the flow passage and minimum mass flow distribution variance to the thrust-chamber cooling tubes and the primary injector. The oxidizer diffuser vanes were machined on the outside of the inner wall dome and inserted through slots in the outer wall dome and welded in place to give maximum strength to the critical dome structure. The T-section was made conical to reduce the intersection diameter. The T-section had drilled holes to form the oxidizer discharge and return passages.

(U) The fuel housing was also moved toward the oxidizer end by approximately 1 in. The fuel housing was designed as an Inconel 718 weldment to contain the two fuel pumps and provide the required discharge volutes, contain the bearings, seal, thrust balancer and primary injector valve, and to supply each of these with fuel through a series of internal passages. Oxidizer fluid was bled off the return passage of the oxidizer housing and fed to the hydrostatic combustion seal via a passage covering the internal face of the fuel housing. This ensured cooling of the fuel housing face from the turbine exhaust gases.

### (1) Stress Analysis

(U) The stress limits and load criteria used for the Housing B analyses were the same as for the three-wall structural prototype. The finite element analysis method was used to determine basic stress levels. These stresses were then altered in areas around the thrust pad and T-section to main cylinder intersection to reflect the stress concentration factors determined from the photoelastic model testing. The oxidizer dome and profile was studied to minimize axial deflections. The dome curvature is critical as shown in Figure IV-27, which shows axial deflection as a function of radius of curvature and wall thickness for the three-wall structural prototype, Metal Model 1, Metal Model 2, and Housing B.

(U) The ordinate and abscissa values for Figure IV-27 are as follows:

$$\Psi = \frac{R\,\theta}{h}$$

where R is the mean radius of curvature of the oxidizer dome, θ is the angle of radians from the intersection of the main cylinder and dome to the top of the oxidizer diffuser vanes of approximately 65 degrees or 1.33 radians, and h is the effective thickness of the dome based on equivalent section moment of inertia.

$$X_b = \frac{2.44\ q\ R^4\ R_I}{(2\ R_o + R_i)\ EI}$$

where q is the internal pressure, $R_i$ is the radius from the housing center line to the oxidizer bearing housing hot-gas surface at the turbine nozzle attachment location, $R_o$ is the radius from the housing center line to the midpoint of the wall at the intersection of the dome and main cylinder, E is the elastic modulus, and I is the moment of inertia of a 1-in.-wide section of the wall.

(U) This shows that the axial deflection of the oxidizer dome end is directly dependent on R, the moment of inertia of the dome wall and the pressure applied.

### (2) Heat Transfer Analysis

(U) The heat transfer analysis of the oxidizer housing showed that the wall temperature on the hot-gas side varied significantly with hot-gas velocity and insignificantly with coolant velocities above 35 fps. With a gas velocity of 5 fps next to the 0.020-in.-thick housing wall the temperature was 400°F. At a gas velocity of 20 fps the wall temperature rose to 640°F. The hot-gas shields in the primary combustion area and the turbine exhaust area were designed to reduce the gas velocity between the shield and the housing wall to less than 5 fps. To accomplish this, a single row of holes on the upstream side of each shield was used to vent the cavity between the shield and wall for start and shutdown pressure change conditions. The single entry point allows extremely limited circulation and, subsequently, low gas velocities at the housing wall. The effectivity of the shield design will have to be substantiated by test.

### (3) Fluid Dynamic Analysis

(U) A preliminary fluid dynamic analysis showed relatively uniform fluid velocities in the main cylinder passages except the velocity at the T-section at the bottom of the main cylinder on the fuel housing end, which was high due to lack of sufficient space to enter that portion of the T-section. The air test program was expected to clarify this area. The air test results were not available until after the design was completed.

### (4) Summary

(U) The calculated weight of the Housing B design was 89 lb less than the three-wall structural prototype. The housing axial deflections between bearing locations was reduced to 0.0256 in. with no permanent deformation under maximum operating conditions.

(U) The fabrication quotations received were excessive in price and delivery. This eliminated the possibility of receiving Housing B in time for a second round of structural testing. The preliminary results of air testing showed a pressure loss of 417 psi in the oxidizer discharge passage near the fuel housing end and the mass flow variation was ± 10 to 14%. The design pressure loss was limited to 125 psi in each of the housing flow passages. To decrease this pressure loss and reduce the mass flow variation, a change in passage design was required.

### c. Three-Wall Housing C

(U) The three-wall C design housing (Figure IV-1) was required to achieve a lower unit cost, reduce the pressure losses in the oxidizer flow passages, and provide a uniform mass flow distribution to the thrust-chamber cooling tubes and to the primary injector.

(U) To accomplish these objectives, changes were required from the B design housing. The outer passage height was increased from 1/4 to 3/8 in. The passage guide vane patterns (Figure IV-28) were changed from continuous vanes to intermittent vanes. The housing length on the fuel end was increased 0.5 in. The oxidizer housing was divided into six investment castings of Inconel 718C material. The use of the cast material required a slight increase in wall thicknesses which increased the housing weight to 33 lb above the calculated weight of Housing B. The castings were welded together by electron-beam welding and by plug-welding the rib-to-shell joints from the inside and outside surfaces. The third wall of the main cylinder was shortened to extend only from the primary injector to the fuel housing end. The T-section was modified to include a manifold area in both the discharge and return passages. The fuel housing was changed to a 17-4 PH casting and modified by adding ribs on the outside to decrease the axial deflections experienced by the structural prototype.

(U) The pressure losses were reduced to acceptable values and the mass flow distributions improved as described in Section VIII,A. The quotations received for fabrication showed a substantial cost reduction although casting delivery times were relatively long. The reliability of the welding and fabrication processes was improved by designing the wall-to-rib welds to be performed from an external surface. The stresses and deflections calculated for the C design housing were approximately the same as those for Housing B.

### d. Conclusions

(U) The results of the T-configuration turbopump housing program were highly satisfactory. The test results on the first full-scale prototype, Housing A, met all work statement requirements. The stress levels were lower than the design but the deflections were higher than the design. By

IV, C, Engine Housing, T-Configuration (cont.)

judicious placement of ribs the deflections have been reduced in the final design as shown in the following table. In addition, the weight in the final housing has been reduced to 82% of the weight of Housing A.

| | | Housing A | Housing B | Housing C |
|---|---|---|---|---|
| Axial deflection between bearing locations at 140% of nominal design conditions | Total<br>Permanent | 0.0305 in.<br>0.008 in. | 0.0314 in.<br>0 in. | 0.0300 in.<br>0 in. |
| Radial deflection between bearing locations at 140% of nominal design conditions | Total<br>Permanent | 0.010 in.<br>0.003 in. | 0.007 in.<br>0 in. | 0.004 in.<br>0 in. |
| Weight | | 100% | 71.3% | 82% |
| Cost | | 100% | 200% | 48% |

(U) The short lead time of the Phase I program required that the housing be made as weldments using forgings, plate, and sheet material. This increased the cost of the housings. The final design uses many castings which are ultimately assembled by welding, which reduces the cost. With some development it is expected that the oxidizer housing and fuel housing each can be cast as single units. This would further reduce the cost to 19% of the cost of Housing A. The lead time required for obtaining usable castings is approximately 30 weeks. It is recommended that the tooling for these castings be procured and approved by sample castings prior to Phase II. This would reduce the lead time by approximately 20 weeks.

(U) The final housing is designed for a 100% regeneratively cooled thrust chamber. If a transpiration-cooled thrust chamber is used, considerable simplification could be made to the housing design. Preliminary investigations show that a weight reduction of approximately 40 lb can be achieved. In addition, the housing would be simplified by the reduction to a two wall construction thereby reducing manufacturing costs and thus improving the reliability as a result of the reduced number of welds.

## D. BACKUP TURBOPUMP

### 1. Objectives

(C) A basic objective of this program is to design and test a reliable flight-weight turbopump for a 100,000-lb-thrust engine utilizing high pressures in the staged combustion cycle and storable propellants.

(U) Because ARES is an advanced engine with stringent requirements for ease of operation, limited maintenance and servicing, lightweight components, minimum size envelope, and avoidance of external leakage, together with a high degree of integration and relatively high engine performance goals, heavy demands on advancing the state of the art of turbopumps were imposed. In certain components, specifically seals, bearings, and high-pressure housings, it was beneficial to incorporate several component concepts to achieve overall engine design objectives that would to a significant degree advance the state of the art. Although programs for improved components were established, it was believed prudent to investigate an alternative, or backup turbopump design, because of inherent uncertainties in achieving successful operation of the several new concepts.

(U) The overall objective of the backup turbopump design effort was to evolve a turbopump which met most of the operational requirements of the advanced turbopump, yet incorporated only conventional components. "Conventional" in this case was interpreted as a design concept or analysis technique which had previously been successfully used, demonstrated, or tested. For example, conventional dynamic shaft seals were to be used in place of an advanced hydrostatic combustion seal, a semi-integrated housing is used which is easier to fabricate than the integrated advanced T-engine housing, and does not subject the rotating elements to effects of pressure and temperature distortion. In addition, the propellant-cooled bearings were to operate at more conservative DN values. Turbopump size and weight were secondary considerations to simplified, conservative design, and ease of fabrication of parts of known high reliability. These conventional components were to be arranged in a manner designed to minimize the interrelationship of one component to another, so that a high degree of success was predictable.

(U) The practical approach of evolving a backup turbopump design using state-of-the-art design practice ensured that the benefits of advanced turbopump technology could be safely pursued without jeopardizing the goals or schedule of the ARES engine program. This requirement also made it desirable that maximum use of the development of primary and secondary combustors and valves be utilized in the backup turbopump.

## 2. Concept Selection

### a. Concept Alternatives Considered

(U) The concept selection involved a "morphological" survey of candidate configurations, tempered by experience gained in previous Aerojet-General high-pressure engine programs.

(U) Using results of a prior study program to avoid pitfalls in the design, four configurations were chosen for more detailed design investigations. These concepts, shown schematically in Figure IV-29, were:

Vertical shaft-end mounted turbine (ultimately selected)
Horizontal shaft, center-mounted turbine
Horizontal shaft, end-mounted turbine
The Y-engine concept

(U) Features of each of the four candidate concepts and relative advantages and disadvantages are discussed in the following section.

### (1) Vertical Shaft Concepts

(U) The single shaft, vertical configuration, is most logically arranged with the turbine at the thrust chamber end. This permits the turbine to exhaust directly into the secondary injector with a minimum of manifolding. The primary combustor, contained by the oxidizer discharge housing, is annular, similar to the basic advanced design. All high-temperature parts are localized and thermal distortion is virtually eliminated from the power transmission and pump housing.

(U) The oxidizer pump is placed next to the turbine to eliminate the need of a dynamic shaft seal for the turbine. This arrangement also permits the oxidizer-pump discharge flow to be carried by drilled passages in the housing directly to the down-flow tubes of the thrust chamber without further manifolding. The oxidizer housing also provides the necessary structural support to contain the primary combustor chamber pressure. The oxidizer flow cools the housing. A perforated primary chamber liner is provided to prevent high velocity gas from scrubbing against the housing walls. Symmetry of the oxidizer-housing flow passage and a vaned diffuser section at the impeller discharge provide assurance that radial hydraulic loads on the impeller are minimized. Thus, associated potential rubbing problems on the pumps and radial bearing loading are also minimized. This location of the oxidizer pump requires that oxidizer enter the pump radially through an inlet scroll.

(U) The fuel pump is placed at the end opposite the turbine. Engine thrust is carried axially through the turbopump housing to a fixed or gimbaled thrust pad at the top (fuel) end of the housing. The fuel pump can be oriented for either an axial or radial inlet.

(U) If an axial flow inlet were selected for the fuel pump, the thrust pad or gimbal would have to be a ring to admit the fuel to the pump inlet. Thus, a somewhat unconventional gimbal would be required and some weight penalty would be anticipated. In addition, with the fuel impeller oriented for the axial inlet, the back of the impeller would be toward the oxidizer pump. This arrangement would create a potential seal problem because of the high pressures developed in the fuel cavities behind the second-stage impeller, which must be sealed from the adjacent oxidizer inlet passage. Radial inlet of the fuel would eliminate all of the above problems; however, an additional inlet manifold is required to guide the flow into the fuel inducer.

(U) A dual exit volute with a vaned diffuser provides symmetry of flow out of the first stage of the fuel pump to minimize radial hydraulic loads. In addition, the maximum cross section of the fuel pump volute carries only half the total flow, thus its cross-sectional area is minimized for a given volute velocity. This fact in turn reduces the wall thickness required to contain the pressure and minimizes weight. The two volute tongues, located 180 degrees apart provide additional symmetrical structural support.

(U) The inducer hub diameters of both pumps must be large to carry the required shaft diameter for torque transmission. As a result, inducer hub-tip ratios are somewhat larger than would normally be used. Because of the radial inlet manifolds and the large inducer hub-tip ratios, a slight loss of cavitation performance may occur. However, boost pumps will provide more than adequate NPSH, so no problem is expected.

### (2) Horizontal Shaft Concepts

(U) The original vertical-shaft configuration, described above, results in an engine size envelope which is slightly longer than the advanced turbopump concept. For upper-stage applications where additional length of interstage structure may be required to accommodate a longer engine, a possible vehicle weight penalty exists. This consideration led to investigations of horizontal shaft concepts which could potentially reduce engine length.

(U) Center-mounted and end-mounted turbine versions of the horizontal shaft concept were investigated. The center-mounted turbine creates a fuel-to-turbine gas-sealing problem, axial thermal growth of the shaft must be accommodated, and unsymmetrical thermal distortion of the housing could occur. Also, manifolding of the turbine exhaust flow into the secondary injector would be required. In general, the potential problems with this design were so similar to those of the advanced turbopump that it did not offer a good backup approach and the concept was discarded.

(U) With the end-mounted turbine, horizontal shaft configuration, the turbine exhaust gas would be ducted around a 90 degree bend and into the secondary injector; and thus an L-shaped engine would result. Thermal distortion of the hot turbine exhaust elbow dictated that separate struts be provided to support the turbopump on the engine. In addition, a separate thrust-take-out structure was required. These added structural members imposed a significant weight penalty. It also became evident that the internal configuration of the turbopump would be virtually identical to the interior of the vertical shaft concept. Finally, for the horizontal shaft, end-mounted turbine, a set of external oxidizer lines from the pump to the thrust chamber were necessary unless the 90 degree turbine exhaust bend was made tubular-walled to carry the oxidizer flow. Because of the increased structural weight and added complexity of plumbing, this concept was also discarded.

### (3) Y-Engine

(U) Early studies of two separate turbopumps in a Y-Engine arrangement indicated two advantages: (1) external leak paths to atmosphere were virtually eliminated and (2) small, very high-speed turbopump units were possible since short bearing spans and reduced power levels of the individual units made small bearings possible without critical speed problems. It also appeared that the engine envelope length could be relatively short. Therefore, further consideration was given to this concept.

(U) Several shortcomings were found inherent in the Y-Engine which ultimately caused it to be rejected.

(U) The turbine seal on the fuel pump was required to be a positive high-pressure seal to prevent fuel from leaking into the oxidizer-rich turbine gas. This requirement was beyond current conventional dynamic seal capability unless a purge fluid at high pressure was used.

(U) Separate turbines on the oxidizer and fuel units cause a loss in turbine efficiency. The turbines could not readily be mechanically linked, which created potentially difficult speed control and engine mixture ratio control problems.

(U) Other drawbacks included multiplicity of components (such as two turbines, two shafts, extra bearings, etc.), requirement for a primary combustor substantially different from that to be evolved for the advanced turbopump, and complex turbine-to-turbine gas manifolding. Weight, complexity, and thermal stress in the high-pressure hot-enclosure dome were additional negative factors. These factors led to rejection of this concept.

### b. Speed Selection

(U) As the various concepts were evaluated, the range of potential operating speeds available to each configuration was given consideration because of the effect on bearing DN, shaft critical speed, shaft seal surface speed, engine size and weight, component efficiency and NPSH requirements of the selected design.

(U) A design speed of 30,000 rpm was selected. This section presents the justification for this speed selection.

#### (1) Power Transmission Considerations

(U) Bearing DN, critical shaft speed and rubbing velocity of the seal are important considerations in the design of the power transmission. A bearing DN value of $1.25 \times 10^6$ was considered to be a conservative value since it had been demonstrated with these propellants on a previous program. Some increase in this value was considered to be reasonable as long as it was significantly lower than the $1.6 \times 10^6$ value used on the advanced turbopump.

(U) Bearing DN, shaft stress, and critical speed are closely interdependent. A smaller bearing reduces DN for a given speed, but requires a smaller shaft, which correspondingly increases shaft torsional and bending stresses. Also, the smaller shaft is more flexible and the smaller bearing provides less radial stiffness. The combined effects reduce the shaft-whirling critical speed. Two approaches were studied in iterating these three parameters.

(U) The first approach (ultimately used) was to place the bearings inboard of the turbine with the ground rule that operating speed was to be a minimum of 20% below the first critical speed. In this case, the turbine roller-bearing bore had to be large enough to transmit full turbine torque. In addition, the turbine coupling had to be small enough to allow the roller bearing to slip over it, since it is installed from the turbine end.

(U) With these limitations, the bearing size narrowed to 40 mm or larger with a design speed of approximately 30,000 rpm. Preliminary turbopump layouts were made to provide input for critical speed analysis.

(U) Critical speed is an important parameter in the ARES turbopump, where the high reliability of rub-free operation and long bearing life are considered mandatory. Parametric plots of the critical speeds, showing effects of bearing span, impeller weight and overhang, and gyroscopic (inertial) effects of turbine and fuel impellers were prepared.

(U) Preliminary results of an analysis of the critical speed indicated first critical speed values to be approximately 35,000 rpm for 40 mm bearings. Increasing the oxidizer bearing size to 45 mm and optimizing bearing spacing as well as turbine and fuel impeller overhang increased the critical speed to above 37,000 rpm. However, at 30,000 rpm, bearing DN was $1.35 \times 10^6$.

(U) The interpropellant dynamic shaft seal or seals tentatively selected were face-riding rubbing contact seals, chosen because of their low leakage and static sealing capability. Shaft diameter which is fixed by stress and critical speed fixed the diameter of the seal face at 2.50 in. At 30,000 rpm, seal rubbing velocity is approximately 325 ft/sec, a relatively high value for this type of seal. Since the seal is in a cool environment, satisfactory operation is expected. However, higher surface velocities would require empirical demonstration testing.

(U) An alternative approach was also investigated in which the ground rule was to operate at least 20% above the first critical speed and at least 20% below the second critical speed. In this case, the turbine-end roller bearing was placed outboard of the turbine. Thus a smaller turbine bearing could be used. It was concluded that reliability problems of maintaining alignment and operating the bearing in the hot turbine exhaust stream would be potentially more severe than those associated with operating the bearing at $1.35 \times 10^6$ DN. Various other problems such as increased turbopump length and possibility of excessive shaft deflection at the oxidizer impeller location while passing through the critical speed regime also contributed to the rejection of the outboard bearing concept.

### (2) Component Efficiencies

(U) For the ARES turbopump operating requirements, the pump efficiencies improve somewhat in the 30,000 to 40,000 rpm range. Figure IV-30 shows the Worthington curve of pump efficiency as a function of specific speed. Also shown is an approximately average curve of rocket-engine turbopump efficiency versus design specific speed. The inline oxidizer and fuel pump efficiency at 30,000 rpm are shown on the curve relative to the advanced turbopump design points operating at 40,000 rpm. Two to four percentage points in efficiency are lost by operating at 30,000 rpm rather than 40,000 rpm. The efficiency degradation becomes more severe as design speed is decreased further. The characteristics of this curve provide incentive to maintain design speed as high as practical, contingent on other limitations such as bearing DN.

IV, D, Backup Turbopump (cont.)

(U) Studies indicate that turbine efficiency remains relatively constant over design speed ranges from 20,000 to 40,000 rpm as shown in Figure IV-31 and indicate turbine efficiencies of 75 to 80% and possibly even higher can be obtained.

### (3) Turbopump Weight

(U) Early in the conceptual design effort, layouts of turbopumps at 20,000, 30,000, 40,000, and 50,000 rpm design speed were prepared. These concepts were sufficiently close to the configuration ultimately chosen to allow a realistic weight comparison to be made. Figure IV-32 shows the curve of weight versus speed for the designs evolved.

(U) Because of the bearing DN restraint, which made outboard turbine-end bearings essential as speeds approach 40,000 rpm, the weight curve has an abrupt and significant discontinuity between 30,000 and 40,000 rpm. The additional structure necessary to support the outboard bearing and the overall increase in turbopump length resulted in a substantial increase in turbopump weight. Speeds approaching 50,000 rpm were found to be required to offset this weight gain. While such high speeds are not undesirable per se, it was found that the turbine design became highly unconventional. To accommodate the required gas weight flow, an approximately fixed turbine annulus area is required. As turbine tip diameter was reduced (to maintain a reasonable range of turbine U/Co) the blade heights increased until the wheel became virtually "all blade." In addition, fluid vorticity dictated that the long blades be highly twisted to accommodate radial equilibrium requirements of the gas flow.

(U) The engine specification provides for 20-ft NPSH for both propellants at the engine-to-vehicle interface. Without boost pumps, a speed of less than 20,000 rpm (or exceptionally advanced inducers) would be required for normal operation. This low speed would result in substantial weight and component efficiency penalties. Because of the additional suction head, a turbopump design speed of 30,000 rpm or higher is warranted with the boost pumps. Thus bearing DN, weight, and turbine design considerations, as well as such practical considerations as standard spline and bearing sizes, led to a nominal design speed of approximately 30,000 rpm. (Without the bearing DN limitation the optimum speed would have increased to about 35,000 rpm.)

### c. Selection Summary

(U) Based on established ground rules and design objectives, a vertical shaft (inline with the thrust chamber axis) turbopump with centrifugal pump impellers and an end-mounted, single-stage axial flow turbine was selected (Figure IV-33).

(U) Major reasons for selecting this concept include:

1. The low-pressure, ambient-temperature, dynamic shaft-seal environment allows conventional seals to be used.
2. All hot parts are localized at the turbine end, thus minimizing potential thermal distortion problems.
3. Symmetry of flow passages throughout will minimize radial hydraulic loading.
4. Ease of engine integration.
5. Power transmission simplicity.
6. No turbine-end seal required; the oxidizer bleeds into oxidizer-rich gas.
7. Acceptable turbopump weight of approximately 350 lb.
8. Ease of housing fabrication.

(U) A detailed description of the selected inline turbopump is presented in the following section.

## IV, D, Backup Turbopump (cont.)

### 3. Design and Analysis

#### a. Description of Inline Turbopump

(U) This section presents a more detailed description and discussion of design features of the selected vertical-shaft concept for the inline turbopump. A cross section of the unit is shown in Figure IV-33. All performance data for this TPA are presented in the ARES Engine Handbook, (Appendix I).

#### (1) Turbopump Assembly

(U) The inline turbopump consists of a two-stage centrifugal fuel pump, a single-stage centrifugal oxidizer pump, and a single-stage, low-reaction, axial-flow turbine installed on a common shaft. Design operating speed is 30,000 rpm. Estimated weight of the unit including primary injector initially was 350 lb. This estimate was reduced to 300 lb as the design was refined.

#### (2) Fuel Pump

(C) The fuel pump flow enters radially through a "radial in-flow" scroll to a separate inducer. The inducer discharges into the inlet of the first-stage centrifugal impeller. This stage provides a discharge pressure of approximately 3700 psi and feeds approximately 80% of its total flow to twin discharge lines (from which boost-pump turbine flow is tapped) and then through a valve to the secondary injector. The remaining 20% of the flow is tapped off symmetrically from the first-stage volute and fed to the second-stage impeller. In the second stage, the fuel pressure is increased to approximately 6000 psi and supplied to the primary combustor.

Predicted efficiency of the first-stage fuel pump is approximately 66%. Efficiency of the second-stage fuel pump is predicted to be 55%.

### (3) Oxidizer Pump

(C) Oxidizer enters the pump radially through an inlet scroll to a separate inducer. The inducer discharges into the inlet of the single-stage oxidizer pump. The shrouded centrifugal impeller increases the pressure to approximately 6000 psi. Predicted oxidizer pump efficiency is approximately 68%. From the impeller, the oxidizer passes through tandem vaned diffuser downstream of which oxidizer boost-pump turbine-drive flow is tapped, and then into the annular oxidizer housing. Flow from the oxidizer housing enters the thrust chamber down-tubes and returns in the up-tubes to enter the annular primary combustor enclosed by the oxidizer housing. The primary combustor supplies oxidizer-rich gas to the turbine.

### (4) Turbine

(C) The turbine consists of a single-stage, low-reaction, axial-flow design which develops approximately 10,500 bhp at a pressure ratio of 1.5 at a nominal inlet temperature of 1240°F. Predicted efficiency is 75% at design speed. The turbine gas exhaust with virtually no residual whirl component when operating at design speed. However, during engine start-up at low turbine speeds, considerable exit whirl exists which could cause nonuniform flow to the secondary injector. Therefore, exit-straightening vanes are provided. These vanes also support a heat shield over the turbine disc to minimize radiation heating of the disc from the flame in the secondary combustor. The heat shield also provides a diffusing passage for the exhaust gas to minimize diffusion loss in the turbine exit plenum.

IV, D, Backup Turbopump (cont.)

### (5) Power Transmission

#### (a) Thrust Bearings

(U) Axial thrust of each rotor element will be balanced as closely as possible, and the design features a fully self-compensating axial-thrust balance system. Thus, axial bearing loads should be relatively light, on the order of 300 to 500 lb. However, the design incorporates a match-ground pair of 40 mm ball bearings with a total axial load capacity on the order of 3000 lb.

(U) The ball bearings provide axial restraint during transient operation. They are carried in a radially flexible support to avoid radial loading. The flexible support will be strain-gaged to serve as a double-acting (bidirectional) axial thrust measuring sleeve.

#### (b) Roller Bearings

(U) Completely symmetrical flow passages within the turbopump and operation well below the first critical speed, provide assurance that radial bearing loads will be minimized. The radial load-carrying bearings are 35- and 45-mm roller bearings. Radial-load capacity of 500 lb has been demonstrated for long term and 1000 lb for transient operation as discussed in Section IV,G.

#### (c) Dynamic Seals

(U) The turbopump configuration was arranged to permit the dynamic seals to be located in an ambient temperature, low-pressure environment by sealing between liquid oxidizer and liquid fuel at the pump inlets.

IV, D, Backup Turbopump (cont.)

(U) A pair of commercially available, conventional face-riding, carbon-nosed seals are used between the two pump inlet housings. Rubbing velocity is 327 ft/sec. An inert purge fluid (DuPont PR 143) is admitted to the inter-seal cavity. Any inert fluid leakage will lubricate the face seals as it flows toward either pump inlet. An inert fluid reservoir is located on the pump housing.

(U) Both seal running rings are immersed in and cooled by propellant. The dynamic seal location has ample room to allow alternative seal concepts such as hydrostatic and visco-seal (shaft screw-type) designs to be installed, if desired.

(U) No other positive dynamic seals are required in the turbopump assembly. At the turbine end, oxidizer that cools the turbine-end roller bearing is permitted to pass through a labyrinth into the turbine plenum. Pressure drop across the bearing and labyrinth can be controlled by an upstream orifice.

### (d) Wear Rings and Other Potential Rubbing Surfaces

(U) Symmetry of the housing is expected to minimize radial hydraulic loads and distortion. However, the inline turbopump incorporates inserts at all areas at which close running clearances are required in both the oxidizer and fuel pumps.

(U) In connection with the rub-precipitated explosion hazard, the oxidizer inducer and centrifugal impeller have been designed to use steel to minimize the possibility of vane failure and potential hard rubbing of a resulting broken piece against the oxidizer housing. In the inline turbopump design full use was made of information obtained from the wear ring program conducted for the T-engine TPA. Size envelopes were provided to permit fixed labyrinths or floating hydrostatic seals to be installed, as desired.

### (e) Instrumentation

(U) Conventional instrumentation can be installed with relative ease in the inline turbopump. Thrust bearing thermocouples can be installed in the flexible bearing mount and the leads carried together with the thrust measurement strain-gage leads, out to an external connector. The turbine-end roller bearing thermocouple can be inserted directly from the outside, through the oxidizer diffuser vanes and housing to the bearing race. A double-seal arrangement with an inter-seal vent to pump inlet pressure is used to minimize leakage problems along the instrumentation leads. The fuel-pump roller-bearing thermocouples are installed through the housing body. A pair of electromagnetic speed pickups can be installed at the periphery of the fuel-seal running ring. The periphery of the running ring is notched to provide conventional indication of rotational speed.

### (f) Static Seals

(U) All static seals to atmosphere throughout the assembly are paired, with an interseal vent back to pump inlet pressure. This arrangement effectively avoids high-pressure static seals to atmosphere. Conventional O-ring seals are planned. The turbopump has no internal positive static seals, no bellows, and no interpropellant welds or bulkheads.

(g) Primary Combustor Injector Flooding

(U) In design reviews of the inline TPA it was speculated that since the primary combustor injector fires upwards in this design, the result could be the potential of the leading propellant (oxidizer) to fall back and drain into the fuel orifices. This event would cause internal explosions when the hypergolic fuel reached the injector manifold.

(U) Consideration of this possible occurrence reveals that the possibility exists only on ground start where gravitational influences and atmospheric pressure exist. Zero-g starts in a space vacuum should be entirely safe since the oxidizer propellant will flash rapidly and also will not tend to fall back, since gravity forces are absent. Safe starts in space have been achieved with these propellants on numerous occasions: Titan III and Transtage, for example.

(U) In view of the fact that this is a ground-start problem only, several effective solutions exist. The most promising approach, once the engine is developed, is to simply seal the orifices with a thin membrane. Other approaches suited to repetitive development firings are to use inert liquid or gas purges in the fuel system. Also the fuel system downstream of the primary fuel valve up to the injector can be prefilled with an inert viscous liquid to prevent entry of the oxidizer into the fuel system. Thus, it is apparent that effective means of eliminating the potential problem are available in the event that the problem exists.

## b. Turbopump Assembly Analysis and Design

### (1) Engine Requirements and Cycle Considerations

(C) The ARES engine is a 100K, high-pressure, gas-liquid, staged-combustion topping cycle, engine using propellants $N_2O_4$ and AeroZINE 50 as the oxidizer and fuel, respectively. This engine uses the inline TPA, without significant changes in basic performance or transient characteristics.

(U) A computer model of the engine was used to obtain a preliminary power-balanced engine pressure schedule from which the necessary pump and turbine operating parameters and performance values were obtained.

(C) The inline turbopump design makes some of the engine-cycle requirements less rigorous than the advanced turbopump. Most obvious is the absence of the combustion seal which makes approximately 10 lb/sec more gas available to the turbine (since it is not used by the seal), providing additional power.

(U) A second factor is the lower operating speed: 30,000 rpm compared with 40,000 rpm for the advanced version. Assuming identical suction specific speeds for both designs, NPSH can be reduced by the speed ratio (0.75) to the 4/3 power, or approximately 33%. Thus, the power involved in the boost pump hydraulic drive loop can be reduced by a similar amount after a small adjustment is made for the extra pressure drop in the inlet scrolls.

(U) Other differences include reduced pressure loss in the turbine exhaust to secondary injector as well as reduced oxidizer housing and manifolding pressure losses.

(U) The net cycle benefits of increased power availability and reduced power losses can be used to varying degrees in one or more of the following typical ways: (1) reduced turbine gas temperature, (2) less stringent component efficiency, (3) single stage instead of two stage fuel pump, (4) increased bearing coolant flows, or (5) larger running clearances with higher leakages but less danger of rubbing. At the present, full advantage is taken of Item (2). Turbine temperature required is only slightly above that required for the advanced turbopump, in spite of lower component efficiencies.

### (2) Oxidizer Pump Analysis and Design

(U) The oxidizer pump is a single-stage centrifugal design with a separate inducer to obtain optimum cavitation performance. The impeller flow discharges radially across tandem diffuser vane rows and turns axially to enter 52 drilled holes in the housing which match the thrust chamber tubes. The analysis followed conventional practice throughout. The impeller is double shrouded and has front and back labyrinth or hydrostatic seals to minimize axial thrust without excessive leakage flow. Leakage losses were initially estimated for stepped labyrinths and later refined to account for the use of hydrostatic seal devices.

#### (a) Oxidizer Inducer

(C) The four vaned inducer is designed for a suction specific speed ($N_{ss}$) of 30,000 rpm $(gpm)^{1/2}/(NPSH)^{3/4}$. Inlet flow coefficient is 0.104, solidity with leading edge fairing is 1.75. Inlet tip diameter is 4.04 in., inlet hub-tip ratio ($r_n/r_t$) is 0.594. The hub tapers with an 8 degree half angle, with the vanes normal to the hub. The tapered inducer hub permits a more optimum main impeller hub contour and helps to avoid backflow along the inducer hub. The forward canted blades cause centrifugal force to partially off-set fluid loading, to minimize bending stress. In addition, such blades have a "cupped" geometry which gives them a modest increase in section modulus. Inducer material is AM 350.

(U) The inducer has an inlet vane angle of 10.42 degrees, giving an incidence to vane angle ratio (i/β) of 0.425 with vane blockage ignored. Optimum i/β has been empirically shown by Stripling to be 0.425.

(U) The inducer has been designed for leading edge loading, with only sufficient camber to account for the area change caused by the tapered hub. Design inducer head rise is 835 ft.

(U) Stress analysis of the inducer initially indicated excessive stress near the leading edge, especially in the tip region, requiring a moderate change in the fairing taper and a thickening of the leading edge. A positive margin of safety was achieved in this manner, on the basis of a modified Goodman Diagram, using a 1.25 factor of safety.

### (b) Pump Impeller

(C) The oxidizer-pump impeller is designed to accept the inducer exit flow with 3 degrees of incidence. Vane exit angle is 28 degrees and exit-flow coefficient is 0.120. Design pump head coefficient is 0.512 with an 11 vane impeller. Design exit diameter is 6.0 in.

(C) Impeller vane-angle (β) distribution was established to provide uniform vane loading conditions from inlet to exit. Design pump head rise is 9183 ft, at a flowrate of 1589 gpm. Overall pump specific speed is 1275. Stress analysis shows this impeller to have very low stress levels, under 60,000 psi throughout.

IV, D, Backup Turbopump (cont.)

### (c) Diffuser Vanes

(U) The required high headrise of the oxidizer impeller together with a relatively low pump-exit fluid velocity, requires that effective, efficient diffusers be employed. Thus, two diffuser vane rows have been used. The conventional first-diffuser row is designed in accordance with Aerojet practice which has been empirically verified on other programs. The design of the second row is an adaptation of cascade designs by Wislicenus, resulting in airfoil vane profiles.

(U) The first vane row diffuses the absolute evelocity from 395 to 270 ft/sec based on experience with conical diffusers. Design point incidence is 3.2 degrees. Predicted stall margin is slightly over 20% based on Titan IIA data. The fluid leaving the diffuser vanes retains a significant whirl, but eventually must enter the axially drilled passages, and the residual whirl energy would be lost. Thus the second vane row was added to remove a major portion of the residual whirl prior to entry into the axial passages. This second vane row turns the fluid approximately 30 degrees and reduces the absolute velocity from 220 to 130 ft/sec. Design stall margin is predicted to be approximately 20% on the second vane row as well. However, the actual performance of the two vane rows in series including the effects of channel wall boundary layer and channel wall curvature in the second vane row will require empirical resolution.

### (3) Fuel Pumps

(U) The fuel pump is a two-stage design, in which the first stage serves as an axial thrust piston as well. The second stage pumps approximately 20% of the flow to a high pressure to feed the primary combustor. The fuel pump also incorporates a separate inducer to obtain optimum suction performance. Design of this pump follows closely the methods mentioned previously.

### (a) Inducer

(C) The fuel inducer design is similar to the oxidizer inducer, featuring cylindrical tip and tapered hub. Design suction specific speed is 30,000 rpm. Inlet flow coefficient is 0.101, solidity with leading edge fairing is 1.75. Tip diameter is 3.60 in., hub-tip ratio (§) is 0.613. The hub has an 8 degree taper, and the blades are canted forward 8 degrees to optimize structural characteristics. Blade camber is only sufficient to account for hub taper. The inducer inlet angle is 10 degrees which results in an i/β ratio of 0.425 with vane blockage ignored. Design head rise is 660 ft. This inducer required changes similar to the oxidizer inducer to achieve acceptable stresses and a positive margin of safety.

### (b) First-Stage Fuel Impeller

(C) The first-stage fuel pump is designed to produce a head rise of 9500 ft at a flow rate of 1140 gpm. It uses a double shrouded impeller of 6 in. in diameter and a 28 degree vane exit angle. Inlet-flow coefficient is 0.134, discharge flow coefficient is 0.100. The predicted pump head coefficient is 0.542. Vane inlet angle is 13.8 degrees, giving 3.45 degrees of incidence. The vane angle distribution was established to achieve uniform head rise distribution. The impeller shrouds have radial and axial orifice faces, which provide automatic axial thrust balance capability.

(U) The thrust-balance function of this impeller required an unconventional shroud shape, and pressure relief holes in the hub. Stress analysis initially indicated yielding would occur at the pressure relief holes, presenting a low cycle-fatigue problem. Also the heavy shroud contour, required for the radial orifice faces at the impeller periphery, resulted in a relatively low burst speed of 39,000 rpm. A modification was made to the impeller to eliminate these problems which included extending the main vanes toward the impeller suction to provide better shroud support, reducing the shroud thickness, and shifting the impeller center of gravity to reduce localized bending stresses.

### (c) Diffuser

(U) The fuel diffuser is of conventional geometry, designed as straight-walled diffuser elements. Design incidence is 1.55 degrees. The absolute fluid velocity is diffused from 408 to 258 ft/sec. Exit angle is 13 degrees which closely approximates the volute spiral angle. Volute velocity is 100 ft/sec. The volute has twin exits into lines which join downstream in a Y-section just ahead of the secondary-injector fuel valve.

### (d) Second-Stage Fuel Pump

(C) The second-stage fuel pump receives flow from the first-stage volute through ten ports drilled in the housing. The impeller has swept-back vanes with an exit vane angle of 22-1/2 degrees. Impeller diameter is 4.5 in. Exit flow coefficient is 0.075. Design head rise is 5349 ft at a flowrate of 168 gpm. The low specific speed of this stage, 621 $\left(\frac{\text{rpm (gpm)}^{1/2}}{\text{ft}^{3/4}}\right)$, led to the use of an open-faced design to eliminate windage and leakage losses associated with the front shroud. The low specific speed, and low exit flow coefficient of this design also resulted in a very small fluid-exit angle, such that diffuser vanes were impractical. Since efficiency of this stage is not a significant factor, diffuser vanes were not used on this stage. A double exit collector was also used on this stage to minimize radial hydraulic loads. As on the first stage, the discharge lines form a "Y" just upstream from the control valve.

### (4) Turbine Design

(U) The turbine receives gas from an annular gas generator (preburner) surrounding the unit and exhausts across the secondary injector into the thrust chamber.

IV, D, Backup Turbopump (cont.)

### (a) Basic Sizing

(C) The turbine was designed to produce 10,500 bhp at a pressure ratio of 1.5. Turbine design inlet temperature was 1240°F. The cycle requires that the turbine receive the entire preburner gas flow at an inlet pressure of 4780 psia. The nozzle area is fixed by this requirement for a design flowrate of 238 lb/sec.

### (b) Turbine Nozzle

(U) Physical size of the turbine bearing housing dictated a slightly slanted nozzle passage. This geometry also reduces inlet losses from the primary combustor and improves the velocity profile at the rotor-blade inlet on the basis of considerations of radial equilibrium.

(C) The design conditions permit a favorable nozzle geometry. There are 17 nozzles with a height of 1.02 in., an efflux angle of 15 degrees and a total throat area of 4.60 $in.^2$. The nozzle material is Hastelloy 25, chosen because of its adequate high-temperature strength and good ductility. Material 713C is a suitable alternative.

### (c) Turbine Rotor Blading

(C) The rotor has 22 blades designed for radial equilibrium nozzle efflux conditions. The static pressure ahead of the blades varies from 3150 psia at the root to 3860 psia at the tip. Reaction varies from 3 to 52% from blade root to tip. The resulting blade is moderately twisted, with exit angles of 25 and 17 degrees at the root and tip, respectively.

(U) The blade profile is designed for good efficiency while maintaining acceptable structural and vibration characteristics.

The root section duplicates an impulse-type configuration found in a 1964 test program by NASA to have excellent efficiency, yet is relatively insensitive to fluid entrance angle. The tip section is similar to accepted commercial blading. Figure IV-34 shows the turbine cross section and blading profiles.

(U) The diagram efficiency of the turbine is 84%. Approximately 20 lb/sec tip leakage is predicted for a running clearance of 0.030 in. and reduces the efficiency to 77%. Assumed additional parasitic losses result in a predicted total to static efficiency of 75%.

### (d) Mechanical Design

(U) The rotor blade width was established from considerations of stress and vibration. Tension, bending, and shear stresses were considered, including oscillating loads caused by the nozzle wakes. The fluctuating loads include a magnification factor depending on the proximity of the forcing frequency to the natural frequency of the blade. The forcing frequency at 30,000 rpm is 8500 cps. Hollow blades were used to obtain a natural frequency of 12,800 cps, sufficiently above the 8500 cps forcing frequency to achieve an acceptably low magnification factor. The hollow blades also minimize the overhung weight of the turbine, giving a moderate improvement in critical speed. Blade stresses are acceptable with positive margins of safety using a 1.25 factor of safety. The mean stress levels are on the order of 80,000 psi.

(U) The rotor disc is mounted on the shaft by involute splines. (The required spline size dictated the 45 mm size of the turbine-end roller bearing which is installed from the turbine end.) The turbine disc is an approximately constant stress geometry. However, some first cycle yielding of the rim is predicted. This is a common and acceptable condition, resulting from combined thermal and centrifugal stresses. It occurs only on the first use cycle, thus does not create a cyclic fatigue problem.

IV, D, Backup Turbopump (cont.)

(U) The rotor disc and integral blades are designed to be machined from a one-piece forging of Udimet 700. Udimet 500 is an alternative material because of its excellent ductility. However, Udimet 700 has better high-temperature strength, and thus remains the first choice.

(U) At design conditions, the axial thrust of the turbine is under 1000 lb. The effect of a 5% pressure deviation ahead and behind the wheel, cause a 12,000-lb thrust. However, such a pressure deviation corresponds to a significant shift in turbine power, and represents an extreme condition, not associated with normal operation. The axial thrust balance system has a capacity of 30,000 lb, thus could accommodate such a condition if it did occur.

(U) The turbine gas exhausts with virtually no residual whirl at design conditions. The exhaust gas flows across guide vanes which serve to straighten the flow during start transient conditions, and then across the secondary injector and into the secondary chamber.

(U) The effect of heat radiation to the turbine from the high-temperature flame of the thrust chamber is predicted to increase the blade trailing edge temperature by only 32°F for the worst conditions, which assumes no shadowing by the secondary injector. This small temperature rise is insignificant.

(U) Predicted characteristic power, torque and weight-flow parameter curves for this turbine are presented in the ARES Engine Handbook.

### (5) Power Transmission Design

(U) The power transmission design involved several major aspects which are discussed in this section: critical-speed and deflection analysis, axial thrust analysis, bearing design, shaft design and seal design.

#### (a) Critical Speed

(U) A parametric critical-speed analysis was conducted during the concept selection phase of work and has been discussed in that section.

(U) Critical-speed analysis is performed with the aid of a comprehensive computer program to permit investigation of bearing and support stiffness effects in addition to the basic rotor rigidity and weight. It allows the use of nonlinear spring rates and damping for the various elements, thus gives an accurate prediction of the critical speed of the assembly.

(U) For the final design the first critical speed is predicted to be slightly over 42,000 rpm, giving more than 40% critical-speed margin. The second critical speed is well above the range of interest.

(U) Shaft deflection was also calculated. Maximum deflection occurs at the oxidizer impeller location. At nominal operating speed, the predicted deflection is approximately 0.0035 in., well within acceptable limits. All other locations have negligible deflections.

### (b) Axial Thrust Balance

(U) A computer study was performed to investigate the engine cycle effects of using the first-stage or second-stage fuel impeller as the axial thrust balance piston. Use of the second-stage impeller was originally considered because it appeared that less flow recirculation would result, and the fabrication and assembly sequence could be simplified. However, use of the second-stage impeller can have pronounced effects on the engine cycle balance even though total flow recirculation is less.

(U) The second-stage impeller supplies fuel to the primary combustor, and the potential H-Q Variations associated with thrust-balancer movement cause a shift in primary combustor mixture ratio. This in turn shifts the power balanced operating point by a substantial percentage. First-stage H-Q variation effects were found to be less by an order of magnitude. The results of this study were a deciding factor in selecting the first-stage fuel impeller as the thrust-balance piston.

(U) The main rotating elements, turbine oxidizer impeller, first- and second-stage fuel impeller were designed to be balanced individually to reduce axial forces on the shaft and to minimize effects of pressure variations. The mainstage oxidizer impeller is designed to have low pressure on the backside to match the force on the inlet side. The wear rings are located approximately the same radius at inlet and backside. The second-stage fuel impeller has backvanes to reduce backside force

(U) The thrust balancer on the first-stage fuel impeller consists of a labyrinth-land combination on both impeller shrouds (double acting). The labyrinth-land combination of flow restrictors in series is sensitive to axial movement and produces a load capacity of plus or minus 30,000 lb. A nominal operating clearance of 0.007-in. labyrinth and 0.010-in. land was chosen as a compromise between flow rate, balancer stiffness and variables affecting clearances such as pressure, thermal and centrifugal distortions. The total flow rate for the thrust balancer is 173 gpm in the neutral position.

### (c) Bearing Design

(U) Because of flow symmetry in the design, hydraulic loads are not expected to cause significant radial bearing loads. Bearing loads versus operating speed are obtained from the computer program for critical speed. Predicted nominal loads of 385 lb per bearing are significantly less than those successfully demonstrated during the bearing development program.

(U) The inline TPA bearings, their analysis, design and testing is discussed in Section IV,G.

### (d) Shaft Design

(C) The turbopump shaft transmits 10,500 hp at 30,000 rpm. Its stiffness is a significant factor in establishing critical speed. In addition, configuration of the shaft is closely related to the sequence by which the TPA must be assembled. Further, the shaft must be carefully designed to permit precise control of position of all shaft riding elements, since the relationship of rotating and stationary components is critical in high-speed, high-performance turbomachinery. Also, the required shaft size for adequate torsional strength and stiffness, establishes the required bearing size. Because of limitations on bearing DN, the shaft size must be as small as possible within the previous limitations.

(U) All the foregoing factors have been considered in defining an acceptable shaft configuration. A hollow shaft of AM 350 was also considered. However, it is not required for critical speed and does not achieve significant weight reduction. Thus there are no apparent advantages to warrant the added machining cost.

### (e) Interpropellant Seals

(U) Physical arrangement of the inline turbopump results in an interpropellant dynamic shaft seal between the propellant inlets. The seal environment is therefore cool and seal ΔP is always low, being related only to pump inlet pressure.

(U) Three methods of sealing were considered. One method was to leave a cavity open to atmosphere between back-to-back positive contact (rubbing) seals. This approach was rejected because the potential for contaminating the engine compartment with propellant in the event of seal failure. A second method was to enclose the interseal area and pressurize the cavity with an inert fluid. Dupont fluid PR143 was selected for this purpose. This method appears most effective in assuring positive separation of the propellants, even in the event of seal failure. However, the added complexity and weight of a seal purge supply system is necessary.

(U) The third design is essentially the same as the second method, except the rubbing contact seals are replaced by hydrostatic liftoff seals. Surface rubbing velocity is 325 ft/sec, dictated by turbopump speed and shaft-size. Such velocities are near the upper limit for rubbing contact seals. Hydrostatic liftoff seals do not rub in operation; therefore, they are not constrained by allowable surface speed limits. They do have a higher nominal leakage rate, and thus would require a larger purge fluid system. Both approaches provide a static seal when the pump is stopped.

(U) The inline turbopump has been designed to accommodate either of the latter two approaches interchangeably. Test results would be used to make the final dynamic seal selection.

(U) The purge fluid supply system consists of a one pint-container with a spring loaded bladder containing a low viscosity grade of Dupont PR143 fluid. The container is pressurized by oxidizer propellant to pump inlet pressure, which augments the spring loaded bladder and provides purge fluid to the seal cavity at slightly above the inlet pressure of either propellant.

(U) The purge-fluid flow is controlled by a valve made integral with the oxidizer inlet valve. Initial valve actuator travel opens only the purge valve, admitting purge fluid to the seal cavity. Further, valve travel opens the oxidizer valve a controlled time interval later. In closing, the oxidizer valve closes first, with terminal travel of the actuator closing the purge valve.

### (6) Housing

(U) In addition to the design effort on the inline TPA, design fabrication and proof testing of the housing were required by the Work Statement. A discussion of this effort is presented in Section IV,E.

### (7) Materials Summary

(U) Materials selected for the inline TPA were chosen on the basis of propellant compatibility and corrosion resistance, adequate strength, availability, ease of machining and welding, good ductility and toughness, and for high-temperature parts, the ability to withstand the thermal environment. The following table shows the selected materials.

| Item | Component | Material | Basis for Selection | Alternative | Remarks |
|---|---|---|---|---|---|
| 1 | Fuel pump housing elements | Forged Inconel 718 | High strength | | |
| 2 | Oxidizer housing elements | Forged Inconel 718 | High strength thermal environment | | |
| 3 | Shaft | Forged Inconel 718 | High strength thermal environment at turbine end | AM 350 | Alternative is acceptable if stress concentration avoided |
| 4 | Turbine rotor (integral blades) | Forged Udimet 700 | High temperature strength, ductility and toughness | Udimet 500 | Alternative is adequate but slightly less ductile |
| 5 | Turbine nozzle | Wrought Haynes Alloy 25 | High temperature strength, low coefficient of expansion, good weldability | 713 C | Either material equally acceptable |
| 6 | Turbine retainer nut | AM 350 | Machinability, adequate strength | Inconel X750 | Shaft to be chrome plated if of AM 350 |
| 7 | Primary combustor liner and turbine exhaust parts | Hastelloy X Sheet | Oxidation resistance at elevated temperatures weldability | Hastelloy 235 | |
| 8 | Pump inlets | Wrought AISI 347 | Good formability, good weldability | | |
| 9 | Oxidizer impeller | Forged AM 350 | High strength, fatigue resistance, weldable | Cast Al 359 | Cast impeller desirable for production |

| Item | Component | Material | Basis for Selection | Alternative | Remarks |
|---|---|---|---|---|---|
| 10 | Oxidizer inducer, first and second stage | AM 350 | High strength | | |
| 12 | Fuel impellers | Precedent 71A | Light weight | Al 356 | |
| 13 | Fuel inducer | AM 350 | AM 350 | High strength | |
| 14 | Turbine labyrinth | Felt metal | Thermal resistance tolerant to rubbing contact | | |
| 15 | Bearing races and rolling elements | 440C | Hardness, wear resistance, development experience history | K5-H (rolling elements) | K5-H is harder and more wear resistant, not readily machined |
| 16 | Bearing cages | Rulon P (with aluminum support ring) | Development experience, propellant compatibility | | |
| 17 | Fixed labyrinth over impellers (if used) | Glass-filled Teflon compression molded on aluminum support ring | Extrusion resistant, tolerates rubbing contact, test experience | | |
| 18 | Shaft spacers | SS 347 | Adequate strength, ease of machining | | |
| 19 | Shaft nuts and fuel end bolt | AM 350 | High strength, ease of machining, non-galling on Inconel 718 shaft | | |

IV. Turbopump Assembly (cont.)

## E. ENGINE HOUSING, INLINE CONFIGURATION

### 1. Objectives and Approach

(U) The objectives of the inline housing effort were to design, fabricate and test a housing to demonstrate its structural integrity. The design of the housing was constrained by several requirements including: direct adaptation to the ARES thrust chamber interface, incorporation of an integrated annular primary combustor, utilization of the same primary and secondary combustor fuel control valves, transmission of the thrust through the housing to the same gimbal block as the T-engine, a less integrated housing than the T housing which would be easier to fabricate, minimum size and weight, avoidance of high pressure static seals to atmosphere, and low deflections of a symmetrical type.

### 2. Structural Test Housing

#### a. Design and Analysis

##### (1) Design

(U) The in-line housing design shown in (Figure IV-35-a) was evolved within the constraints previously described. A transition section is provided between the turbopump housing and the thrust chamber which incorporates the annular primary injector, secondary injector and the manifolding required for each. This system increased the design flexibility of both the turbopump and thrust chamber assemblies and ensured minimum TPA/TCA interface problems.

(U) An annular primary injector similar to the primary injector designed and tested for the T-engine configuration was incorporated in the housing design. The turbine size limitations incurred by lower shaft speed caused a slight increase in diameter of the primary injector and combustion zone from 10.5-in. outside diameter and 7.00-in. inside diameter to 11.0-in. and 8.15-in., respectively. This increases the L* of the primary combustor slightly which should not adversely affect the performance of the primary injector. The thermal analysis of the oxidizer housing and turbine bearing and nozzle support revealed the desirability of a heat shield to protect the walls from the high velocity hot gases of the primary combustion zone. The heat shield was designed to reduce the gas velocity at the housing wall to less than 5 ft/sec.

(U) The primary and secondary valves designed for the T-engine turbopump are incorporated in the short adapter section with no changes required.

(U) All high pressure static seals include a redundant seal with the interseal cavity vented to inlet pressure through drilled passages.

(U) The thrust of the engine is transmitted from the thrust chamber to the thrust pad through an outer shell. This allows the fuel housing, oxidizer housing and inlet housings to be made as separate symmetrical units. Each of these units is aligned and welded in place. The turbopump housing is then stabilized by the welding of the two halves of the outer shell to the oxidizer housing and the fuel housing. The outer shell is pierced by symmetrical cutouts which provide exit for the inlet manifolds and access for instrumentation. The high moment of inertia of the outer shell provides a high resistance to radial misalignment of the fuel and oxidizer roller bearings. The stiffness of the outer shell also allows only small axial deflections between bearing housings.

IV, E, Engine Housing, Inline Configuration(cont.)

(U) The more conventional and symmetrical design of the fuel housings, propellant inlet manifolds and oxidizer housing allow the use of simple tooling and standardized methods for fabrication. This decreases tooling and manufacturing costs.

(U) The fuel and oxidizer housings were made of Inconel 718 forgings. The inlet manifolds were made of AISI 347 stampings and the outer shell halves were made of rolled Inconel 718 sheet material. This combination of materials provided the maximum strength where it was required as well as high resistance to corrosion. In addition it provided minimum weight. The housing as shown in (Figure IV-35-b) weighed 173 lb. The calculated weight of the fuel end cap, closure insert, and bearing support was 21 lb and that of the turbine bearing and nozzle support, 20.6 lb. The miscellaneous bolts, nuts and lines were estimated to weigh 39 lb. The primary injector and liner were combined with the secondary injector as a single unit. This would result in a weight saving over two separate units. The primary injector and liner portion was estimated at 56 lb.

(U) The structural test housing is shown in (Figure IV-35-b). The fuel end cap, closure insert and bearing support, turbine bearing and nozzle support, and the primary injector were simulated by test tooling. The test tooling was designed to produce equivalent loads on the housing that would be induced by the actual part. This allowed a considerable reduction in housing fabrication costs through the use of mild steel parts with no reduction in validity of testing.

(U) The main features of the in-line housing design are the symmetry of the inlet manifolds, the symmetry of load carrying members, the symmetry of loading and the placement of all hot parts on one end. The symmetry of loading and load carrying members reduces bending resistance requirements to a minimum. This results in a minimum weight structure. The hot parts contained on one end reduce the expansion and radial misalignment problems.

### (2) Analysis

#### (a) Stress Analysis

(U) The inline housing was analyzed for three load conditions: 1.21 x nominal design operating pressures and thrust without temperature, 1.21 x nominal design operating pressures and thrust with temperature, and the hydrotest pressures and thrust. The 1.21 x nominal design operating pressure and thrust condition was equivalent to the 10% turbine overspeed condition. The hydrotest pressures and thrust were 1.4 times the nominal design operating pressures and thrust, without temperature. No flight loads due to yaw, pitch, roll or gimbaling were considered.

(U) The inline housing was analyzed by using the finite element analysis method (Reference 7). The symmetrical features of the in-line housing simplified the analytical task. The results from the finite element analysis in many cases required no alteration. Some of the results required alteration by appropriate stress concentration factors to obtain the true stress and deflection values. The thermal gradient factors were approximate and stress values should be adjusted when new data from hot testing becomes available. The maximum calculated stress occurred on the inside of the oxidizer cylindrical wall near the oxidizer dome of 119,600 psi at 1.4 x nominal design pressure and thrust conditions. This was satisfactory based on the allowable stress of 140,000 psi. The stresses in the pump inlet sections were very low and the wall thicknesses used were based on structural stability rather than on stress considerations. The maximum outer shroud stress of 30,600 psi occurred at the junction of the outer shroud and the oxidizer housing.

### (b) Material Analysis

(U) Several materials such as AM350, AM355, Inconel 718, Haynes alloy 25, and AISI 347, were analyzed for the low- and high-pressure parts under corrosive and high-temperature conditions. The best combination was AISI 347 for the low-pressure components and Inconel 718 for the high-pressure components. AM350 showed promise except that the heat treatment process was time-consuming and expensive.

### (c) Welding Analysis

(U) The information available on the welding on Inconel 718 to AISI 347 was very meager. A small investigation of this potential problem revealed that Inconel 718 and AISI 347 could be readily welded with AISI 349 weld rod.

### b. Fabrication

(U) The fabrication of the in-line housing was relatively simple because it consisted primarily of machined forgings, plates, tubes, and stampings welded together. The various assemblies were stress relieved following each weld operation and dye penetrant and/or X-ray inspected. Because of the singular requirement only minimum tooling was used. This caused some alignment problems because of weld shrinkage but these were resolved by use of the weld shrinkage phenomena. The final housing assembly, Figure IV-36, was heat-treated and final machined without difficulties.

### c. Test

(C) The contractual requirements were to demonstrate the structural integrity of the inline housing. This included vibrational testing to define critical modes of vibration and structural testing with internal hydrostatic and external thrust loads applied. A thrust load of 140,000 lb and internal pressures to 1.4 times the nominal design operating pressure should be applied simultaneously.

(C) The testing of the inline housing was completed in four test series. The first series was the nominal design pressure without thrust test and the second series was the 50% of nominal thrust test without pressure. The third series was the 1.4 times nominal design operating pressure and thrust load test and the fourth series was the vibrational response test. The nominal design pressures were 5900 psi in Zone 1, Figure IV-38-a, 4575 psi in Zone 2; 3750 psi in Zone 3; 3035 psi in Zone 4; and 200 psig in Zone 5. The nominal thrust load was 100,000 lb.

(U) A total of 48 strain gages were applied to various surfaces of the inline housing. The hydrotest tooling was assembled as shown in Figure IV-37. The housing was placed in the external load test fixture, the 22 deflection transducers were attached and all instrumentation was connected to recorders and balanced. The pressure lines were attached, checked, and the unit was ready for testing.

### (1) Inline Housing Design Pressure Test

#### (a) Test Procedure

(U) The design pressure test required pressurization of all pressure zones, Figure IV-38-a, to nominal design pressure. The housing was held at nominal design pressure for approximately three minutes. The pressures were applied in increments simultaneously to each zone. The instrumentation was continuously recorded throughout the test.

IV, E, Engine Housing, Inline Configuration (cont.)

(b) Test

(U) The first test was discontinued at 57% of the nominal design pressure because of leakage through an instrumentation lead wire fitting which had been sealed with a plastic compound.

(U) The second test was performed after the leakage was repaired. The pressure levels for each zone were held for 160 sec. A quick review of the data revealed that the three deflection transducers on the oxidizer bearing location were inoperative. The unit was disassembled, the system repaired and reassembled as shown in Figure IV-38-b.

(U) The third test was successfully performed at nominal design pressure in each zone and held for 75 sec.

(c) Test Results

(U) The deflection between roller bearing locations, Figure IV-39-a in Test 3 was -0.0199 in. The maximum stress in the third test was 73,000 psi at the oxidizer housing flange. The fuel diffuser vane strain gage was not functioning during Test 3 but on Test 2, the fuel diffuser vane stress was -96,000 psi. The overall deflection of the housing from the oxidizer flange to the thrust plate was 0.018 in. at nominal design pressures. The outer shroud deflected inward slightly in the center between the hand holes in the shroud. There was neither damage nor permanent yielding during the test series.

IV, E, Engine Housing, Inline Configuration (cont.)

### (2) Inline Housing Thrust Test

#### (a) Test Procedure

(U) The thrust test required that a 50,000-lb load be placed on the housing in the axial direction while the housing was in an unpressurized condition. The housing was loaded by a hydraulic cylinder in the thrust loading fixture.

#### (b) Test

(U) A maximum thrust load of 50,000 lb was applied to the housing at the thrust pad and held for 200 sec. All instrumentation was continuously recorded throughout the test. The housing was filled with oil but each zone was vented to prevent pressure buildup due to the compressive loading.

#### (c) Test Results

(U) The thrust test showed that the outside shroud carried the thrust load as expected. The maximum stress was 17,600 psi on the inside of the conical portion of the outside shroud. The overall compression of the housing was 0.0094 in.

### (3) Inline Housing Proof Pressure and Thrust Load Test

#### (a) Test Procedure

(U) The inline housing proof pressure and thrust load test required that pressure and thrust loads equivalent to 1.4 times nominal design pressure and thrust be applied to the housing simultaneously. During this test no excessive deflections or any structural damage could occur. The thrust and pressure loads were applied simultaneously in increments by use of a 10,000 psi load marginator supplied by a 4.5 gal/min 10,000 psi pump.

### (b) Test

(U) The first test was discontinued after 25 sec at 1.4 times nominal design pressure and thrust due to two separate seal leaks which prevented the thrust load and Zone 1 pressure from reaching the full load level. The housing instrumentation plug and the line leading to the thrust jack had leaks. The leak in the line was repaired and a second pump was attached to Zone 4 only to supply sufficient oil capacity at the required 4500 psi.

(C) The second test was successfully held for 52 sec at proof pressure and thrust load. The test was discontinued when the potting compound in the instrumentation lead wire fitting in Zone 4 blew out. The sudden release of Zone 4 pressure caused a pressure differential increase across the oxidizer bearing housing simulator from 1850 to 6350 psi which resulted in failure of the 16 attachment bolts. Since the failure which resulted in test termination was structurally independent of the test specimen it was decided not to retest.

### (c) Test Results

(U) The results of the inline housing proof pressure and thrust load test are shown in Figure IV-39-b. The oxidizer end displacement was negligible. The fuel end displacement was linearly negative to approximately 90% of nominal design loads. At this point the fuel housing deflection reversed and a rapid expansion occurred. The cause for this appears to be due to a rolling tendency of the fuel housing under pressure and thrust load. The rotation of the fuel housing causes a column bending effect in the shroud and a reduction in the roll restraint on the fuel housing. This allows the fuel housing to move outward. Measurements before and after testing show no permanent set in any part of the inline housing after completion of testing. The deflection between bearing locations could be minimized by placing ribs along the outer shroud between the lightening holes and by increasing the roll resistance of the fuel housing. The roll resistance would be increased either by better location of the centroid of mass with respect to the shell load line, increasing the mass of the fuel housing to increase the moment of inertia or a combination of these two methods.

### (4) Inline Housing Vibration Test

#### (a) Test Procedure

(U) The inline housing as shown in Figure IV-36 was mounted vertically with the electrodynamic exciter attached to the thrust chamber end and supported from the thrust pad end by a shock cord. The housing was empty except for the test tooling. An input acceleration of 1g from 100 cps was applied by the electrodynamic exciter and acceleration outputs at various points were recorded by a hand held probe.

(U) (b) The first housing response was recorded at 403 cps. This was the response of the two inlet housings. The primary fuel pipe responded at 856 cps and the outer shroud at 913 cps. No other responses were found within 100 cps of the critical range as shown in Figure IV-40. The test results show that the inline housing has no critical modes of vibration in the operating range.

IV, E, Engine Housing, Inline Configuration (cont.)

### 3. Recommendations

(U) Some updating and modifications (Figure IV-33) were made to the in-line housing after initial fabrication and prior to testing. The housing shown in Figure IV-33 will require some additional redesign and analysis to incorporate the knowledge gained from the structural test program. The areas which will require examination are the oxidizer housing discharge flange, the oxidizer housing dome radius, the outer shroud, and the fuel housing resistance to rolling.

#### a. Oxidizer Housing Discharge Flange

(U) The oxidizer housing discharge flange exhibited a relatively large amount of roll during testing which caused high bending stresses in the outer cylindrical portion of the oxidizer housing. The stresses and rotation can be reduced by increasing the wall stiffness and/or by reducing the bending moment imposed by the bolt loads and internal pressure. In addition some bending moment is being induced in the outer cylinder by the small radius of curvature of the oxidizer dome. This area requires additional analysis and revision to optimize the dome radius.

#### b. Outer Shroud

(U) The outer shroud is a low stressed cylindrical unit which has several cutouts for hand holes and inlet ducts. The outer shroud provides stabilization between the oxidizer and fuel housings and transmits the thrust load from the oxidizer discharge flange to the thrust pad. As the fuel and oxidizer housings expand under pressure, the outer shroud ends are forced outward inducing a bending moment in the center portion. When an axial thrust load is applied, the unit reacts similar to a slender column which allows the fuel end to rotate outward. The outer shroud can be restrained by welding longitudinal strips along the outside of the shroud between the cutouts to stiffen this area.

c. Fuel Housing

(U) The fuel housing of the structural test model was a compact weldment which contained both the first and second fuel pump volute sections. The revised design in Figure IV-33 separates the two volutes. An analysis should be made of this area to determine the resistance to rolling, such as experienced in the structural test model, if the design is used.

IV, Turbopump Assembly (cont.)

## F. BOOST PUMP

### 1. Introduction

(U) The pump suction requirements for the ARES engine of 20 ft minimum net positive suction head (NPSH) would cause a severe weight penalty to the engine if boost pumps were not incorporated. The difference in weight between the present turbopump operating at 40,000 rpm and a design operating at less than 10,000 rpm, due to suction limitations, would be several thousand pounds. In comparison, the oxidizer and fuel boost pump weight is only 70 lb.

(U) The ARES boost pumps have a separate hydraulic turbine mounted on the boost-pump impeller (Figure IV-41). The hydraulic turbine requires approximately 16% of the main-stage pump flow at pump discharge pressure to drive the boost-pump impeller. This fluid-coupled method of driving the boost pumps was selected over other concepts such as gear reductions or coaxial drives because it is much simpler and less expensive. Another significant advantage of the separate turbine is that it allows flexibility in boost pump location. This flexibility permits tank-mounted units, eliminating boost-pump suction line losses. It minimizes the dynamic depression in suction pressures, which contributes significantly to boost pump cavitation during the engine start transient. It also reduces the engine gimballed weight and results in lighter weight gimbal actuators and support structure.

(U) A design similar to the ARES boost pumps has been designed and tested by Aerojet-General to demonstrate the feasibility of this concept (Reference 8). This program evaluated the steady-state performance. The dynamic performance of this unit coupled to a gas-generator-turbine-driven pump was conducted by the Air Force Rocket Propulsion Laboratory, Edwards, California (Reference 9) and the characteristics of this fluid coupled system were found to be very stable under various rapid start sequences.

(U) The Air Force gas-generator-turbine-driven pump tests noted above and the ARES tank head start engine have start transient accelerations times of approximately one second. Consequently these tests, plus Aerojet's dynamic computer model of the ARES engine, demonstrate that the selected fluid-coupled boost-pump concept can meet the NPSH requirements of the main-stage pump during the rapid acceleration phase of the engine start transient.

## 2. Design Requirements

(U) The ARES work statement specification for pump suction performance requires that the boost pumps operate at 20 ft minimum NPSH. Both the "T" and "Inline" turbopumps have been designed to meet this specification. The boost pumps were designed to meet the T-engine pump head requirements, since they are approximately 430 ft, whereas the "Inline" engine only requires 350 ft. The boost pumps will also meet the "Inline-design" requirement, but must operate slightly off-design and at lower speeds (Figure IV-41). The current operating points for the "T" and "Inline" boost pumps are given in Appendix I, Sections 2 and 9, respectively.

(U) To minimize low frequency pressure oscillations generated by inducers under severe cavitating conditions, conservative operating suction specific speeds of approximately 25,000 to 30,000 were selected. The inlet diameters, which are primarily a function of NPSH and independent of speed, were sized for approximately 10 ft of NPSH, resulting in maximum suction specific speeds of 45,000 for both fuel and oxidizer at 8000 rpm. The suction specific speeds at 20 ft of NPSH are 30,000 and 24,400 for the oxidizer and fuel, respectively. Under these operating conditions the predicted head loss due to cavitation is less than 1%.

(U) Utilizing component design information obtained from the hydraulic-turbine-driven low-speed inducer tests (Reference 8), the final boost-pump and hydraulic-turbine-design requirements were established; the design specification is given in Appendix I, Section 4.

3. Configuration

(U) The boost-pump specific speeds are in the range, 2500 to 3000, which indicates the design can be either a mixed-flow impeller design (discharges between the radial and axial direction) or axial flow.

(U) Preliminary studies showed the axial flow design was smaller, but inherently had a high axial thrust and would require a thrust compensating device. However, the mixed flow design does not have this high-axial-thrust problem since the larger impeller discharge diameter permits the use of backvanes for pressure balancing. Consequently, the mixed-flow configuration, which weighs 35 lb, was selected due to simplicity in the design. If the aluminum components (impeller and discharge housing) were replaced with steel parts in the $N_2O_4$ oxidizer boost pump to eliminate the potential "salting" problem, the weight would increase by approximately 15 lb.

(U) Preliminary studies also revealed that the size and hydraulic design requirements of the fuel and oxidizer boost pumps were very similar. Therefore, the decision was made to use as many interchangeable parts as possible. This approach significantly reduces engineering, fabrication, and hardware replacement costs with only a slight penalty to engine weight of approximately 7 lb. As a result of this approach, the power transmission, boost-pump discharge housing, hydraulic turbine rotor, and hydraulic-turbine-nozzle design were made interchangeable between the two units.

IV, F, Boost Pump (cont.)

### 4. Design Analysis

(U) This section discusses the detailed design of the pumps, turbine, propellant lubricated bearings, axial thrust balance, and shaft critical speed.

#### a. Pumps

##### (1) Hydraulic Design

(C) The oxidizer boost pump (Figure IV-42), has a design capacity of 1243 gpm and design head rise of 444 ft at the 8000 rpm operating speed. The corresponding specific speed of 2950 is in the range of conventional mixed-flow impeller designs.

(U) The impeller inlet diameter was established by the inducer design criteria of having the inlet velocity head equal to one third the NPSH. The required inlet diameter is 5.66 in. The design inlet tip flow coefficient is 0.084, and the corresponding tip blade angle is 8.4°. This blade setting is obtained from inducer test results which show the optimum fluid incidence to vane angle ratio is approximately 0.425.

(U) The impeller discharge diameter and flow coefficient were selected on the basis of test data obtained from the hydraulic-turbine-driven low-speed inducer program (Ref 1), and also the criteria of matching a single diffuser design to both boost-pump impeller-discharge flow conditions.

IV, F, Boost Pump (cont.)

(C) The fuel boost pump (Figure IV-43), has a design capacity of 824 gpm and a design head rise of 409 ft at the 8000 rpm operating speed. The specific speed of 2500 is also within the range of mixed-flow impeller designs.

(U) The inlet diameter was made the same as the oxidizer pump for interchangeability of housings; however, inlet tip flow coefficient is 0.071 and the corresponding blade angle for a fluid-incidence-to-vane-angle ratio of 0.425 is 7.10°.

(U) The oxidizer fluid angle at the stator inlet, including the hydraulic turbine discharge flow, is 26° while the fuel fluid angle is 20°. The discharge housing diffuser design consists of eight vanes with a mean inlet angle of 27°. This blade angle setting appears optimum for matching both flows based on our experience with similar types of designs such as the M-1 fuel pump inducer. The diffuser discharges the flow in an axial direction and has acceptable outlet-to-inlet absolute velocity ratios of 0.71 and 0.54 for the oxidizer and fuel, respectively.

(C) A summary of the significant design parameters for both boost pumps is listed below:

BOOST-PUMP DESIGN PARAMETERS

| | FUEL | OXIDIZER |
|---|---|---|
| Speed, rpm | 8000 | 8000 |
| Flow, gpm | 824 | 1243 |
| Head rise, ft | 409 | 444 |
| Impeller inlet diameter, in. | 5.66 | 5.66 |
| Impeller inlet vane angle (TIP), degree | 7.10 | 8.50 |
| Impeller inlet hub/tip ratio | 0.5 | 0.22 |

IV, F, Boost Pump (cont.)

| | FUEL | OXIDIZER |
|---|---|---|
| No. of impeller inlet vanes | 3 | 3 |
| No. of impeller outlet vanes | 6 | 6 |
| Impeller-discharge flow coefficient | 0.14 | 0.18 |
| Impeller-discharge diameter (mean), in. | 6.0 | 6.0 |
| Impeller discharge port width, in. | 0.596 | 0.740 |
| Impeller discharge angle (mean), degree | 20.0 | 26.0 |
| No. of diffuser vanes | 8 | |
| Diffuser inlet diameter (mean), in. | 7.24 | |
| Diffuser inlet port width | 0.600 | |
| Diffuser inlet angle (mean), degree | 27.0 | |
| Diffuser outlet diameter (mean), in. | 2.58 | |
| Diffuser outlet angle, degree | 90 | |

(2) Mechanical Design

(U) The highest stressed area of high suction specific speed impellers is generally located at the root of the impeller vane near the inlet. The combined stresses (centrifugal plus hydraulic loads) at this location are 25,200 and 15,600 psi for the oxidizer and fuel impellers, respectively, at the 110% overspeed condition. The allowable stress for the impeller material, forged AL-7075, is 38,000 psi, which allows an adequate margin of safety.

(U) The boost-pump discharge-housing pressure of 300 psi or less results in very low stator vane housing stresses. The housing will be cast from AL-356, and the minimum wall thicknesses requirements preclude high stresses.

IV, F, Boost Pump (cont.)

### (3) Performance

(U) The predicted inducer performance is shown in Figure IV-41 and referenced in Appendix I, Section 4. The characteristic shape of the head versus flow was obtained from test data of a similar type pump (Reference 8). The estimated efficiency at design flow for the ARES boost pumps was assumed to be the same as that obtained from the pump noted above.

(U) The inducer suction specific speed performance, percent head loss versus suction specific speed referenced in Appendix I, was based on test data from the 43,000 suction specific speed M-1 fuel inducer.

### (4) Component Tests

(U) Performance evaluation of the boost pump impeller in Phase II will consist of two test series in AGC pump facilities. The first series will be cavitating and noncavitating tests where the impellers will be driven at rated speed with an electric motor. These tests will establish the noncavitating head and efficiency versus flow from 0 to 120% of design flow and the cavitating performance up to suction specific speeds of 45,000. The second test series will consist of bootstrap tests where the main stage pumps are driven by the electric motor, and boost pumps will be driven with the pump-fed hydraulic turbine. This test series will simulate engine operations and will provide interaction effects and overall performance characteristics of the pumping systems.

IV, F, Boost Pump (cont.)

### b. Turbine

#### (1) Hydraulic Design

(U) The hydraulic designs of the fuel and oxidizer drive turbines are based on the nominal operating conditions, specified in Appendix I, Section 4. Studies of the oxidizer and fuel drive turbines showed that both designs could be identical without effecting the turbine efficiency substantially. The requirements result in a low specific speed and, consequently, low partial admission. The estimated turbine efficiencies are difficult to predict accurately because reliable information on low partial admission turbines is scarce. Therefore, the turbine rotor blades were shrouded to improve the efficiency and also lower blade stresses.

(U) The rotor and stator blades have constant-sections (no twist) with constant hub and tip annulus radii. The selected blade heights of 0.3 in. result in nozzle admissions of 4.96 and 3.6% for the oxidizer and fuel turbine, respectively. A summary of the significant design parameters is as follows:

DESIGN PARAMETERS

| | OXIDIZER | FUEL |
|---|---|---|
| shp - shaft horsepower | 306 | 118 |
| N - Speed, rpm | 8000 | 8000 |
| $\Delta P$ - pressure drop, psi | 5248 | 3251 |
| H - head, - ft | 8440 | 8330 |
| Q - flow, $ft^3/sec$ | 0.447 | 0.320 |
| $N_s$ - specific speed, $ft^{3/4}\ sec^{-1/2}\ min^{-1}$ | 6.09 | 5.20 |
| $D_s$ - specific diameter, $ft^{1/4}\ sec^{1/2}$ | 9.00 | 10.60 |
| Um - mean blade speed, ft/sec | 253 | 253 |

IV, F, Boost Pump (cont.)

| | OXIDIZER | FUEL |
|---|---|---|
| $C_o$ - fluid jet velocity, ft/sec | 738 | 732 |
| $Um/C_o$ - velocity ratio | 0.343 | 0.346 |
| $\eta$ - efficiency | 0.50 | 0.43 |

(U) The efficiencies are near optimum for the given conditions. The optimum efficiency moves to lower velocity ratios, $U_m/C_o$, with reducing admission. The predicted design efficiencies of 0.50 and 0.43 for the oxidizer and fuel turbine respectively, may be optimistic; however, the hydraulic turbine efficiency does not affect the overall engine performance critically.

### (2) Mechanical Design

(U) The maximum mechanical load occurs with the oxidizer turbine at 8800 rpm and 427 hp. At this condition, the maximum rotor fluctuating stress (centrifugal stresses are negligible) is 15,400 psi. The endurance limit of the rotor material, AM 355, is 80,000 psi, and thus the safety factor is 5.2. This high safety factor is a result of the following reasoning. No satisfactory method is known to account for the adverse effect of partial admission rotor blade stresses. As the efficiency and weight penalties are not significant, the conservative approach was taken to ensure a high reliability against blade failures.

(U) The maximum nozzle stresses assuming simply supported ends are 43,700 psi. These stresses are also conservative for the selected material AM 355, which has a yield strength of 181,000 psi.

IV, F, Boost Pump (cont.)

### (3) Component Test Plan

(U) During Phase II, component tests will be conducted in AGC pump-test facilities to verify predicted turbine-design and off-design performance. The turbine will be mounted on a dummy inducer (no vanes) coupled to an electric dynamometer. High pressure water from a pump located in the adjacent test bay will be used as the turbine drive fluid and tests will be conducted with partial admission nozzles of 3.60, 4.96, and 6.50% to verify the relationship of turbine efficiency versus percent admission over a wide range of speeds and flows. Test fixtures have been designed for this work.

## c. Power Transmission

### (1) Design Requirements

(U) The boost pump power transmission requirements were established by the oxidizer design since this pump has the higher axial and radial loads. These requirements are: (1) the first lateral resonant frequency (critical speed) must be 20% above the design speed of 8000 rpm and (2) the propellant-lubricated bearings must have the capacity to carry 1200-lb axial load and 800-lb radial load with a minimum life of 10 hr.

(U) The bearing radial loads are caused by the partial admission turbine and not by the pump, which has a symmetrical discharge housing. The maximum force generated by the single-entry turbine results in an 800-lb radial load on the bearing nearest the impeller and 270 lb on the bearing nearest the boost pump discharge (Figure IV-42). In order to ensure the thrust-bearing axial load is always greater than the radial load, a roller bearing was selected for the high-radial-load side and a ball bearing was chosen to carry the smaller radial load and the 1200-lb axial-thrust load.

### (2) Critical Speed

(U) The critical speed analysis performed with an aluminum impeller and steel turbine rotor indicates the first lateral resonant frequency is over five times (44,000 rpm) the nominal operating speed, with expected bearing stiffnesses of 2.5 x $10^5$ lb/in. The critical speed of the rotating shaft assembly with a steel impeller and steel turbine rotor is 34,000 rpm. Both figures exceed the design requirement considerably. Substituting a steel oxidizer impeller for the aluminum impeller would increase the boost pump weight by six lb.

### (3) Axial Thrust

(U) The axial thrust of mixed-flow impeller designs is considerably lower than that for axial flow impellers, and this was a major factor in selecting the mixed flow design. The calculated axial thrust for the selected design is 600 lb acting towards the pump suction (Figure IV-44) while a corresponding thrust of 4100 lb would result from an axial-flow design without the use of a balance piston.

(U) The key parameter which controls the impeller axial thrust in the mixed-flow design is the impeller-back-bane pressure distribution. The pressure is a function of the back-vane height, clearance, and diameter ratio. Empirical data from Aerojet-General Corporation pump tests and test results from other investigators was used to establish the boost pump value of K = 0.82, where "K" is the ratio of the fluid tangential velocity to the back-vane tangential velocity. Since the axial thrust can be modified by changes in the back-vane geometry, boost-pump water tests in Phase II will be used to make final adjustment in the back-vane geometry and corresponding axial thrust.

### (4) Bearing Design

(U) The boost-pump shaft is supported radially by a 205 (25 mm bore) size roller bearing located at the impeller end and a 304 (20 mm bore) size ball bearing at the pump discharge end. Axial load support is provided by the 304 ball bearing. These larger bearings (205 and 304 versus 105 and 104) were selected for longer life expectancies. At this relatively low speed (8000 rpm) the rolling element centrifugal forces are insignificant (2 lb per element) and the larger bearings are practical. The $B_{10}$ life at the boost pump loads were calculated to be 190 hr for the 205 roller bearing and 86 hr for the 304 ball bearing.

(U) A1S1 440C stainless steel was selected for the races and rolling elements of both bearings. The cages are of the configurations used in the successful 40,000 rpm bearing testing. Both ball- and roller-bearing cages are 25% glass-filled Teflon with stainless steel containment shrouds. The ball-bearing cage is inner race riding while the roller-bearing cage is outer race riding.

(U) The roller bearing has 11 rollers of 7.5 mm dia x 9 mm long (L/D = 1.2). The ball bearing has eight balls of 11/32 in. dia and has a 25° contact angle. The ball bearing outer and inner race curvatures are 52 and 53%, respectively.

(U) A 10-micron filter is located at the discharge end of the boost-pump diffuser center body (figure IV-42 and -43), where 5 to 10 gpm of propellant is recirculated to the impeller discharge by the impeller back vanes for bearing lubrication. The flow rate is controlled by the filter element pressure drop.

## G. PROPELLANT-LUBRICATED BEARINGS

### 1. Objectives and Approach

(U) The objectives of the propellant lubricated bearing program were to demonstrate $N_2O_4$ and AeroZINE 50 lubricated rolling contact bearings at DN values of $1.25 \times 10^6$ and $1.6 \times 10^6$. Program requirements as specified by the contract work statement were as follows:

(U) a. Conduct initial testing at 25,000 rpm using 210 size (50 mm bore) bearings to evaluate improved cage designs for operation in $N_2O_4$. The criteria for success was a test series with a total of 12-min cumulative duration at a rotative speed of 25,000 rpm with 2500-lb axial load on a single ball bearing, and 1000-lb radial load on each of two roller bearings.

(U) b. Conduct testing at 31,250 rpm using 108 size (40 mm bore) $N_2O_4$ and AeroZINE 50 lubricated bearings to provide demonstration data of ball and roller bearings for the inline (backup) turbopump design. The criteria of success was a single test of 6-min duration at a rotative speed of 31,250 rpm with minimum steady state loads of 2200-lb axial on a duplex load sharing ball bearing set and 500-lb radial on the single roller bearing. Peak loads of 4400-lb axial and 1000-lb radial were to be applied for at least 8 sec during the in duration.

(U) c. Conduct testing at 40,000 rpm using 108 size (40 mm bore) $N_2O_4$ and AeroZINE 50 lubricated bearings to provide demonstration data of ball and roller bearings for the T-engine (advanced) turbopump design. The criteria for success was a minimum of two tests on a given set of bearings with a total of 12-min cumulative duration at a rotative speed of 40,000 rpm with minimum steady state loads of 1500-lb axial on a duplex load sharing ball bearing set and 500-lb radial on the single roller bearing. Peak loads of 2500-lb axial and 1000-lb radial were to be applied for at least 8 sec during the 12-min duration. During this test series, bearing minimum operating clearances and misaligned operation of the roller bearing were to be investigated.

(U) The bearings had to be in reusable condition after the achievement of the cumulative durations to be considered satisfactory tests. The test hardware was made available for the Air Force Project Officer or his designee at the completion of each achievement test series.

(U) The feasibility of flooded rolling contact bearing operation in $N_2O_4$ and AeroZINE 50 was proven under the pre-ARES ICP program contract AF 04(611)-8548 (Reference 10). During that testing, several 210 series roller bearing cages fabricated of Armalon material operated satisfactorily in $N_2O_4$ at 20,000 rpm but failed at 25,000 rpm. Successful operation was obtained with both Rulon-A and carbon graphite roller bearing cages at 25,000 rpm in AeroZINE 50. Rulon-A was also successfully demonstrated at 20,000 rpm in $N_2O_4$. The maroon color of the Rulon-A bleached out during the $N_2O_4$ exposure, but no structural problem was noted. During the ICP program various methods of propellant lubrication were studied. The simplest system, flooded lubrication with series flow, was selected and successfully demonstrated. The same approach was used during the ARES program.

(U) The ARES bearing program consisted of three phases. The first phase, 25,000 rpm testing of 210 series (50 mm bore) ball and roller bearings in $N_2O_4$, was directed at solving the residual cage problems mentioned above. The second phase, 40,000 rpm testing of 108 series (40 mm bore) ball and roller bearings in both $N_2O_4$ and AeroZINE 50, was directed at evaluating

IV, G, Propellant-Lubricated Bearings (cont.)

designs for the T-engine turbopump. The third phase, 31,250 rpm testing of 108 series (40 mm bore) ball and roller bearings in both $N_2O_4$ and AeroZINE 50, was directed at evaluating bearing designs for the inline turbopump and included higher loads on the ball bearings.

(U) All phases of testing were completed with excellent results. All of the requirements of the work statement were met, and all of the bearing components used in the work statement certification tests were in reusable condition.

### 2. Design and Testing of 25,000 rpm Bearings in $N_2O_4$

(U) This task was to design and evaluate new bearing cage designs utilizing residual 210 size ball and roller bearings from the pre-ARES ICP bearing program. Successful designs were to then be incorporated in the 40,000-rpm and 31,250-rpm test bearings. Based upon the ICP test results, 25% glass-filled Teflon was selected as the cage material. Design was mainly directed at alternative Teflon containment configurations (shrouds) and the method of guiding the cage (outer race versus inner race guiding). Primary concern was cage web thickness. Minimum web thickness at the rolling element pitch line was held to 0.150 in.

(U) Successful ball and roller bearing cage designs are shown in Figure IV-45. The Teflon was contained by a single-piece machined aluminum shroud consisting of two side plates connected on the OD by axial rails located over each Teflon web. The cage was designed to ride the outer race on Teflon pads located on the outer diameter and on each side of each pocket.

(U) Testing was completed with excellent results. All of the requirements of the work statement were met in the first three tests; all of the bearing components were in perfect condition after testing. The total time accrued on the bearing cages during this test series was 16 min of which 14 min and 35 sec were at 25,000 rpm or better. These tests are summarized in Figure IV-46 and consisted of seven starts with durations varying from 15 to 353 sec. Maximum speed was 26,500 rpm (DN = $1.33 \times 10^6$); maximum radial load was 2985 lb on a single ball bearing and maximum radial load was 2329 lb shared by two roller bearings (the test configuration consisted of a single ball bearing straddled by two roller bearings). The bearings were loaded by hydraulic load cylinders and were lubricated in series by the flow of $N_2O_4$.

(U) Additional tests, not required by the work statement, were conducted for turbopump design. Successful bearing operation at flows of 15 gpm, more than three that required for cooling, was achieved during Test 5. The bearings were again in excellent condition.

(U) A failure of the ball bearing occurred during Test 4. The test was terminated after approximately 5-1/2 min because of rising test bearing temperatures. Disassembly of the test hardware revealed that the ball bearing had failed. The race shoulders were rolled over, and the loaded side of the inner race was brinnelled and showed evidence of severe misalignment. The failure was not a result of the bearing design but the result of an improper assembly. The normal assembly procedure was to shim the outer race bearing stack 0.001 to 0.002 in. loose. This allows the ball bearing outer race freedom to center radially in a housing outer race relief when subjected to centrifugal and axial forces. This design and assembly procedure isolates the ball bearing from externally applied radial loads. An error in the buildup prior to this test resulted in outer race lockup which in turn subjected the ball bearing to combined high radial and axial loads under a misaligned position. Both roller bearings and all cages were in good condition and were considered reusable. The temperature rise of both the propellant and ball bearing outer race was about 50°F for steady-state conditions. At the indication of trouble the temperature deviation from these steady-state values was instantaneous and the temperature rises were about 70°F for the propellant and about 100°F for the bearing.

(U) During this test series the bearings were disassembled and cleaned after each test. Pitting occurs in 440c material if it is exposed to atmospheric conditions without proper cleaning. Between Tests 5a and 5b, to prevent atmospheric exposure, the bearings were left immersed in $N_2O_4$ for 24 hr. After Test 5d the bearings were removed, cleaned, and found to be like new.

### 3. Description of 40,000- and 31,250-rpm Tester

(U) A new tester for testing $N_2O_4$ and AeroZINE 50 lubricated bearings at speeds up to 40,000 rpm was designed as shown in Figure IV-47. The tester consisted of a turbine drive, power transmission, and a test head. The power transmission imparted the required torque through a shaft, which was radially supported in the drive housing by two roller bearings; one of these bearings was the test roller bearing and was lubricated by the test propellant. Axial positioning was provided by a hydrostatic thrust bearing. A separate positive displacement pump supplied 20 gpm of 4000 psig oil to the hydrostatic bearing pockets. Before scavenging, the oil discharge from this bearing lubricated the two centrally located radial loading roller bearings and the shaft support roller bearing at the turbine end.

(U) Power was supplied to the shaft by a single stage partial admission impulse drive turbine attached directly to the shaft as shown. Ambient-temperature nitrogen gas flowing through two sonic nozzles provided energy to the turbine rotor. The test propellant and the oil lubricating the power transmission were kept separate by a combined purge and drain labyrinth shaft seal system.

(U) The test bearings were mounted on the shaft end and encased in a cover housing (refer to Figure IV-47). The test ball-bearing tandem-load-sharing set was mounted in a cantilevered flexible housing, designed for the turbopumps. This housing was stiff in the axial direction but flexible in the radial direction.

(U) Axial load was applied to the ball-bearing set by means of a loading piston provided in the test bearing cover housing. Radial load was applied by a loading piston, which pulls upward on the shaft center by means of two "slave" bearings mounted in a loading ring.

### 4. Design of Ball Bearings for 40,000 rpm Propellant-Lubricated ($N_2O_4$ and AeroZINE 50) Operation

(U) Both the T-engine and inline engine turbopumps incorporate 108 size ball bearings lubricated with AeroZINE 50. The bearing arrangement required for the turbopumps is discussed in Sections IV-B and IV-D. Ball bearing operation in $N_2O_4$ was not required for the final turbopump designs but was a requirement of the program work statement. The high loads required by the work statement made it necessary to match-grind two ball bearing races for load sharing.

(U) This design incorporated two split inner race bearings with full curvature outer raceways. Bearing internal geometry was optimized for the requirements using the existing computer program.

(U) This geometry is summarized as follows:

| | |
|---|---|
| Ball complement | 14 |
| Ball diameter | 11/32 in. |
| Contact angle (free) | 25° |
| Outer race curvature | 52% |
| Inner race curvature | 53% |
| Axial play* (unmounted) | 0.009 to 0.012 in. |
| Class | ABEC-7 |

(U) Both races were 440C and the balls were K-5-H (tungsten-titanium carbide manufactured by Kenametal, Latrobe, Pa.) for AeroZINE 50 operation. This combination resulted in superior performance in AeroZINE 50 during the ICP bearing testing (Reference 10). The balls were 440C for $N_2O_4$ operation.

(U) A comparison of the ball to race mean stress levels for bearings with K-5-H balls and 440C races for the 25,000, 31,250, and 40,000 rpm requirements are summarized below.

---

*For the DB arrangement, required for the T-engine and inline engine turbopumps, the races are ground so all axial play of the bearing assembly is removed.

IV, G, Propellant-Lubricated Bearings (cont.)

| Bearing Size<br>Speed, rpm | 210<br>25,000 | 108<br>31,250 | 108<br>40,000 |
|---|---|---|---|
| Steady State | | | |
| Axial load, lb | 2500 | 1320* | 900* |
| Inner race stress, psi | 292,000 | 273,000 | 243,000 |
| Outer race stress, psi | 266,000 | 247,000 | 220,000 |
| Peak Load | | | |
| Axial load | Same as steady state | 2640* | 1500* |
| Inner race stress, psi | Same as steady state | 336,000 | 288,000 |
| Outer race stress, psi | Same as steady state | 304,000 | 250,000 |

(U) It should be noted that the stress levels at the highest speed turbopump applications were not higher than those demonstrated during the 25,000 rpm ICP bearing testing.

(U) Several ball-cage designs were fabricated for testing. All designs incorporated Teflon with a 25% glass fill. Both inner and outer race designs with variations of containment shrouds were fabricated and tested. The cages similar to the design successfully tested at 25,000 (see Figure IV-45) were not of good quality (the aluminum rails were not contained in channels of Teflon) (refer to Figure IV-45) and were never tested. A replacement order was placed but cancelled when successful operation was obtained with an alternative design. This alternative design, shown in the right side of Figure IV-48, incorporated 14 pockets with 0.100-in.-thick webs between the pockets and was inner race riding. The design shown on the left is a modification of the same design made during the 40,000 rpm testing in AeroZINE 50. This modification incorporated rivets in each web (the original design incorporated rivets in only two webs) and radial cutouts of the guiding surface (inside diameter) at each ball pocket. This modification provided additional coolant flow over the ball and inner race contact area.

---

*Axial load was applied to a tandem load sharing set of ball bearings. The highest loaded bearing in the set is assumed to carry 60% of the applied load.

### 5. Design of Ball Bearings for 31,250 rpm for Propellant-Lubricated ($N_2O_4$ and AeroZINE 50) Operation

(U) The design for the 31,250 rpm ball bearing testing was the same as that initially used for the 40,000 rpm testing. The cage design modifications discussed above were not necessary for the 31,250 rpm requirements but were also incorporated in the final design for the inline turbopump to provide extra margin of safety. The race to ball stress levels at the required test conditions are summarized above in the 40,000 rpm ball bearing design for comparisons.

### 6. Design of Roller Bearings for 40,000 rpm Propellant-Lubricated ($N_2O_4$ and AeroZINE 50) Operation

(U) The roller bearing designs for either $N_2O_4$ or AeroZINE 50 operation were the same. The internal geometry of the final bearing after testing is summarized as follows:

| | |
|---|---|
| Roller complement | 13 |
| Roller size | 0.320 in. dia x 0.360 in. long |
| L/D | 1.125 |
| Roller crown | 28 in. radius x 0.075 long (both sides) |
| Radial play (unmounted)* | 0.001 to 0.0014 |
| Class | RBEC 7 |

---

*Roller bearings with radial play (unmounted) of 0.0015 to 0.0019 in. were also tested.

(U) Misaligned operation required that the roller bearing have a built-in aligning mechanism. Figure IV-14 shows how roller bearing life ($B_{10}$-oil lubricated) decreases rapidly with the misaligned operation when no alignment device is used. The mechanism used for this design was a spherical mounting of the outer race (refer to Figure IV-14). The outer race incorporated a spherical outer diameter and was mounted in a mating spherical ring. To reduce the coefficient of friction, a 0.004-in.-thick glass-filled Teflon film was bonded on the inside spherical surface of the mounting ring. The bearing outer race was fitted to the spherical mounting ring with a slight interference fit, in the order of 0.0002 in.

(U) Two bearings of this design were fabricated of two different material combinations. The primary design incorporated both races and rollers of 440C material. This bearing was planned for the testing in $N_2O_4$ and was available for the testing in AeroZINE 50. The second design incorporated a 440C inner race, K-5-H outer race, and K-5-H rollers. This bearing was planned for testing in AeroZINE 50. During the test program appreciable roller end wear resulted during the testing in AeroZINE 50; only slight burnishing was noted in the tests conducted in $N_2O_4$. The material combination of K-5-H on 440C was selected on the basis of the good results obtained during both a four ball bearing material investigation and tests of 210 size bearings at 25,000 in AeroZINE 50 with the K-5-H and 440C combination conducted during the ICP bearing program (Reference 10).

(U) The comparison of the mean stress levels of these two bearing designs at 40,000 rpm and under radial loads of 500 to 1000 lb is given below:

IV, G, Propellant-Lubricated Bearings (cont.)

| Design | Both races and rollers 440C | 440C inner race<br>K-5-H rollers<br>K-5-H outer race |
|---|---|---|
| 500 lb | | |
| Inner race stress, psi | 130,000 | 162,500 |
| Outer race stress, psi | 110,000 | 206,000 |
| 1000 lb | | |
| Inner race stress, psi | 182,000 | 228,000 |
| Outer race stress, psi | 167,000 | 313,000 |

(U) The Teflon-lined spherical mounting housing was 17-4 PH for both designs.

(U) Several roller-cage designs were fabricated for testing. As in the ball cages, all of the roller cage designs were made of Teflon with a 25% glass fill. Both inner and outer race designs with variations of containment shrouds were fabricated and tested. Two of these designs were used in the work statement achievement tests. These two cages are shown in Figure IV-49. The inner race design shown on the right has 15 pockets and a web thickness at the pitch diameter of about 0.075 in. and incorporate a full containment shroud of aluminum. An aluminum rivet adds strength to each web. It was found necessary to modify the aluminum cutout around the pocket during the testing to assure that the rollers did not contact the shroud. The aluminum open area around the pocket was increased so as to expose 0.020-in. Teflon around the perimeter. This design was successfully used in the 31,250 rpm successful tests in both $N_2O_4$ and AeroZINE 50 and in the 40,000 rpm tests in $N_2O_4$. Failures of this cage occurred during the 40,000 rpm tests in AeroZINE 50.

(U) The cage shown in the left of Figure IV-49 was the design used successfully in the 40,000 rpm tests in AeroZINE 50. This cage is the same "thin-line" design demonstrated in the 25,000 rpm test series and provides more area for propellant through flow but contains two less rollers than the inner race riding design. The web thickness was 0.110 in. Tests were also conducted with cages of this design, but with 15 pockets. The web thicknesses of the 15-pocket cage was only 0.060 in., and was found to be inadequate. Consequently, to obtain increased web thickness of 0.110 in., two rollers were dropped. This change resulted in about a 30% decrease in bearing life. However, as noted in Figure IV-14, the $B_{10}$ life for the 13 roller bearing at the steady-state load requirement of 500 lb at 40,000 rpm is still 1550 lb. This $B_{10}$ life was calculated for oil lubrication and is used as a criteria of comparison as to upper limit of life expected in propellants. With cages of nonmetallics the web thickness is most important. The 13 roller "thin-line" cage is considered the optimum design for this application.

### 7. Design of Roller Bearings for 31,250-rpm Propellant-Lubricated ($N_2O_4$ and AeroZINE 50) Operation

(U) The roller bearing design for the 31,250 test series in $N_2O_4$ and AeroZINE 50 was the same as the 15-roller design with inner race riding cage as discussed for the 40,000-rpm requirement except for the alignment capabilities. The outer race was of standard 108 (68 mm) dimensions. The internal geometry was the same as that tabulated in the 40,000-rpm design except for the number of rollers. Figure IV-49 shows the bearing and cage design along with the 13-roller 40,000-rpm design.

## IV, G, Propellant-Lubricated Bearings (cont.)

### 8. Testing at 31,250 rpm

(U) No bearing problems were encountered during any of the testing at 31,250 rpm. The ball and roller bearing work statement requirements were met in one test (Test 7) in $N_2O_4$ and one test (Test 10) in AeroZINE 50.

(U) Figure IV-50 tabulates steady-state data for Test 7 in $N_2O_4$. The test duration was 7 min and 15 sec, of which 6 min and 53 sec were at a speed of 31,250 to 32,000 rpm. Minimum and maximum axial loads were 1770 and 4200 lb. The axial load was greater than 2200 lb for 6 min 10 sec and was more than 4200 lb for 26 sec of the test duration. The radial load was greater than 500 lb during the entire test duration, and was between 980 and 985 lb for 47 sec. Figure IV-51 shows the excellent posttest condition of these bearings.

(U) Figure IV-52 tabulates steady-state data for Test 10 in AeroZINE 50. The test duration at 32,000 rpm was 7 min 20 sec of which 6 min 58 sec were above 32,000 rpm. The minimum axial load was 2700 lb, and an axial load of 4600 lb was maintained for 20 sec. The minimum radial load was 600 lb, and a peak radial load of 1115 lb was applied for 18 sec. Radial load was above 1000 lb for 31 sec. Figure IV-53 shows the excellent posttest condition of these bearings. As can be seen from this photograph (Figure IV-53), slight roller end wear of the 440C rollers was experienced; however, this was considered acceptable for the turbopump application.

### 9. Testing at 40,000 rpm

(U) It was considerably more difficult to obtain satisfactory (U) test results at 40,000 rpm. A large portion of these problems were tester and facility problems since the tester was of new design and the facility was a new installation. The same tester and test setup was used during the testing at 31,250 rpm discussed previously; however, the initial tester and facility checkout and bearing tests were conducted at 40,000 rpm in $N_2O_4$ as tabulated in Figure IV-50. The first four tests were considered checkout tests and are not tabulated in Figure IV-50 since no significant bearing test data were obtained.

(U) Work statement objectives for the testing at 40,000 rpm in $N_2O_4$ were met in two tests (Tests 5a and 6b) on the same bearings. Figure IV-50 tabulates steady-state data for these tests. Test 5a was conducted with the roller bearing mounted in an aligned position and the other (Test 6b) with the roller bearing mounted in a misaligned housing. The misalignment was equivalent to a radial displacement of 0.016 in. of the bearing bores of the T-engine turbopump housing, which was twice the allowable radial displacement of the housing stipulated in the work statement. Figure IV-14 shows this amount of misalignment and the probable life if an alignment mechanism is not used.

(U) In addition to Tests 5a and 6b, three starts were made on these bearings that did not generate significant data for work statement requirements because of difficulties encountered in the test systems. They are included in the tabulation of Figure IV-50 only to present a complete history of the work statement achievement bearings.

(U) Total accrued duration of Tests 5a and 6b was 14 min and 9 sec. During Test 5a, the roller bearing was installed in the aligned position. Test duration was 4 min and 57 sec, of which 4 min and 29 sec was at speeds of 38,000 to 39,600 rpm. Minimum and maximum axial loads were 1170 and 2950 lb. The 2950 lb was maintained for 20 sec and over 2300 lb was maintained for 43 sec. The radial load for the entire duration was 500 lb. The test was terminated prematurely during a radial load increase to 870 lb because the turbine speed signal was lost. The bearings were removed, examined, and found to be in excellent condition.

IV, G, Propellant-Lubricated Bearings (cont.)

(U) The same bearings were reinstalled for the next test. The roller bearing was installed in a misaligned housing. The duration of the next significant test (Test 6b) was 9 min and 12 sec of which 8 min and 50 sec were at speeds of 38,800 to 40,400 rpm. Minimum and maximum axial loads were 1450 and 2500 lb. The 2500 lb was maintained for 36 sec. Minimum and maximum radial loads were 500 and 1000 lb. The radial load peak was applied twice during this test for a total duration of 32 sec. Figure IV-54 is a test data plot of Test 6b. Figure IV-55 exhibits the excellent posttest condition of these bearings.

(U) The 40,000 rpm series in AeroZINE 50 was the most difficult of the test requirements because AeroZINE 50 is an extremely poor lubricant. A problem of roller bearing operation in AeroZINE 50 is severe roller end wear. Roller skewing and skidding problems are accentuated by this wear since the guiding land clearance increases with operation. This in turn causes high drag on the roller cage. Also, large cage moments result unless pocket clearances are large enough to accept the roller skewing. For this reason, the first design incorporated K-5-H rollers, K-5-H outer race, and 440C inner race. This combination was selected on the basis of the results of four ball tests and bearing tests conducted on the pre-ARES ICP bearing program (Reference 10).

(U) The first test (Test 8) conducted in AeroZINE 50 at 40,000 rpm was performed on a bearing of this material combination. No problems were noted during the test; full duration of 450 sec was obtained, with 429 sec of operation at 40,300 rpm. Minimum and maximum axial loads were 1820 and 2690 lb, whereas minimum and maximum radial loads were 500 and 1110 lb. Steady-state data points are tabulated in Figure IV-52. Upon disassembly and inspection of the roller bearing, it was found that considerable wear had occurred on the K-5-H rollers and in the loaded zone of the K-5-H outer race. This bearing was of the self-aligning design mounted with a misalignment equivalent to a

0.016-in. radial displacement of the T-engine roller bearing span. Figure IV-14 shows this data point on the life plot as a function of radial displacement. The curve represents the probable life for a bearing without an aligning device. The roller bearing cage was in good condition.

(U) This cage had 15 roller pockets and was of the same "thin-line" design that was successfully tested in the 25,000 rpm series in $N_2O_4$ (Figure IV-45). Later failures of this cage resulted in the redesign which decreased the roller pockets to 13 to increase the web thickness. Also, the shroud material was changed from aluminum to 302 stainless steel.

(U) The load sharing ball bearing set was in excellent condition. This bearing set incorporated K-5-H balls in 440C races and experimental outer race riding cages. This cage design was a "halo" type fabricated of 25% glass-filled Teflon molded around a stainless-steel ring located at the pitch diameter. Posttest condition of the ball bearing cages was good; however, the same cages failed in the next test (Test 9) and the design was not evaluated further.

(U) Measurements of the K-5-H race and roller wear were taken. The race wear covered about 120° of the outer race track. The wear was tapered and measured from 0.0008 in. to 0.0015 in. deep axially across the track. Approximately half of the rollers had circumferential wear of about 0.001-in. radial depth which resulted in a dumbbell shape. In addition, profilometer measurements were taken of new K-5-H rollers which passed the normal roundness inspection but were found to be of poor quality with more precise inspection. They had irregular crowning, small flats, and very small holes. This poor condition probably contributed heavily to the wear. K-5-H material is most difficult to grind, and better results would be obtained if diamond grinding wheels were used instead of carborundum wheels.

(U) It is also believed that a finer-grain material with a minimum of cobalt binder probably would be less prone to wear. Stress does not appear to be the primary cause of the wear since the bearings with K-5-H balls operated successfully at higher stresses. Further testing with improved K-5-H rollers would be necessary to determine the cause.

(U) Because of the poor quality of the K-5-H rollers on hand, the remainder of the tests in AeroZINE 50 were conducted with 440C races and rollers. Appreciable end wear of the 440C rollers resulted, but was demonstrated to be acceptable for work statement life. This end wear can be seen in the posttest photographs of the AeroZINE 50 tests (Figures IV-53 and IV-56).

(U) Failures of the "thin-line" roller bearing cages with 15 pockets occurred during Test 11 and during two tests on the wear ring program, which was being conducted concurrently and used the same bearing design (water-lubricated). Because of these failures the cage was redesigned with 13 rollers to obtain thicker webs between roller pockets (refer to Figure IV-49).

(U) Two failures of the ball-bearing load-sharing set occurred. The first was in Tests 12 through 15 and the second was in Test 16. Both failures were similar fatigue failures of the races and balls. Both tests were conducted with an AeroZINE 50 flow of 8 to 9 gpm while previous tests were conducted at AeroZINE 50 flows of about 12 gpm. The flow was decreased to lessen the fluid-loading forces on the cages, which in turn loads the rollers against the downstream guiding land and increases the roller end wear. From previous bearing experience in AeroZINE 50 and from the completed tests at 40,000 rpm in $N_2O_4$ at flows of 9 to 11 gpm no problem was expected in reducing the flow to the 8 gpm value and no problem was seen in the roller bearing. However, because the ball bearing set is at close proximity, almost all of the heat generated in the upstream ball bearing was input to the downstream ball bearing. In both failures the downstream bearing was in the worse condition and showed evidence of high temperature. In addition to the lower flow, the ball bearing set in Test 16 was subjected to an extremely high peak axial load. An error in the axial load piston pressure resulted in an axial load of 6000 lb for 22 sec and a peak of 7080 lb as noted in Figure IV-52. The failure probably started during this high-load period. However, it was about 3 min later when the test was terminated because of excessive vibration. The load at shutdown was 1960 lb.

(U) The accrued duration, rotational speed, and bearing loads all met work statement requirements during Tests 12 through 15. However, the posttest condition of the ball bearings was unacceptable. The roller bearing was accepted as a work statement achievement exhibit for the 40,000 rpm AeroZINE 50 lubricated requirement. The roller bearing was mounted aligned for Tests 12 and 13 for a total duration of 8 min and 14 sec and in a misaligned housing for Tests 14 and 15 for a duration of 4 min and 1 sec. The cumulative duration was therefore in excess of the 12-min requirement. Speed was between 40,000 to 40,500 rpm. Minimum and maximum radial loads were 540 and 1070 lb. The peak load of 1070 lb was maintained for 27 sec. Figure IV-52 tabulates steady-state data for these tests.

(U) The bearing was removed, inspected, and reinstalled in a misaligned housing after Test 13. Some damage had been experienced from the dirt generated from the failing ball bearings. Race spalling had started in three small areas and there were many dirt dents on both raceways. Also, small dents were visible on the rollers. The cage was in excellent condition. The cage was the improved thin-line design with 13 rollers and the stainless-steel shroud web was contained in a Teflon channel preventing contact between the roller and stainless-steel shroud. After Tests 14 and 15 this bearing was in the same condition as noted above at assembly and found acceptable for work statement achievement. Figure IV-56 shows this roller bearing along with the achievement ball bearings.

IV, G, Propellant-Lubricated Bearings (cont.)

(U) Work statement objectives for testing of the ball bearings at 40,000 rpm in AeroZINE 50 were met in Tests 17 through 19. Figure IV-52 tabulates steady-state data for these tests. AeroZINE 50 flow was increased to 14 gpm for these tests. The accrued duration for these tests was 13 min and 35 sec. A total of seven starts were made on these bearings as noted in Figure IV-52. Maximum peak and steady-state loads were 2750 and 1600 lb. A peak load of more than 2500 lb was maintained for 27 sec during Test 19c. The axial load was more than 1500 lb for the entire 12 min and 35 sec duration of Test 19c and was between 1200 and 1700 for the 1-min duration of Test 17. Rotational speed was in excess of 40,000 rpm for the total cumulative duration. Since work statement requirements were completed for the roller bearing, the radial load was 250 lb during these tests. The ball bearings were in excellent posttest condition (see Figure IV-56). The balls were K-5-H and races were 440C. The cages were the modified inner race design, shown in Figure IV-48, which allows through flow at each ball race contact area.

### 10. Summary and Conclusions

(U) a. All work statement objectives were satisfactorily demonstrated.

(U) b. The final roller bearing design for both turbopumps incorporate the 13-roller thin-line outer-race riding cage since roller-bearing life with 13 rollers is more than adequate and the lesser number of rolling allows more space for heavier webs on the bearing cages.

(U) c. The ball-bearing design for both turbopumps incorporate the 14-ball inner race riding cage with increased area for through flow.

(U) d. In AeroZINE 50 the ball bearing incorporating K-5-H balls in 440C races gave superior performance.

IV, G, Propellant-Lubricated Bearings (cont.)

(U) e. The amount of end wear experienced on the 440C rollers during the AeroZINE 50 work statement achievement tests is acceptable to turbopump life. However, elimination of end wear is desirable. Better tooling and control is required to fabricate K-5-H rollers of the quality required. Finer grain material with a minimum of cobalt binder should be used.

(U) f. Misaligned operation was successfully demonstrated at 40,000 rpm in both $N_2O_4$ and AeroZINE 50 with the spherical outer-race design.

(U) g. In addition to the bearing work statement requirements, the following data was obtained during the bearing, wear ring and seal test programs:

(1) Operation without filters was demonstrated for 5 min in $N_2O_4$. More information on bearing life and reliability is needed to eliminate filters.

(2) Most reliable operation was obtained at 40,000 rpm with 10 to 20 gpm of flow.

(3) Operation without propellant flow for several seconds caused no damage.

(4) Acceleration to 50,000 rpm in 1 sec has been demonstrated.

(5) Satisfactory operation during retest of $N_2O_4$ lubricated bearings, after 24- to 48-hr downtime with freon flush on shutdown and a continuous $GN_2$ purge, was demonstrated.

f. Retest of AeroZINE 50 lubricated bearings, after 24 to 48 hr downtime without purges, was demonstrated.

(U) g. Rapid (1 sec) changes in pressure from 100 to 3000 psi, like those experienced in the turbopump start transient, produced no problems.

### 11. Application to the ARES Turbopumps and Further Requirements

(U) Both the T-engine and inline engine turbopumps incorporate a thrust balancer, integral with the first-stage fuel impeller. Consequently, the ball bearings are only required to carry start- and stop-transient loads in normal operation. This arrangement requires a different ball bearing arrangement than the tandem load-sharing set demonstrated at work statement requirements. The work statement loads were much higher than the 400-lb ball-bearing load expected during a normal start transient. Section IV,B discusses the turbopump thrust balance and bearing arrangement and expected operation. Figure IV-12 shows the load-life relationship for a single ball bearing of the final design for both high-load (as required by the work statement) and light-load operation (as expected in the turbopumps). The 108-size ball bearing duplex "DB" set, designed for both turbopumps, should be tested at the actual design requirements even though higher loads were demonstrated on the same bearing design in a load sharing arrangement. The "DB" arrangement is more sensitive to temperature caused clearance changes and some design optimization may be required before turbopump operation.

(U) The T-engine turbopump roller bearing design is the same for both the AeroZINE 50 and $N_2O_4$ lubricated bearings. The races and rollers are 440C, the outer race is mounted in a spherical housing and the cage is the 13-roller outer-race riding thin-line design (shown in Figure IV-49). Figure IV-14 shows the effect of radial misalignment on the $B_{10}$ life of this bearing without the aligning mechanism for the T-engine turbopump bearing span, while operating at 40,000 rpm and under a 500 lb radial load. Further work should be done to eliminate roller end wear when operating in AeroZINE 50.

Also further testing should be conducted on the corrosion effects of $N_2O_4$ on 440C bearings and to develop methods of cleaning and preserving bearings between tests to prevent corrosion after $N_2O_4$ exposures.

(U) The inline engine turbopump incorporates a 107-size (35 mm bore) fuel lubricated roller bearing and a 109-size (45 mm bore) oxidizer lubricated roller bearing. No misalignment device was required. The races and rollers are 440C and the cages are of the same outer race riding thin-line design selected for the 108 size bearings used in the T-engine turbopump.

IV, Turbopump Assembly (cont.)

## H. PUMP WEAR RINGS

### 1. Objectives and Approach

(U) The primary objectives of the pump wear-ring program were to design and evaluate wear rings for both the fuel and oxidizer pump impellers. The pumps use fully shrouded impellers as shown in Figure IV-57. The criteria for success of the test program were that the final designs (selected for the turbopump) would (1) satisfactorily limit or control internal leakage in the pump to a value consistent with the turbopump efficiency and thrust-balance requirements and (2) operate safely and reliably with intermittent rubbing in both $N_2O_4$ and AeroZINE 50.

(U) Secondary objectives were to establish insert materials for other close-running components, such as shaft labyrinths, inducers, and boost pumps.

(U) Two design approaches were taken in solving the wear-ring sealing and explosion hazard problems. The first approach was to allow intermittent rubbing of the impeller wear ring on inert, compatible inserts; straight labyrinth seals were designed and tested with various combinations of insert materials and pressure retention mechanisms.

(U) The second approach was to allow low-speed transient rubbing, but to prevent high-speed contact by maintaining a fluid film between the impeller rubbing surfaces and the seal itself. Hydrostatic face and journal seals, based upon this concept, were designed and tested.

(U) The test approach was to conduct preliminary screening tests in water. Both rotating tests (at 30,000 rpm and 2000 to 2500 psi pressure differential) and nonrotating tests (at 4000 psi pressure differential) were

IV, H, Pump Wear Rings (cont.)

conducted. Selected designs were then tested in $N_2O_4$ or AeroZINE 50 at 40,000 rpm and turbopump simulated operating conditions. During the rotating tests, rubbing conditions were simulated by actual displacement of the test seal toward the rotating wear ring by an amount greater than the measured radial clearance.

## 2. Design Requirements

(U) The wear-ring seals had to satisfy four basic design requirements:

a. They must efficiently limit internal leakage in the pump.

b. They must follow the movements of the pump impeller and housing and operate safely and reliably in highly explosive fluids.

c. They must be simple, small, and light.

d. They must be able to control the axial thrust forces to a reasonable value which the thrust bearing can absorb.

(U) The specific operating requirements of the wear rings for the oxidizer pump required sealing of a 4000-psi pressure differential while operating at 600 ft/sec surface velocity and accommodating axial movements of 0.040 in. and radial movements of 0.015 in.

(U) The specific operating requirements for the fuel-pump wear ring necessitated sealing of a 2000-psi pressure drop while operating at 820 ft/sec surface velocity, and accommodating axial movements of 0.005 in. and radial movements of 0.010 in. In addition, the fuel wear rings serve as constant-area restrictors that supply flow to each side of the double-acting thrust-balancing piston. This balancing piston (discussed in detail in Section IV-B), is made integral with the fuel impeller and is capable of compensating for unbalance axial forces of ± 15,000 lb.

(U) The first basic design requirements (limiting internal leakage) becomes very important at high pressures. Figure IV-58 shows how pump efficiency varies as a function of wear-ring radial clearance (leakage) and pressure differentials for a bushing, straight labyrinth, and stepped labyrinth of comparable axial length and diameter.

(U) The importance of the second basic requirement (prevention of explosions) is obvious. Oxidizer pumps are the most prone to this type of failure; metal-to-metal rubbing generates both fuel (in the form of small metal particles) and heat to initiate burning.

(U) If the burning is confined, as it would be in a close-running wear-ring seal, detonation is likely to follow. Also it is known that, as pressures go up, ignition temperatures of metals go down. Consequently, the explosion hazard increases when pumping to high pressures.

(U) Rubbing of metals in high-pressure $N_2O_4$ pumps has resulted in catastrophic failure (Reference 11); however, severe rubbing in a similar high-pressure AeroZINE 50 pump was sustained without explosion (Reference 12). Previous investigations report that AeroZINE 50 may detonate if its temperature exceeds several-hundred degrees. Therefore, consideration should be given to preventing rubbing or at least minimizing temperature rises during rubbing conditions in the AeroZINE 50 pump as well.

(U) The third basic requirement (simple, small, and light) is part of the overall engine concept, which demands the elimination of redundancy and complexity. Also, at 40,000 rpm, the masses of the wear rings attached to the shrouds of the impellers must be small in order to keep the centrifugal stresses at an acceptable level.

(U) The fourth basic requirement (axial thrust balance) also is more critical in high-pressure pumps. The axial forces acting on the turbopump rotating assembly are very large (summation of 200,000 lb in either direction). A steady-state operating thrust balance is attempted in the design by the appropriate radial location of the impeller wear-ring seals.

(U) Theoretically, such a thrust balance could yield zero thrust at design operating conditions. However, with load summations of such large magnitudes, an error of only a few percent in estimated pressure distributions, plus variations in practical manufacturing tolerances could result in unbalance forces in the range of 5,000 to 10,000 lb.

(U) As discussed in Section IV-B, the fuel impeller is designed to serve as a thrust-balancing piston which compensates for these steady-state loads as well as for off-design transient loads. The flow requirement for proper operation of this thrust balancer is appreciable (70 gpm per side). For this reason only straight labyrinth wear rings were considered for the fuel pump.

(U) In the design of the wear rings for the oxidizer pump, all four of the basic requirements were considered. The first two basic requirements (low leakage and safe operation in high-pressure $N_2O_4$) could not be easily met in a conventional bushing or labyrinth type of seal at the specific operating requirements of 4000 psi pressure differential and 600 ft/sec surface velocity. The first demands operation at close clearances (less than 0.010 in.), whereas the second requires either the elimination of high-speed rubbing or the use of materials that will not lead to an explosion if rubbing should occur.

(U) To successfully satisfy these requirements, the oxidizer pump wear rings must follow or conform to the relatively large axial (0.040 in.) and radial (0.015 in.) movements and clearance changes of the impeller and housing. Housing movements result from combined pressure and temperature changes, whereas impeller movements result from pressure and temperature changes, radial and axial hydraulic unbalance, internal bearing clearance, rotating assembly unbalance, centrifugal growth, and operational vibration.

### 3. Wear-Ring Design

(U) Several basic wear-ring-seal design concepts were analyzed to meet the oxidizer and fuel-pump requirements. Of these, four concepts (straight labyrinth, stepped labyrinth, face hydrostatic, and journal hydrostatic) were selected for preliminary evaluation in water. The four selected configurations are discussed below.

#### a. Straight-Labyrinth Seal

(U) Little information is available on liquid-labyrinth seals. However, published annular-orifice data (Reference 13) and a paper prepared by G. Vermes (Reference 14) yielded valuable background information for design and analysis and for optimum tooth geometry.

(U) The primary advantages of straight-labyrinth seals are simplicity of construction, simplicity of operation, and highest reliability, if radial clearances between the rotating cylinder and the stationary sleeve are large enough to preclude rubbing. The minimum clearance to preclude rubbing was analyzed to be 0.015 in. However, the allowable leakage rate established by oxidizer pump-efficiency requirements was 120 gpm, instead of 260 gpm for two labyrinths each with a clearance of 0.015 in. Therefore, it

IV, H, Pump Wear Rings (cont.)

was concluded that the running clearance would have to be approximately 0.007 in. and that rubbing must be allowed by the design for severe movements.

(U) To permit such rubbing, the stationary member of the labyrinth had to be made from a relatively soft and chemically inert material that can deform under the rubbing action of the rotating labyrinth teeth. This approach minimizes the variation in leakage due to rubbing, and most importantly minimizes the possibility of an explosion.

(U) Literature searches discovered only a few prospective materials that are compatible with the test propellants nitrogen tetroxide ($N_2O_4$) and AeroZINE 50. Only Teflon (TFE and FEP) is compatible with both, whereas Kel-F, Kynar, Vespel, and Hystel show promise for limited service in one or the other. The compatibility of these materials with the propellants studied is indicated in the following table:

| Material | Manufacturer | Compatible With<br>$N_2O_4$ | <br>AeroZINE 50 |
|---|---|---|---|
| TFE Teflon | E. I. duPont de Nemours & Co. | x | x |
| FEP Teflon | E. I. duPont de Nemours & Co. | x | x |
| Kel-F | Minnesota Mining and Mfg. Co. | | x |
| Kynar | Penn Salt Corp. | | x |
| Vespel | E. I. duPont de Nemours & Co. | x | |
| Hystel | Thompson Ramo Woolridge | x | |

(U) While it is the most compatible, virgin Teflon (both TFE and FEP) is the least desirable because of its unsatisfactory cold-flow properties. Fillers (glass, ceramic, graphite) were therefore added to increase the strength of this material.

IV, H, Pump Wear Rings (cont.)

(U) In designing these close-running labyrinth seals, consideration was given to the retention of the soft inserts at high pressure differentials and during rubbing. Several designs (Figure IV-59) were evaluated in both static (nonrotating) and preliminary rotating-rubbing tests in water. The retention mechanisms selected for futher evaluation in propellants (see Figure IV-57) are briefly described in the following paragraphs.

### (1) Dovetail Insert

(U) The soft insert was sandwiched between a two-piece flange. Axial compression on the insert depended upon the thickness of the Teflon shim and on the torque on the bolts. In order to prevent the insert from being forced out of the flange by trapped pressure, the insert outer diameter was vented to the downstream side of the labyrinth by relief holes in the flange. This concept provided good pressure retention but required several parts. Its main disadvantage is a wide axial clamp on the upstream side of the labyrinth, which requires that the labyrinth teeth be located either axially away from the impeller proper or that the number of teeth be reduced (with an attendant increase in the leakage).

### (2) Pressure-Relieved Insert

(U) In this concept, a series of radial holes connects the outside and the inside of the insert. Sets of eight equally spaced holes were drilled in each of three planes, and each set of holes was connected by a circumferential groove. The pressure gradients on the inside and on the outside were thereby equalized, and the probability that the insert would be displaced by pressure was thus reduced.

IV, H, Pump Wear Rings (cont.)

b. Stepped Labyrinth

(U) The attractive feature of the stepped-labyrinth seal is a higher head loss per tooth than in the straight labyrinth designs. Leakage rates would be about 20% less than with a straight-labyrinth seal having a comparable clearance and number of labyrinth restrictions. Because the teeth must be spaced to act as restrictors during all phases of turbopump operation, the number of teeth is determined by the relative axial movements of housing and rotating assembly. For the oxidizer pump application, this necessitated fewer labyrinth restrictions within the given space or a greater axial space to obtain the same number of restrictions. Even with the greater length, the leakage requirements still required close clearances, so that rubbing had to be anticipated. Therefore, inert materials capable of withstanding rubbing would be required. Insert retention would be more difficult and would require more space than the straight-labyrinth design. Consequently, the advantage of a low leakage rate must be weighed against increased complexity, size, and cost. In addition, the stepped features of this seal result in additional axial thrust variation which must be considered in the thrust balance of the overall rotating assembly. For these reasons, the stepped labyrinth was dropped from the test program after preliminary tests.

c. Hydrostatic Face Seal

(U) A major advantage of the hydrostatic face seal over that of labyrinth concepts is the low leakage rate of the former, which results in higher pump efficiency. The leakage rate for the hydrostatic face seal is 19 gpm or about 30% that of the straight labyrinth design for the oxidizer pump at an operating clearance of 0.007 in. To achieve this relatively low leakage at a pressure differential of 4000 psi, the seal was designed to operate at an axial clearance of 0.001 in.--a somewhat arbitrary value influenced by previous test experience.

IV, H, Pump Wear Rings (cont.)

(U) An equally important feature (for pumping explosive liquids) is the elimination, by design, of any high-speed metal-to-metal rubbing. The seal operates on a fluid film which is maintained by the design features of seal stiffness, force balance, and orifice compensation. However, since low-speed transient rubbing cannot be avoided, the contacting faces are hard-coated with a suitable material. Many rubbing tests were conducted to evaluate numerous materials at various loads and operating speeds. Linde flame spray LC-1c on LC-1c (chromium carbide) was finally selected as the best combination for this application.

(U) Two other features of the all-metal hydrostatic seal that make it attractive is storage life and insensitivity to pressure. Properties of the labyrinth plastic inserts will deteriorate with time and successive propellant exposures. Also the plastic inserts are pressure-limited, i.e., at some pressure differential depending upon the material properties and the retention mechanism, they will be extruded. Use of the all metal hydrostatic seal would eliminate these two problems.

(U) The hydrostatic wear-ring seal design had eight pockets and was orifice-compensated (Figure IV-60). The primary difference between this seal and similar hydrostatic orifice-compensated seals consists in supplying the orifice by the pressure being sealed rather than be a separate higher-pressure source. Flow therefore enters the seal through each of the eight pocket orifices and also across the high-pressure seal land. This combined flow then exits across the low-pressure seal land. Consequently, the pocket pressure at the design clearance is less than the supply pressure.

(U) Secondary sealing is provided by a piston ring located in the seal at a diameter calculated to obtain a proper balance of forces. The high pressure drop across the seal (4000 psi) and the small cross section of the seal could produce extremely large pressure-area moments, which could

IV, H, Pump Wear Rings (cont.)

cause the seal to rotate past operating clearance and make the seal unworkable. These unbalanced moments, about the centroid of a cross section of the seal, were reduced to tolerable values by selecting an appropriate cross section for the seal.

(U) The design approach taken for this specific seal is outlined in the following paragraphs.

(U) The flows, $Q_i$ and $Q_e$, past the primary sealing surfaces (lands) were calculated by using the thin-slot flow equations of Tao and Donovan (Reference 15). These flow equations were programed for the computer so as to allow for calculations where the flows across the sealing lands are turbulent across one land and laminar across the other and where the running clearances at the two lands are not identical.

(U) The flow through the orifices, $Q_o$, is defined by the orifice equation. A pocket pressure was selected, and the first iteration pressure drops were thereby established. These pressure drops were then modified by a speed-effect function and the running clearance was calculated to satisfy the continuity equation, $Q_i + Q_c = Q_e$. Knowing the pressure drops, the required balance radius for the piston ring was then computed. The seal stiffness (k) was calculated after the continuity equation was satisfied.

(U) There are many parameters involved in the design of a hydrostatic seal. However, pocket pressure ($P_p$), and orifice diameter ($d_o$), appear to be the most important because the seal flow rate ($Q_e$), the stiffness (k), and the running clearance (c) can be adjusted from very large values to nearly zero. Q, k and c are plotted in Figure IV-60 as functions of $P_p$ and $d_o$ for the seal-face geometry of the final design and for fluid properties of water and $N_2O_4$; the "fixed" parameters are also listed in this figure. The plots clearly indicate that certain limits exist for the possible values of $P_p$. At the lower limit of $P_p$, both flow and clearance are large and change rapidly with small changes in $P_p$; the corresponding stiffness is very low. The seal therefore should not be designed too close to this lower limit. At the upper limit of $P_p$, both stiffness and clearance are very small, and the upper limit should therefore also be avoided. Since previous testing in $N_2O_4$ and AeroZINE 50 had demonstrated successful hydrostatic-seal operation at a clearance of about 0.001 in., it was decided to design the seal for this clearance. After a clearance is selected, the choice of orifice diameter becomes a compromise between low flow rate (small orifice) and high stiffness (large orifice), and requires selecting a point along the line c = constant = 0.001 in. The design point for each fluid is circled on the curves.

(U) In addition to being able to follow axial movements, the seal must respond to high-speed shaft wobble induced by a combination of normal runouts, mass unbalance, and bearing internal clearances. Wobble, of the same order of magnitude as the seal running clearance, occurs at rotational speed or a frequency of 667 cps (40,000 rpm). Since the resonant frequencies are calculated to be quite high, above 4600 cps, no forced-vibration problem is expected. Also, since the angular spring rate, $k\alpha$, is high (above $3 \times 10^6$ in.-lb/rad), and since the piston-ring friction moment is low (less than 300 in.-lb), the seal is able to follow impeller-face wobble.

### d. Hydrostatic Journal Seal

(U) In operation, this seal is very similar to the hydrostatic face seal. The seal (see Figure IV-61) is basically a floating journal bearing, which is able to follow the radial displacements of the pump-impeller wear ring by virtue of pressure changes in eight circumferentially equally spaced orifice-compensated pockets. Secondary sealing is accomplished by a radial sealing dam, which is kept in contact with the vertical face of the housing by a slight pressure-area unbalance. As in the hydrostatic face seal, each pocket orifice is supplied by the pressure being sealed and not by a separate higher pressure. Consequently, the pocket pressures at concentric operations are equal and are less than the pressure being sealed. Parallel flows enter the seal through the orifices and across the high-pressure land where they combine and exit past the low-pressure land. The flows past the primary sealing surfaces (lands) were calculated using the thin-slot flow equations of Tao and Donnovan (Reference 15) with an exponent and coefficient of $N = 0.21$ and $C = 0.316$ respectively. The flow through the orifices was calculated using the orifice equation.

(U) A concentric, nonrotating design clearance of 0.0025 in. was chosen. This choice was a compromise between expected clearance changes (i.e., centrifugal growth of the wear ring, pressure distortions, and temperature growth) and seal stiffness, and it results in a concentric operating clearance of 0.0014 in. at 2500 psi $\Delta P$ and 30,000 rpm. Stiffness must be high if the seal is to follow the high-frequency shaft movements and is to overcome the friction forces at the semistatic radial sealing dam. The design stiffness was $1.6 \times 10^6$ lb/in. and the undamped natural frequency of the seal was about 200,000 cpm. analysis of frequency responses showed that the seal operating clearance need only change by less than 0.0003 in. to overcome the estimated friction forces.

(U) The seal design parameters, total flow ($Q_e$), land capacity (w), and stiffness (k), are plotted in Figure IV-61 as a function of eccentricity ratio ($\varepsilon$) for the nominal design operating clearance of 0.0014 in. and for the expected manufacturing tolerance extremes of ± 0.0006 in. or operating clearances of 0.0008 to 0.0020 in. These curves assume a uniform axial slot. Also, from these design curves, it can be seen that the lower operating clearances (0.0008 in.) would result in the best seal performance, i.e., higher stiffness and higher restoring forces. However, the 0.0014-in. nominal clearance was selected to ensure a safe operating clearance on the prototype seal. Future seals of this type would be designed for closer operating clearance.

### e. Bushing Seals

(U) Since many commercial pumps use simple bushings for wear-ring seals, these were considered in the preliminary analysis.

(U) Generally, for small clearances (≈0.002 in.), the bushing seal achieves lower leakage rates and thus results in higher pump efficiencies than the comparable labyrinth (see Figure IV-58). However, at the larger clearances required to prevent high-speed rubbing and for the small axial space available in the specific application, the leakage rate would greatly exceed that of the comparable labyrinth. Consequently bushing seals were not considered for the test program.

## 4. Description of Tester

(U) The wear-ring tester for testing in propellants at speeds up to 40,000 rpm is shown in Figure IV-62. The tester consisted of a drive-power transmission and a test head.

(U) The power transmission imparted the required torque through a shaft, which was radially supported in the drive housing by two roller bearings; one of these bearings was located in the test cavity and was lubricated by the test fluid, i.e., water, oxidizer, or fuel. Axial positioning was provided by a hydrostatic thrust bearing, capable of supporting a load of

± 15,000 lb. A separate positive-displacement pump supplied 20 gpm of 4000 psig oil to the hydrostatic bearing pockets. Prior to being scavenged, the oil discharge from this bearing lubricated the two centrally located shaft-loading roller bearings and the shaft-support roller bearing at the turbine end.

(U) An integral system consisting of a pneumatic cylinder, a loading ring, and two "slave" roller bearings provided radial loading of the shaft system as required to prevent skidding of the bearings.

(U) Power was supplied to the shaft by an electric motor gear drive for the concept-screening tests in water at speeds up to 30,000 rpm. For the propellant tests, a single-stage partial-admission impulse drive turbine was attached directly to the shaft as shown. Ambient-temperature nitrogen gas flowing through two sonic nozzles provided energy to the turbine rotor. The test fluid and the oil lubricating the power transmission were kept separate by a combined purge and drain labyrinth shaft-seal system.

(U) The test head consisted of a housing, mounting flanges for the test wear ring seals, and an end cover plate. Two test seals were installed back-to-back. This configuration provided an axial thrust balance and allowed obtaining a maximum of data in each test. Two opposed actuation cylinders provided the means of misaligning and aligning the entire test head, by which the test wear-ring seals were displaced with respect to the rotating disk, thereby introducing potential interference and high-speed rubbing.

### 5. Test Setup and Procedure

(U) Figure IV-63 shows a typical test-seal arrangement and identifies the test parameters. The inlet flow, $Q_1$, of high-pressure fluid is supplied through a filter to the test head, where the fulid is divided between the outboard seal, $Q_3$, and the inboard seal, $Q_2$. The inflow, $Q_1$, and the outboard seal outflow, $Q_3$, were measured directly. The inboard seal flow, $Q_2$, is simply $Q_1 - Q_3$. A small portion of the inboard seal flow was utilized to lubricate and to cool the test-cavity roller bearing. The main inboard-seal outflow was monitored and designated $Q_2'$, and the bearing flow at this location was $Q_1-Q_3-Q_2'$. The inlet pressure, $P_1$, and the outlet pressures, $P_2$ and $P_3$, were monitored so that the pressure drops across the seals were known. In addition, temperature rises of the fluid across the seals were measured.

(U) The normal test procedure was to pressurize the cavity between the two seals (refer to Figure IV-63) prior to rotation. After assurance that upstream and downstream seal parameters were acceptable, rotation was initiated. At the planned test speed, the nonrotating portion of the seal was displaced towards the rotating disc by actuation of the misalignment piston (refer to Figure IV-62). After the seal was realigned, shutdown was initiated by simultaneously terminating the power for rotation and closing the test-fluid supply valve. The decay rates of the test-fluid and turbine-gas pressures were such that rotation ceased before the test seals were completely depressurized. Data were recorded during the entire test period.

## 6. Test Results

(U) Preliminary screening of wear-ring concepts was conducted in water. Both rotating and rubbing tests (at 30,000 rpm and 2000 to 2500 psi pressure differential) and nonrotating tests (at 4000 psi pressure differential) were conducted. On the basis of these tests, three concepts (hydrostatic face seal), pressure-relieved straight labyrinth insert, and dovetail-retained labyrinth insert) were selected for testing in propellant at simulated

IV, H, Pump Wear Rings (cont.)

turbopump operating conditions. Results of the water and propellant testing are discussed in the following paragraphs.

### a. Straight Labyrinth

(U) The primary concern of the straight-labyrinth test was to find an insert material of sufficient strength and/or a retention mechanism to prevent material "cold flow" or pressure extrusion at high pressures. Only the dovetail seal configuration (see Figure IV-59) of Vespel SP-21 was successful at a pressure differential of 4000 psi. This material and configuration were successfully tested, including rubbing without burning or explosion at 40,000 rpm, in $N_2O_4$ at 4070 psi pressure differential. Test data and a post-test photograph are shown in Figure IV-64. A few materials and configurations that were successful in the screening tests in water at pressure differentials of about 2500 psi failed at higher pressure differentials in $N_2O_4$. Two materials, Kynar and Kel-F, fabricated in the pressure-relieved configuration (see Figure IV-59) were successfully tested, including rubbing without detonation in AeroZINE 50, at 2260 psi pressure differential. Test data and posttest photographs are shown in Figure IV-65.

(U) In Figure IV-66, water, $N_2O_4$, and AeroZINE 50 flow data are plotted as functions of pressure differential for several labyrinth configurations. Using the flow equations from G. Vermes' paper (Reference 14) a discharge coefficient was calculated for each configuration. This $C_D$ value is tabulated with the labyrinth geometry on Figure IV-66. The curves are calculated flows using the $C_D$ value that best fits the test data.

(U) These $C_D$ values are not necessarily exact, since there is no way of knowing exactly what clearance changes occurred after the parts were installed and pressurized. The test data $C_D$ values provided a means of

IV, H, Pump Wear Rings (cont.)

estimating these changes. To establish a base of comparison, by eliminating this clearance variable due to pressure, metal parts were used for two tests in water (Curves A and E). In all other tests plotted, plastic inserts were used. The two all-metal labyrinths were identical except for clearance and had, for all practical purposes, the same discharge coefficient, $C_D = 0.85$.

(U) For the labyrinth configurations incorporating plastic rubbing inserts, the $C_D$ values were calculated to match the test data assuming a constant clearance. The pressure differential where the calculated $C_D$ began to decrease from a reasonable mean value was assumed to be where the plastic began to cold-flow and close off the clearance. The flow curves of Figure IV-66 were calculated using the average value of $C_D$ before this point was reached.

(U) Deviation of the test data from these curves was then assumed to be mainly the result of pressure-caused clearance changes. Temperature rise most certainly had some effect, but, considering other unknowns, it was considered futile to attempt to include these effects in the analysis.

(U) As can be seen from Figure IV-66, the dovetail insert of Vespel SP-21 (Curve F) was the best design as regards cold flow versus pressure differential. The $N_2O_4$ flow deviation shown (noted as point 4) represents a clearance change of only about 0.0004 in. during about a 15-sec period (calculated using the tabulated $C_D$ and the test data). This 8% change, although considered small and acceptable, still represented about 14% (9 gpm) change in flow at this close clearance. The important thing is that the material had stabilized and no further change was noted with respect to time prior to rotation. The still lower data point represents the test flow at 40,000 rpm. From analysis, it was expected that centrifugal growth of the labyrinth rotating teeth would be about 0.001 in. at this speed. As can be seen, this clearance change caused an additional flow decrease, which resulted in an operating flow of about 40 gpm.

(U) On the other extreme, the dovetail insert of Teflon filled with glass and ceramic (Curve B) was reasonably stable to about 3000 psi, where it began to lose clearance rapidly (from Point 1 to Point 2 represents 2.7 sec), and from post-test inspection was found to have contacted the labyrinth teeth even with no rotation.

(U) The clearance changes experienced with the pressure-relieved inserts of Kynar (Curve G) and Kel-F (Curve I) during the AeroZINE 50 were acceptable for the lower pressure-differential (2000 psi) requirement of the fuel-pump application.

(U) During the rubbing tests that were considered successful (i.e., the insert was retained, and pressure-caused clearance change was acceptable and stable), the flow increased during the insert displacement and returned to essentially the original value upon realignment.

(U) A total of 41 tests were conducted on straight labyrinths, of which 30 were in water, 5 were in $N_2O_4$, and 6 were in AeroZINE 50.

### b. Stepped Labyrinth

(U) The stepped labyrinth was tested in water only. The labyrinth parts were made of steel. Labyrinth configuration is shown and test data are tabulated in Figure IV-67. Better correlation with estimated flows existed for the smaller radial clearance (0.0055 in.) than for the larger

IV, H, Pump Wear Rings (cont.)

(0.0097 in.): 35.3 gpm estimated versus 35.8 gpm actual and 61.7 gpm established versus 53.8 gpm actual, respectively. For the stepped labyrinth flow calculation, it was assumed that the labyrinth steps prevent any carry-over of velocity from one tooth to the other. As expected, speed had no noticeable effect upon flow at these relatively large clearances.

### c. Hydrostatic Face Seal

(U) The hydrostatic face seal performed very well during the screening-test series in water. When it was tested in $N_2O_4$ under extreme operating conditions, no seal problems were encountered and the seal performed excellently.

(U) Transient rubbing of the seal was demonstrated in the water and $N_2O_4$ test series. No measurable wear was noted after four rubbing start-and-stop-transient tests in water. In these tests, the seal was flooded with water at atmospheric pressure and rotation was started. At about 5000 rpm, the water pressure was increased to cause the seal to lift off as it would in the turbopump; approximately 50 rubbing revolutions were experienced per transient. During the $N_2O_4$ series, the seal was subjected to a 6-sec dry rubbing test. A maximum speed of 15,000 rpm was reached. This is a surface speed of 250 ft/sec. No appreciable wear occurred (as can be seen in the post-test photograph in Figure IV-64), and testing continued on the same hardware. Test results before and after the dry rubbing test were repeatable.

(U) The flow past the seal was repeatable from test to test. Figure IV-68 is a plot of actual test data showing the correlation to the estimated flow for both the water and $N_2O_4$ testing. Although the actual data on water flow versus pressure differential were not exactly as predicted, the predictions are well within the accuracy needed for turbopump design.

IV, H, Pump Wear Rings (cont.)

The solid and dashed curves are predicted flows as a function of pressure differential. The difference between the two water-flow estimates is that the lower curve includes pressure-distortion effects while the upper curve does not. The distortion corrections were obtained from analysis of the flow after the angular rotation of the seal caused by the pressure moments was considered. This was correlated with data from strain gages on the seals during the tests. From the water data, one might conclude that the actual distortions were less than those measured or analyzed. However, neither of these estimated flow curves includes temperature-distortion effects due to fluid throttling. Temperature increase at the seal face should tend to rotate the outer sealing land away from the rotating wear ring, resulting in a converging flow path and thus a larger clearance and a higher flow. This effect could well compensate for the pressure-distortion effects and result in closer correlation of data.

(U) The correlation of the actual test data with the estimated $N_2O_4$ flow curve (see Figure IV-68) was very satisfactory. The estimated flow curve is approximately the same as an average flow curve drawn through the test data. This estimated flow curve included pressure-distortion effects but not temperature-distortion effects.

(U) During the testing with water and $N_2O_4$, the nonrotating portion of the seal was moved radially with respect to the rotating disk with no effect on seal flow. During the testing with $N_2O_4$, a severe thrust reversal occurred on the tester rotating assembly at 38,000 rpm, which resulted in a large and rapid axial movement: 0.0025 in. (twice the hydrostatic seal clearance) in 0.02 sec and 0.0063 in. (five times the hydrostatic seal clearance) in 7.0 sec. The seal followed this movement with no problems, [illegible] as new, and testing continued on the same hardware.

IV, H, Pump Wear Rings (cont.)

(U) A total of 14 tests were conducted on the hydrostatic face seal shown in Figure IV-64; of these, 9 were in water and 5 were in $N_2O_4$.

d. Hydrostatic Journal Seal

(U) The hydrostatic journal seal was tested in water only. Even though the seal performed excellently, it was not further considered for the oxidizer-pump application and therefore not evaluated in $N_2O_4$. It was eliminated because the test program had funds sufficient to test only two concepts. Also, there was some question as to whether the desired radial fit between the wear ring and the seal could be guaranteed at the time of this decision. Further analysis and results of the water testing showed that the seal can be designed to be pressure sensitive so that, even with a relatively large initial clearance, a small operating clearance would result. This feature is discussed in detail below.

(U) No seal problems were encountered during the water testing. Transient rubbing and steady-state tests demonstrated seal performance and repeatability at pressure differentials up to 2500 psi. In the transient tests, the seal was flooded with water at atmospheric pressure and rotation was started. At about 5000 rpm, the water pressure was increased to cause the seal to lift off as it would in a pump; approximately 50 rubbing revolutions were experienced per transient. No measurable wear was noted after rubbing start-and-stop transients, as can be seen in Figure IV-69. Water test data is also summarized in this Figure. A total of 10 tests including 4 rubbing transients were conducted on this seal.

(U) The flow past the seal was repeatable from test to test. Figure IV-70 shows the correlation of the flow data with estimated flows for the test seal. The test data are very close to the estimated data. The solid curve, just below the data, includes pressure-distortion effects but not temperature-distortion effects, while the dashed curve just above the data includes distortion effects due to both pressure and temperature. The other three curves are shown to illustrate a very attractive feature of this seal. The seal is radially flexible; that is, as the upstream or external pressure on the seal is increased, the seal distorts radially inward, resulting in a decrease in clearance and in a higher stiffness value. This results in lower leakage and higher restoring forces for wear-ring radial displacements. This feature tends to be self-compensating, since as the clearance closes the pocket pressure increases toward its supply, which is the external pressure, thus decreasing the radial pressure differential. As can be seen from the seal data of Figure IV-70, the result was a flat flow curve or a nearly constant flow over a wide range of pressure differentials. The three additional curves show how the flow would vary with pressure differential for rigid seals (essentially hydrostatic journal bearings) for radial clearances of 0.0008, 0.0014, and 0.0025 in. The significance of the latter two curves is that the test seal had an initial radial clearance of 0.0024 in. and was analyzed to result in a running clearance of 0.0014 in. at a 2500-psi pressure differential and 30,000 rpm. The significance of the 0.0008-in.-clearance curve is that, with design optimizing of the seal cross-section, it is expected that the seal flexibility could be increased, thereby resulting in a running clearance and thus a leakage flow comparable to those of a rigid seal with only 0.0008 in. clearance from an initial clearance of about 0.0025 in. In addition, because the seal is floating and is flexible, its ability to follow radial movements of the running ring without contact is excellent.

(U) Also, since a close running clearance could be achieved even with relatively large buildup clearances, the radially flexible hydrostatic journal seal would lend itself to volume production without costly tight-tolerance requirements. This is particularly important in commercial pumps.

## 7. Conclusions

### a. Oxidizer-Pump Wear Rings

(U) (1) The hydrostatic face seal and the straight labyrinth with Vespel SP-21 inserts limited flow through the wear ring to very low values at the required 4000-psi pressure differential. Both withstood intentional attempts at rubbing at 40,000 rpm without causing fire or explosion and were in reusable condition.

(U) (2) A number of the other plastic inserts for labyrinths passed water tests but failed at the 4000-psi pressure differentials in $N_2O_4$.

(U) (3) The hydrostatic journal seal passed the water tests and shows considerable promise for these applications. It was eliminated because the test program had funds sufficient to test only two concepts. One of the concepts was the very successful hydrostatic face seal and the other was the straight labyrinth with inert inserts. The inert-insert concept had to pass rubbing tests in $N_2O_4$ for other labyrinths in the turbopump shaft system.

(U) (4) The stepped labyrinth with inert inserts does not appear to be practical for application to the oxidizer-pump wear ring.

### b. Fuel-Pump Wear Rings

(U) The fuel pump is designed integrally with the thrust balancer in a manner which requires a straight labyrinth seal at the outside diameter of the fuel-pump impeller. The optimum design of this labyrinth seal requires operation at a clearance of 0.007 in. Two inert inserts of (Kynar and Kel-F) were satisfactorily designed and tested under simulated conditions. This included repeatable flow rate before and after rubbing at high speed and pressure differentials of 2250 psi. Kynar was selected for the fuel-pump application on the basis of its slightly better properties after exposures to AeroZINE 50 in laboratory tests.

### 8. Application to Turbopump

(U) On the basis of this program and analysis of the turbopump requirements, hydrostatic face seals were selected for the oxidizer-pump wear ring and straight labyrinths with pressure relieved Kynar inserts were selected for the fuel-pump wear ring. These designs are shown for the advanced turbopump in Figure IV-1 and the backup turbopump in Figure IV-33.

(U) The hydrostatic face seal as shown in the advanced turbopump layout has a 50% smaller cross section than the seal tested so that it will fit the space limitations better. The smaller seal can also tolerate larger impeller distortions which cause nonparallelism of the sealing surfaces. Figure IV-71 shows how this nonparallelism affects the performance of the tested seal (0.300-in. face width) and the half-size seal (0.150-in. face width); both seals were analyzed with the same balance diameter of 3.504 in. and for the same operating clearance of 0.001 in. From this figure, it can be seen that, for increasing $\alpha$ (divergence of the flow path) the minimum running clearance, $t_i$, decreases until the faces contact at the outside diameter of the seal; the point of contact (or close to it) may be considered an upper limit on $\alpha$ for seal operation. It is thus seen that, for good seal performance, limits exist for the acceptable angular distortions, and, by decreasing the seal-face width, the amount of distortion that can be tolerated is increased. The angular distortions of the oxidizer impeller were analyzed to be within

IV, H, Pump Wear Rings (cont.)

the range of + 0.0017 to - 0.0021 radians. The main disadvantage of a narrower seal is an increase in flow from 19 to 28 gpm at a 4000-psi pressure differential. However, for the application, this increase in flow is relatively small and can be accepted. An apparent disadvantage is that the seal stiffness is decreased by roughly 50%. Further testing of a half-size seal is recommended.

(U) The straight labyrinth with pressure-relieved Kynar inserts, selected for the fuel pump of the T-engine turbopump, is designed to operate at a radial clearance of 0.007 in. and has the following labyrinth geometry per side.

| | |
|---|---|
| Number of teeth, N | 7 |
| Pitch, P, in. | 0.068 |
| Axial length, W, in. | 0.408 |
| Tooth width, L, in. | 0.0075 |
| Diameter, D, in. | 4.700 |

(U) For application in a restartable engine, some further improvement of the insert's ability to resist softening and extrusion is warranted. The cross section and thickness of the Kynar ring could be reduced by adding an internal (molded in place), perforated metal ring. Hardware of this design was purchased but received too late to test. It is recommended that this design be tested along with soft S.O. aluminum rings. The soft aluminum should be safe in AeroZINE 50 at the 0.007-in. clearance and may be more reliable with respect to deterioration from repeated exposures to propellant.

## I. COMBUSTION SEAL

### 1. General

#### a. Background

(C) The ARES "T" engine requires a rotating shaft seal between the fuel pump and the 3000 psi, 1100°F oxidizer-rich turbine exhaust gas, as shown in Figure IV-1. At the operating speed of 40,000 rpm, the seal surface velocity is over 600 ft/sec, which, at the design temperatures and pressures, is considered excessive for rubbing contact seals. A hydrostatic seal was therefore designed for the TPA. The hydrostatic seal (Figure IV-72) operates with a thin film of fuel separating the nonrotating seal face from the rotating face. Part of the fuel flows inward to the shaft, where it is returned to pump suction. The outward flow of fuel enters the oxidizer-rich turbine exhaust gas, where it is consumed, eliminating the need for external vents or purges. The rotating shaft is cooled and combustion is controlled by streams of oxidizer flowing through holes around the shaft periphery, just upstream of the seal face. Oxidizer also flows through an annular slot downstream of the seal face, and serves to control combustion and protect the seal, bellows, and external surfaces from the combustion temperatures.

(U) The hydrostatic combustion seal was designed and its feasibility of operation is an inert environment established on the Hydrostatic Combustion Seal Feasibility Demonstration Program under Contract AF 04(611)-10784. Details of this program are presented in the final report, AFRPL-TR-66-79.

(U) Major work completed on contract AF 04(611)-10784 included the following:

(1) Design of a hydrostatic combustion seal.

IV, I, Combustion Seal (cont.)

(2) Design and fabrication of testers and test hardware for use in water tests (Hydrolab).

(3) Design of a preburner, burnoff stack, and other hardware for hot testing.

(4) Hydrolab seal tests under reduced pressures and at speeds up to 30,000 rpm. These tests demonstrated that closer operating clearances were more feasible than originally expected.

(5) Combustion tests, at reduced pressure, of a small segment of the seal (2D tests).

b. Objectives

(C) The Phase I portion of the ARES program required a 60-sec demonstration of a hydrostatic combustion seal or a purge seal while operating under conditions simulating those expected in the ARES engine.

(C) The test condition goals were as follows:

| | | | |
|---|---|---|---|
| Operating pressure | 3100 ± 600 psi | Gas temperature | 1100 ± 50°F |
| Pressurizing time | 0.75 to 1.25 sec | Speed | 40,000 rpm |
| Acceleration time | 1.0 to 1.5 sec | Gas velocity | 200 to 250 fps |
| Duration | 60 sec including 50 sec at 40,000 rpm | | |

IV, I, Combustion Seal (cont.)

c. Technical Approach

(1) Design Refinements

(U) To meet the program objective, refinements were made to the seal and associated hardware. The design changes evolved during the testing, and consisted of the following:

(a) Reduction of exposed peripheral area of the rotating ring to minimize thermal distortion.

(b) Replacement of the single-ply bellows with a two-ply bellows, to increase reliability.

(c) Relocation of the bellows attachment point and weld modification, to reduce susceptibility to failure from external pressure.

(d) Redesign of the burnoff area shield.

(e) Increased oxidizer flow upstream and downstream of the seal.

(2) Testing

(U) The following series of tests were conducted to attain the program objectives:

(a) Additional 2D tests, in which combustion was further examined with the modified cross-section of the seal developed on Air Force Contract AF 04(611)-10784, but with a clearance of 0.001 in. rather than 0.002 in.

IV, I, Combustion Seal (cont.)

(b) Cold rotating tests to 40,000 rpm, wherein the seal-fuel flows and the tester operating characteristics were evaluated while using fuel, but without combustion.

(c) Hot rotating combustion tests, in which the combustion-seal objective was to be reached.

## 2. Design

(C) The hydrostatic combustion seal is a radial face type seal which has six pockets supplied with fuel from a high-pressure source to maintain a fluid film between the stationary and rotating faces. The stationary face pressure areas are balanced so that external pressure tends to reduce the operating clearance. The fuel flows from the seal pockets radially inward to the bearing cavity and outward to combustion; the flow rate being jointly controlled by an orifice in each pocket supply passage and by the seal clearance gap. The fluid film thickness is maintained regardless of axial shaft movement and/or running ring wobble due to the relationship of seal pocket pressure to clearance (i.e., decreasing clearance increases pocket pressure which re-establishes design clearance, and vice-versa).

(C) To allow axial motion of the nonrotating face, the hydrostatic combustion seal requires two secondary seals for the 2600-psi pressure differential. One of these seals must maintain absolutely zero leakage because it seals fuel from the oxidizer. A single-convolution metal bellows was selected for the zero leakage secondary seal, and a metal piston ring is the other seal. The bellows is fabricated from two plies of 0.006-in. Inconel 718, and is formed into the shape of a torus of circular cross-section. A configuration of the bellows-to-end-piece welds was designed to minimize the stress in the area of welds. It has been determined through analysis that a two-ply bellows is superior to a single-ply bellows from the standpoint of

IV, I, Combustion Seal (cont.)

resistance to failure from both high internal pressure and from pressure differential reversal (which may occur during tester system transients). The modified Goodman diagram shown in Figure IV-73 illustrates the relationship between pressure stresses and fatigue life of the bellows. Point A on Figure IV-73 indicates the conditions associated with the bellows in the hot rotating Test 11, where the single-ply bellows failed. From this, it appears that the cyclic flexure resulting from the high unbalance vibration was in excess of 0.001 in. Point B indicates the conditions under which the two-ply bellows have been tested, and point C shows the cyclic life to be expected with a bellows axial compression corresponding to engine conditions. The cyclic life of the bellows in the ARES engine would therefore be expected to be more than $10^8$ revolutions, and would not limit the engine life.

(U) Because of the close clearance between rotating and nonrotating seal faces, it is important that distortion of the seal parts be minimized. Heat-transfer and stress analyses of the seal parts were performed and the results were applied to the seal design. Invar (low thermal expansion alloy) was selected for the nonrotating seal face to minimize thermal distortion. The seal was also designed to minimize distortion from the effect of pressure forces on the seal nonrotating face. One of the functions of the combustion seal is to maintain leak-tight contact prior to and after engine firing. Since some rubbing occurs during transients, the sealing surfaces are flame-plated with Linde LC-1B chromium carbide to resist degradation of the surface finish.

(C) The fuel flow from the seal is of primary importance because of the need to maintain a mixture ratio with the oxidizer streams that will ensure safe operating temperatures. When a mixture ratio of 30 to 40 has been used, there has been no combustion damage to downstream hardware. The stress and distortion analyses determined that the minimum allowable running clearance should be approximately 0.001 in. The fuel flow to maintain the required gap is therefore a function of the differential pressure between the seal pockets and the surrounding oxidizer-rich gas. The differential pressure must be higher than any surge in gas pressure, to eliminate the possibility of forcing oxidizer into the seal. This differential pressure was set at 500 psi, which was higher than any expected spikes in gas pressure. The resulting fuel flows were about 0.45 lb/sec outward and 1.3 lb/sec inward. The optimum fuel flows will be established when the ARES engine pressures have been evaluated and the proper differential pressure is selected. If the differential pressure is 200 psi, for example, outward seal flow will be 0.32 lb/sec and inward flow will be 0.81 lb/sec.

## 3. Tests

### a. Refined Two-Dimensional (2D) Combustion Tests

### (1) Objective

(U) The 2D tests were conducted to obtain further information on flame patterns, oxidizer-fuel ratios, surface temperatures, and test techniques, using comparatively inexpensive hardware and test facilities, prior to the rotating tests on the full-scale seal. The 2D test series were an extension to the tests conducted under Contract AF 04(611)-10784. However, the seal gap was reduced from 0.002 to 0.001 in. on the basis of the successful demonstration of seal operation at the closer clearance.

### (2) Description of Hardware

(U) The tester (Figure IV-74a) was designed to produce oxidizer-rich gas at conditions simulating the ARES engine, except that facility limitations restricted the operating pressure to 1000 psi. Combustion in the seal test zone was observed by close-circuit television and photographed through a quartz window in the side of the tester.

IV, I, Combustion Seal (cont.)

(U) The test segment (Figure IV-74b) duplicated the cross-section of the hydrostatic combustion seal at the point of fuel introduction. Temperatures were monitored at a point 0.1 in. below the surface and 0.1 in. upstream of the fuel inlet, and also at two points along the downstream ramp. A 0.001-in.-thick slot was formed by fabricating the seal in two parts, using a 0.001-in.-thick shim to maintain the required gap while the parts were gold-brazed in a vacuum furnace.

### (3) Description of Tests

(U) The tester was installed in accordance with the flow diagram shown in Figure IV-74a. A total of 11 seal-segment tests were attempted during eight firings. A summary of these tests is shown in Figure IV-75. During the first three firings, two segments were tested simultaneously, but, because of technical difficulties with the bottom segments, it was decided that more expeditious testing could be accomplished by eliminating the bottom segments in the later tests. Two parts were tested for total durations of 8.3 and 40.5 sec, respectively. No test hardware was damaged. An inert purge fluid was used for filling the fuel-segment tubing to reduce the possibility of interpropellant contamination during startup. A significant development during the last three tests was the introduction of fuel to the segment before the preburner was activated. During the engine startup transient, fuel at low pressure may leak from the seal prior to precombustor ignition, which poses the possibility of damage to hardware during this time. The 2D test results indicate that there will be no hardware damage if the fuel and oxidizer flows to the seal precede combustor ignition.

(U) During 2D testing, the flow of fuel to the test segment was to be representative of prototype seal flow rate. This resulted in a lower fuel flow rate through a smaller slot than had been accomplished during the 2D tests on Contract AF 04(611)-10784. Examination of test data revealed that the seal-segment fuel-circuit pressure drop increased markedly within about 1.5 sec after stable preburner combustion had been attained, reducing fuel flow to about one-third of the nominal value. The added restriction was not permanent, and occurred only during preburner operation. An examination of possible causes led to the conclusion that this flow restriction had been caused by surface thermal expansion. This condition will not be significant on the hydrostatic seal since this seal can automatically adjust its average clearance.

(U) Temperatures at 0.1 in. below the surface of the upstream half of the segment rose steadily during all tests, but surface temperatures along the downstream ramp were less than 200°F, as can be seen from the data from test 030, Figure IV-76.

### (4) Conclusions from 2D Testing

(C) The 2D test program led to the following observations:

(a) Mixture ratios in the range of 10 to 20:1 appear to be acceptable.

(b) An average axial seal operating clearance of about 0.001 in. appears to be practical. If the initial seal operating clearance is reduced to lesser values, the seal distortion due to temperature of the rotating portion may cause rubbing. If the initial seal clearance is increased to more than 0.0015 in., the fuel flow rate will be excessive.

(c) The original rotating ring design exposed too much surface to the hot gases, and thermal expansion would distort the seal.

IV, I, Combustion Seal (cont.)

The rotating ring was therefore redesigned to provide a minimum of exposed area, and the upstream oxidizer flow was increased to cool the perimeter of the ring.

### b. Cold Rotating Tests in AeroZINE 50

(U) Before attempting the hot rotating tests, 12 tests were conducted without combustion to accumulate tester and seal performance and test sequence data without the hazards of combustion. Instead of combustion, nitrogen gas was used to pressurize the tester.

(1) The objectives of these tests were:

(a) Determination of fuel fill time at 60 psi.

(b) Determination of the drive-turbine gas pressure and flow necessary to rotate the tester at 40,000 rpm.

(c) Tester component evaluation.

(d) Determination of tester acceleration and deceleration rates.

(e) Determination of fuel flow from the seal at operating speed for two axial clearances and two seal-to-gas operating pressure differentials.

(f) Test installation checkout and evaluation.

IV, I, Combustion Seal (cont.)

### (2) Description of Hardware

(U) The tester shown in Figure IV-77 was used for the cold test series, except that the internal shielding and the velocity-control equipment were removed for the cold tests. The tester is described in Paragraph I,3,c,(3).

(U) The test seal was a prototype combustion seal, with a single-ply bellows. The rotating face was a simple disc with no provision for upstream oxidizer. No burnoff shield was installed.

### (3) Description of Tests

(U) For the cold rotating tests, the seal test chamber was pressurized with gaseous nitrogen and fuel supply pressure was computer-controlled to increase as the seal test chamber pressure increased. Data from the cold rotating tests are listed in Figure IV-78. Considerable difficulty was experienced in obtaining a workable test sequence which adequately represented the ARES engine. A reliable test system was developed in six tests.

(U) Tests 7 through 10B were conducted to refine the tester speed indication system and to eliminate defects in the test control system.

(C) Test 11 was conducted with a seal which was balanced to maintain a 200-psi pocket-to-gas differential pressure and an operating clearance of 0.00076 in. This test was completely successful with a maximum rotative speed of 39,400 rpm. The test duration of 84 sec included 60 sec at over 38,000 rpm. The test hardware was in excellent condition with no evidence of rubbing contact. The total AeroZINE 50 flow to the seal was 1.30 lb/sec. The outward flow was 0.27 lb/sec.

IV, I, Combustion Seal (cont.)

(C) Test 12, the final test in the series, utilized a seal which was designed to maintain a 500-psi pocket-to-gas differential pressure. This test was completely successful. All objectives were met; seal fuel flow to combustion was 0.43 lb/sec and speed was 40,000 rpm. Total rotating time was 78 sec, with a duration of 63 sec at 40,000 rpm. Surface velocity was over 600 ft/sec and the pressure on the installed face was 19.5 psi. The seal was installed with an initial compression of 0.016 in. There was no evidence of seal contact and no damage to the hardware.

(4) Conclusions from Cold Rotating AeroZINE 50 Tests

(C) The following results were obtained from the cold rotating tests:

(a) The seal has performed at fuel flows and pocket-to-gas differential pressures throughout the expected range of operating conditions.

These Include:

| | |
|---|---|
| Pocket-to-gas differential pressure | 200 and 500 psi |
| Fuel flows (to combustion) | 0.27 to 0.43 lb/sec |
| Calculated operating clearance | 0.00076 to 0.001 in. |
| Operating speed | 40,000 rpm |

(b) Axial wobble of 0.0004 in. at operating speeds can be accommodated with an average clearance of 0.00076 in.

(c) The tester components were checked out at engine operating speeds and pressures for the desired duration of 60-sec tests.

IV, I. Combustion Seal (cont.)

(d) Fill times, turbine gas pressures, acceleration and deceleration rates, and pressure drops were established.

(U) The cold rotating tests revealed a weakness in the seal bellows structural resistance to pressure reversal. As a result of these tests, the method of bellows attachment was redesigned and the use of two-ply bellows was initiated.

(U) During Test 8, the pressurizing fuel flow to the seal interior was interrupted and the seal faces contacted while rotating. This contact resulted in welding the faces together. This is significant in that, if restart in the vacuum-condition of space is required, consideration must be given to the demonstrated tendency of the flame-plated seal faces to cold weld, and further investigation of face materials will be required, since there will be momentary rubbing contact during restart.

c. Hot Rotating Tests

(1) Technical Approach

(U) The hot rotating tests were designed to simulate as closely as possible the conditions to be expected in the ARES engine during atmospheric startup. The tests were therefore prepared to meet the conditions as listed in Paragraph I,1,b.

(U) Attainment of the objective included the following tasks:

(a) Simulation of the ARES engine start transients.

(b) Operational checkout of the test area pressure intensifier system.

IV, I, Combustion Seal (cont.)

(c) Determination of the operating characteristics of the gas generator.

(d) Determination of the effects of thermal distortion of the seal.

(e) Rotating tests under full operating conditions.

(2) Start Transient Simulation

(U) The ARES start transients were simulated as closely as practical (Figure IV-79). Pressure rise-rates were controlled by regulating the pressurizing rate of the nitrogen, which operated the propellant pressure intensifiers. Acceleration was controlled by adjusting the nozzle size and nitrogen pressure which operated the tester drive turbine. It was necessary to modify the start transients somewhat to ensure the proper sequence of events, because a malfunction could occur if the mixture ratio should shift during the start transient. It was also necessary to ensure that fuel was admitted to the seal interface during startup rotation. The requirements were accomplished by initiating the oxidizer pressure rise, which, at 800 psig started the fuel pressurizing system. When the fuel pressure reached 200 psig, the turbine speed was initiated. The resulting start transient is shown in the test data plot for Test 14 in Figure IV-80 and includes the following information.

(a) Startup pressures: approximately 100 psig.

(b) Time elapsed from start of pressurization to operating pressure: 1.25 sec.

(c) Time elapsed from start of pressurization to 90% of full rotation: 1.0 sec.

IV, I, Combustion Seal (cont.)

(U) Engine simulation required an extremely precise, interconnected, computer-controlled test system. Despite efforts to simplify the test as much as possible, the sequences, safety interlocks, and shutdown parameters resulted in a complexity which was sufficient to result in several malfunction shutdowns.

### (3) Description of Test Hardware

(C) The hydrostatic combustion seal tester is shown in Figure IV-77. The tester was fabricated from stainless steel and was designed for an operating internal pressure of 3000 psi. The tester consisted of three basic parts: (1) a gas generator or preburner, to supply the oxidizer-rich hot gas environment simulating the ARES engine; (2) a test chamber, which contained a gas velocity control element to create the gas velocity expected in the ARES engine, and served as a combustion chamber for the seal testing; and (3) a drive housing, containing a turbine-driven shaft, the test seal and burnoff shield, and most of the test supply connections. Axial thrust was carried by an oil-operated hydrostatic bearing.

(U) This tester was designed on Contract AF 04(611)-10784 and is described in detail in the final report, AFRPL TR-66-79, Section III,C.

(U) The test seal, installed in the tester, is shown in Figure IV-81. The seal consisted of a rotating face made of AM-350, containing 180 0.014-in.-dia pheripheral holes for upstream oxidizer coolant, and a stationary face of Invar, which contained six pockets around the face. The seal faces were coated with LC-1B (80% $Cr_3C_2$ + 20% Ni Cr) applied by the Linde flame-plating method. The stationary face was attached to a flange by a single convoluted toroidal bellows, made of two 0.006-in.-thick plies of Inconel 718.

IV, I, Combustion Seal (cont.)

(U) A burnoff shield made of 0.050-in.-thick Type 304 stainless steel served as a passage for downstream cooling oxidizer admission. Thermocouples were welded into the outside surface of the shield.

(U) Fuel entered each seal face pocket through a 0.035-in.-dia orifice. The flow was divided so that about 60% passed inward into the fuel cavity and the remainder flowed outward, where it combusted in the upstream and downstream oxidizer and the oxidizer-rich gas stream.

(U) A detailed description of the seal design and operation appears in Final Report AFRPL-TR-66-79, Section II,B.

### (4) Description of Tests

#### (a) Preburner Checkout

(U) Seven tests were conducted to evaluate the preburner gas generator, to check out the pressure intensifier system, to calibrate the gas generator cavitating venturis, and to investigate the gas generator start characteristics at various fill pressures. All equipment functioned properly and the gas generator demonstrated ability to start successfully at 60 psi. This established that engine start transients could be simulated with the existing facilities.

#### (b) Seal Distortion Tests

(U) Three nonrotating tests were conducted in which the preburner was operated, but $N_2O_4$ was substituted for fuel at the seal, so that thermal distortion, oxidizer fill times, and operating clearances could be determined without combustion at the seal. These tests

IV, I, Combustion Seal (cont.)

demonstrated that the seal could operate at engine temperatures without excessive distortion. At the conclusion of the tests, the flame plate had blistered, attributable to chemical attack of the bond surface. This condition will require further action if it develops during hot tests.

### (c) Hot Rotating Tests

(U) The tester was installed in the test stand in accordance with the flow diagram, Figure IV-77. This depicts all flows, pressures, and purges used during hot rotating tests.

(U) Eleven tests were conducted in an effort to reach the program objective of 60 sec of operation under engine conditions. Data from these tests are tabulated in Figure IV-82. Test accomplishments are summarized as follows:

| | |
|---|---|
| Tests completed | 11 |
| Total combustion duration | 82.25 sec |
| Total rotation time | |
| Over 30,000 rpm | 29.65 sec |
| Over 35,000 rpm | 21.25 sec |
| 40,000 ± 500 rpm | 4.1 sec |

(U) Tests 5 through 8 were conducted with the same seal, without inspection between restarts. This was significant because it established that the seal is capable of restarts. Tests 4, 10, 11, and 12 were terminated with substantial damage, but all malfunctions were due to problems not associated with the prototype seal. The burnoff shield, downstream of the seal face, was found to be a major contributor to test malfunctions in Tests 8, 11, and 12 and a redesign was necessary. The annular space under the burnoff shield was made free from any obstructions so that all of the under surface of the shield was continually cooled by the flowing oxidizer. A velocity below the shield of 10 fps was calculated to be minimum flow for efficient regenerative cooling of the shield; therefore, the flow rate was kept above 10 fps. Test 13 was conducted to test one version of the new design, wherein cooling oxidizer was allowed to flow to the outside of the shield through slots near the oxidizer exit annulus. The test continued for the expected duration with no combustion damage, but the tip of the shield cracked at the slots because of structural weakness. The shield was changed so that 40 holes, 0.030 in. in diameter, replaced the slots. Test 14 confirmed the new design, operating for the expected duration without damage to the shield, as can be seen from the posttest photograph, Figure IV-83. A malfunction of the upstream velocity control equipment caused minor damage to the rotating ring during Test 14, so that the necessary tests to attain the program objective could not be completed. It will be necessary therefore, to continue testing during the Phase I extension.

### (C) (5) Conclusions and Recommendations

#### (a) Conclusions

##### 1 Propellant Flows

Propellant flows from the seal will be as follows:

| | |
|---|---|
| Fuel to combustion | 0.43 lb/sec |
| Upstream oxidizer | 5 to 6 lb/sec |
| Downstream oxidizer | 10 to 12 lb/sec |

(C) The prototype seal is designed to maintain a fuel flow to combustion of at least 0.40 lb/sec. This flow separates the seal faces about 0.001 in., which is an acceptable clearance to accommodate thermal and pressure-induced conical deflections of the seal face. Further testing is required to ascertain minimum clearances.

(C) The tests have proved that both upstream and downstream oxidizer flows are essential to reliable seal operation. Downstream flow must be at a velocity of approximately 70 fps, in order to create sufficient velocity head to prevent the hot gas from forcing fuel under the burnoff shield. The optimum oxidizer flows have not been established, and reductions in oxidizer flow require further testing beyond the scope of this contract.

## 2 Gas Supply Conditions

(C) The gas generated by the preburner closely resembles that in the ARES engine. During Test 14, the measured temperature was 1100°F, pressure was 3300 psi, and the gas velocity at the seal was 211 fps. The ARES engine gas temperature will be 1100°F, pressure will be 3100 psi, and gas velocity will be about 225 fps.

## 3 Seal Performance

(C) Short duration test results have demonstrated that steady state is reached in 3.5 sec, burnoff-area conditions reach equilibrium in about 7 sec, and the maximum burnoff area temperatures are less than 500°F. Seals have been operated in steady-state conditions without surface contact, and cold-flow tests have shown that at 40,000 rpm, the seal will follow an axial runout of at least 0.0004 in. without contacting. Combustion test results indicate that the chief problem to be solved is the protection of associated hardware. This can be accomplished by (1) increasing oxidizer coolant, (2) changing the direction of oxidizer injection, (3) redesigning the hardware to redirect the flame, and (4) redistributing the oxidizer to improve cooling efficiency. All of these modifications will be investigated. Although the program objective of 60 sec duration has not yet been achieved, test results indicate that the combustion seal will function properly if the hardware immediate to the seal can be protected.

### (b) Recommendations

### (U) 1 Additional Tests to Meet Program Objective

A total of ten additional tests have been planned to meet the program objective. Limitations to the test area oxidizer supply will require at least two tests of one assembly to reach the required total duration. Hardware is being obtained for five separate tests. Testing will continue as a Phase I extension until the test objective is reached. If an unexpected development should make it appear that the hydrostatic combustion seal is not practical for extended-duration tests, an inert purge seal will be substituted for duration testing.

### 2 Recommended Future Work

### a Reduced Fuel Flow

(U) The seal pocket-to-gas differential pressure has been set at 500 psi, to ensure that the pocket pressure will exceed any combustion pressure spikes that might force oxidizer-rich gas into the seal. When the maximum pressure spikes from the ARES precombustor are determined, the seal should be redesigned for a lower differential pressure. In this way the operating clearance can be maintained at a lower fuel flow. Additionally, tests should be conducted to determine the minimum operating face clearance, with the consequent reduction in fuel flow.

IV, I, Combustion Seal (cont.)

b Reduced Oxidizer Flow

(U) The oxidizer flow rates at the seal were selected to give maximum protection and are probably in excess of the required amount. The determination of proper oxidizer flow rates for existing and future fuel flows will permit more efficient engine operation, and tests should be conducted to accomplish this.

c Bellows Redesign

(U) In the prototype seal design, the bellows operates with a differential pressure of about 2600 psi. Preliminary design studies have been made on a configuration that will permit the bellows to function at essentially no differential pressure. This feature will add to the reliability of the seal, and the design should be investigated.

d Bellows Compression

(U) The prototype bellows has been hot tested with an axial compression of 0.010 in. The total axial travel in the ARES turbopump has been calculated to be close to 0.020 in.; therefore, further testing at the new compression is indicated.

e Restart and Throttling

(U) Testing of the prototype seal has been conducted with all propellant passages purged with nitrogen during startup and shutdown. If restart capability is required of the seal, investigations must be made to determine the best materials and face design to effect a dependable static seal after shutdown and prior to restart. If vacuum shutdown and

IV, I, Combustion Seal (cont.)

restart is required, it will be necessary to determine face materials that will resist vacuum welding. If engine throttling is expected, the operation of the seal and components must be evaluated under the pressures and flows that will result.

## IV, Turbopump Assembly (cont.)

### J. PURGE SEAL

### 1. General

#### a. Background

(U) A purge seal was required for the T-engine turbopump as a backup in the event the hydrostatic combustion seal should prove impractical. The purge seal designed for this application (Figure IV-84) operates on the same hydrostatic principle as and is similar in design to the hydrostatic combustion seal. Inert purge fluid will be contained in a pressurized tank, external to the ARES engine, and will flow through orifices in the six seal-face pockets to the face of the seal, thus providing an inert barrier separating the fuel from the oxidizer-rich gas. The purge seal was designed to fit in the advanced TPA in the same location as the hydrostatic combustion seal and will not require extensive modification of the TPA.

(U) An initial design study of this purge seal was completed under Contract AF 04(611)-10784 and is discussed in Section II,D of the final progress report, AFRPL-TR-66-79.

#### b. Objective

(C) The [illegible]ram objectives for the purge seal were to design, fabricate, and test the seal. Testing was required under the following TPA operation conditions:

Gas pressure, 3100 psig ± 600 psi
Gas temperature, 1100 ± 50°F
Gas velocity, 200 to 250 fps

IV, J, Purge Seal (cont.)

Rotative speed, 40,000 rpm

Test duration was to be 60 sec (including start and stop transients), and the seal must be reusable after the test.

c. Approach

(U) The objective was reached via the following steps:

(1) Design of the seal
(2) Selection of a purge fluid
(3) Cold rotating tests of the purge seal system
(4) Hot rotating tests under full engine conditions

## 2. Design

### a. Seal Design

(U) The purge seal was designed to be interchangeable with the hydrostatic combustion seal in the ARES T-configuration TPA with a minimum of different parts. Because of the high relative surface speed encountered in this seal application (500 fps at 3-in.-dia) it was determined that a hydrostatic face seal would provide the most reliable operation. Requirements for small leakage and low weight excluded fixed-clearance labyrinth seals from consideration. The purge seal (Figure IV-84) is similar in design to the hydrostatic combustion seal (Figure IV-72), except that a purge fluid instead of fuel is introduced at high pressure into six orificed pockets in the seal face. The purge fluid, in separating the fuel from the oxidizer, flows outward to the hot gas and inward to the bearing cavity, where it mixes with the fuel from the bearings, and flows to the fuel-pump suction.

IV, J, Purge Seal (cont.)

(U) The orifices in the seal pockets were sized to operate the seal at purge-fluid flows of 1, 2 or 3 cu in./sec, so that the operating face clearance could be adjusted between tests. The seal dimensions were selected to give an optimum balance of minimum flow rate and limited temperature rise of the purge fluid due to viscous friction. For the fluid selected, the optimum width of the seal land was about 0.1 in. This dimension results in a fluid temperature rise of about 600°F at the minimum design total flow rate of 1 cu in./sec (3.9 lb/min) (Figure IV-85). This temperature rise and flow rate correspond to a seal running clearance of approximately 0.00085 in. Heat-transfer and distortion studies showed that this running clearance and minimum flow rate would be feasible if the seal face were fabricated from a material having a low coefficient of thermal expansion (e.g., Invar) and an oxidizer coolant flow were directed over the backside of the seal. The face and the inside (bore) of the seal was coated with a hard material to prevent galling caused by rubbing and by foreign particles which might be carried in the purge fluid. Two sets of three-piece piston-ring seals were designed for use as secondary purge-fluid seals in this application, since these seals are subjected to axial motion only and a small amount of purge-fluid leakage could be tolerated.

(U) The stability of the seal was investigated to ensure that the seal would not be excited into axial vibration by wobbling of the rotating ring. The natural frequency of axial vibration is 534,000 cpm, or 13 times the shaft speed; therefore, the seal will not be excited by the shaft rotation frequency. Additional stability is obtained from viscous damping due to squeeze-film effects and from the friction damping caused by the piston-ring secondary seals.

IV, J, Purge Seal (cont.)

### b. Selection of Purge Fluid

(C) The requirements for a purge fluid for use in the ARES engine were as follows:

(1) Must not react with $N_2O_4$ or AeroZINE 50 in a 600°F, 3500-psi environment.
(2) Must be noncorrosive in combination with AeroZINE 50.
(3) Low specific gravity is desirable.
(4) High specific heat is desirable.
(5) Must not decompose in 600°F, 3500-psi environment.
(6) Must not be adversely affected by radiation of the level encountered in space environment.

(U) The purge fluid selected, E. I. DuPont's Fluid PR 143 AB, ("Krytox"), is a perfluorinated hydrocarbon with a specific gravity of 1.8 and a viscosity of 11 centistokes at 210°F. The fluid is stable to 600°F; its autoignition point is above 1300°F, and its specific heat is 0.30 at 400°F. It was selected for this application because of its chemical inertness and high-temperature stability. These characteristics outweigh the relatively high specific gravity and low specific heat. Tests by the manufacturer indicate good radiation stability. Laboratory tests at Aerojet-General determined that the fluid does not react with either propellant, and it does not increase the shock, adiabatic compression, or spark sensitivity of the propellants. The viscosity at operating temperatures was considered optimum for minimum purge flow at the desired operating clearances.

(U) During testing, it was discovered that the purge fluid exhibits a fivefold viscosity increase when pressurized to operating conditions (Figure IV-86). As a result of the viscosity increase due to pressure, filters which were adequate for low-pressure flows were much too restrictive

IV, J, Purge Seal (cont.)

at operating pressures. Because of the high purge fluid viscosity in comparison with $N_2O_4$ and AeroZINE 50, two problems were experienced during the tester start transient. One problem was that the purge fluid flowed outward from the seal into the downstream oxidizer coolant circuit before the start of the test. When high-pressure oxidizer was introduced, the resistance to flow caused by the purge fluid in the circuit resulted in grossly increased back pressure, which distorted the shield over the seal. The shield has been redesigned to resist distortion, but the new design has not been tested. The other problem associated with the purge-fluid viscosity was restriction of the bearing-cavity outlet labyrinth. Before the tester was started, purge fluid filled the bearing-cavity labyrinth passages. When high-pressure fuel was introduced into the bearing cavity, the increased resistance to flow through the labyrinth caused the bearing cavity pressure to rise higher than anticipated, resulting in the flow of purge fluid and fuel from the bearing cavity, across the seal face, and into the downstream oxidizer coolant stream. Figure IV-87 illustrates the effect of the purge fluid on the pressure-rise rate of the bearing cavity. This effect can probably be eliminated by adjusting the valve-opening sequence of the tester. This approach, plus the re-evaluation of candidate purge fluids of lower viscosity, will be taken if purge-seal testing is resumed. During initial engine testing, when a purge seal may be used and there is no minimum weight requirement, it may be preferable to use a less viscous fluid to eliminate problems associated with the viscosity increase with pressure.

### c. System Weight

(U) The system weights of purge fluid (1.8 specific gravity) and container, exclusive of valves, lines, and other auxiliary equipment, for a 3-min operation of the purge seal are as follows:

IV, J, Purge Seal (cont.)

| Flow, cu in./sec | Weight, lb |
|---|---|
| 1 | 18 |
| 2 | 35 |
| 3 | 53 |

### 3. Test Program

#### a. Tester and Installation

(U) The tester used for testing the purge seal was the same as that used for the hydrostatic combustion seal (Figure IV-75), except that the fuel-supply passages were modified to permit introduction of purge fluid to the seal (Figure IV-88). Installation of the tester in the test stand was also similar to that of the hydrostatic combustion seal tester, except that the fuel supply to the seal was replaced with a reservior of purge fluid pressurized by the fuel intensifier. The installation flow diagram is shown in Figure IV-89.

#### b. Simulation of TPA

(U) As in the hydrostatic combustion seal tests, an attempt was made to simulate the engine start transients. The sequence of operations during startup required precise control to avoid malfunctions in the tester which would not occur in the engine, and minor adjustments to the sequence were necessary to ensure the proper balance of pressures and to accommodate the pressure surges resulting from changes in the viscosity of the purge fluid. Despite the viscosity change, the pressures, rise rates, acceleration, gas velocity, and temperatures were close to the expected TPA conditions. In Test 7, the most successful test, engine operation conditions were reached 1 sec after the start of pressure increase.

## IV, J, Purge Seal (cont.)

### c. Testing

(U) Nine tests were conducted; the results are summarized in Figure IV-90.

#### (1) Cold Rotating Tests

(U) During Tests 1, 2, and 3, the tester was gradually pressurized with $GN_2$ instead of hot gas, so that the seal operating clearances could be determined without thermal distortion. As an added precaution, fuel was used instead of oxidizer beneath the downstream shield. The seal was orificed for a purge flow of 2 cu in./sec. Tests 1 and 2 were terminated because of the unexpected high purge-fluid viscosity, which was sufficient to virtually stop flow through the filter. This led to an investigation of the purge fluid viscosity at high pressure, which revealed the characteristic of the fluid to increase in viscosity with increasing pressure. The filter area was then increased, and, in Test 3, operation continued for 38 sec, including 27 sec at 40,000 rpm. Post-test examination revealed that the seal faces had contacted slightly, and that two pocket orifices were partially plugged. The purge-fluid flow during this test was 1.4 cu in./sec instead of the design flow of 2 cu in./sec. The seal was orificed for a purge-fluid flow of 3 cu in./sec for the remaining hot tests, since some thermal distortion was expected.

#### (2) Hot Tests

(U) Six hot tests were conducted in an attempt to meet program requirements. The most successful, Test 7, operated for 55.3 sec at over 40,000 rpm, but because of damage to the purge-seal parts from high internal bearing-cavity pressure during the start transient of Test 6, fuel and purge fluid flowed outward into the oxidizer-rich atmosphere, causing combustion damage to the seal faces. The instrumentation gave little indication of this malfunction (see Figure IV-87), and the test appeared successful before the hardware was examined. The test data indicated that the initial damage to the shield occurred during Test 6, but it was not detected in the test records, and since the hardware was not inspected after Test 6, the next test was started with the damaged hardware.

(U) In Tests 8 and 9, attempts were made to control the shield distortion by adjusting fill-times and clearances, but it was finally concluded that a complete redesign of the shield was necessary. At the end of Test 9, the computer-controlled shutdown sequence failed to operate, and during the manual shutdown the oxidizer valve was mistakenly closed before the fuel valve. Because of this improper sequence, the gas generator mixture ratio went from oxidizer-rich to fuel-rich, causing extensive damage to the hardware.

(U) No further testing of the purge seal was attempted because the hydrostatic combustion seal had given favorable results, and testing will not be resumed unless it is found that the hydrostatic combustion seal is not practical.

### (3) Conclusions from Tests

(U) Every failure of the purge seal during hot testing started with failure of the downstream shield. This part was underdesigned for the high pressure experienced during startup. The redesigned shield will not flex with startup pressure and should prevent recurrence of this failure. The cold rotating tests established that the purge fluid prevents mixing of fuel and oxidizer-rich gas. It is therefore expected that the seal will perform as required when operated with the redesigned shield. The purge-fluid flow rate will be 12 lb/min; tankage and fluid for an engine to operate 3 min will weigh about 53 lb, exclusive of valves, supports, and piping.

(U) If the purge seal is to be used in the TPA, either in testing or in the ARES engine, at least one 60-sec test should be conducted with the redesigned shield. If the purge seal is used in the engine, additional tests will be necessary to establish the minimum flow for safe operation in order to reduce the system weight.

### 4. Application to TPA

(U) The turbopump assembly (Figure IV-1) has been designed to accommodate either the purge seal or the combustion seal. The purge seal is expected to be used in preliminary testing, and the combustion seal in the final tests. In this case, a minimum purge flow is not essential, since weight reduction will not be important, and an alternative purge fluid may be investigated. If the purge seal is to be used in the ARES engine, it will be necessary to design the tankage, pressurizing system, controls, and installation of the purge system.

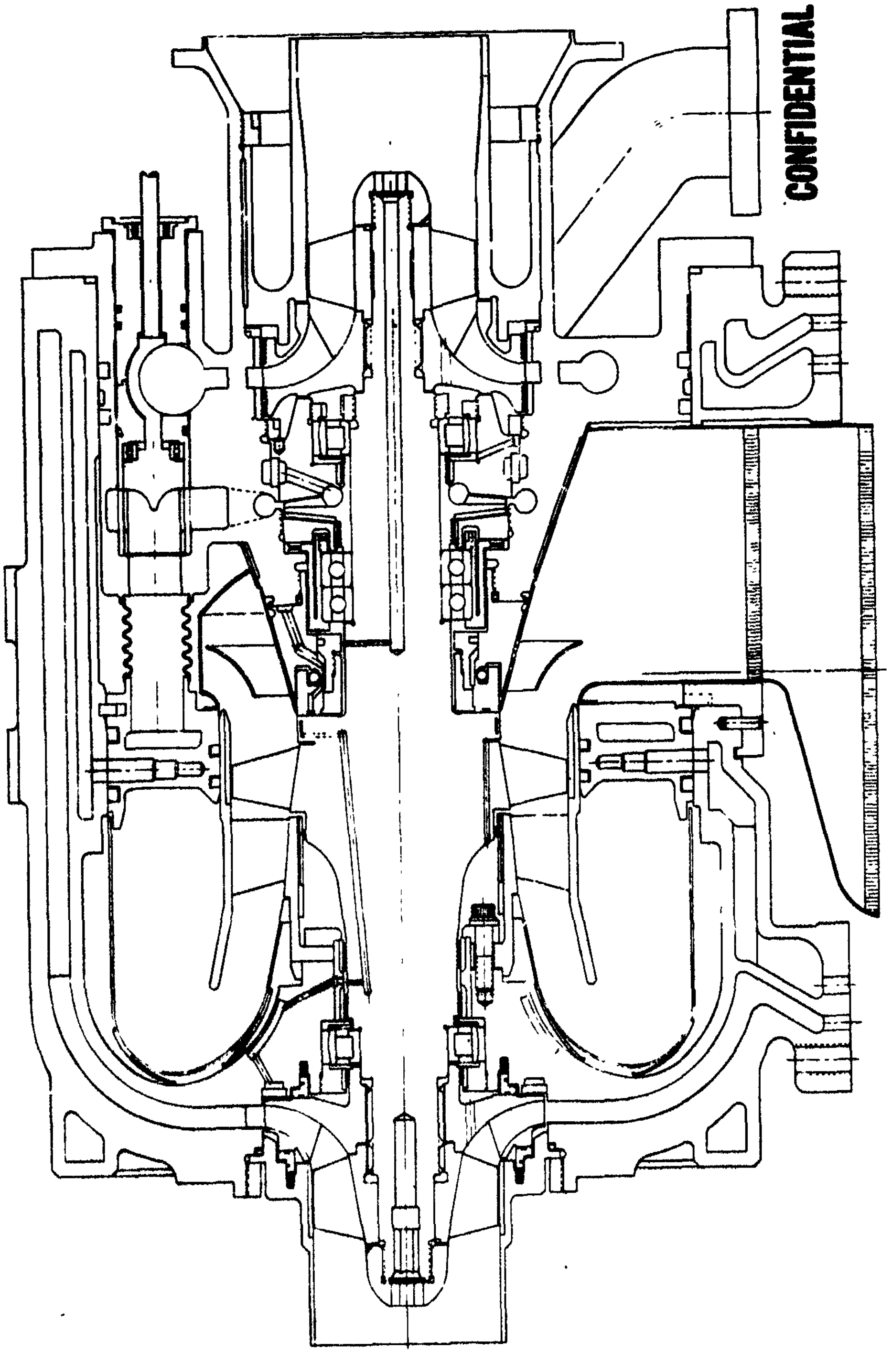

CONFIDENTIAL

C Design TPA Layout (u)

Figure IV-1

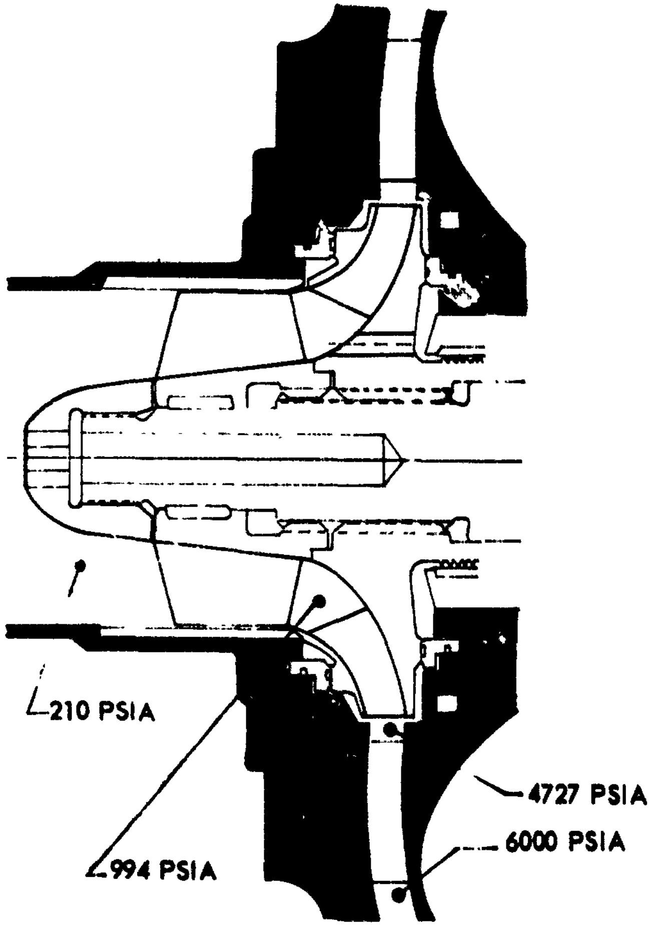

| | INDUCER | IMPELLER |
|---|---|---|
| FLOW, GPM | 1444 | 1444 |
| HEAD, FT | 1660 | 7990 |
| SPEED, RPM | 40,000 | 40,000 |
| EFFICIENCY | 70 | 78 |
| HORSEPOWER | 1240 | 5330 |
| SPECIFIC SPEED | 5850 | 1790 |
| MAXIMUM SUCTION SPECIFIC SPEED, RPM | 28,600 | 6500 |
| MATERIAL | AM-355 | CAST 17-4 PH |
| STRESS | | |
| MAXIMUM STRESS, PSI | 42,000 | 55,000 |
| MAXIMUM ALLOWABLE, PSI | 105,000 | 140,000 |

CONFIDENTIAL

Oxidizer Pump Design Data (u)

Figure IV-2

| | INDUCER | IMPELLER | |
|---|---|---|---|
| | | FIRST | SECOND |
| FLOW, GPM | 945 | 945 | 173 |
| HEAD, FT | 1360 | 8175 | 6150 |
| SPEED, RPM | 40,000 | 40,000 | 40,000 |
| EFFICIENCY, % | 70 | 66 | 57 |
| HORSEPOWER | 416 | 2660 | 424 |
| SPECIFIC SPEED | 5090 | 1430 | 750 |
| MAXIMUM SUCTION SPECIFIC RPM SPEED | 30,000 | 5590 | |
| MATERIAL | TITANIUM 6 AL 4 VA | CAST 17-4 PA | AM-355 |
| STRESS | | | |
| MAXIMUM STRESS, PSI | 49,000 | 77,000 | 80,000 |
| MAXIMUM ALLOWABLE, PSI | 70,000 | 112,000 | 144,000 |

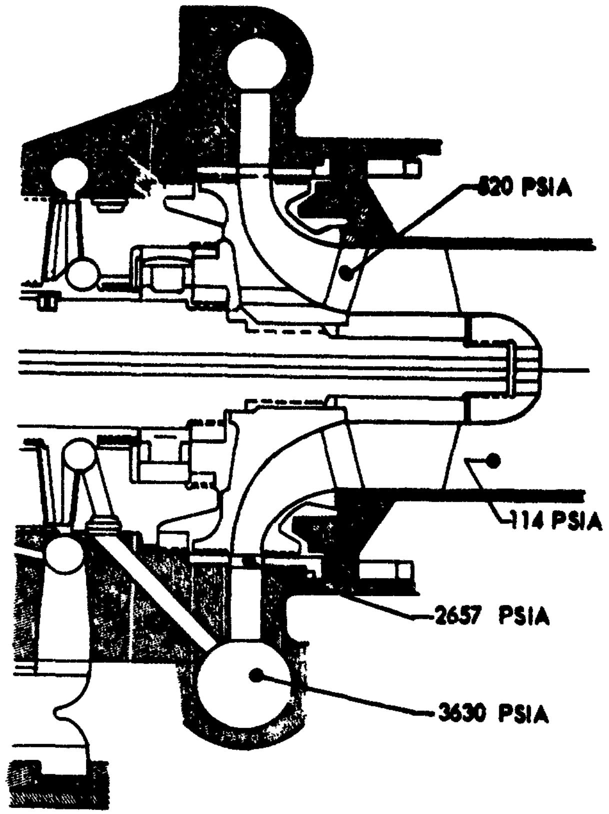

CONFIDENTIAL

Fuel Pump Design Data (u)

Figure IV-3

UNCLASSIFIED

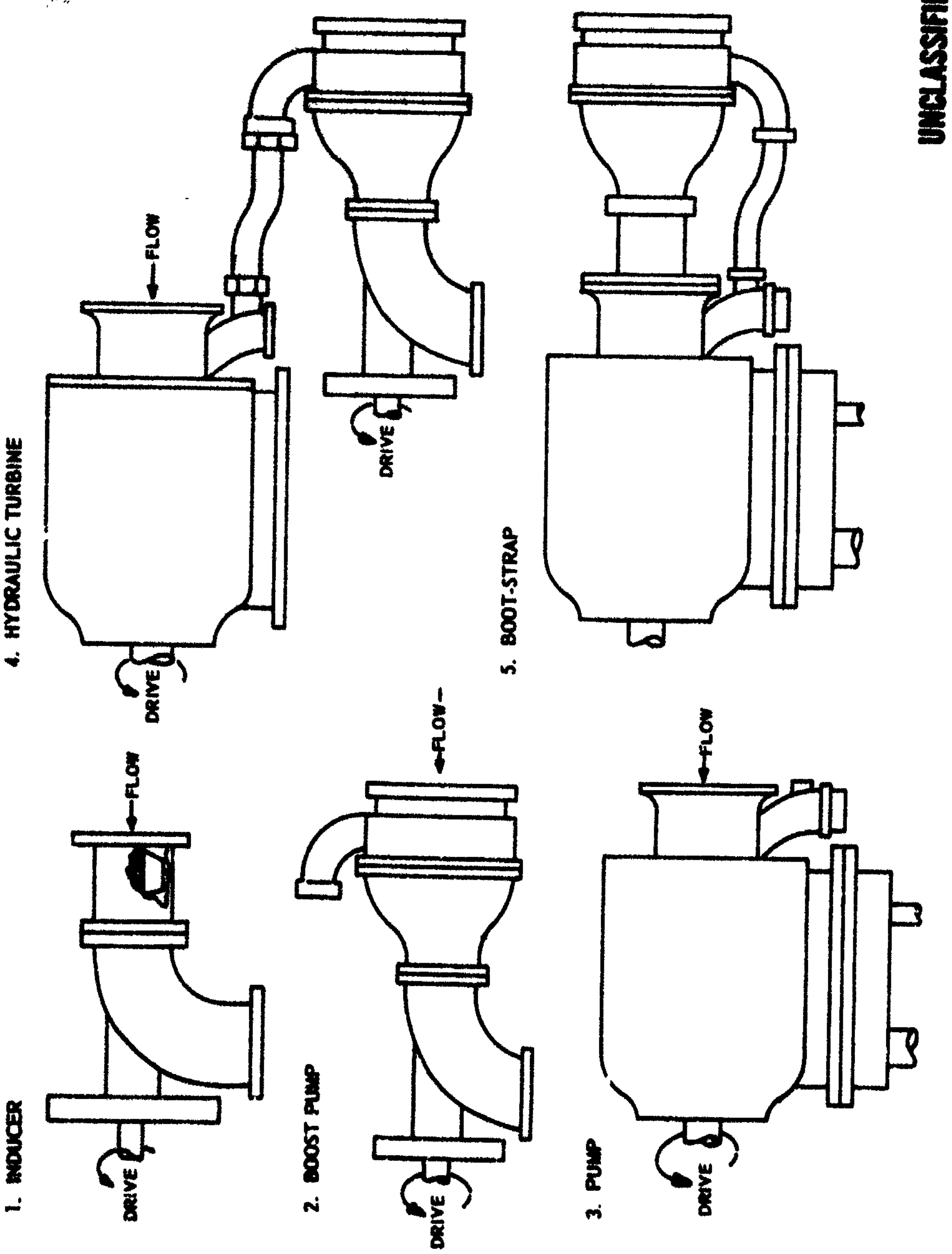
1. INDUCER
DRIVE
FLOW
2. BOOST PUMP
DRIVE
FLOW
3. PUMP
DRIVE
FLOW
4. HYDRAULIC TURBINE
DRIVE
FLOW
DRIVE
5. BOOT-STRAP

TPA Water Test Sequence

Figure IV-4

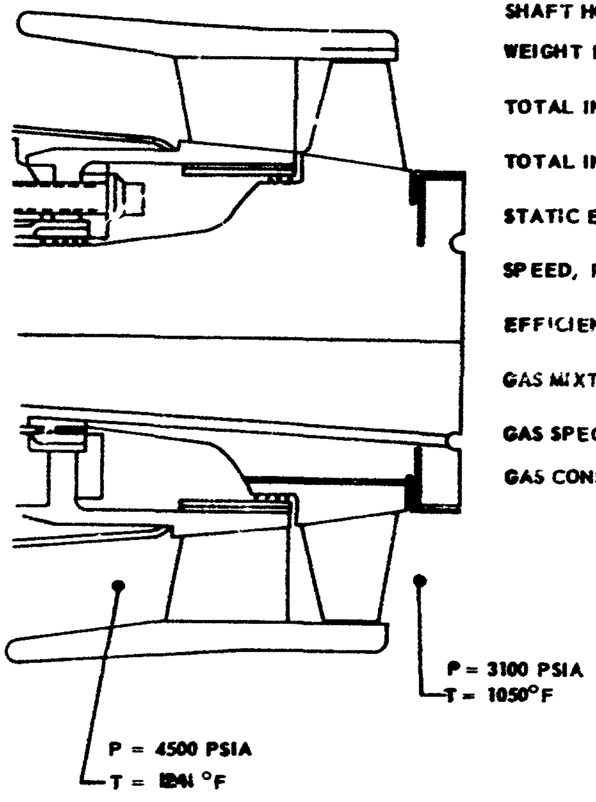
P = 3100 PSIA
T = 1050°F
P = 4500 PSIA
T = 1240 °F

| | |
|---|---|
| SHAFT HORSEPOWER | 10,070 |
| WEIGHT FLOW, LB/SEC | 233 |
| TOTAL INLET TEMP, °F | 1240 |
| TOTAL INLET PRESSURE, °F | 4650 |
| STATIC EXIT PRESSURE, °F | 3100 |
| SPEED, RPM | 40,000 |
| EFFICIENCY, % | .77 |
| GAS MIXTURE RATIO | 11.30 |
| GAS SPECIFIC HEAT RATIO | 1.257 |
| GAS CONSTANT, °F | 46.62 |

SHAFT-ROTOR TEMP DISTRIBUTION AT 2 SEC

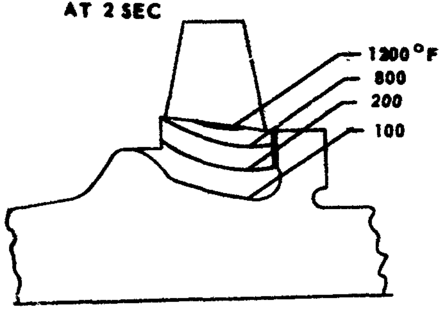
1300 °F
800
200
100

SHAFT-ROTOR STRESS DISTRIBUTION AT 2 SEC

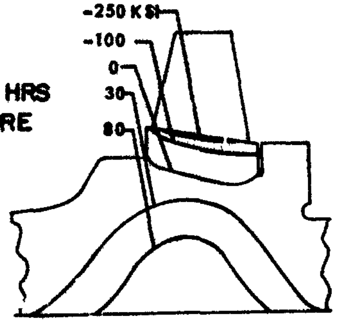
-250 KSI
-100
0
30
80

LIFE = 77 CYCLES

ROTOR BLADE STRESS GOODMAN DIAGRAM

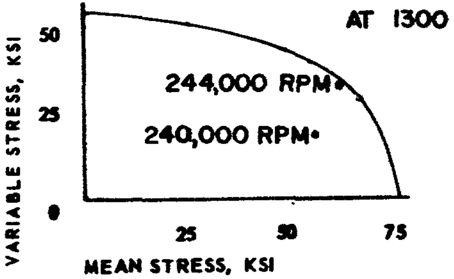

Turbine Design Data (u)

CONFIDENTIAL

Figure IV-5

Air Test Turbine

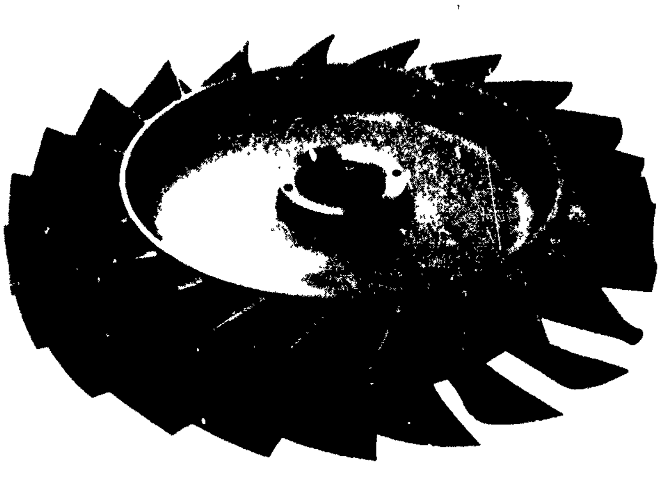

MOD I TURBINE

(TAPERED THICKNESS – TWISTED BLADES)

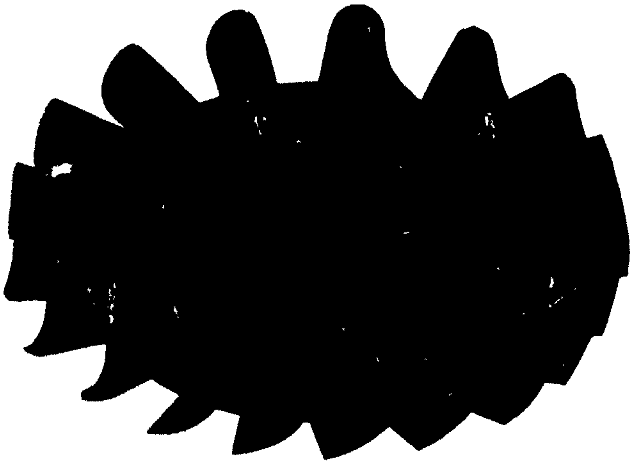

MOD II TURBINE

(CONSTANT SECTION–ZERO TWIST BLADES)

UNCLASSIFIED

Figure IV-6

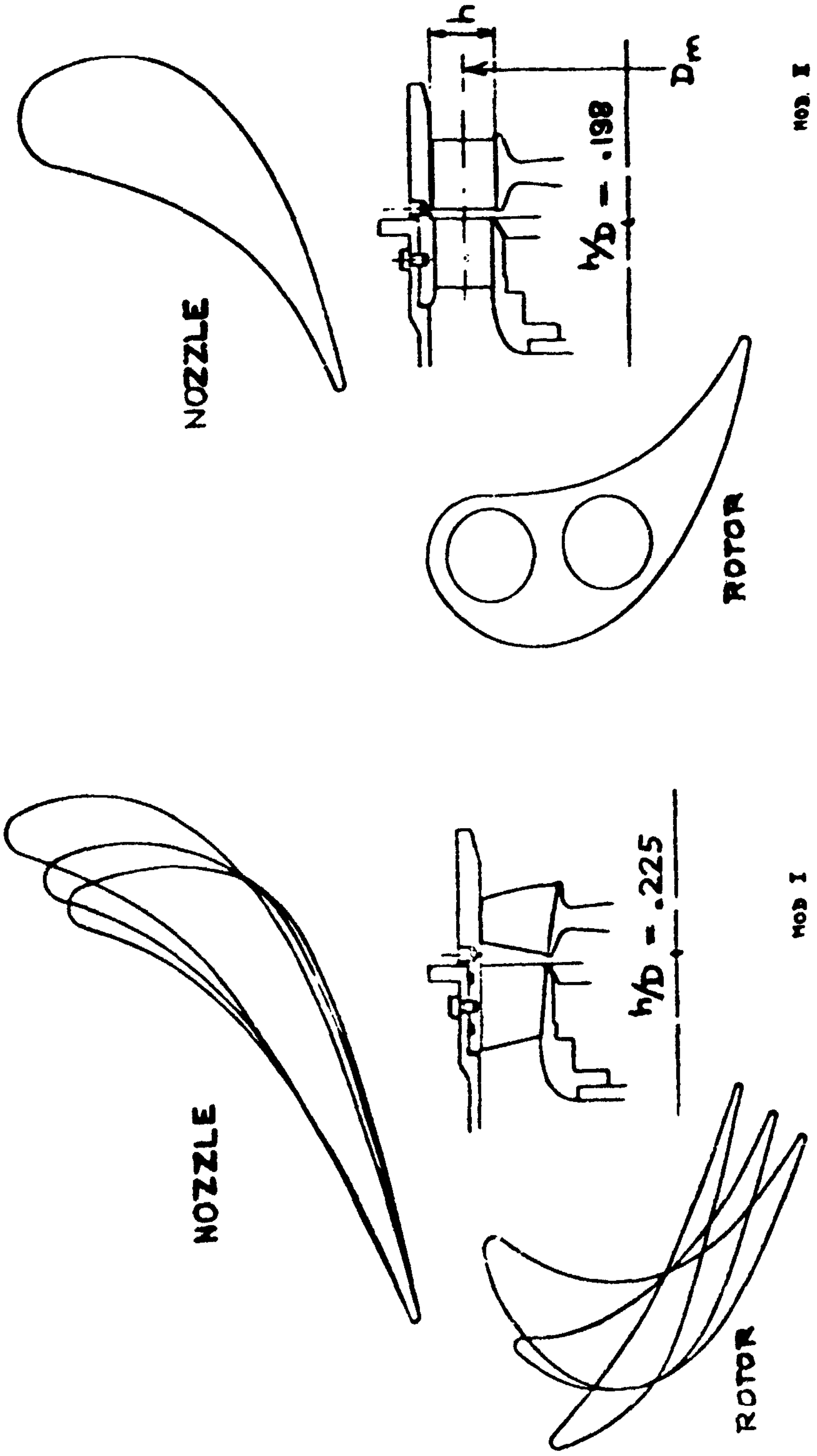
NOZZLE
h
$D_m$
h/D = .198
ROTOR
MOD II
NOZZLE
h/D = .225
ROTOR
MOD I

Turbine Mod I and Mod II Configurations

Figure IV-7

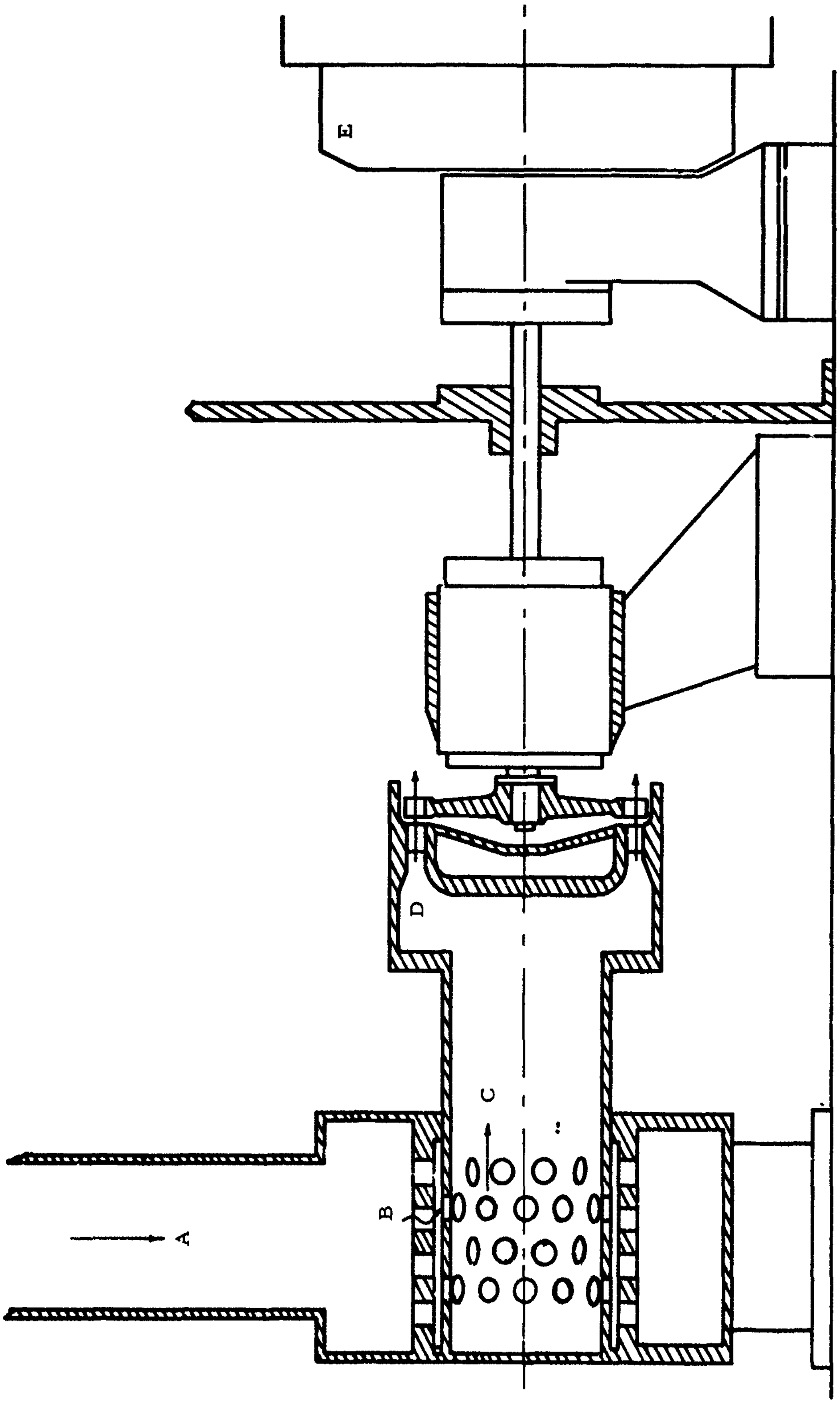

Air Test Setup

Figure IV-8

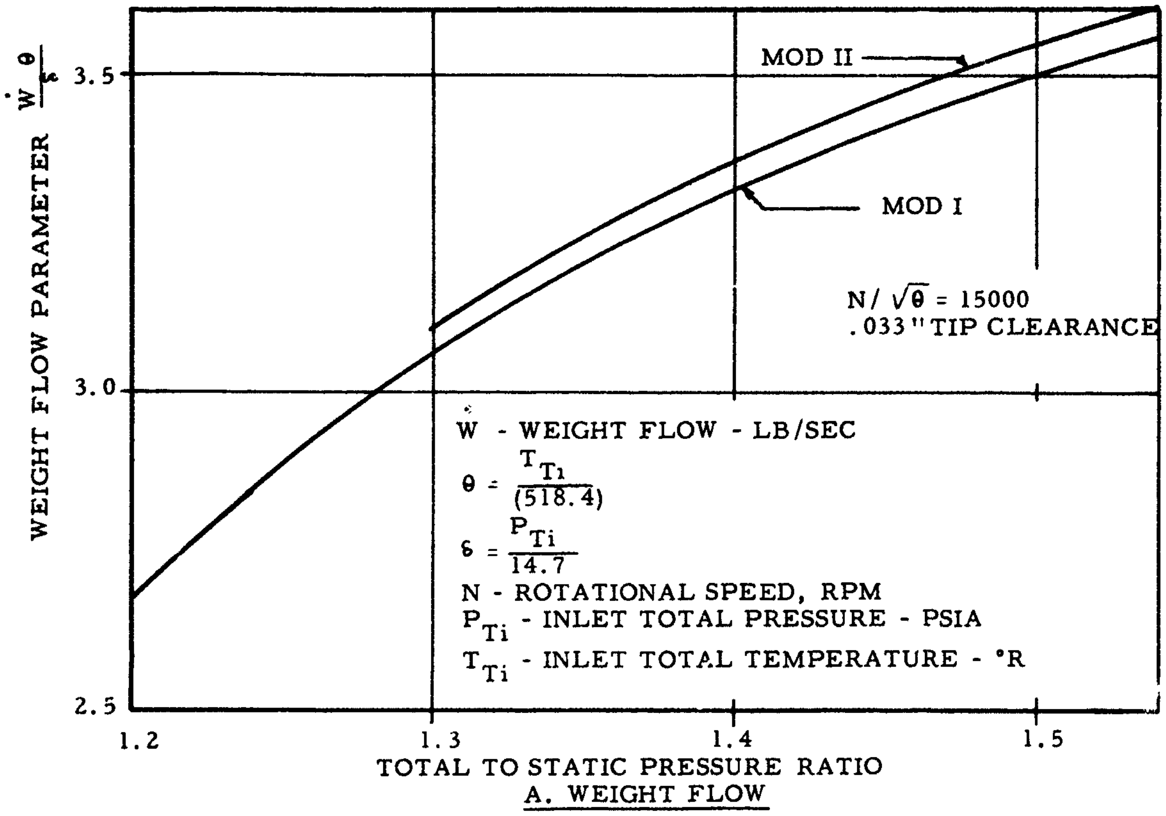

A. WEIGHT FLOW

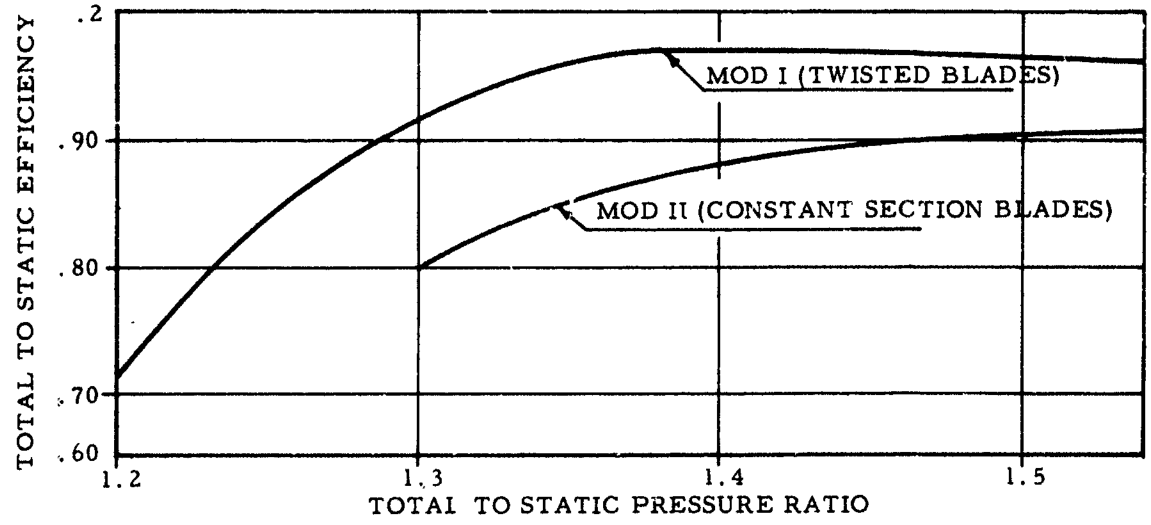

B. EFFICIENCY

Turbine Weight Flow and Efficiency vs Pressure Ratio

Figure IV-9

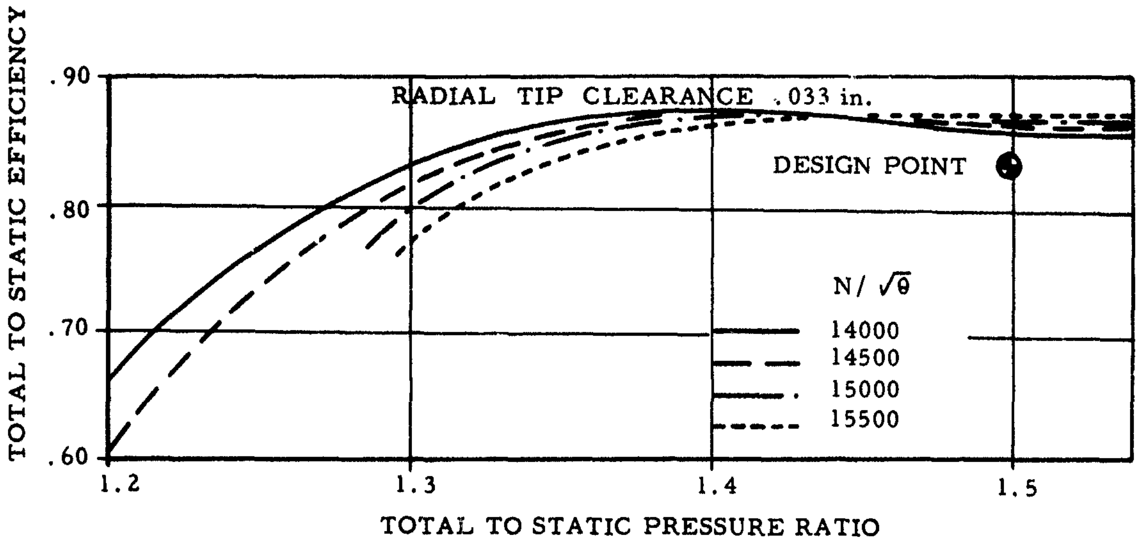

a) MOD I (TWISTED, TAPERED BLADES)

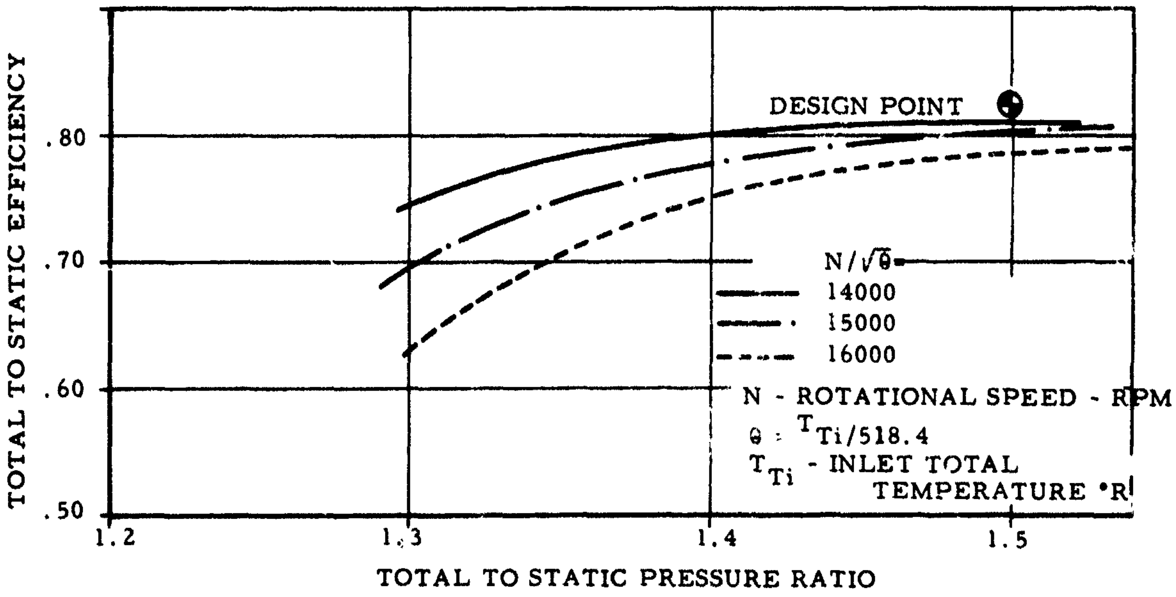

b) MOD II (CONSTANT SECTION, BLUNT LEADING EDGE BLADES)

Turbine Efficiency vs Pressure Ratio and Speed

Figure IV-10

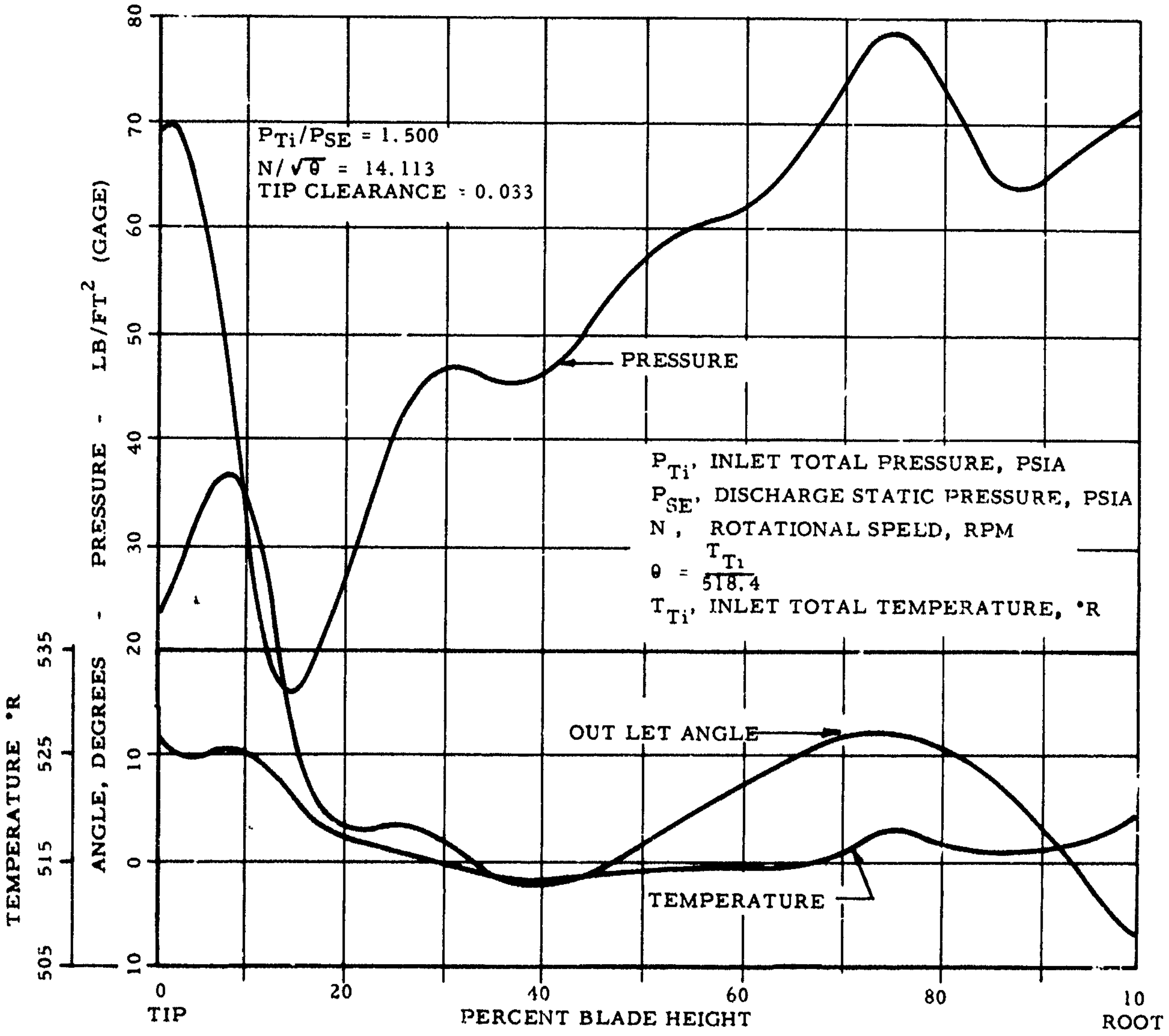

Mod. I Rotor Discharge Survey

Figure IV-11

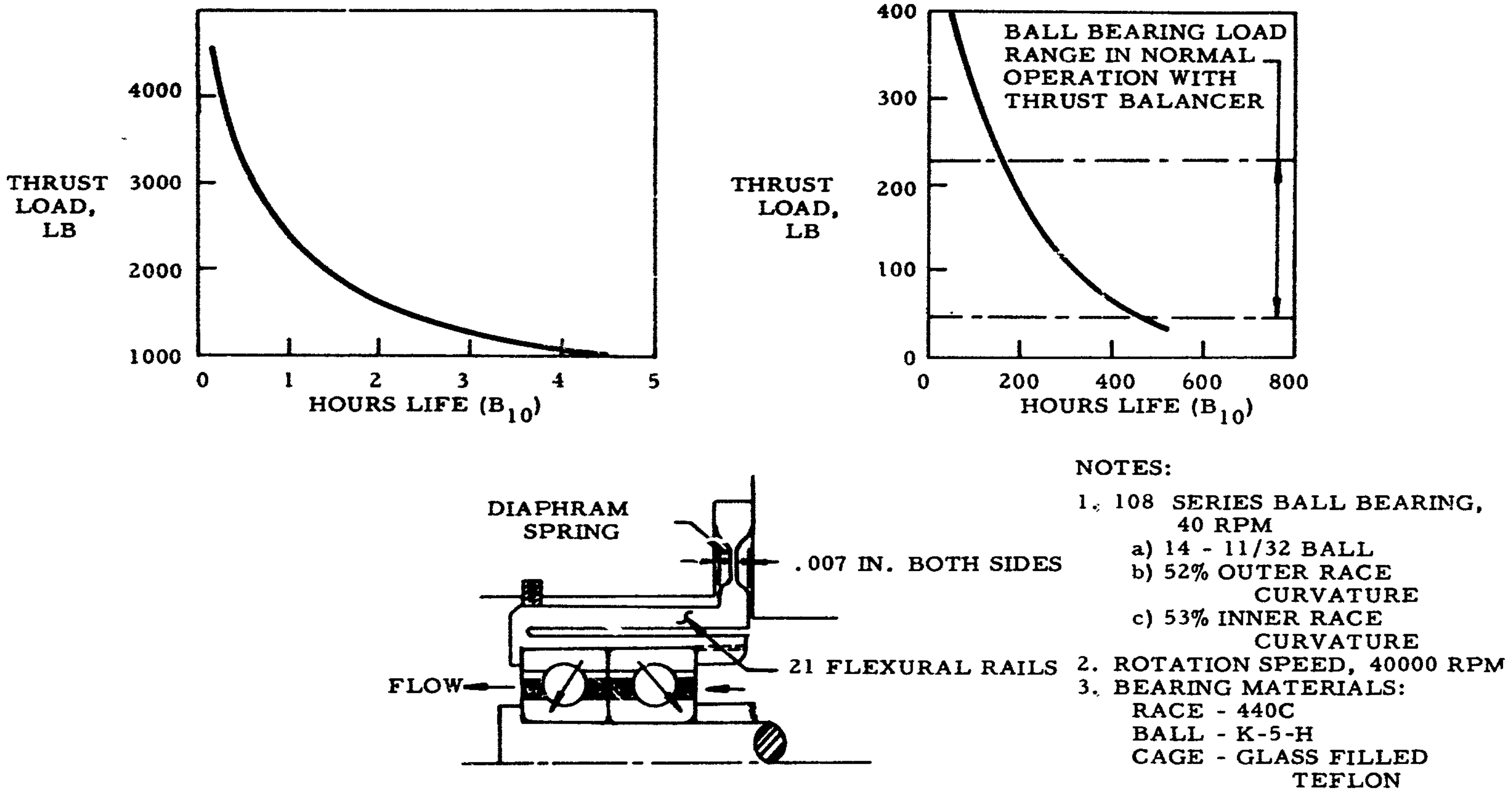

NOTES:

1. 108 SERIES BALL BEARING, 40 RPM
   - a) 14 - 11/32 BALL
   - b) 52% OUTER RACE CURVATURE
   - c) 53% INNER RACE CURVATURE
2. ROTATION SPEED, 40000 RPM
3. BEARING MATERIALS:
   - RACE - 440C
   - BALL - K-5-H
   - CAGE - GLASS FILLED TEFLON

Ball Bearing Life vs Load

Figure IV-12

NOTES:
1. Start-Transient Data per Figure XV-1 of Second Quarterly Report; Two-Stage Fuel Pump, Separate Fuel Valves.
2. Thrust-Bearing-Retainer Diaphragm Deflection, 0.007 in. @ 400 lb

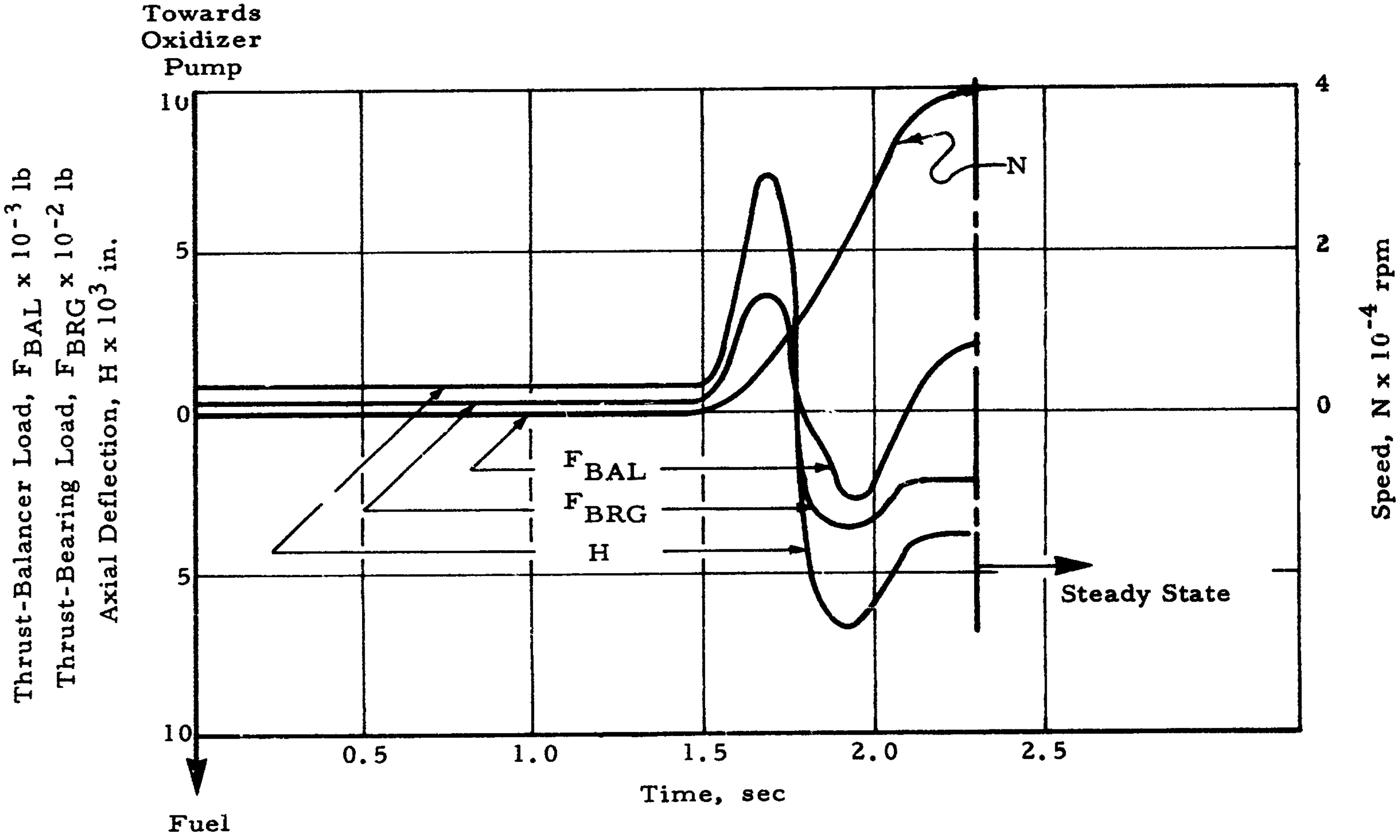

Bearing Thrust Load vs Time--Engine Start Transient

Figure IV-13

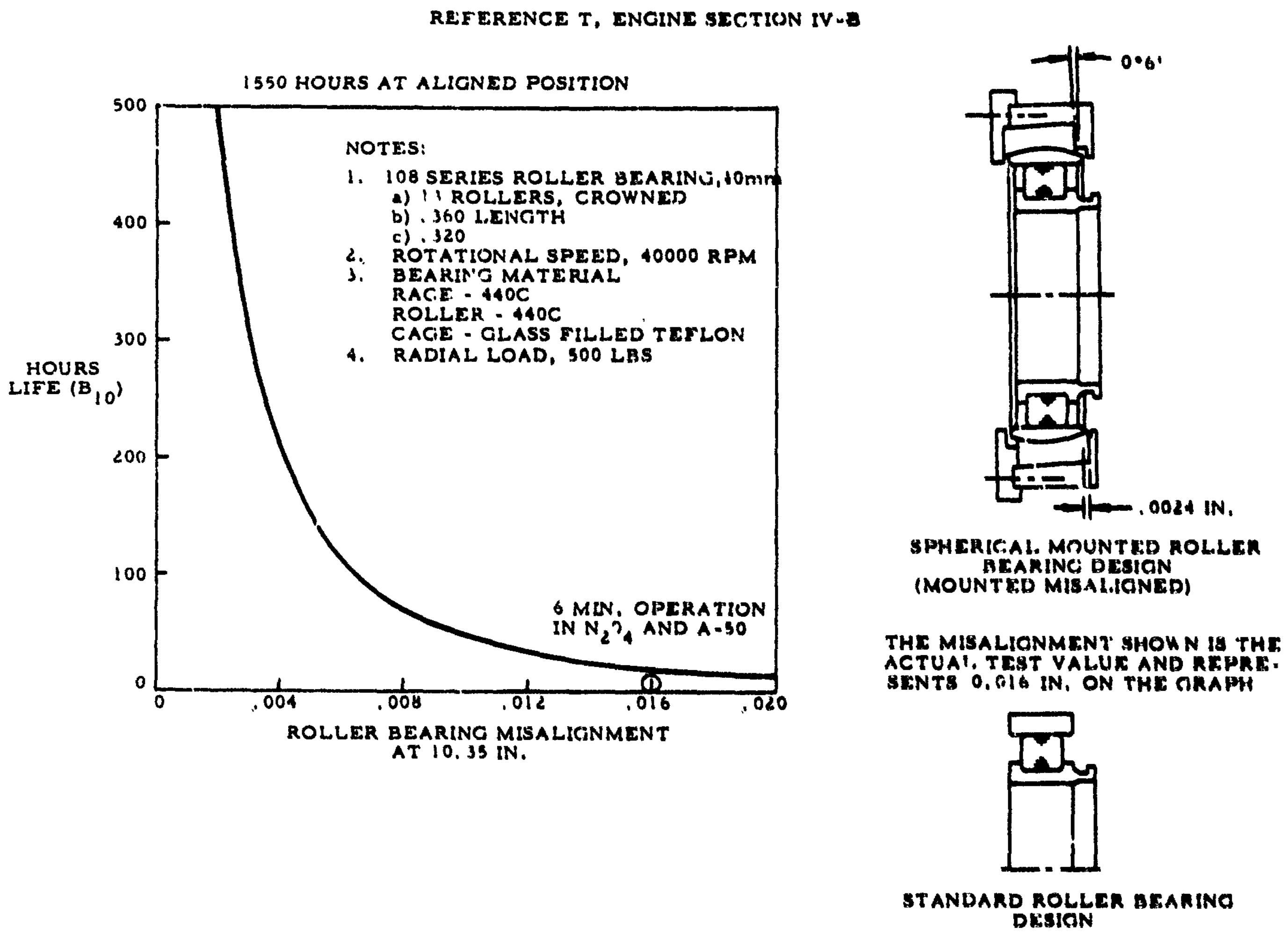

Roller Bearing Life vs Misalignment

Figure IV-14

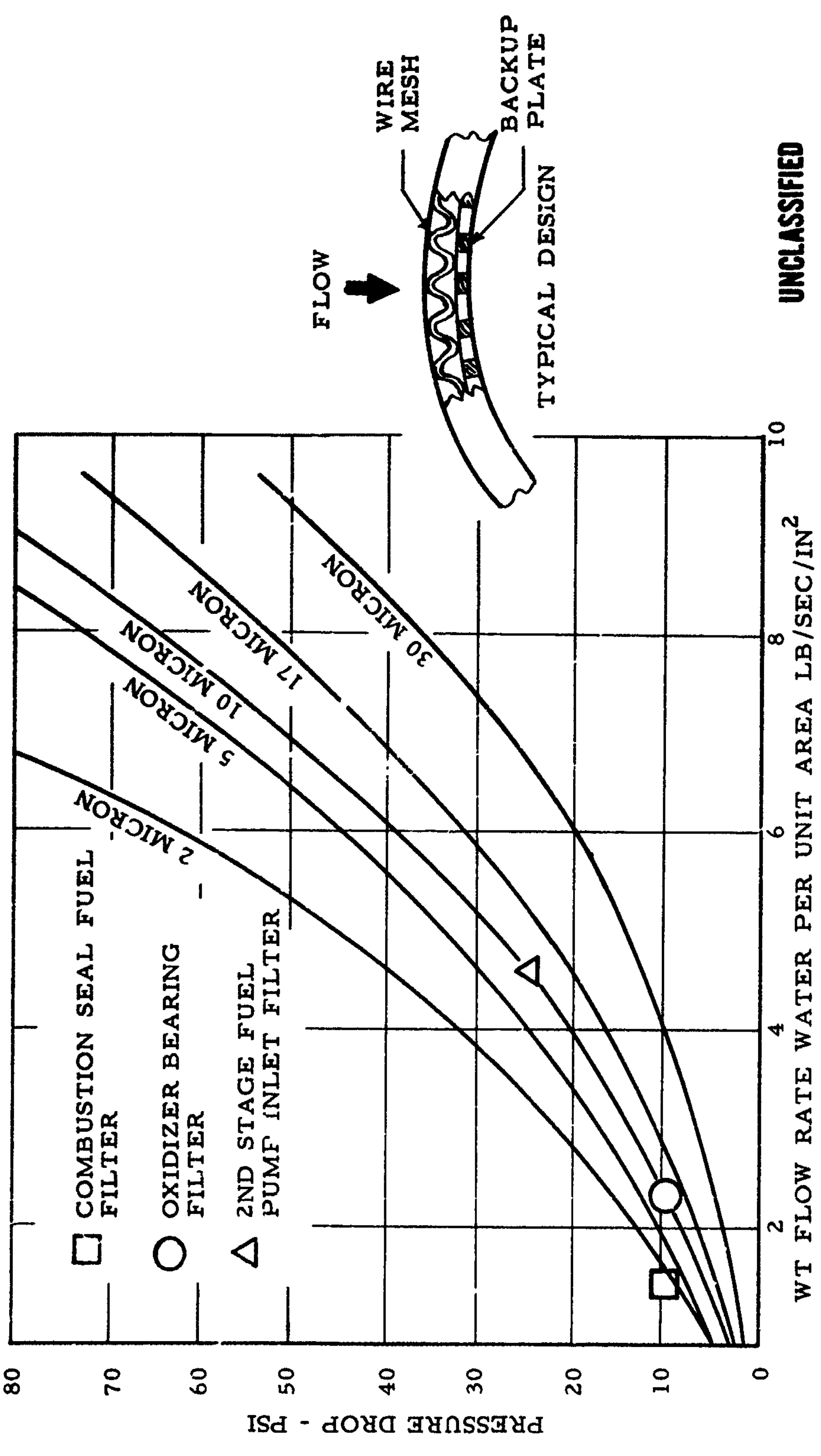

**UNCLASSIFIED**

TPA Filter Pressure Drop Data

Figure IV-15

CONFIDENTIAL

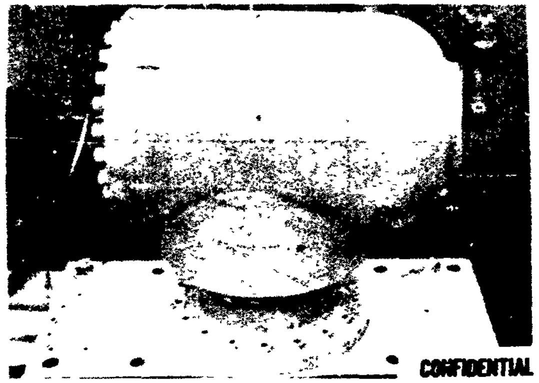
CONFIDENTIAL

Figure IV-16a. Metal Model I (u)

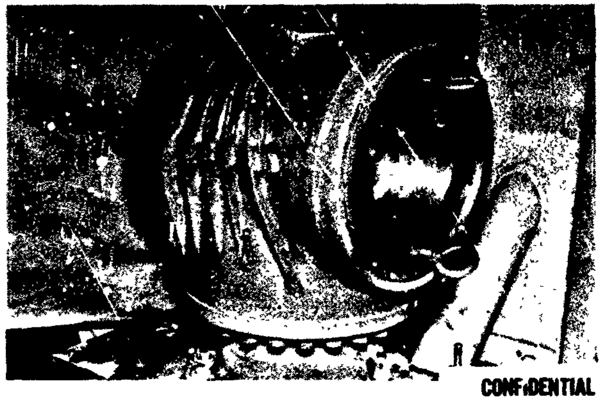
CONFIDENTIAL

Figure IV-16b. Metal Model II (u)

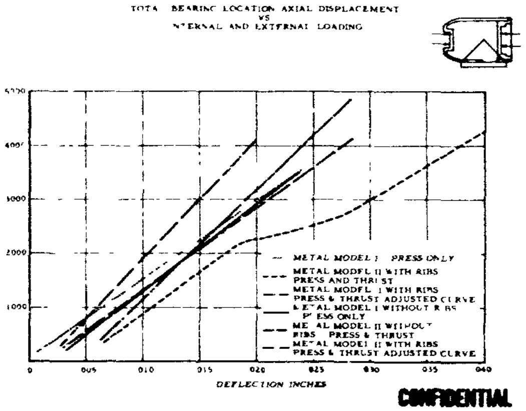

Figure IV-16c. Metal Model Bearing Axial Displacement (u)

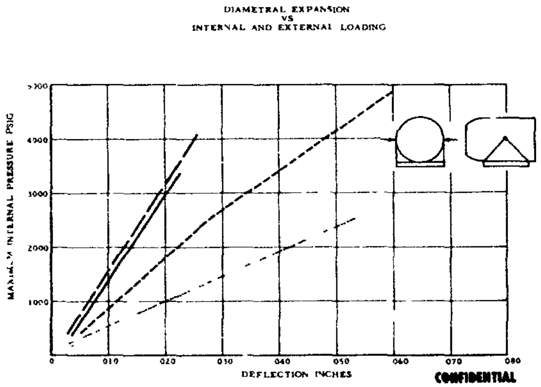

Figure IV-16d. Metal Model Diametral Expansion(u)

Figure IV-16

CONFIDENTIAL

| | METAL MODEL #1 | HOUSING "A" DESIGN |
|---|---|---|
| MATERIAL | 4130 NORMALIZED<br>$F_{TY}$ = 70 KSI<br>$F_{TU}$ = 90 KSI | INCO 718<br>$F_{TY}$ = 150 KSI<br>$F_{TU}$ = 180 KSI |
| WALL CONSTRUCTION AND STIFFNESS | SINGLE WALL, 0.50 THICK<br>$Z_1 = I/c = .0417\ IN^3/IN$ | TRIPLE WALL, TOTAL THICKNESSES<br>0.55 IN REGION (a)<br>0.625 IN REGION (b)<br>$Z_A = .129\ IN^3/IN$ (a)<br>$Z_A = .171$ (b) |
| PRESSURES | 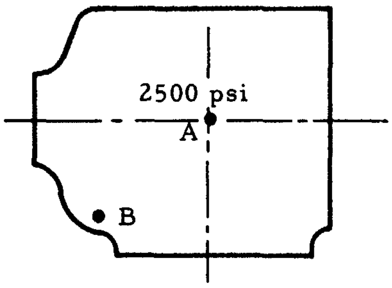 TEST PRESSURE | 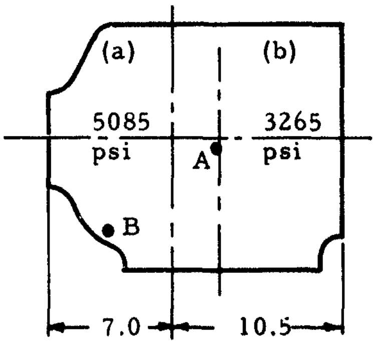 MAX. OPERATING PRESSURES |
| DEFLECTIONS | RELATIVE BRG. AXIAL DISPL.<br>$\Delta = .017 \pm 3\%$<br>RELATIVE BRG. ROTATION<br>B < 3.6 SEC (NIL) | ESTIMATED $\Delta$ =<br>$.017\left[\frac{5085}{2500}X\frac{.50}{.55}X\frac{7}{125}\ \frac{3265}{2500}X\frac{.50}{.625}X\frac{10.5}{17.5}\right]$<br>= .0232<br>(ANALYTICAL = .021)<br>B < 3.6 SEC (NIL) |
| STRESSES | BASIC CYL. HOOP = 33,750 psi<br>AT "A": $f_{OUTER}$ = 107,000 psi<br>($K_1$ = 3.17)<br>$f_{INNER}$ = -57,000 psi<br>($K_1$ = 1.69)<br>AT "B": $f_{OUTER}$ = 10,550 psi<br>($K_1$ = .313)<br>$f_{INNER}$ = 3,780 psi<br>($K_1$ = 1.2) | BASIC CYL. HOOP = (a) 62,200 psi<br>(b) 35,200 psi<br>ESTIMATED $K_A = 1 + (K_1 - 1)\frac{Z_1}{Z_A}$<br>AT "A": $K_A$ = 1.7<br>$f_{MAX}$ = 106,000 psi<br>AT "B": $K_A$ = 1.029<br>$f_{MAX}$ = 36,200 psi<br>CONFIDENTIAL |

Metal Model I Test Results (u)

Figure IV-17

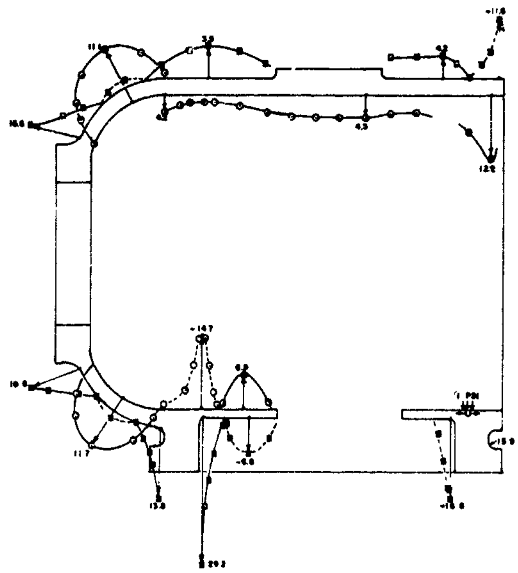

Figure IV-18a. Test 1 Photoelastic Model Longitudinal Section Stresses

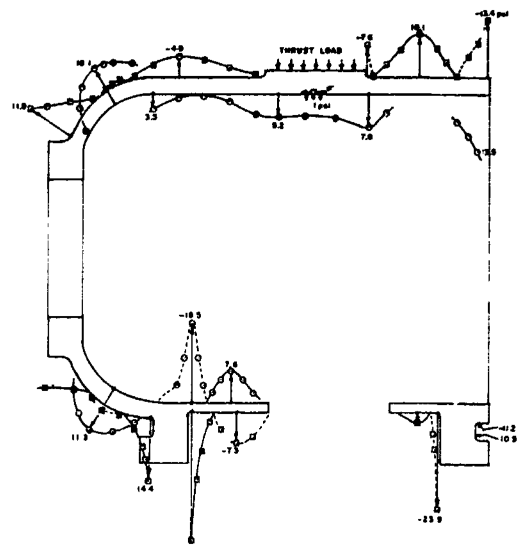
THRUST LOAD
1 psi

UNCLASSIFIED

Figure IV-18b. Test 2 Photoelastic Model Longitudinal Section Stresses

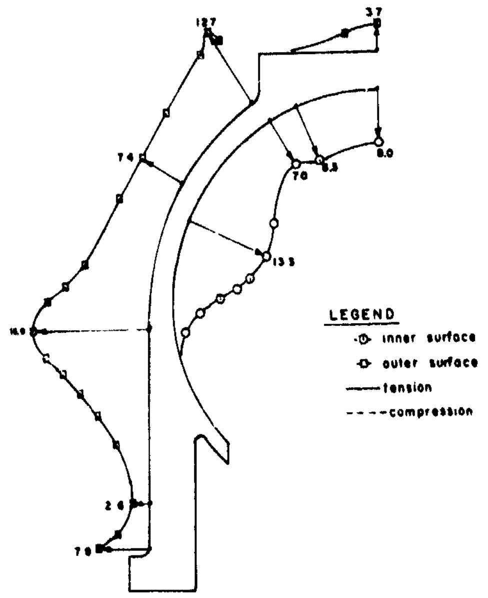
12.7
3.7
7.4
7.0
8.3
8.0
13.3
16.0
2.6
7.0
LEGEND
inner surface
outer surface
tension
compression

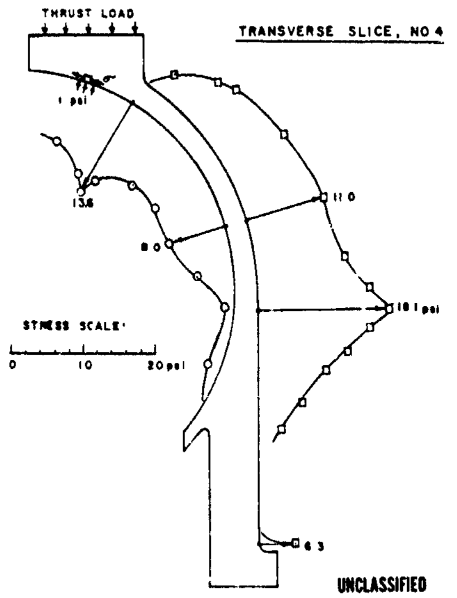
THRUST LOAD
TRANSVERSE SLICE, NO 4
1 psi
13.6
8.0
11.0
18.1 psi
STRESS SCALE:
0
10
20 psi
6.3

UNCLASSIFIED

Figure IV-18c. Test 1 Photoelastic Model Lateral Section Stresses

Figure IV-18d. Test 2 Photoelastic Model Lateral Section Stresses

Figure IV-18

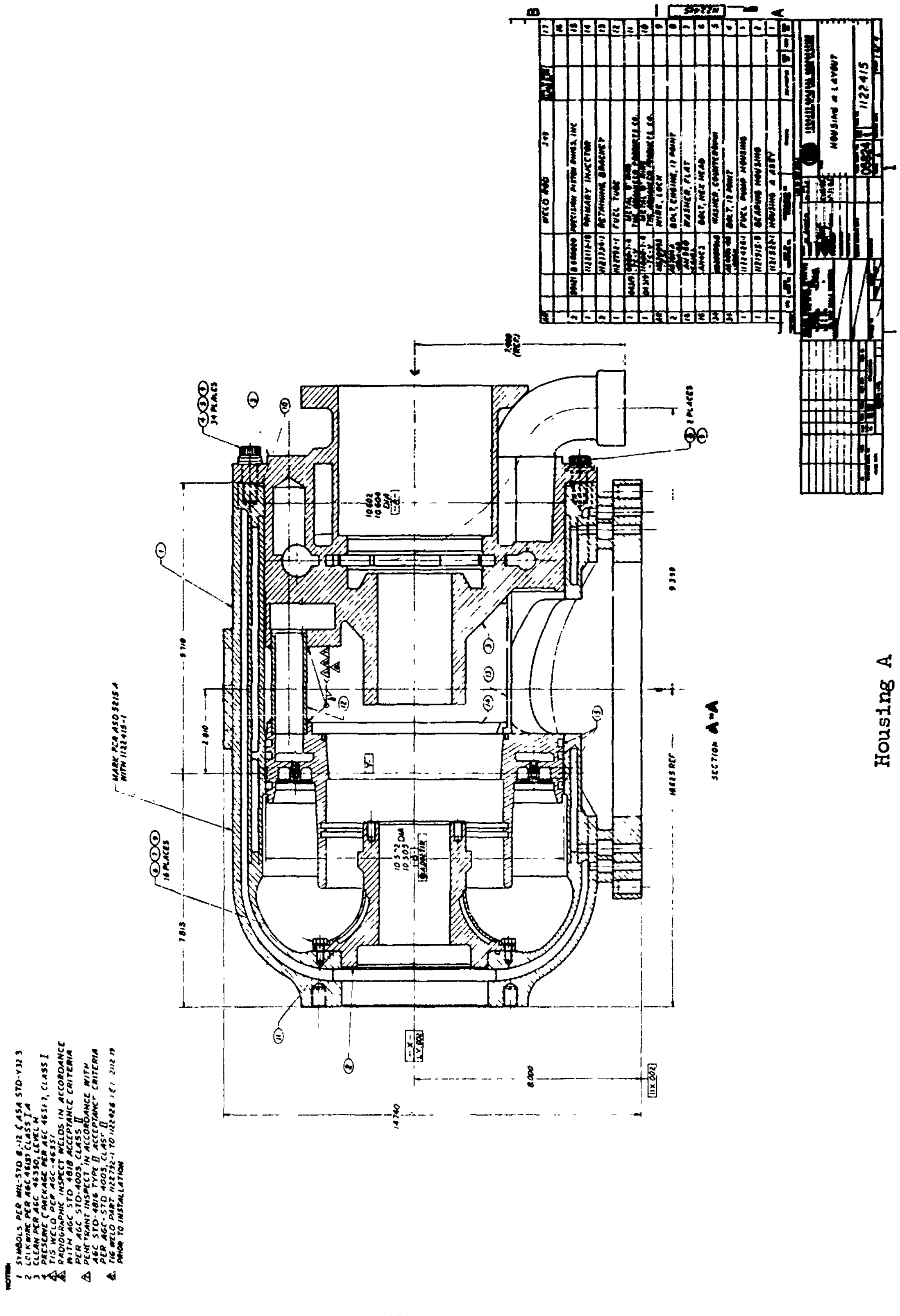
WELD PAD
PRECISION PISTON RINGS, INC
AUXILIARY INJECTOR
RETAINING BRACKET
FUEL TUBE
WIRE, LOCK
BOLT, ENGINE, 12 POINT
WASHER, FLAT
BOLT, HEX HEAD
WASHER, COUNTERSUNK
BOLT, 12 POINT
FUEL PUMP HOUSING
BEARING HOUSING
HOUSING A ASSY
HOUSING A LAYOUT
1122415
SECTION A-A
MARK PER ASD 5215 A WITH 1122415-1
34 PLACES
16 PLACES
2 PLACES
10.602
10.604 DIA
10.505
10.503 DIA
9.710
9.330
7.813
2.810
8.000
14.740
14.615 REF
7.000 (REF)
NOTES:
1 SYMBOLS PER MIL-STD 8,-12 & ASA STD-Y32 3
2 LOCKWIRE PER AGC 46137 CLASS I A
3 CLEAN PER AGC 46350, LEVEL H
4 PRESERVE & PACKAGE PER AGC 46517, CLASS I
5 TIG WELD PER AGC-46551
6 RADIOGRAPHIC INSPECT WELDS IN ACCORDANCE WITH AGC STD 4818 ACCEPTANCE CRITERIA PER AGC STD-4005, CLASS II
7 PENETRANT INSPECT IN ACCORDANCE WITH AGC STD-4816 TYPE II ACCEPTANCE CRITERIA PER AGC-STD 4005, CLASS II
8 TIG WELD PART 1122732-1 TO 1122428 PRIOR TO INSTALLATION
Housing A

Figure IV-19

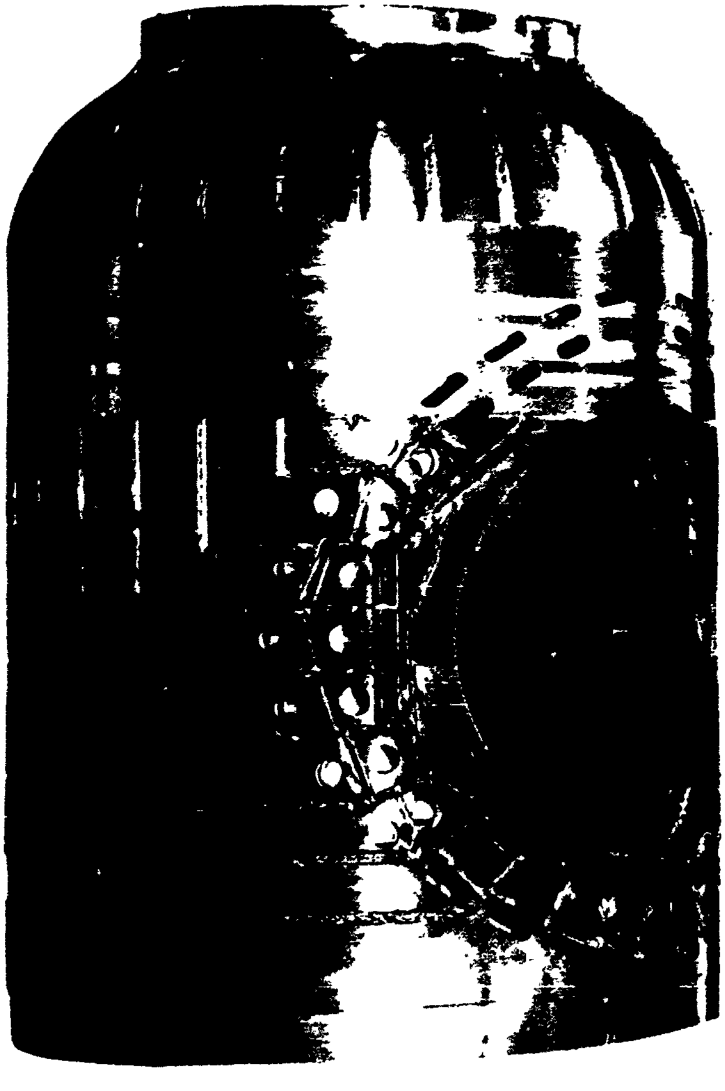

Housing A Rib Pattern

Figure IV-20

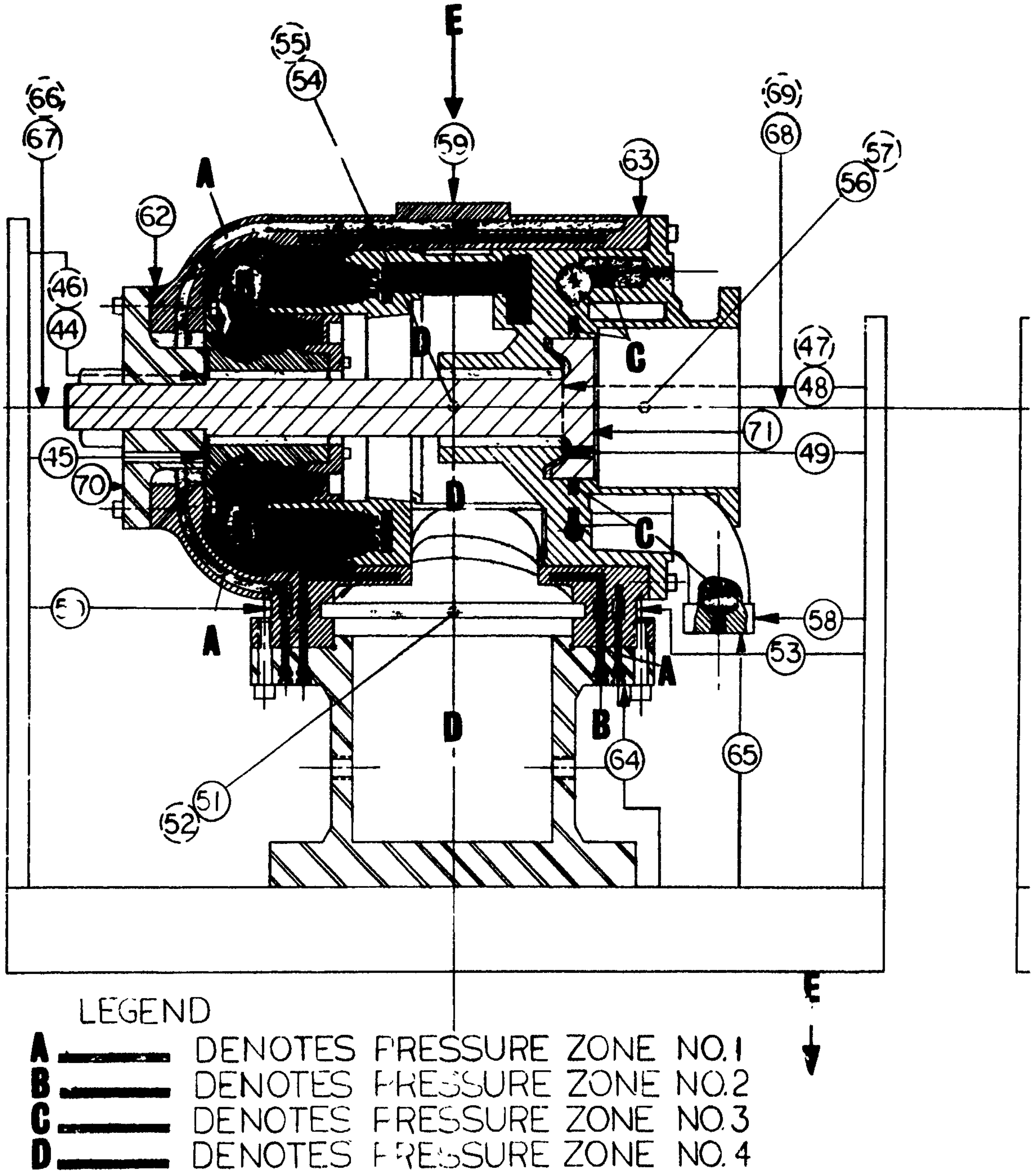
E
55
54
59
66
67
69
68
63
57
56
62
A
46
44
D
C
47
48
71
49
45
70
D
C
58
53
A
A
D
B
64
65
51
52
E
LEGEND
A DENOTES PRESSURE ZONE NO.1
B DENOTES PRESSURE ZONE NO.2
C DENOTES PRESSURE ZONE NO.3
D DENOTES PRESSURE ZONE NO.4

Housing A Hydrotest Pressure Zones

Figure IV-21

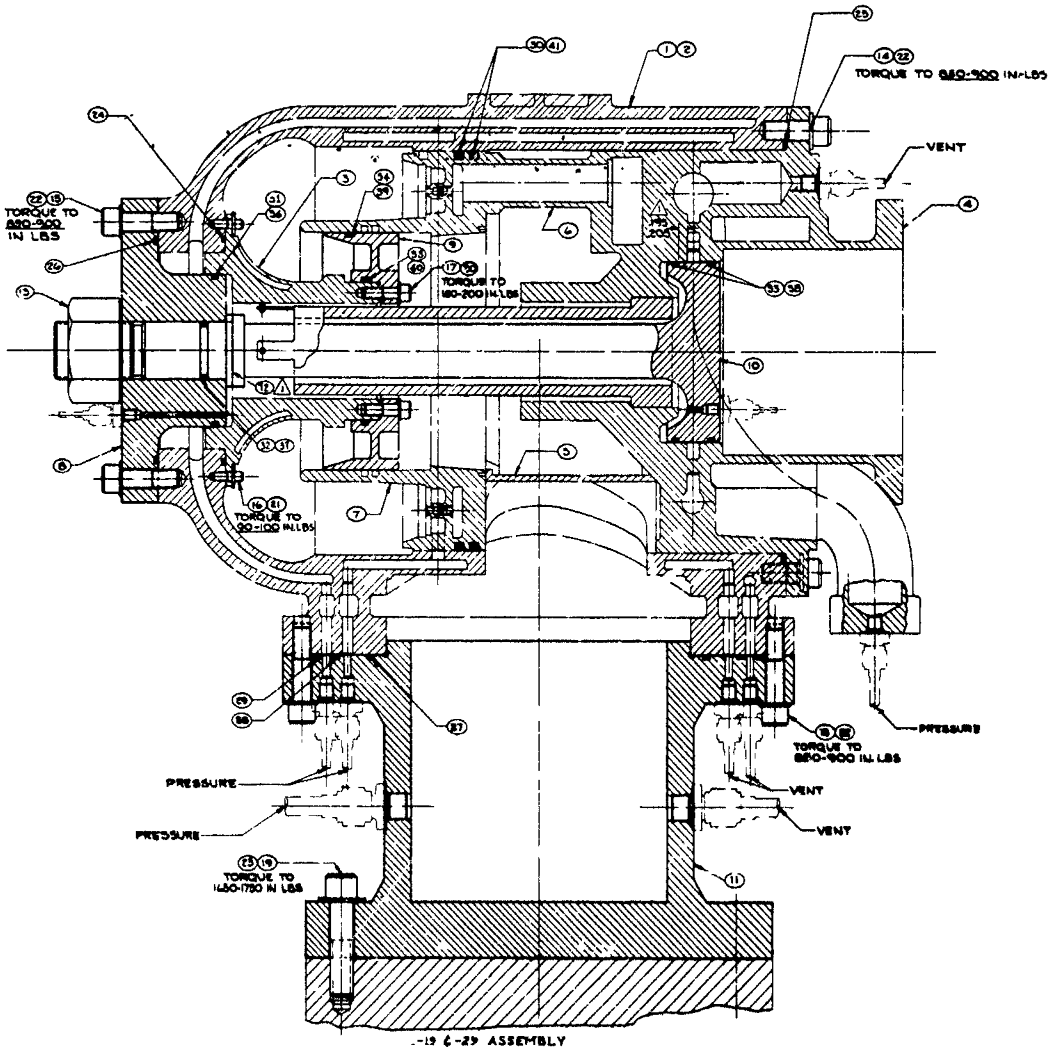
㉕
㉚㊶
①②
⑭㉒
TORQUE TO 880-900 IN-LBS
㉔
VENT
④
③
㉞
㊴
㉛
㊱
㉒⑮
TORQUE TO
880-900
IN LBS
⑥
195
205
㉖
⑨
㉝
㊵
⑰⑳
TORQUE TO
180-200 IN.LBS
㉝㊳
⑬
⑩
⑫
㉜㊲
⑧
⑤
⑯㉑
TORQUE TO
90-100 IN.LBS
⑦
㉙
㉘
㉗
⑱㉒
TORQUE TO
880-900 IN. LBS
PRESSURE
PRESSURE
VENT
PRESSURE
VENT
㉓⑲
TORQUE TO
1650-1750 IN LBS
⑪
-19 & -29 ASSEMBLY

Housing A Hydrotest Assembly

Figure IV-22a

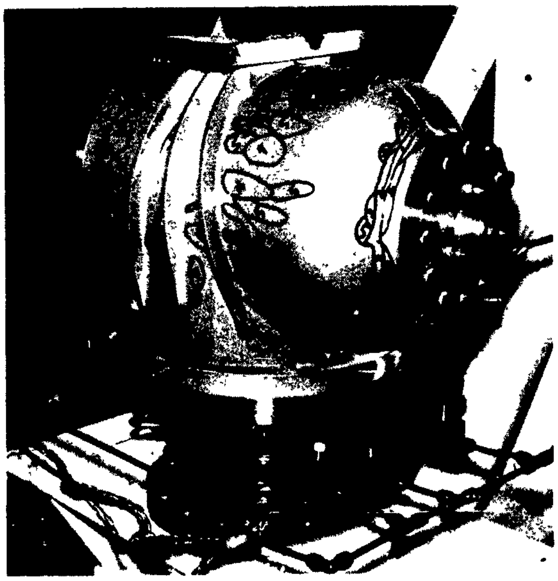

Stress at Test, View 1

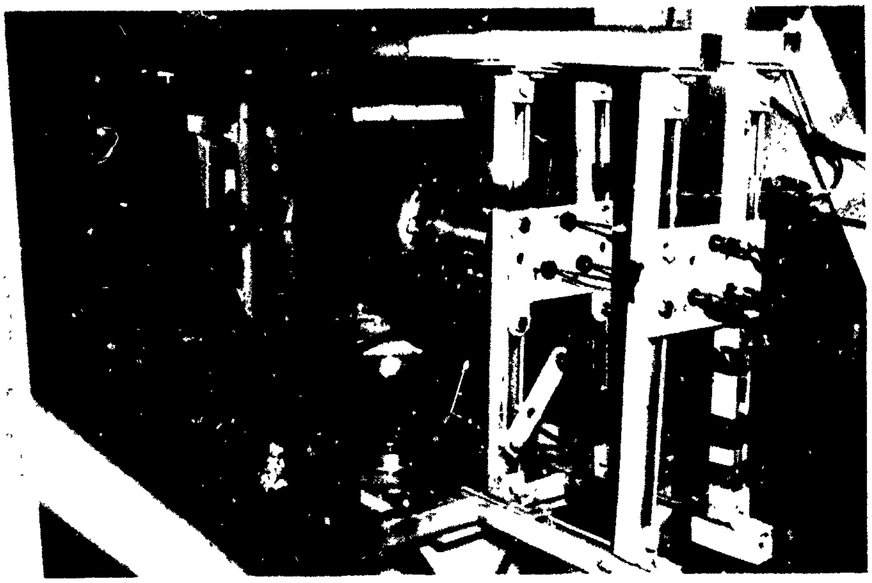

Pressure Test, View 2

Housing A Hydrotest

Figure IV-22b

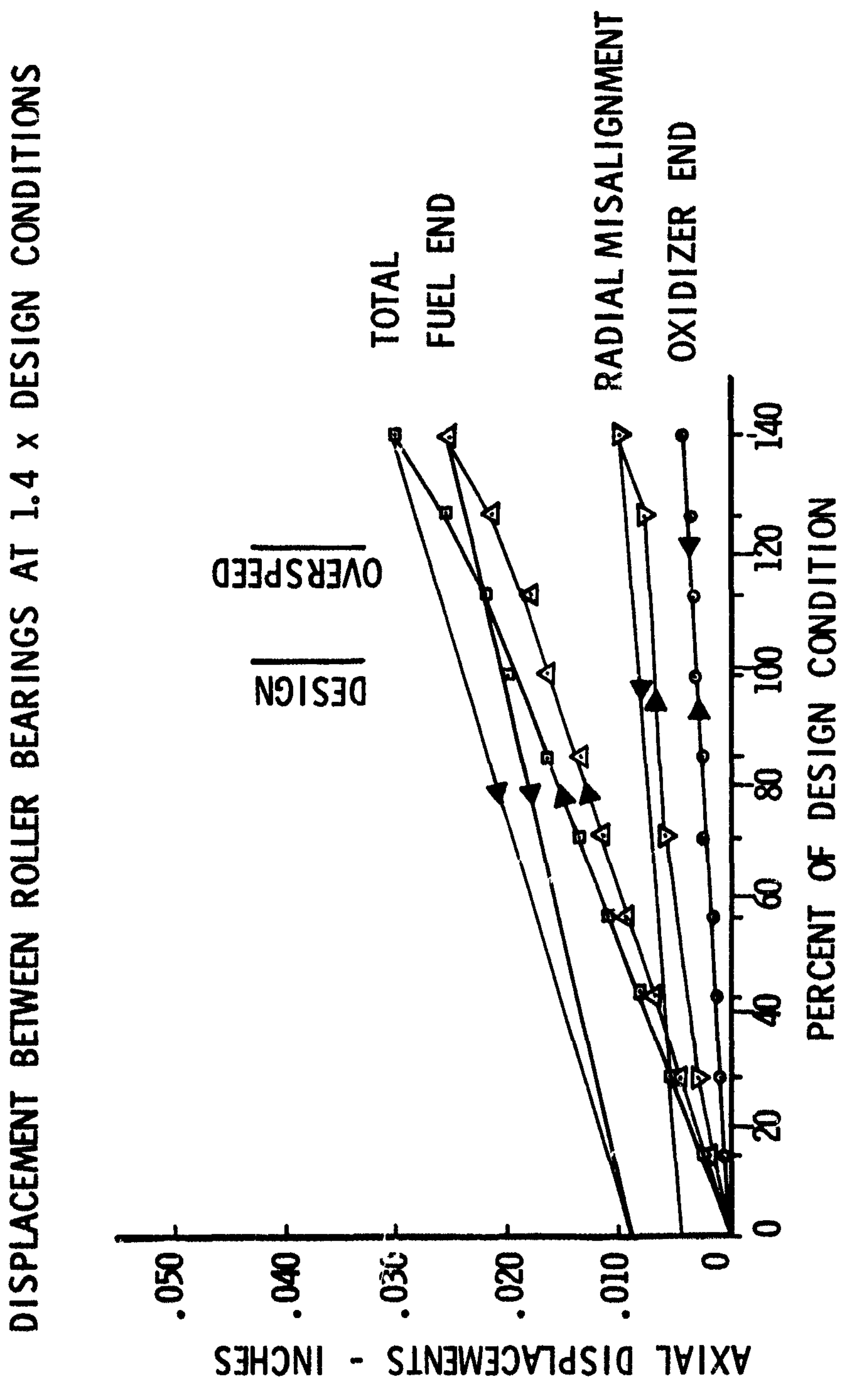
DISPLACEMENT BETWEEN ROLLER BEARINGS AT 1.4 x DESIGN CONDITIONS

Housing A Pressure and Thrust Proof Test Results

Figure IV-23

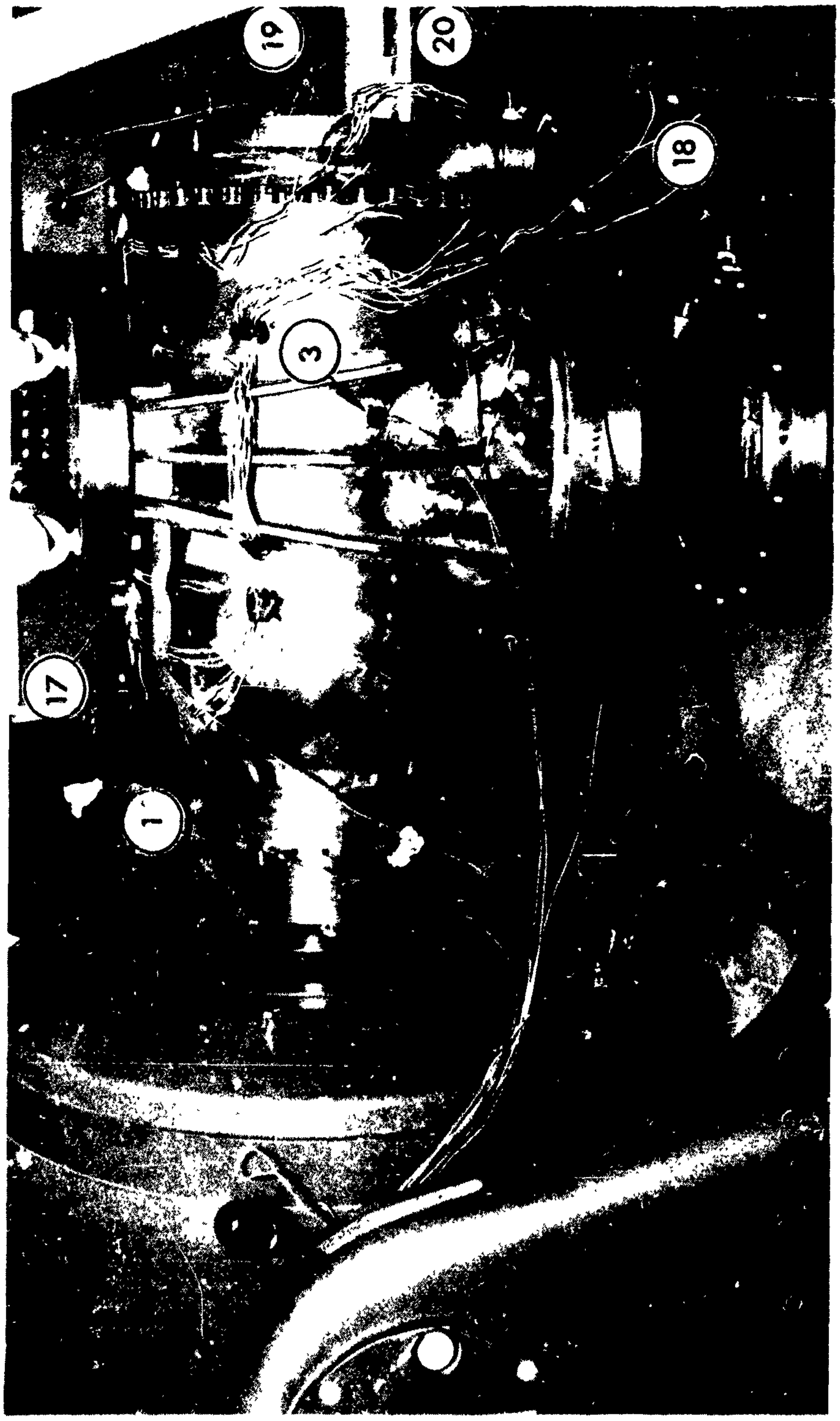
19
20
18
3
17
1

Vibration Test Results

Figure IV-24a

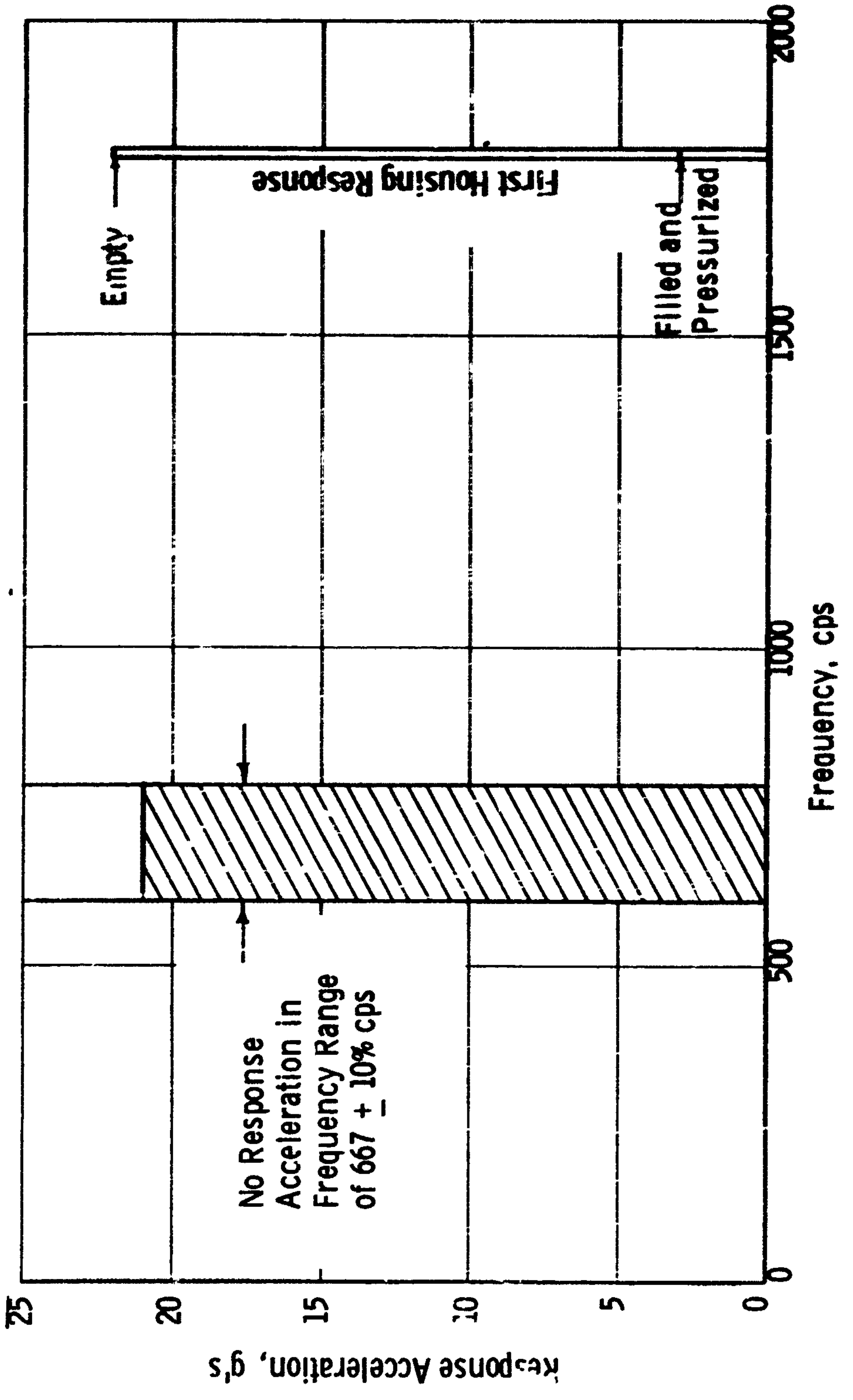

Vibration Test Results

Figure IV-24b

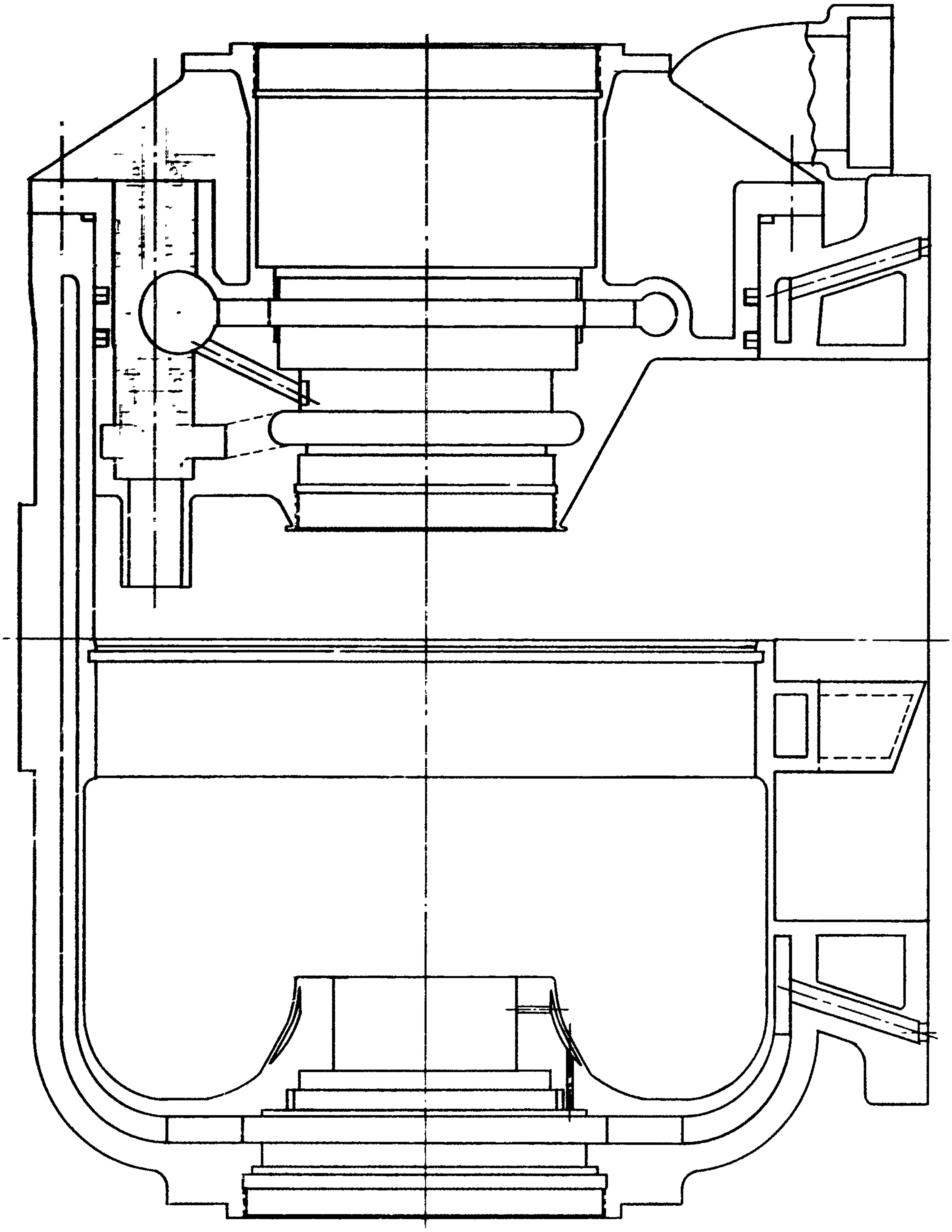

Two-Walled Housing

Figure IV-25

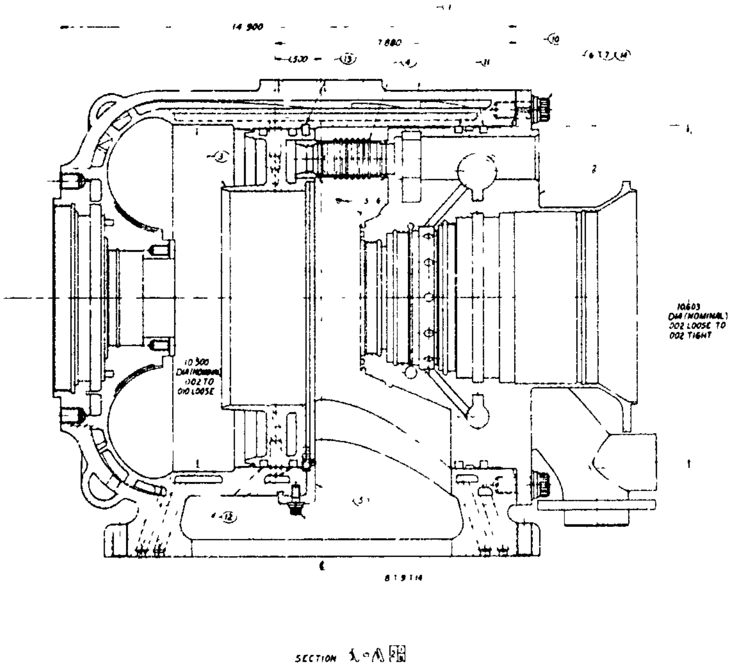
14.900
7.880
1.500
13
4
11
10
6 7 14
3
2
1
12
5
10.500 DIA (NOMINAL) .002 TO .010 LOOSE
10.603 DIA (NOMINAL) .002 LOOSE TO .002 TIGHT
819114
SECTION

Housing B

Figure IV-26

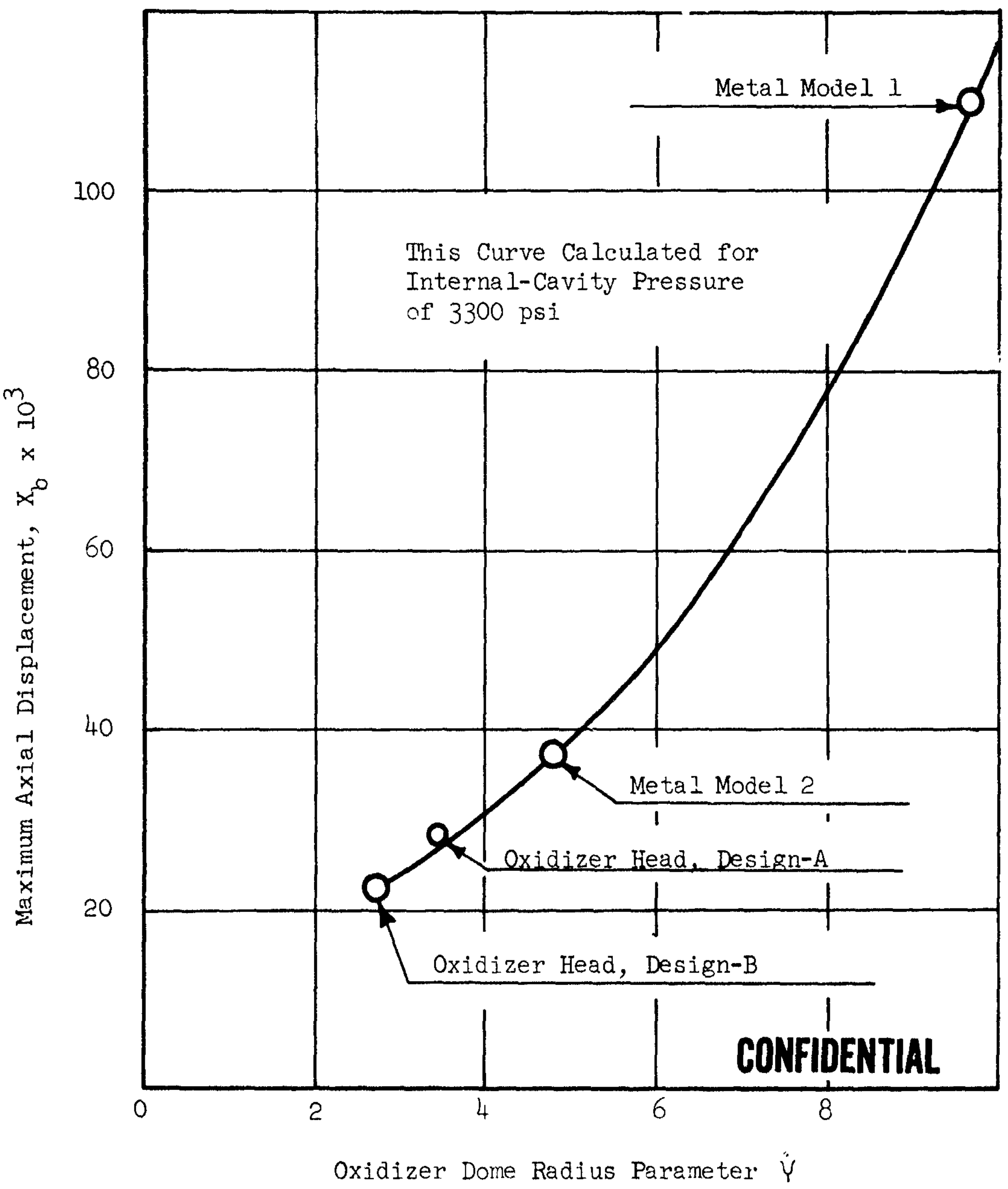

Oxidizer Dome Parameter vs Displacement (u)

Figure IV-27

UNCLASSIFIED

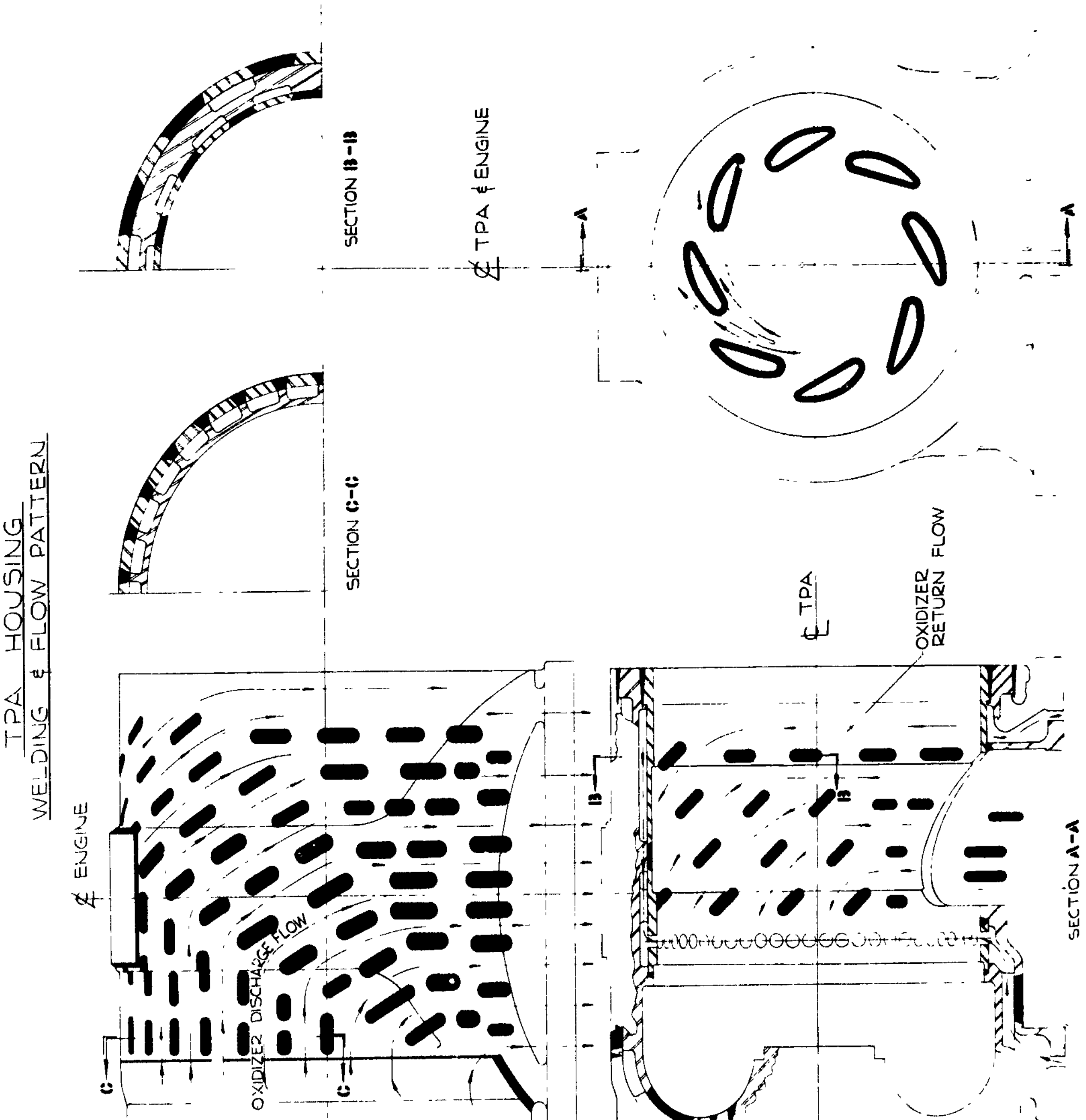
TPA HOUSING
WELDING ¢ FLOW PATTERN
¢ ENGINE
SECTION B-B
SECTION C-C
¢ TPA ¢ ENGINE
A
A
B
B
C
C
OXIDIZER DISCHARGE FLOW
¢ TPA
OXIDIZER RETURN FLOW
SECTION A-A

Housing-C Rib Pattern

Figure IV-28

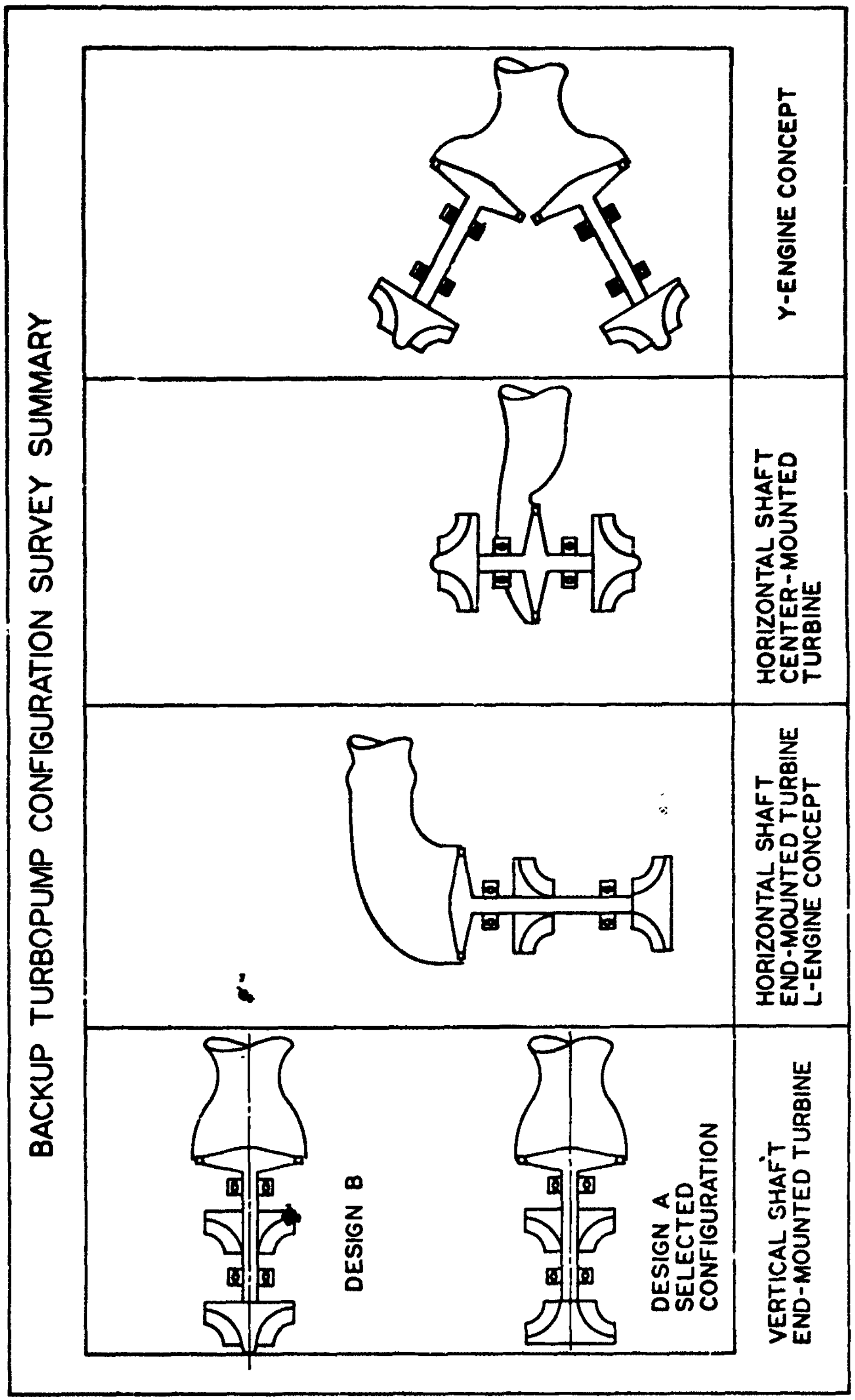

BACKUP TURBOPUMP CONFIGURATION SURVEY SUMMARY

Y-ENGINE CONCEPT
HORIZONTAL SHAFT CENTER-MOUNTED TURBINE
HORIZONTAL SHAFT END-MOUNTED TURBINE L-ENGINE CONCEPT
VERTICAL SHAFT END-MOUNTED TURBINE
DESIGN A SELECTED CONFIGURATION
DESIGN B

Configuration Survey

Figure IV-29

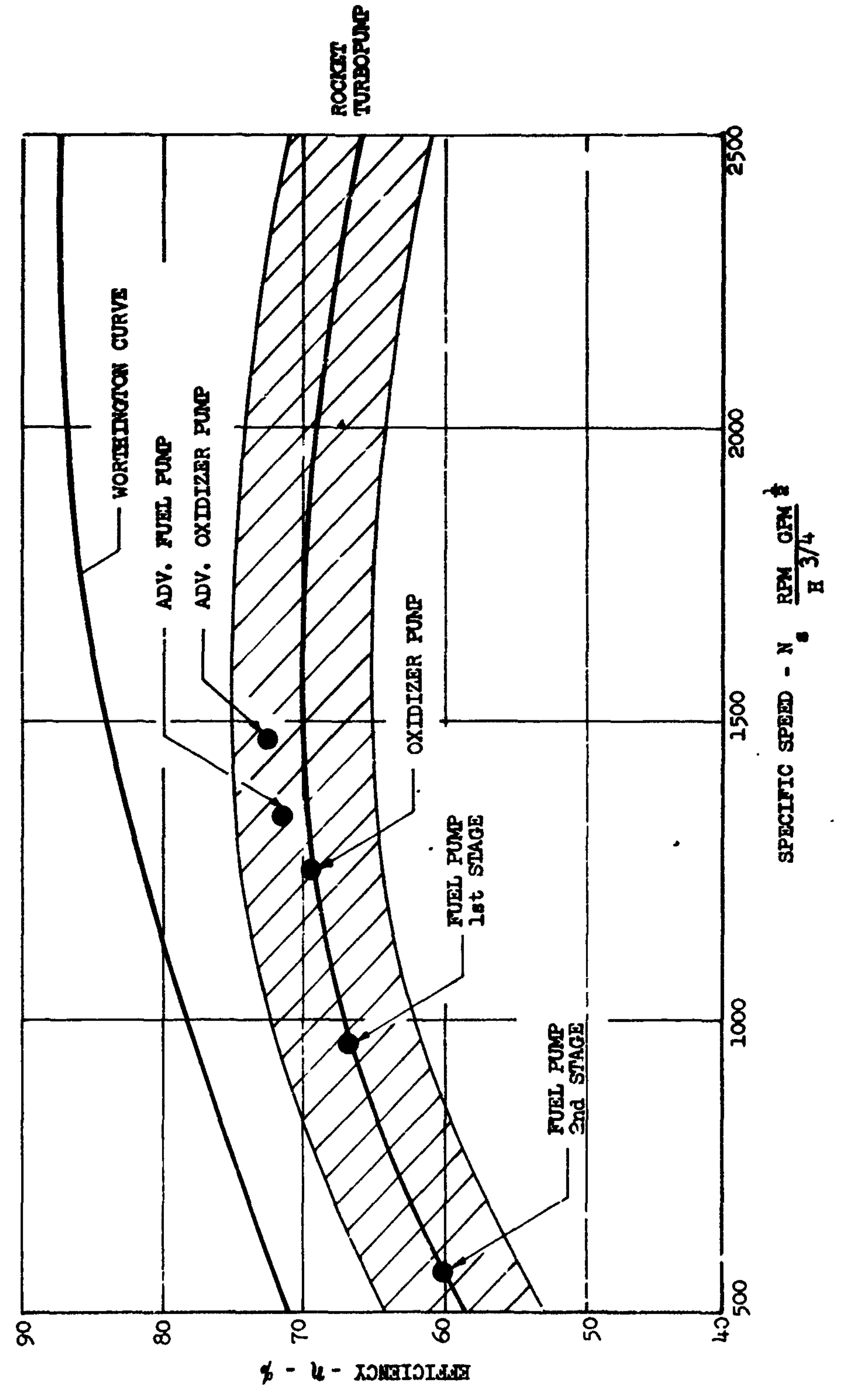

Pump Efficiency vs Specific Speed

Figure IV-30

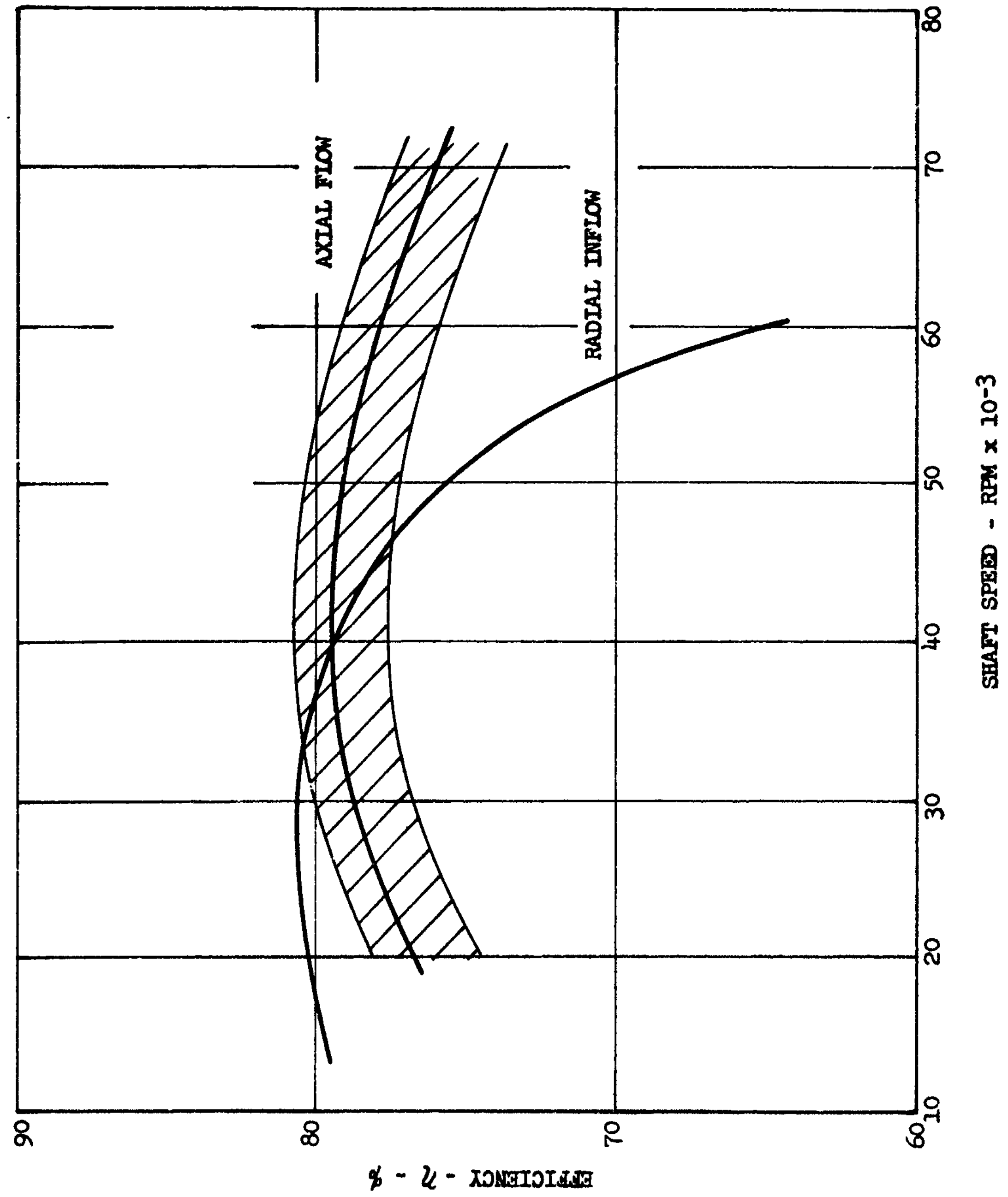

Turbine Efficiency vs Design Speed

Figure IV-31

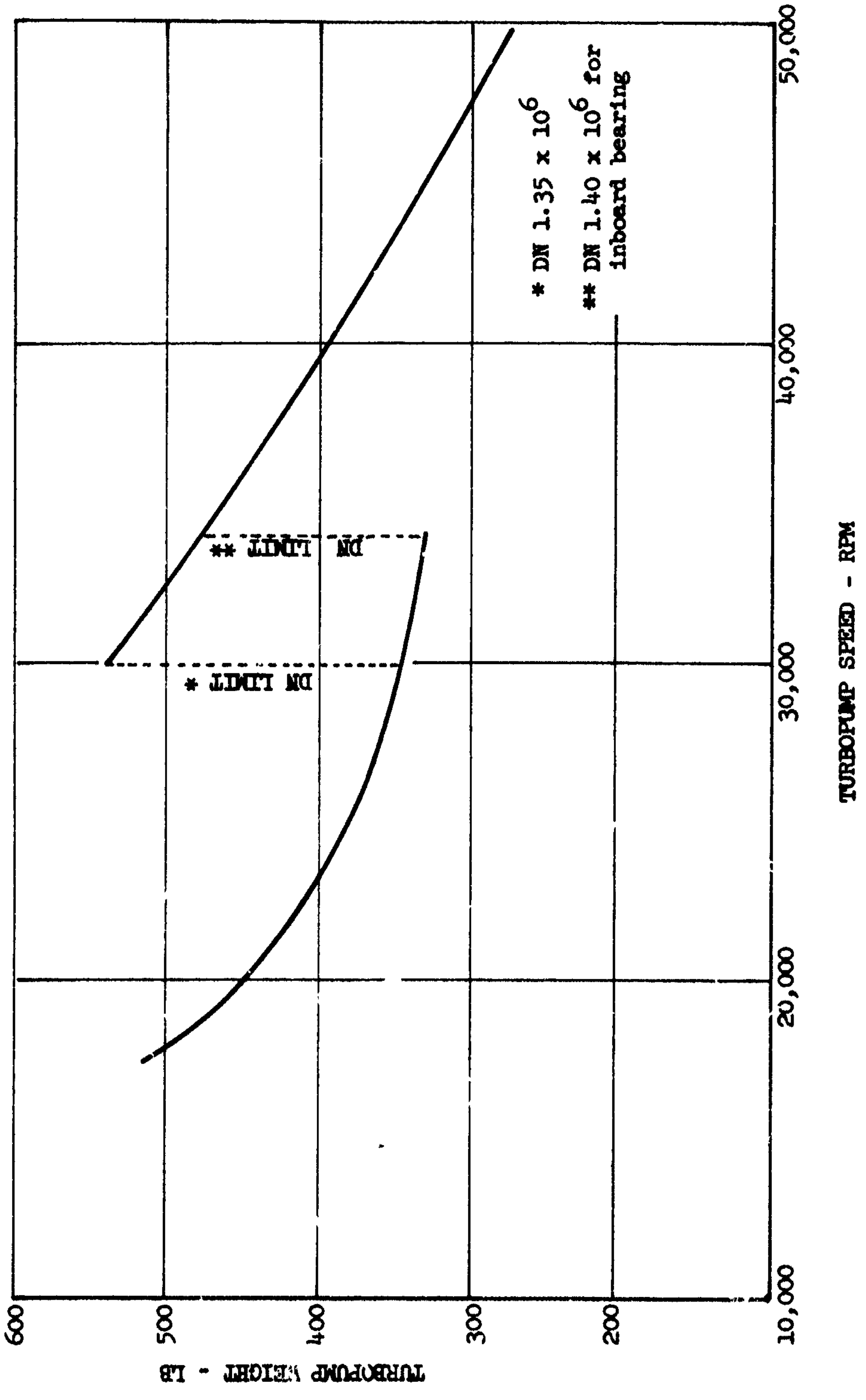

Inline TPA Weight vs Design Speed

Figure IV-32

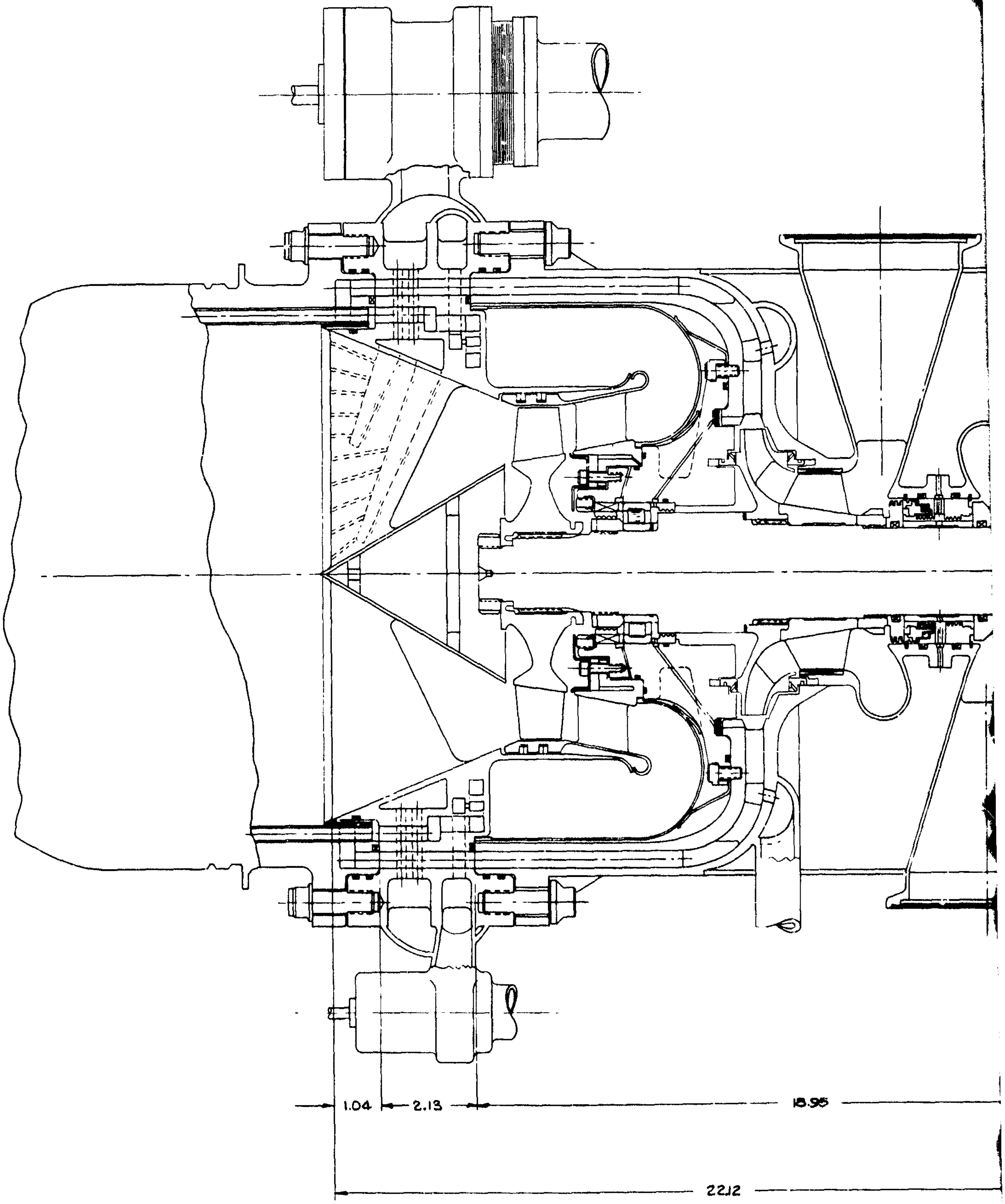
1.04
2.13
18.95
22.12

Report 10830-F-1, Phase I

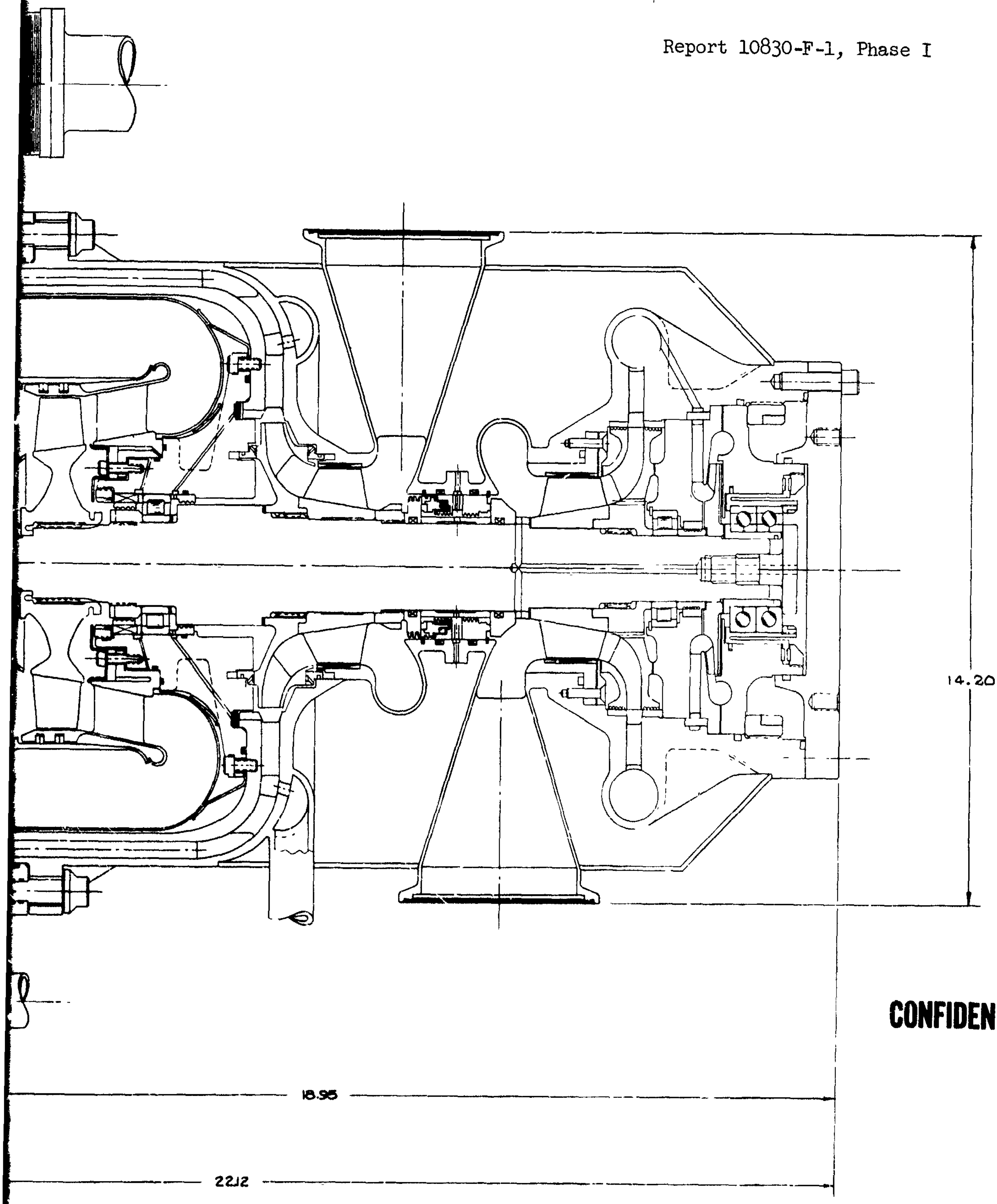
14.20
18.95
22.12

CONFIDENTIAL

Inline TPA Cross Section (u)

Figure IV-33

2

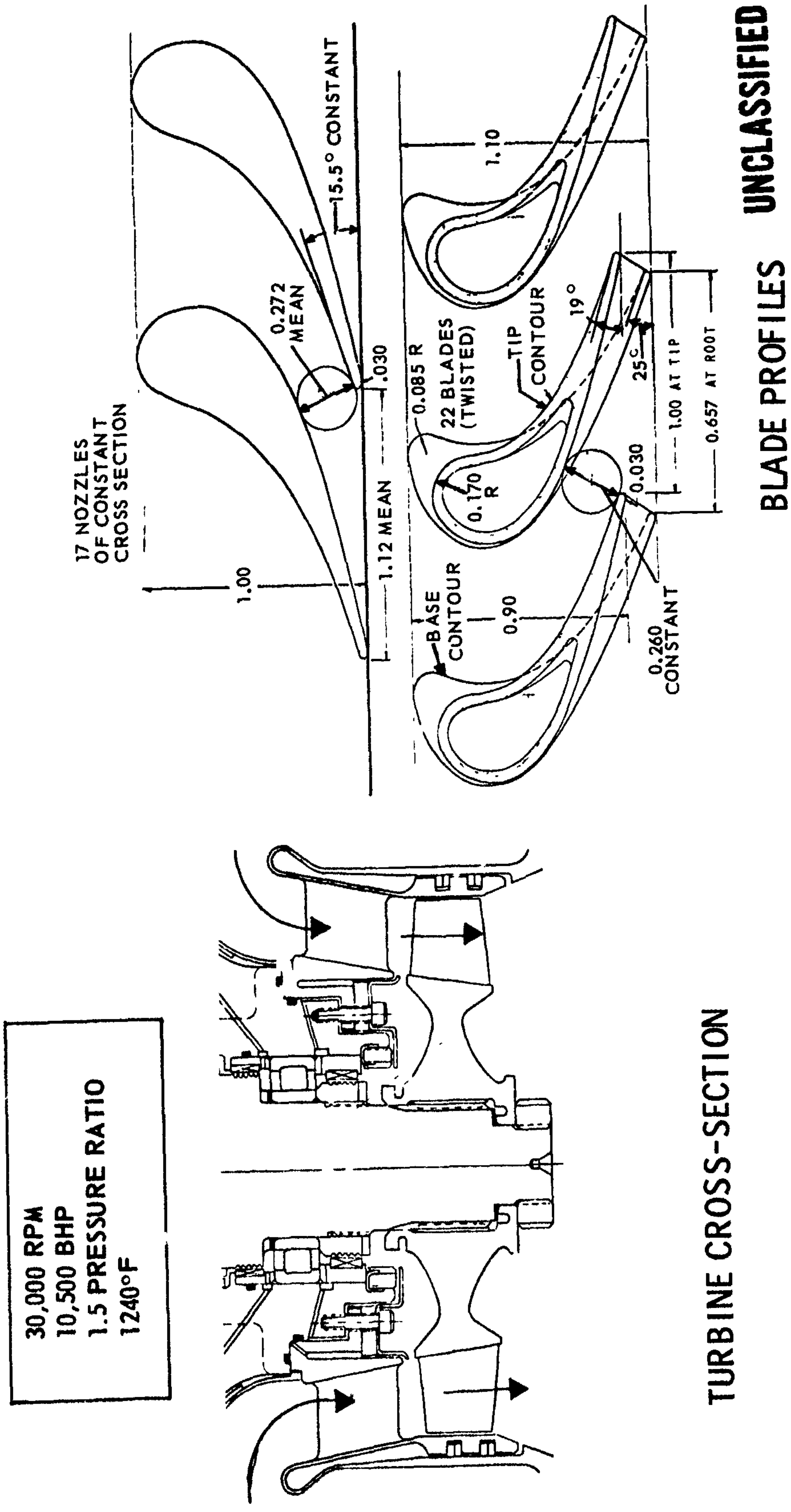
UNCLASSIFIED
BLADE PROFILES
17 NOZZLES OF CONSTANT CROSS SECTION
15.5° CONSTANT
0.272 MEAN
.030
1.12 MEAN
1.00
0.085 R
22 BLADES (TWISTED)
TIP CONTOUR
19°
25°
1.00 AT TIP
0.657 AT ROOT
1.10
0.170 R
0.030
BASE CONTOUR
0.90
0.260 CONSTANT
TURBINE CROSS-SECTION
30,000 RPM
10,500 BHP
1.5 PRESSURE RATIO
1240°F

Turbine Cross Section

Figure IV-34

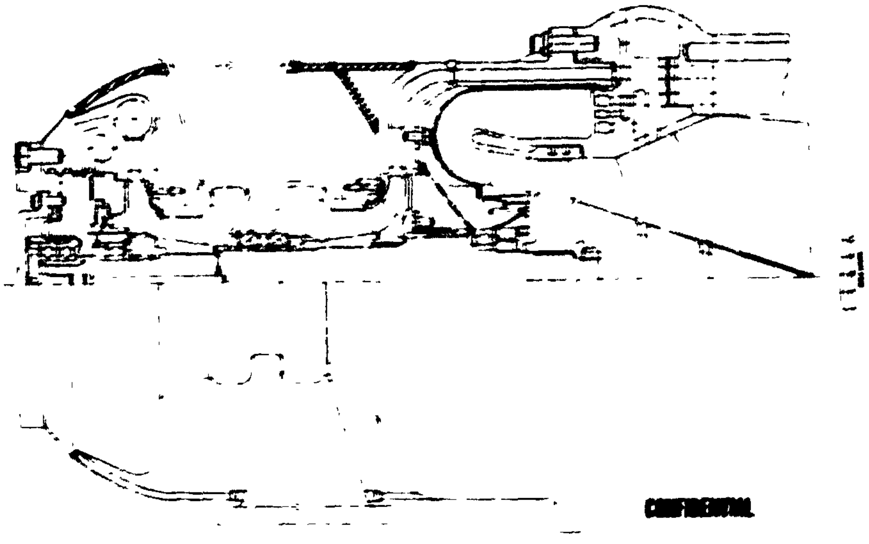
CONFIDENTIAL

Figure IV-35a. In-Line Turbopump Assembly (u)

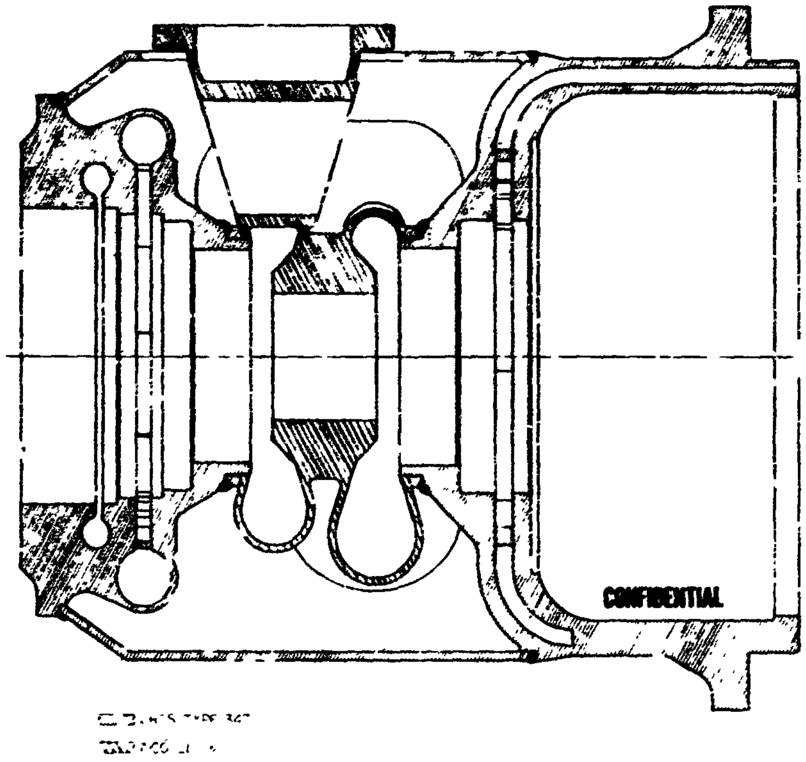
CONFIDENTIAL

Figure IV-35b. In-Line Turbopump Housing Assembly (u)

Figure IV-35

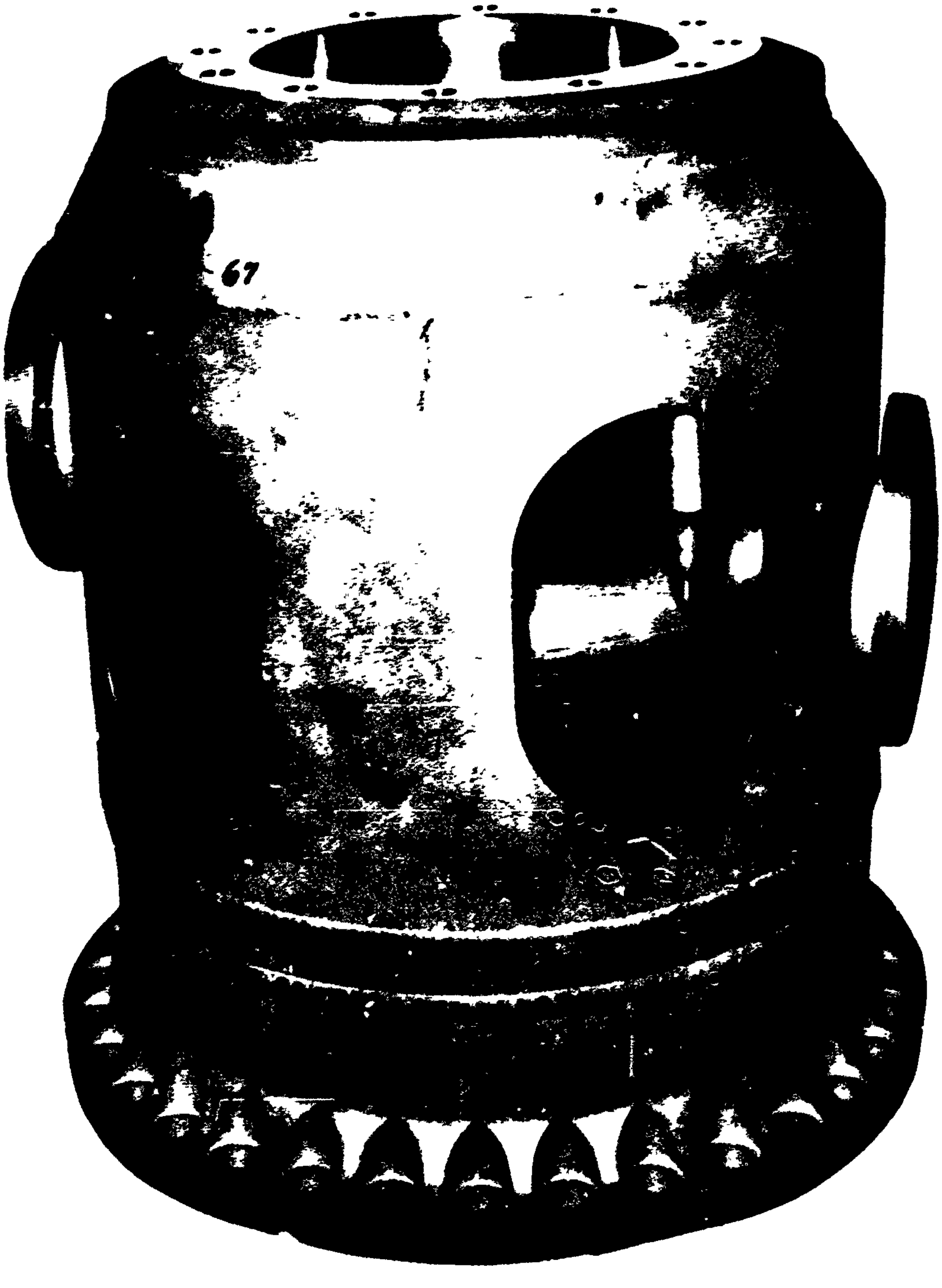

In-Line Turbopump Housing

Figure IV-36

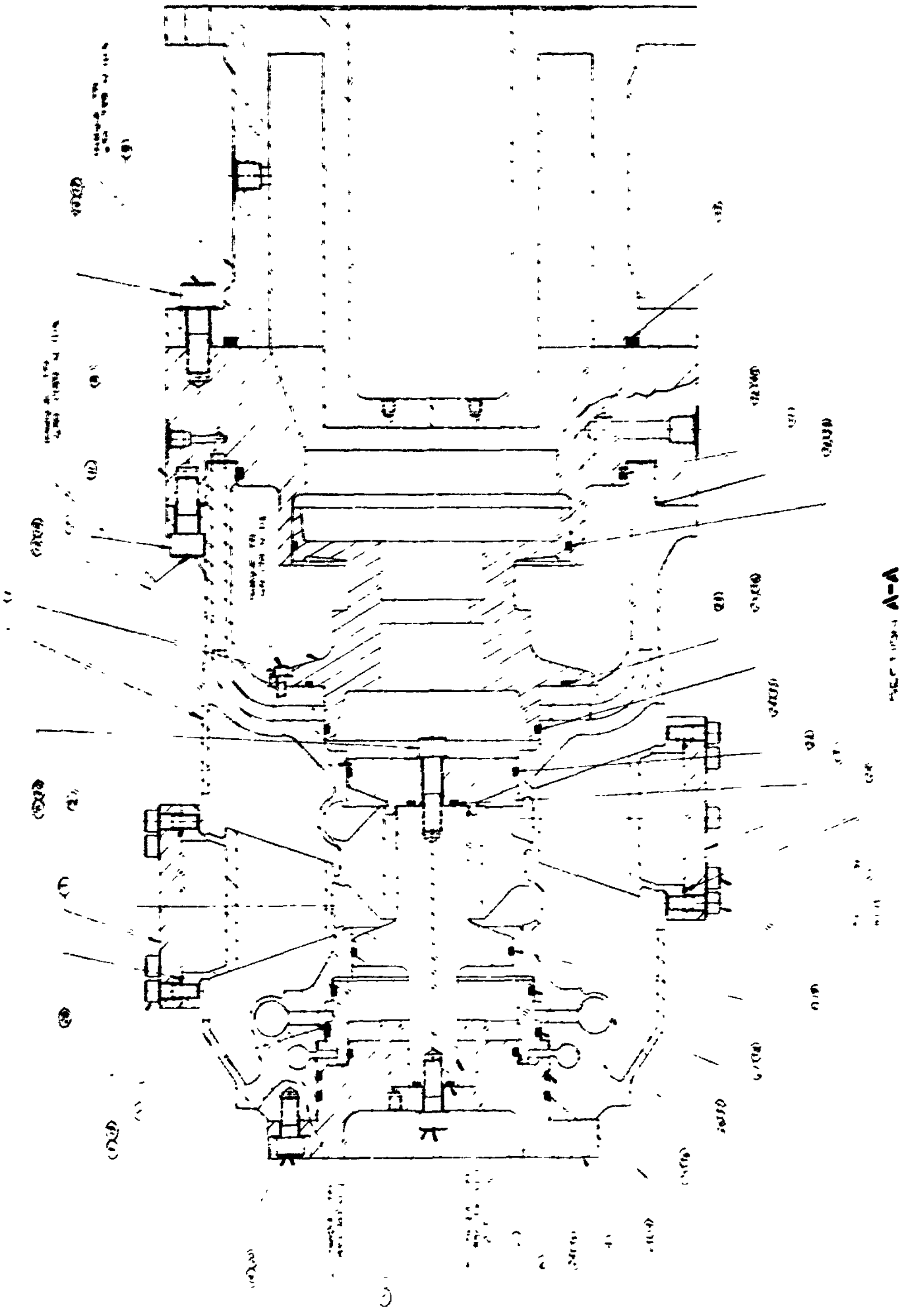

In-Line Turbopump Housing Hydrotest Assembly

Figure IV-37

Figure IV-38b. In-Line Turbopump Housing Test Setup

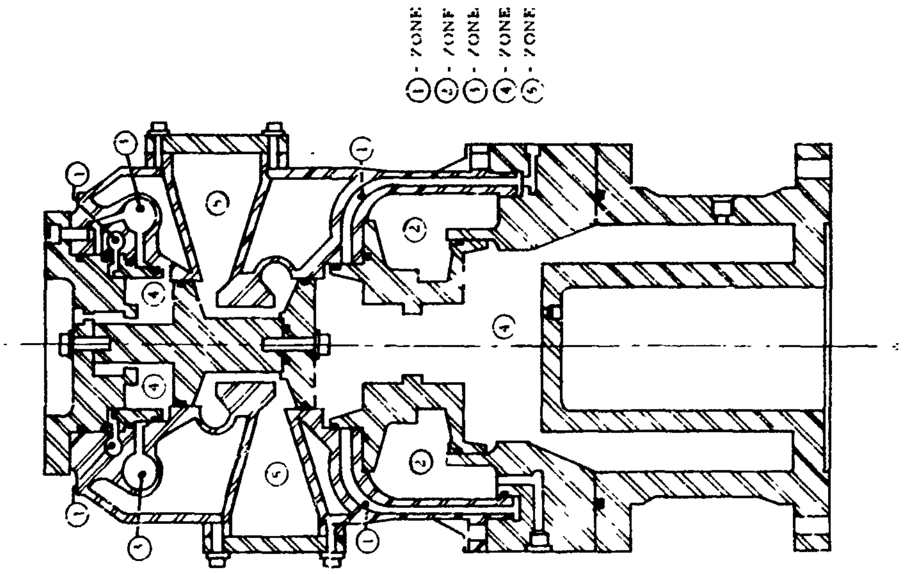
① - ZONE
② - ZONE
③ - ZONE
④ - ZONE
⑤ - ZONE
①
②
④
⑤

Figure IV-38a. In-Line Turbopump Housing Pressure Zones

Figure IV-38

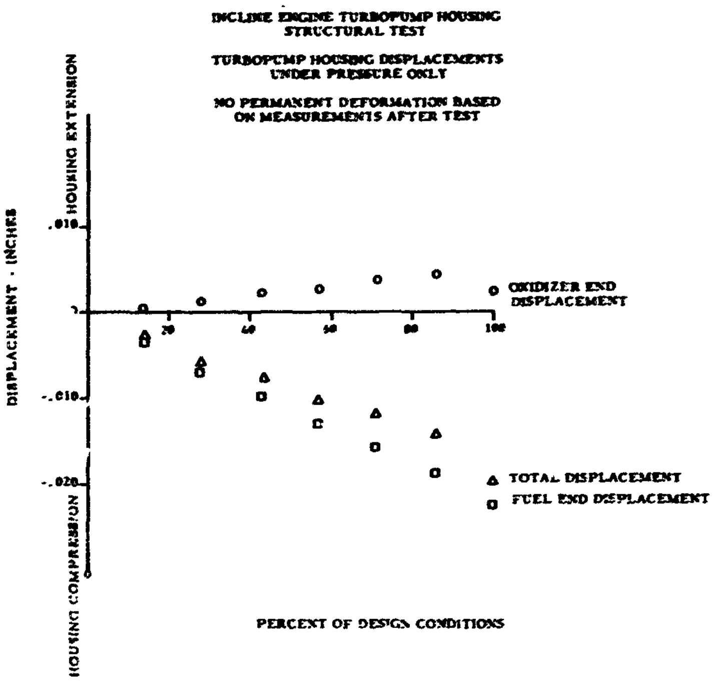

Figure IV-39a. Location of Displacement of In-Line Turbopump Housing Bearing, Pressure Only

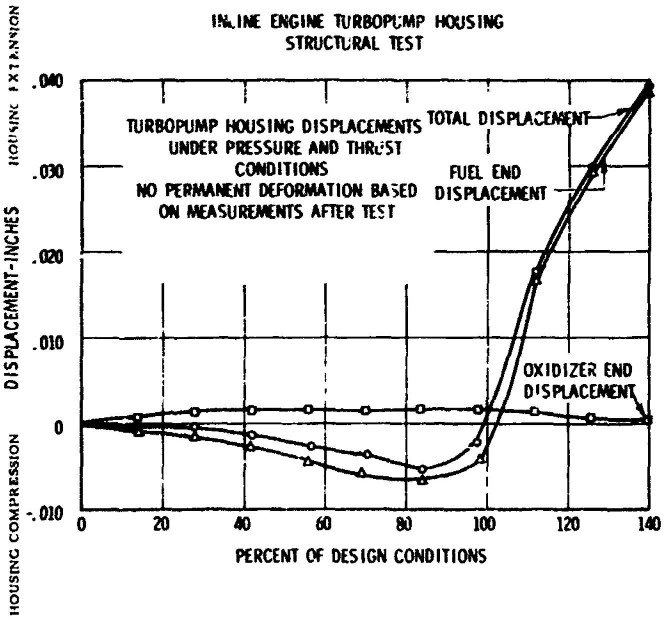

Figure IV-39b. Location of Displacement of In-Line Turbopump Housing Bearing, Pressure and Thrust Proof

Figure IV-39

UNCLASSIFIED

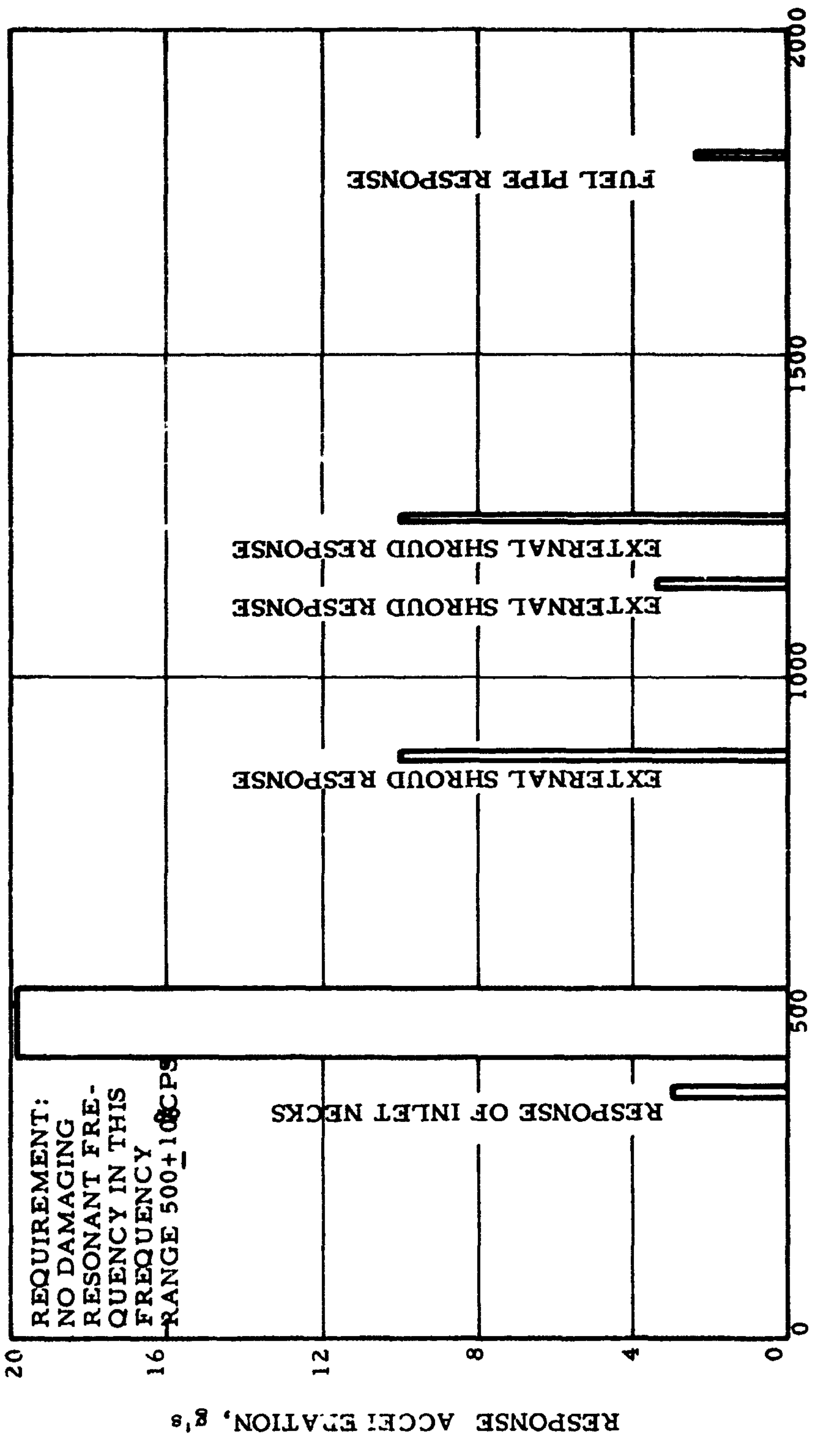

Test Results of In-Line Turbopump Housing Vibration

Figure IV-40

|  | "T" TPA |  | INLINE TPA |  |
|---|---|---|---|---|
| PUMP | FUEL | OXIDIZER | FUEL | OXIDIZER |
| Q GPM | 824 | 1243 | 800 | 1258 |
| $\Delta$H, FT | 409 | 444 | 293 | 325 |
| N, RPM | 8000 | 8000 | 7242 | 7384 |
| $\eta$, % | 65 | 65 | 63.6 | 62.3 |
| SHP | 118 | 308 | 84 | 238 |
| NPSH-FT | 20 | 20 | 20 | 20 |
| $S_{MAX}$, $\frac{\text{RPM GPM}^{1/2}}{\text{FT}^{3/4}}$ | 24,400 | 30,000 | 21,628 | 27,710 |
| HYDRAULIC TURBINE |  |  |  |  |
| W, LB/SEC | 180 | 40.0 | 130 | 31.0 |
| $P_{Ti}$, PSIA | 3430 | 5603 | 3582 | 5527 |
| $P_{Te}$, PSIA | 137 | 262 | 125 | 232 |
| $\eta$, % | 43.0 | 50.0 | 42.0 | 490 |

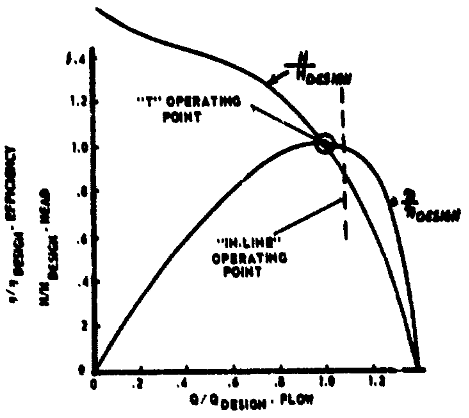

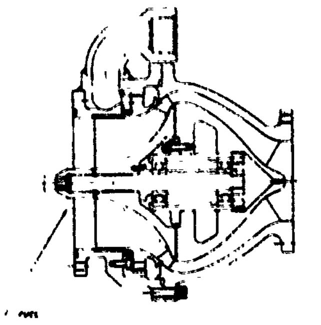

CONFIDENTIAL

Boost Pump Operation Requirements (u)

Figure IV-41

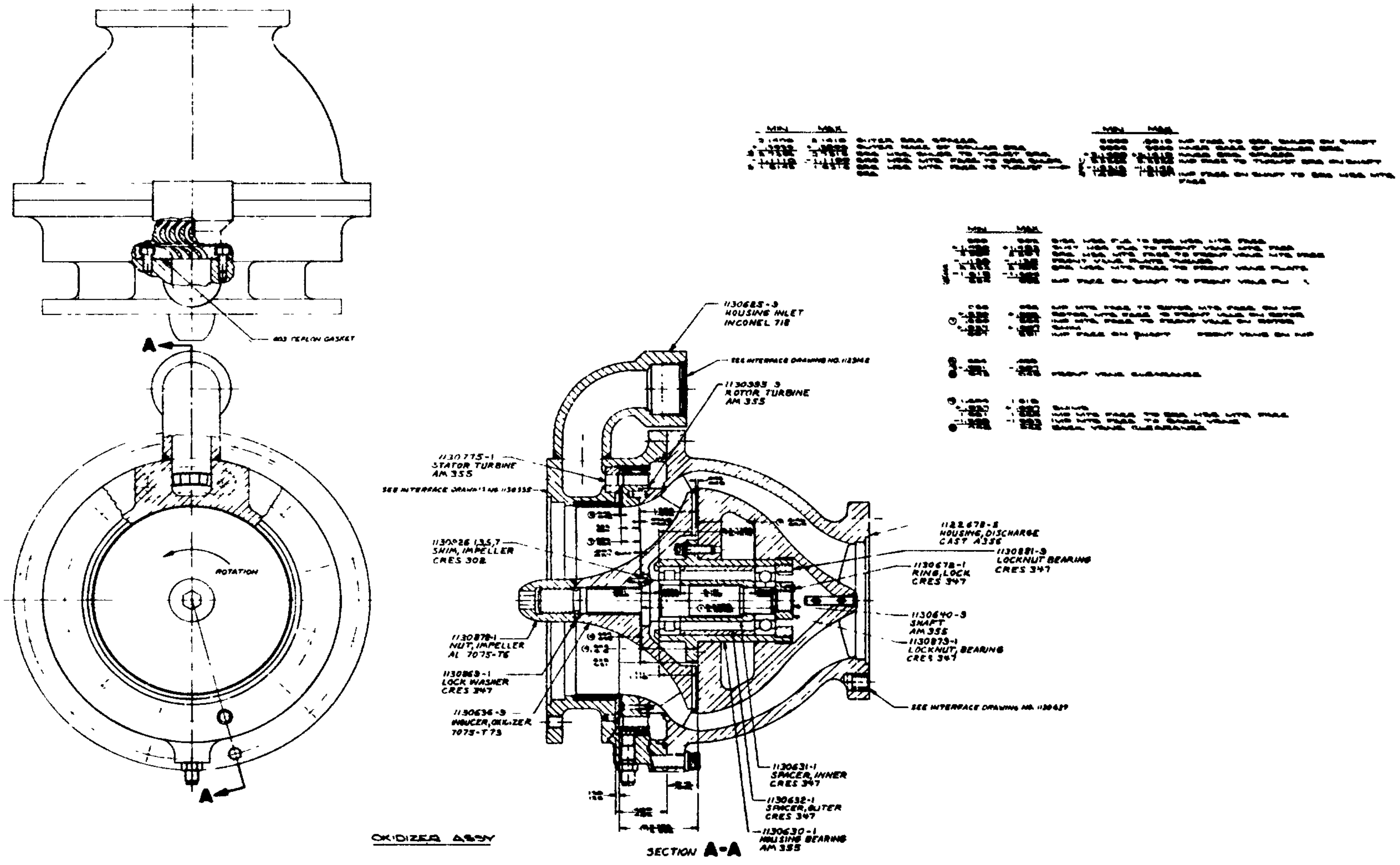
603 TEFLON GASKET
A
ROTATION
A
1130685-3
HOUSING INLET
INCONEL 718
SEE INTERFACE DRAWING NO. 1123142
1130383-3
ROTOR TURBINE
AM 355
1130775-1
STATOR TURBINE
AM 355
SEE INTERFACE DRAWING NO. 1130335
1130826 1,3,5,7
SHIM, IMPELLER
CRES 302
1130878-1
NUT, IMPELLER
AL 7075-T6
1130869-1
LOCK WASHER
CRES 347
1130636-3
INDUCER, OXIDIZER
7075-T73
1122678-5
HOUSING, DISCHARGE
CAST A356
1130881-3
LOCKNUT BEARING
CRES 347
1130678-1
RING, LOCK
CRES 347
1130640-3
SHAFT
AM 355
1130873-1
LOCKNUT, BEARING
CRES 347
SEE INTERFACE DRAWING NO. 1130639
1130631-1
SPACER, INNER
CRES 347
1130632-1
SPACER, OUTER
CRES 347
1130630-1
HOUSING BEARING
AM 355
OXIDIZER ASSY
SECTION A-A
MIN
MAX

Oxidizer Boost Pump Layout

Figure IV-42

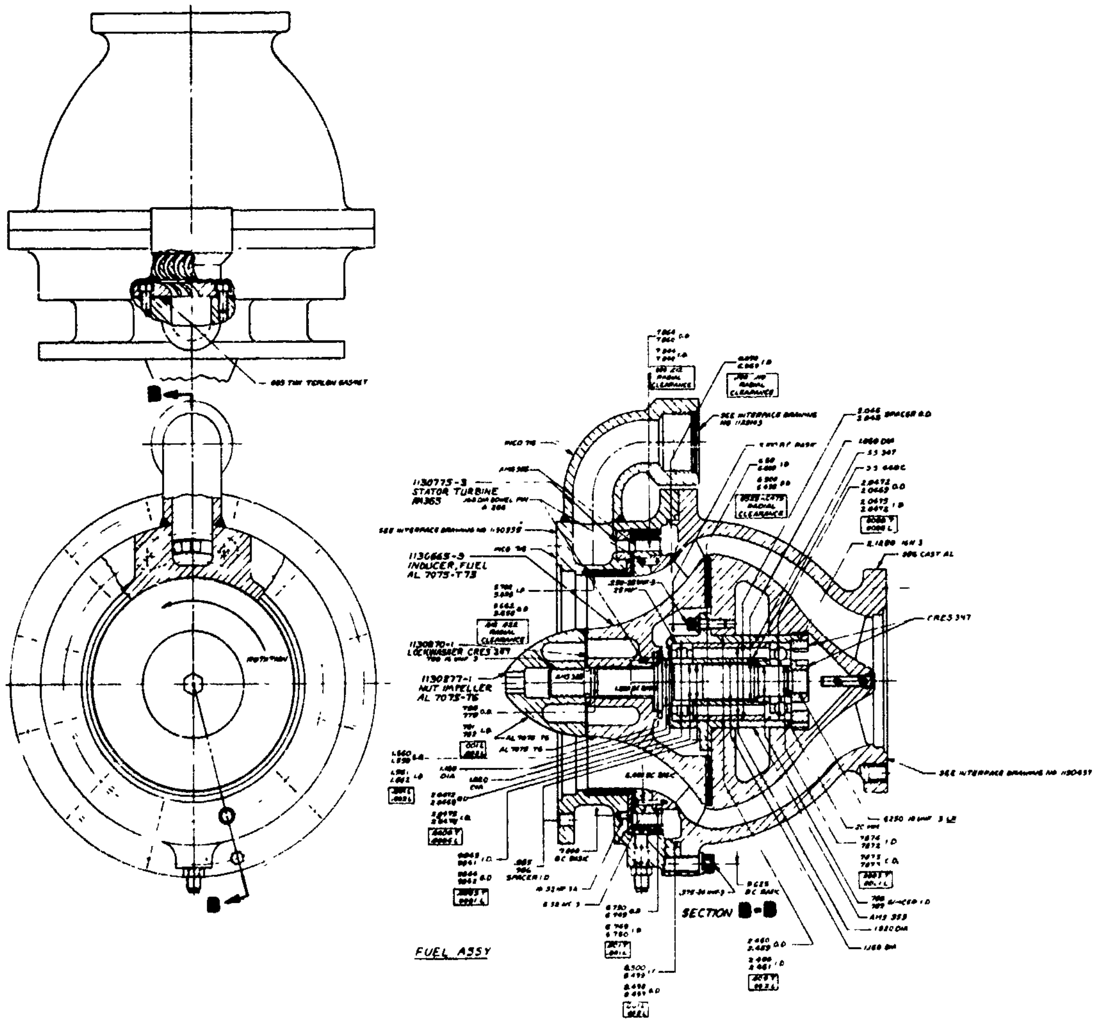
1130775-3
STATOR TURBINE
AM365
SEE INTERFACE DRAWING NO 1130338
1130665-3
INDUCER, FUEL
AL 7075-T73
1130870-1
LOCKWASHER CRES 347
1130877-1
NUT IMPELLER
AL 7075-T6
AL 7075 T6
RADIAL CLEARANCE
CRES 347
SEE INTERFACE DRAWING NO 1130457
SPACER I.D
BC BASIC
AMS 355
SECTION B-B
FUEL ASSY
ROTATION
B

Fuel Boost Pump Layout

Figure IV-43

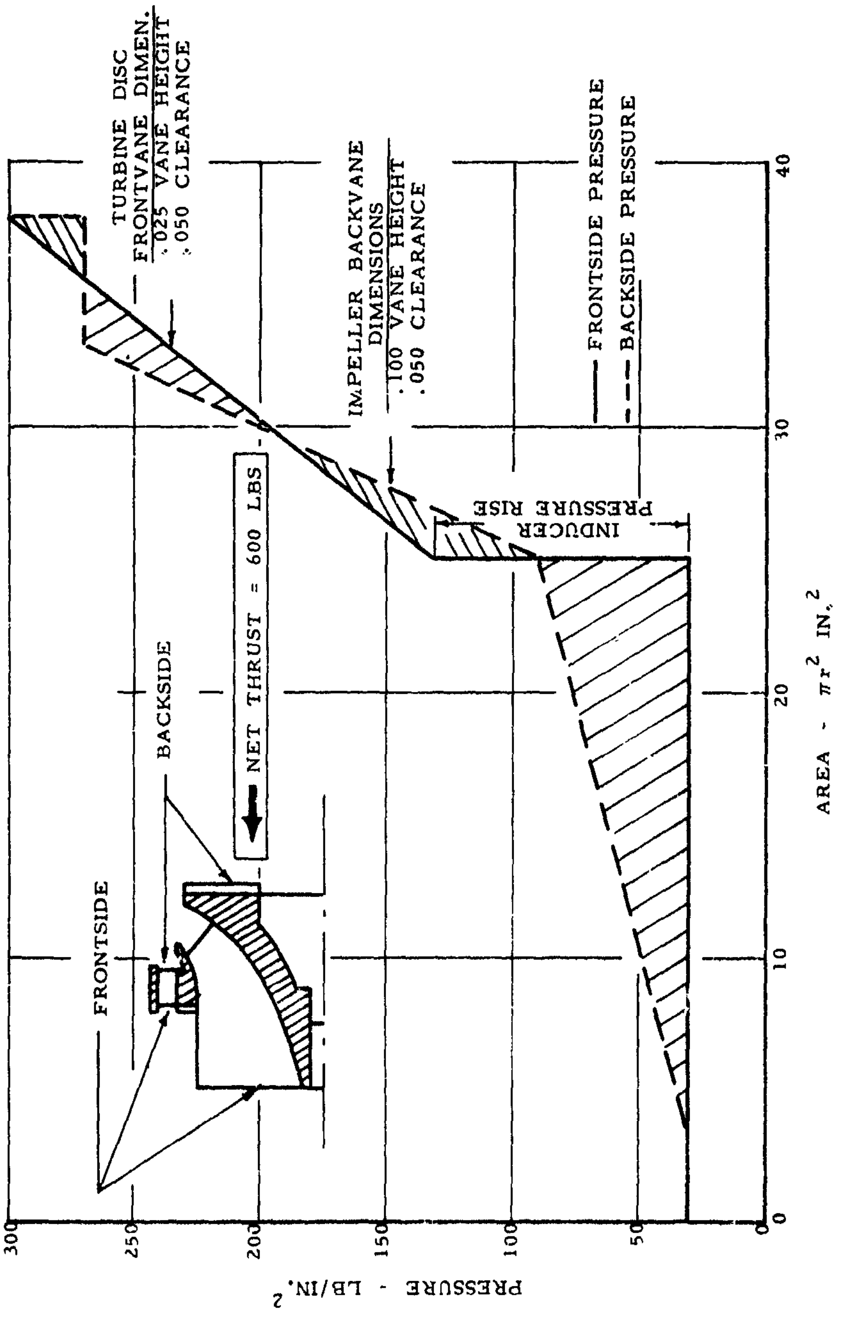

Oxidizer Boost Pump Axial Thrust

Figure IV-44

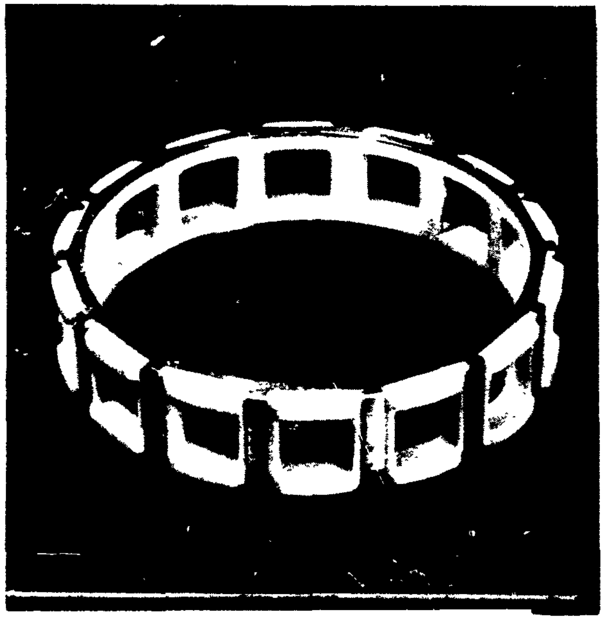

Roller Bearing Cage
Radial Load--1000 lbs

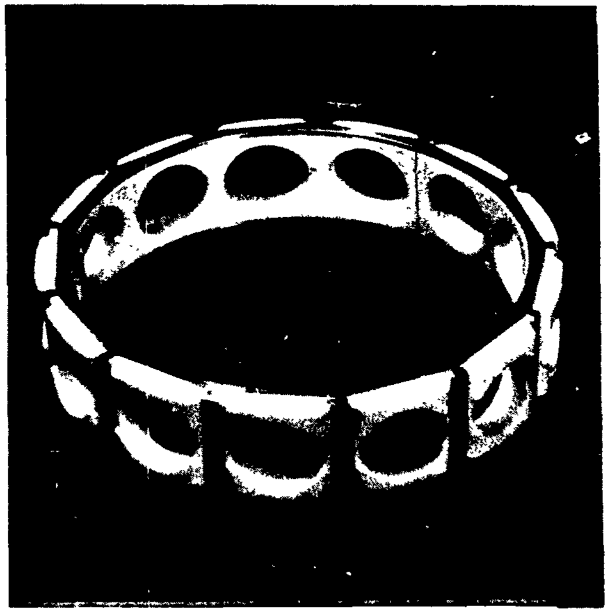

Ball Bearing Cage
Axial Load--2500 lbs

Speed - - - - - - - - 25,000 rpm
Duration - - - - - 14 min 35 sec

25,000 rpm Posttest Bearings Cages--$N_2O_4$ Lubricated

Figure IV-45

| Test No. | Duration Sec. | Rotational Speed RPM | DN (rpm x mm) $10^{-6}$ | LOADS |  | PROPELLANT ($N_2O_4$) |  |  | BEARING OUTER RACE TEMPERATURES |  |  |
|---|---|---|---|---|---|---|---|---|---|---|---|
|  |  |  |  | Axial lb | Radial lb | Flow gpm | Inlet Temp. °F | Outlet Temp. °F | Roller Bearing °F | Ball Bearing °F | Roller Bearing °F |
| 1 |  |  |  |  |  |  |  |  |  |  |  |
| 1-a | 71 | 22,300 | 1.11 | 2576 | 1989 | 5.8 | 67 | 109 | 81 | 95 | 112 |
| 1-b | 172 | 25,700 | 1.28 | 2570 | 2019 | 8.3 | 66 | 110 | 88 | 102 | 128 |
| 2 |  |  |  |  |  |  |  |  |  |  |  |
| 2-a | 15 | 21,600 | 1.08 | 2501 | 2039 | 5.8 | 83 | 101 | 92 | 86 | 99 |
| 2-b | 74 | 25,700 | 1.28 | 2655 | 2049 | 5.8 | 79 | 128 | 109 | 112 | 133 |
| 3 |  |  |  |  |  |  |  |  |  |  |  |
| 3-a | 45 | 25,000 | 1.25 | 2734 | 1993 | 5.5 | 77 | 115 | 112 | 105 | 100 |
| 3-b | 231 | 25,300 | 1.26 | 2615 | 2035 | 6.0 | 74 | 125 | 126 | 122 | 113 |
| 3-c | 353 | 25,300 | 1.26 | 2564 | 2045 | 5.6 | 78 | 129 | 129 | 123 | 116 |
| 4 |  |  |  |  |  |  |  |  |  |  |  |
|  | 344 | 25,300 | 1.26 | 2518 | 1974 | 6.2 | 74 | 124 | 99 | 123 | 136 |
|  | - | 23,400 | 1.27 | 2740 | 2329 | 6.2 | 74 | 147 | 136 | 166 | 170 |
| 5 |  |  |  |  |  |  |  |  |  |  |  |
| 5-a | 198 | 25,300 | 1.26 | 2711 | 1989 | 12.0 | 68 | 95 | 76 | 76 | 81 |
| 5-b | 58 | 25,000 | 1.25 | 2739 | 2024 | 4.0 - 10.0 | 67 | 91 | 76 | 74 | 79 |
| 5-c | 173 | 25,300 | 1.26 | 2775 | 2024 | 12.0 | 66 | 91 | 75 | 74 | 79 |
| 5-d | 221 | 25,000 | 1.25 | 2985 | 2007 | 15.2 | 75 | 93 | 81 | 80 | 84 |

| ELLANT ($N_2O_4$) | | BEARING OUTER RACE TEMPERATURES | | | |
|---|---|---|---|---|---|
| Inlet Temp. °F | Outlet Temp. °F | Roller Bearing °F | Ball Bearing °F | Roller Bearing °F | REMARKS |
| | | | | | 210 Series Bearings<br>Radial load shared by two roller bearings |
| 67 | 109 | 81 | 95 | 112 | Tests 1-a and 1-b: |
| 66 | 110 | 88 | 102 | 128 | Ball bearing, K-5-H balls, 440C races, Thin line cage, 25% glass-filled Teflon & outer race riding. |
| | | | | | Roller bearings (2), outer race roller guiding channel, 440C rollers and races, thin-line cage, 25% glass-filled Teflon outer land riding. |
| | | | | | Bearings inspected and found in excellent condition. |
| | | | | | Tests 2-a and 2-b: |
| 83 | 101 | 92 | 86 | 99 | Same bearings from tests 1-a and 1-b reinstalled |
| 79 | 128 | 109 | 112 | 135 | Bearings inspected and found in excellent condition. Roller bearing not cleaned sufficiently and pitted over night. Ball bearing in excellent condition. |
| | | | | | Tests 3-a, b and c: |
| 77 | 115 | 112 | 105 | 100 | Reinstalled same ball bearing. Two new roller bearings with same cages used in tests 1-a through 2-b. |
| 74 | 125 | 126 | 122 | 113 | |
| 78 | 129 | 129 | 123 | 116 | |
| | | | | | Bearings inspected and found in excellent condition. Work statement objectives met 25,000 rpm bearing operation in $N_2O_4$ with new cage designs. |
| | | | | | Test 4:<br>Ball bearing, Carboloy 44a (Tungsten carbide balls), 440C races, fully shrouded Rulon A (pre-soaked in $N_2O_4$ and maroon color bleached white) cage, inner race riding. |
| 74 | 124 | 99 | 123 | 136 | Steady-state prior to failure. |
| 74 | 147 | 136 | 166 | 170 | Steady-state data. |
| | | | | | Steady-state at shutdown due to ball bearing failure due to improper assembly. Roller bearings in good condition. |
| | | | | | Test 5:<br>New ball and one new roller bearings of same configuration used in tests 1-a thru 3-c. One roller bearing used previously in tests 1 and 2. |
| 68 | 95 | 76 | 76 | 81 | |
| 67 | 91 | 76 | 74 | 79 | Variable flow test |
| 66 | 91 | 75 | 74 | 79 | |
| 75 | 93 | 81 | 80 | 84 | Bearings in excellent post test condition. |

Summary of 25,000 rpm Bearing Tests in $N_2O_4$

Figure IV-46

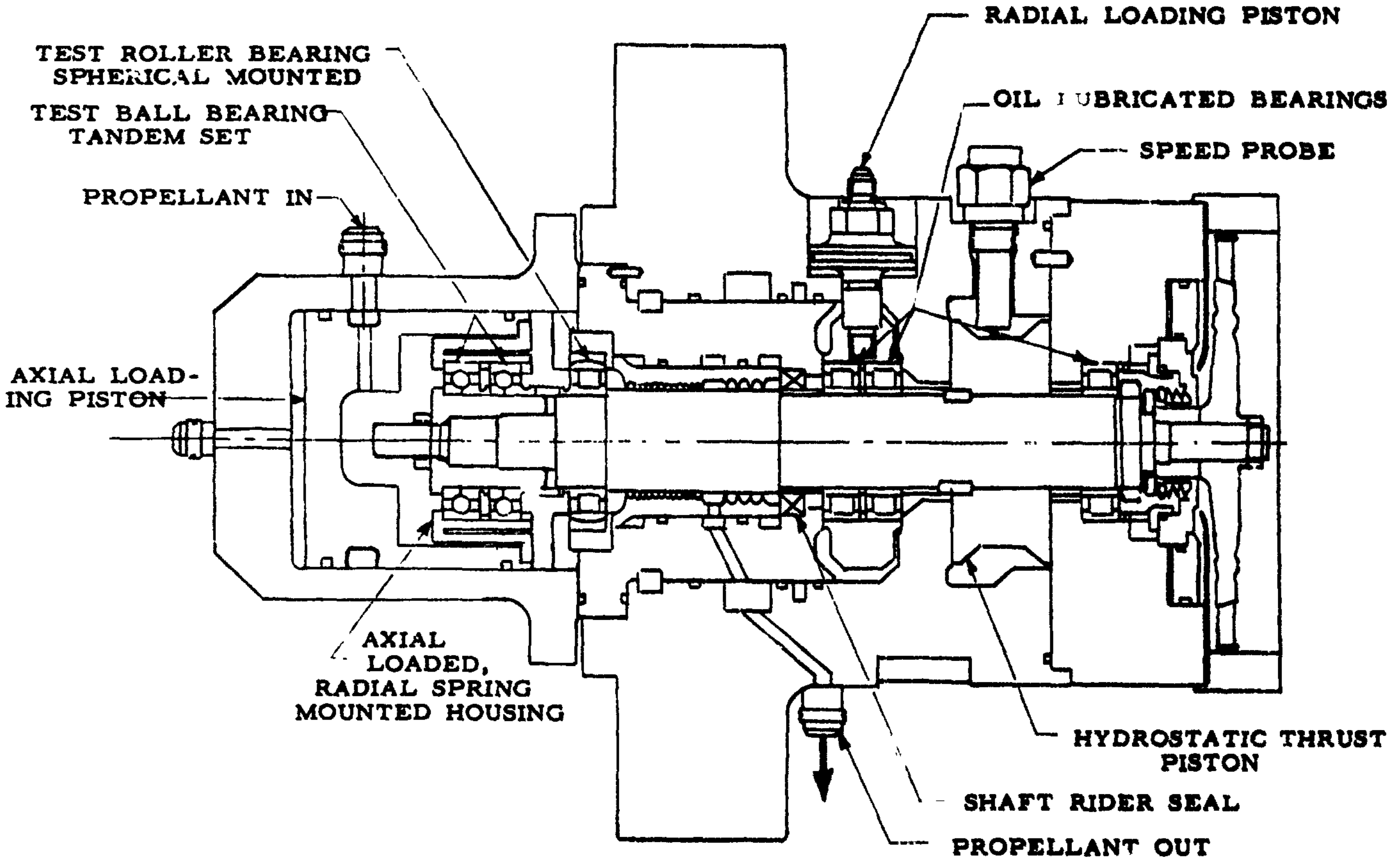
RADIAL LOADING PISTON
TEST ROLLER BEARING SPHERICAL MOUNTED
OIL LUBRICATED BEARINGS
TEST BALL BEARING TANDEM SET
SPEED PROBE
PROPELLANT IN
AXIAL LOADING PISTON
AXIAL LOADED, RADIAL SPRING MOUNTED HOUSING
HYDROSTATIC THRUST PISTON
SHAFT RIDER SEAL
PROPELLANT OUT

40,000 rpm Bearing Tester

Figure IV-47

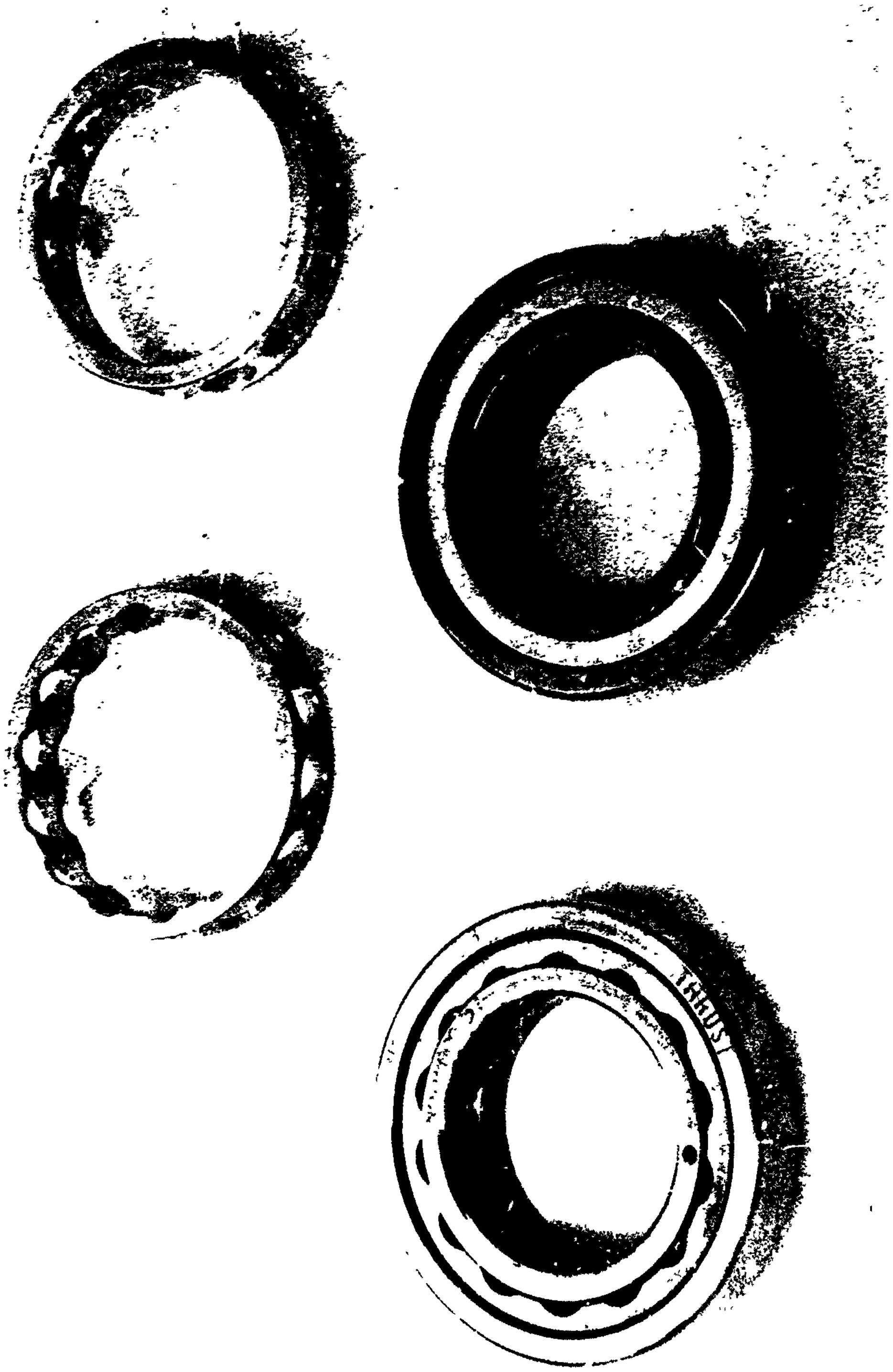

Ball Bearing Cage Designs

Figure IV-48

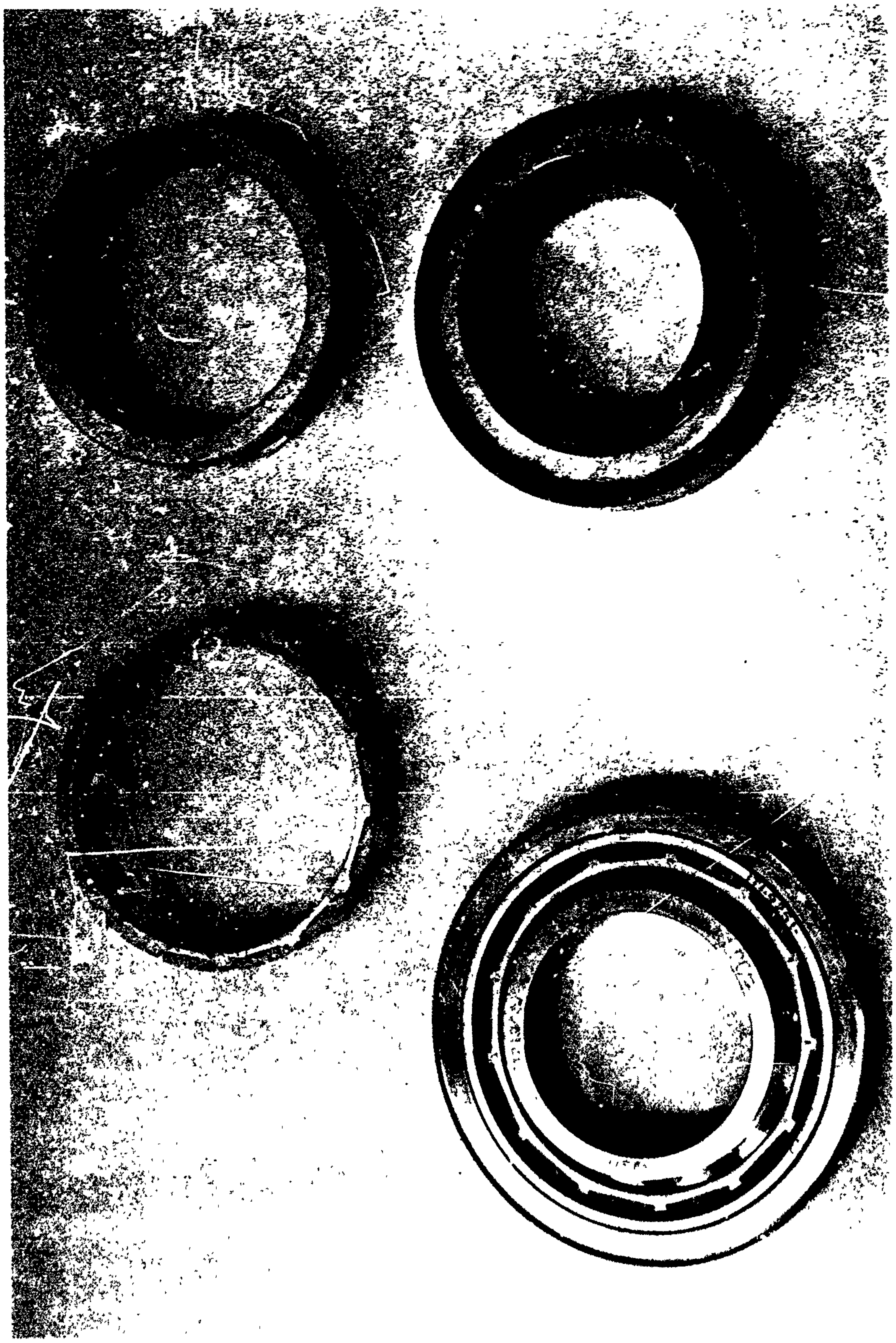

Roller Bearing Cage Designs

Figure IV-49

| Test No. | Full Speed Duration sec 1 | Data Point Sec 2 | Rotational Speed rpm | DN (rpm x mm) $10^{-6}$ | LOAD |  | PROPELLANT($N_2O_4$) |  | RISE OF OUTER RACE TEMP. |  |  |
|---|---|---|---|---|---|---|---|---|---|---|---|
|  |  |  |  |  | Axial lb | Radial lb | Flow gpm | Temp Rise °F | Ball Bearing °F | Ball Bearing °F | Rolle Beari °F |
| 005a | 266 |  |  |  |  |  |  |  |  |  |  |
|  |  | 35 | 39,600 | 1.55 | 1170 | 525 | 9.6 | 9 | 21 | 21 | 37 |
|  |  | 245 | 39,100 | 1.56 | 2955 | 548 | 8.6 | 22 | 22 | 22 | 41 |
|  |  | 297 | 39,000 | 1.56 | 2350 | 880 | 8.2 | 22.6 | 22 | 22 | 41 |
| 005b |  |  |  |  |  |  |  |  |  |  |  |
|  |  | 1 | 39,300 | 1.57 | 835 | 551 | 9.6 | 7 | 17.5 | 18.5 | 34 |
| 006a |  |  |  |  |  |  |  |  |  |  |  |
|  |  | 1 | 27,600 | 1.1 | 1503 | 572 | 9.5 | - | - | - | - |
| 006 b | 530 |  |  |  |  |  |  |  |  |  |  |
|  |  | 120 | 39,890 | 1.59 | 1810 | 560 | 9.0 | 24.1 | 23.9 | 23.9 | 33 |
|  |  | 340 | 39,435 | 1.58 | 2550 | 520 | 8.4 | 26 | 28 | 28 | 39 |
|  |  | 420 | 38,995 | 1.56 | 1840 | 1020 | 8.3 | 26 | 29 | 28 | 40 |
| 007 | 410 |  |  |  |  |  |  |  |  |  |  |
|  |  | 35 | 32,212 | 1.29 | 2320 | 500 | 9.0 | 12 | 10.8 | 13 | 20 |
|  |  | 145 | 31,913 | 1.28 | 4200 | 500 | 9.2 | 13 | 13.1 | 15.5 | 17 |
|  |  | 200 | 31,575 | 1.26 | 2650 | 985 | 8.6 | 13.2 | 15.5 | 15.8 | 24.1 |

NOTES:
1 Duration at full speed
2 Time from turbine start to data point

108 series bearings. Axial load shared by tandem bearing set.

Su

| | PROPELLANT($N_2O_4$) | | RISE OF OUTER RACE TEMP. | | | |
|---|---|---|---|---|---|---|
| al | Flow gpm | Temp Rise °F | Ball Bearing °F | Ball Bearing °F | Roller Bearing °F | REMARKS |
| | | | | | | Ball bearing set, 440C balls and rollers, fully shrouded, 25% glass-filled teflon cage, inner race riding. Spherical seat roller bearing, 440C rollers and races, fully shrouded, 15 pocket, 25% glass-filled Teflon cage, inner race riding. Roller bearing installed aligned. |
| | 9.6 | 9 | 21 | 21 | 37 | Steady State. |
| | 8.6 | 22 | 22 | 22 | 41 | Axial peak load (maintained 20 sec) |
| | 8.2 | 22.6 | 22 | 22 | 41 | Increasing radial load - shutdown due to loss of speed signal. Bearings not inspected. |
| | | | | | | Bearings from Test 005a reinstalled |
| | 9.6 | 7 | 17.5 | 18.5 | 34 | Shutdown due to rupture of burst diaphragm in turbine gas supply. Bearings inspected and found in excellent condition. |
| | | | | | | Bearings from test 005a and b reinstalled. Roller bearing installed misaligned |
| | 9.5 | - | - | - | - | Shutdown due to loss of instrumentation. Bearings not inspected. |
| | | | | | | Retest of bearings reinstalled prior to test 006 a. Roller bearing installed misaligned. |
| | 9.0 | 24.1 | 23.9 | 23.9 | 33 | Steady state |
| | 8.4 | 26 | 28 | 28 | 39 | Axial peak load (maintained 36 sec) |
| | 8.3 | 26 | 29 | 28 | 40 | Radial peak load applied twice for a total of 32 sec |
| | | | | | | Scheduled duration, manual shutdown. |
| | | | | | | Bearings inspected and found in excellent condition. Work Statement objectives met for 40,000 rpm operation in $N_2O_4$ (Tests 005a and 006b) |
| | | | | | | Ball bearing set, 440C balls and races, fully shrouded, 25% glass-filled teflon cage, inner race riding. |
| | | | | | | Standard outer race roller bearing, 440C rollers & races fully shrouded, 15 pocket, 25% glass-filled Teflon cage, inner race riding. |
| | 9.0 | 12 | 10.8 | 13 | 20 | Steady state. |
| | 9.2 | 13 | 13.1 | 15.5 | 17 | Axial peak load |
| | 8.6 | 13.2 | 15.5 | 15.8 | 24.1 | Radial peak load |
| | | | | | | Scheduled duration, manual shutdown. |
| | | | | | | Bearings inspected and found in excellent condition. Work Statement objectives met for 31,250 rpm operation in $N_2O_4$. |

ring set.

Summary of 40,000 and 31,250 rpm Bearing Tests in $N_2O_4$

Figure IV-50

2

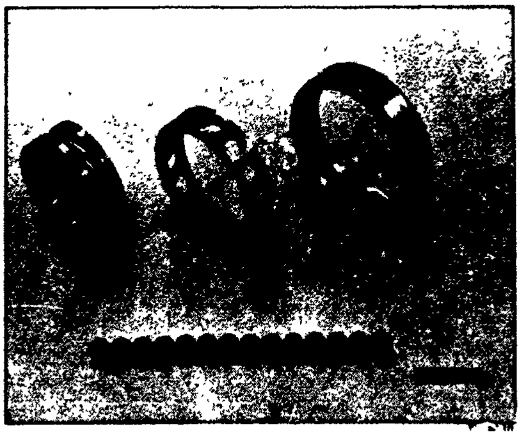

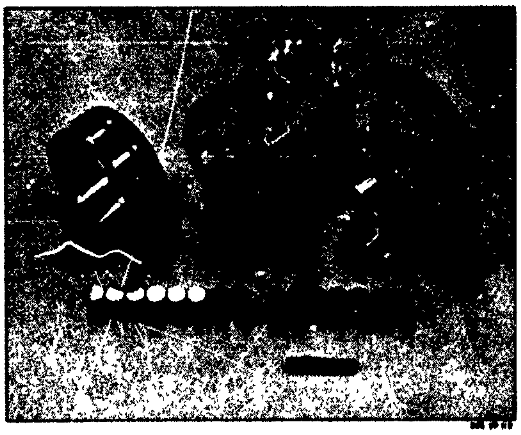

SPEED: 31,250 RPM
DURATION: 413 sec, 6 min. 53 sec.

| | LOAD | DURATION |
|---|---|---|
| AXIAL, NOMINAL: | 2200+ lbs | 384 sec. |
| PEAK: | 4200 lbs | 29 sec. |
| RADIAL, NOMINAL: | 500 lbs | 368 sec. |
| PEAK: | 985 lbs | 45 sec. |

31,250 rpm Posttest Bearings--$N_2O_4$ Lubricated

Figure IV-51

| Test No. | Full Speed Duration Sec 1 | Data Point Sec 2 | Rotational Speed rpm | DN (rpm x mm) $10^{-6}$ | Axial lb | Radial lb | Propellant (A-50) |  | Rise of Outer Race Temperature |  |  |  |
|---|---|---|---|---|---|---|---|---|---|---|---|---|
|  |  |  |  |  |  |  | Flow gpm | Temp Rise $^{\circ}$F | Ball Bearing $^{\circ}$F | Ball Bearing $^{\circ}$F | Roller Bearing $^{\circ}$F |  |
| 008 | 450 |  |  |  |  |  |  |  |  |  |  | Bal<br>mol<br>sea<br>inr<br>rac |
|  |  | 70 | 40,300 | 1.61 | 1800 | 552 | 14.2 | 17.8 | 12.4 | 12.3 | 17.9 | Ste |
|  |  | 100 | 40,400 | 1.62 | 2600 | 552 | 13.9 | 18.6 | 13.3 | 13.5 | 17.9 | Axi |
|  |  | 180 | 40,300 | 1.61 | 2060 | 1115 | 13.6 | 18.9 | 13.6 | 13.0 | 17.9 | Rad |
|  |  | 440 | 40,300 | 1.61 | 1860 | 550 | 13.6 | 19.2 | 13.1 | 13.3 | 19.1 | Ste<br>Bea<br>cor<br>rol |
| 009 | 267 |  |  |  |  |  |  |  |  |  |  | Bal<br>typ<br>440<br>gla<br>bea |
|  |  | 85 | 40,700 | 1.63 | 1960 | 548 | 13.7 | 10.3 | 24.5 | 25.1 | 30.2 | Ste |
|  |  | 107 | 40,800 | 1.63 | 2790 | 548 | 13.7 | 10.5 | 25.2 | 25.8 | 30.7 | Axi |
|  |  | 200 | 41,200 | 1.65 | 2010 | 1118 | 13.4 | 10.1 | 26.2 | 28.7 | 34.6 | Rad |
|  |  | 265 | 40,600 | 1.62 | 1690 | 560 | 8.1 | 10.5 | 33.1 | 32.8 | 51.6 | Dat<br>ris<br>Bea<br>cau<br>dow |
| 010 | 418 |  |  |  |  |  |  |  |  |  |  | Bal<br>inn<br>Sta<br>ra<br>Te |
|  |  | 60 | 32,800 | 1.31 | 2790 | 595 | 14.2 | 10.2 | 7 | 5.3 | 8.1 | St |
|  |  | 100 | 32,600 | 1.30 | 2840 | 1117 | 14.1 | 9.6 | 6.3 | 5.1 | 10.4 | Rad |
|  |  | 190 | 32,300 | 1.31 | 4690 | 605 | 14.1 | 9.7 | 6.0 | 4.4 | 9.4 | Axi |
|  |  | 415 | 32,200 | 1.29 | 2970 | 600 | 14.1 | 10.1 | 2.6 | 1.3 | 5.8 | Ste<br>Bea<br>Wor<br>ope |
| 011 |  |  |  |  |  |  |  |  |  |  |  | Bal<br>shr<br>cag<br>and<br>poc<br>ins |
|  |  | 11 | 10,500 | .42 | 2030 | 595 | 13.7 | - | 4 | 4 | 8 | Rol<br>exc |

Summary o

| Propellant (A-50) | | Rise of Outer Race Temperature | | | |
|---|---|---|---|---|---|
| Flow gpm | Temp Rise °F | Ball Bearing °F | Ball Bearing °F | Roller Bearing °F | Remarks |
| | | | | | Ball bearing set, K-5-H balls, 440C races and Halo molded 25% Teflon cage outer race riding. Spherical seat roller bearing K-5-H rollers & outer race, 440C inner race, thin line, 25% Teflon, 15 pocket outer race riding cage. Roller bearing installed misaligned. |
| 14.2 | 17.6 | 12.4 | 12.3 | 17.9 | Steady state |
| 13.9 | 18.6 | 13.3 | 13.5 | 17.9 | Axial load peak |
| 13.6 | 18.9 | 13.6 | 13.0 | 17.9 | Radial load peak |
| 13.6 | 19.2 | 13.1 | 13.3 | 19.1 | Steady state prior to scheduled shutdown |
| | | | | | Bearings inspected; Ball bearing set in excellent condition, roller bearing had excessive wear on K-5-H rollers and outer races. |
| | | | | | Ball bearing set - 400C balls, races and same Halo type cages from test 3. Spherical seat roller bearing 440C rollers and races, Thin line, 15 pocket 25% glass filled Teflon outer race riding cage. Roller bearing installed aligned. |
| 13.7 | 10.3 | 24.5 | 25.1 | 30.2 | Steady State |
| 13.7 | 10.5 | 25.2 | 25.8 | 30.7 | Axial load peak |
| 13.4 | 10.1 | 26.2 | 28.7 | 34.6 | Radial load peak |
| 8.1 | 10.5 | 33.1 | 32.8 | 51.6 | Data prior to manual shutdown due to abnormal temperature rise in bearings. |
| | | | | | Bearings inspected, cages of ball bearings failed causing damage to all bearing components including downstream roller bearing. |
| | | | | | Ball bearing set, 440C balls and races, fully shrouded inner race riding 25% glass filled Teflon cage. Standard outer race roller bearing, 440C rollers and races, fully shrouded, 15 pocket, 25% glass filled Teflon, inner race riding cage. |
| 14.2 | 10.2 | 7 | 5.3 | 8.1 | Steady state |
| 14.1 | 9.6 | 6.3 | 5.1 | 10.4 | Radial load peak (above 1000 lb for 31 sec) |
| 14.1 | 9.7 | 6.0 | 4.4 | 9.4 | Axial load peak (maintained 20 sec) |
| 14.1 | 10.1 | 2.6 | 1.3 | 5.8 | Steady state data prior to scheduled shutdown. |
| | | | | | Bearings inspected and in excellent condition. Work Statement objectives met for 31,250 rpm A-50 operation. |
| | | | | | Ball bearing set K-5-H balls, 440C races fully shrouded, inner race riding, 25% glass filled Teflon cage. Spherical seat roller bearing, 440C rollers and races, Thin line, 25% glass filled Teflon, 15 pocket, outer race riding cage. Roller bearing installed misaligned. |
| 13.7 | - | 4 | 4 | 8 | Roller bearing cage failure; Ball bearings were in excellent condition. |

Summary of 40,000 and 31,250 rpm Bearing Tests in AeroZINE 50

Figure IV-52, Sheet 1 of 3

| Test No. | Full Speed Duration Sec 1 | Data [illegible] Sec 2 | Rotational Speed rpm | DN (rpm x mm) $10^6$ | Axial lb | Radial lb | Propellant (A-50) | | Rise of Outer Race Tempe | | |
|---|---|---|---|---|---|---|---|---|---|---|---|
| | | | | | | | Flow gpm | Temp Rise °F | Ball Bearing °F | Ball Bearing °F | Rolle Beari °F |
| 012a | 55 | | | | | | | | | | |
| | | 97 | 40,395 | 1.61 | 390 | 532 | 10.8 | 20.0 | 12.6 | 13.0 | 15.0 |
| | | 151 | 41,232 | 1.65 | 1030 | 625 | 8.2 | 18.1 | 20.0 | 19.0 | 21.3 |
| 012-b | 36 | | | | | | | | | | |
| | | 58 | 40,126 | 1.60 | 1145 | 515 | 8.0 | 17.2 | 17.0 | 10.0 | 18.4 |
| | | 94 | 40,654 | 1.62 | 1120 | 710 | 8.0 | 18.5 | 18.0 | 14.0 | 20.0 |
| 013 | 393 | | | | | | | | | | |
| | | 86 | 40,407 | 1.62 | 1410 | 573 | 8.8 | - | 16.4 | 8.6 | 18.4 |
| | | 122 | 40,530 | 1.62 | 1460 | 1094 | 8.8 | - | 18.4 | 14.6 | 19.4 |
| | | 190 | 40,937 | 1.64 | 2640 | 579 | 8.7 | - | 18.4 | 15.6 | 22.4 |
| | | 479 | 40,835 | 1.63 | 1480 | 570 | 8.2 | - | 14.4 | 13.6 | 17.4 |
| 014 | 137 | | | | | | | | | | |
| | | 32 | 40,044 | 1.60 | 1770 | 562 | 8.6 | - | 17.2 | 18.9 | 18.4 |
| | | 174 | 40,527 | 1.62 | 1855 | 550 | 8.1 | - | 38.1 | 39.5 | 35.7 |
| 015 | 103 | | | | | | | | | | |
| | | 31 | 40,258 | 1.61 | 1257 | 567 | 8.9 | - | 25.8 | 32.0 | 21.5 |
| | | 134 | 40,446 | 1.62 | 1385 | 558 | 8.9 | - | 30.3 | 35.7 | 27.2 |
| 016 | 343 | | | | | | | | | | |
| | | 27 | 40,424 | 1.62 | 1560 | 260 | 9.7 | 19.0 | 12.0 | 12.0 | 15.0 |
| | | 118 | 42,392 | 1.70 | 7080 | 261 | 9.5 | 19.0 | 17.0 | 19.0 | 20.0 |
| | | 370 | 40,495 | 1.62 | 1960 | 260 | 9.4 | 19.0 | 31.0 | 34.0 | 29.0 |

Summ

| era<br>er<br>ing | ial | Propellant (A-50) Flow gpm | Propellant (A-50) Temp Rise °F | Rise of Outer Race Temperature: Ball Bearing °F | Rise of Outer Race Temperature: Ball Bearing °F | Rise of Outer Race Temperature: Roller Bearing °F | Remarks |
|---|---|---|---|---|---|---|---|
| | | | | | | | Ball bearing set, K-5-H balls, 440C races, fully shrouded inner race riding 25% glass-filled Teflon cage. Spherical seat roller bearing, 440C rollers and races, redesigned thin line, 13 pocket, outer race riding cage. Roller bearing installed aligned. |
| .0 | 32 | 10.8 | 20.0 | 12.6 | 13.0 | 15.0 | Steady State |
| .3 | 25 | 8.2 | 18.1 | 20.0 | 19.[illegible] | 21.3 | Steady state prior to shutdown due to loss of speed signal. Bearings not inspected. |
| | | | | | | | Retest of bearings installed prior to test 12-a. |
| .4 | 15 | 8.0 | [illegible] | 17.0 | 10.0 | 18.4 | Steady state |
| 0 | 10 | 8.0 | 18.5 | 18.0 | 14.0 | 20.0 | Steady state prior to shutdown due to loss of speed signal. Bearings not inspected. |
| | | | | | | | Retest of bearings installed prior to test 012 a. |
| 4 | 73 | 8.8 | - | 16.4 | 8.6 | 18.4 | Steady state |
| 4 | 94 | 8.6 | - | 18.4 | 14.6 | 19.4 | Radial load peak |
| 4 | 79 | 8.7 | - | 18.4 | 15.6 | 22.4 | Axial load peak |
| 4 | 70 | 8.2 | - | 14.4 | 13.6 | 17.4 | Steady state prior to scheduled shutdown. Bearings inspected and reinstalled. Roller bearing installed misaligned. |
| | | | | | | | Bearings from tests 12-a, 12-b and 13 reinstalled. Roller bearing installed misaligned. |
| 4 | 62 | 8.6 | - | 17.2 | 18.9 | 18.4 | Steady state |
| 7 | 50 | 8.1 | - | 38.1 | 39.5 | 35.7 | Steady state prior to shutdown due to loss of speed signal. Bearings not inspected. |
| | | | | | | | Retest of bearings reinstalled prior to test 014. |
| 5 | 67 | 8.9 | - | 25.8 | 32.0 | 21.5 | Steady state |
| 2 | 58 | 8.9 | - | 30.3 | 35.7 | 27.2 | Steady state prior to scheduled shutdown. Bearings inspected. Roller bearing met Work Statement requirements for 40,000 rpm AeroZINE 50 operation. Ball bearings failed, races and balls overheated and fatigued. |
| | | | | | | | Ball bearing set, K-5-H balls, 440C races, fully shrouded, 25% glass filled Teflin, inner land riding modified with radial cutouts on guiding surface. Spherical seat roller bearing, 440C rollers and races. Thin line, 13 roller, 25% glass-filled Teflon cage, outer race riding. Roller bearing installed aligned. |
| | 60 | 9.7 | 19.0 | 12.0 | 12.0 | 15.0 | Steady state |
| | 61 | 9.5 | 19.0 | 17.0 | 19.0 | 20.0 | Axial load peak (over 6000 lb for 22 sec) |
| | 60 | 9.4 | 19.0 | 31.0 | 34.0 | 29.0 | Steady state prior to manual shutdown due to high vibration reading. Ball bearings failed, races and balls overheated and fatigued (both bearings). |

Summary of 40,000 and 31,250 rpm Bearing Tests in AeroZINE 50

Figure IV-52, Sheet 2 of 3

| Test No. | Full Speed Duration Sec 1 | Data Pt. Sec 2 | Rotational Speed rpm | DN (rpm x mm) $10^6$ | Axial lb | Radial lb | Propellant (A-50) |  | Rise of Outer Race Temperat |  |  |
|---|---|---|---|---|---|---|---|---|---|---|---|
|  |  |  |  |  |  |  | Flow gpm | Temp Rise °F | Ball Bearing °F | Ball Bearing °F | Roller Bearing °F |
| 017 | 61 |  |  |  |  |  |  |  |  |  |  |
|  |  | 31 | 40,140 | 1.60 | 1220 | 277 | 14.8 | - | - | - | - |
|  |  | 92 | 42,072 | 1.68 | 1685 | 278 | 14.6 | - | - | - | - |
| [illegible]<br>b | Start attempts | - | 0 - 40,000 | - | 1600 | 250 | 14 | - | - | - | - |
| 019 &<br>019-b | Start Attempts |  | 0 - 40,000 | - | 1600 | 250 | 14 | - | - | - | - |
| 019-c | 756 |  |  |  |  |  |  |  |  |  |  |
|  |  | 31 | 40,108 | 1.60 | 1575 | 270 | 14.2 | - | 11.7 | 11.7 | 17.6 |
|  |  | 672 | 40,364 | 1.61 | 2860 | 270 | 14.0 | - | 14.3 | 15.1 | 22.6 |
|  |  | 787 | 40,210 | 1.61 | 1720 | 270 | 14.0 | - | 14.3 | 12.6 | 23.2 |

**NOTES:** 1 Duration at full RPM

2 Time from turbine start to data point.

108 series bearings

Axial load shared by tandem bearing set.

Summar

| | Propellant (A-50) | | Rise of Outer Race Temperature | | | |
|---|---|---|---|---|---|---|
| ial | Flow gpm | Temp Rise °F | Ball Bearing °F | Ball Bearing °F | Roller Bearing °F | Remarks |
| | | | | | | Ball bearing set, K-5-H balls, 440C races, fully shrouded 25% glass filled Teflon cages, inner race riding with radial cuts on guiding surface. Spherical seat roller bearing from test 16 ,installed aligned. |
| | 14.8 | - | - | - | - | Steady state |
| | 14.6 | - | - | - | - | Steady state prior to shutdown due to loss of speed signal. Bearings not inspected. |
| | | | | | | Retest of bearings installed prior to test 16.. |
| | 14 | - | - | - | - | Problems with speed signal equipment. |
| | | | | | | Retest of bearings installed prior to test 16. |
| | 14 | - | - | - | - | Problems with speed signal equipment.. |
| | | | | | | Retest of bearings installed prior to Test 16. |
| | 14.2 | - | 11.7 | 11.7 | 17.6 | Steady state |
| | 14.0 | - | 14.3 | 15.1 | 22.6 | Axial load peak (over 2500 lb for 27 sec) |
| | 14.0 | - | 14.3 | 12.6 | 23.2 | Steady state prior to scheduled shutdown. |
| | | | | | | Bearings inspected and in excellent condition. Work Statement objectives met for 40,000 rpm AeroZINE 50 operation of ball bearings. |

Summary of 40,000 and 31,250 rpm Bearing Tests in AeroZINE 50

Figure IV-52, Sheet 3 of 3

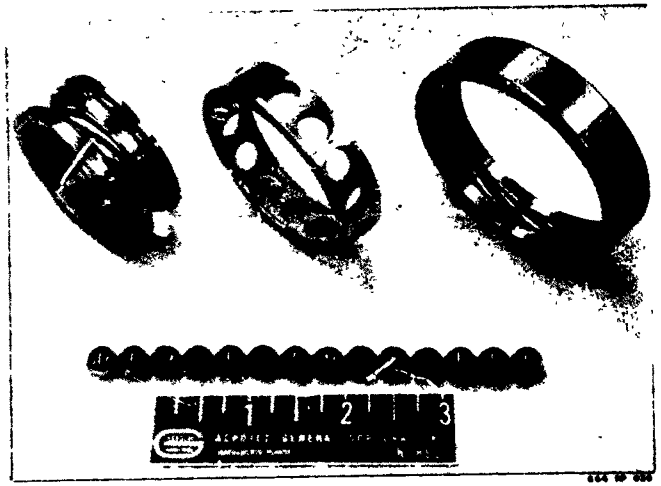

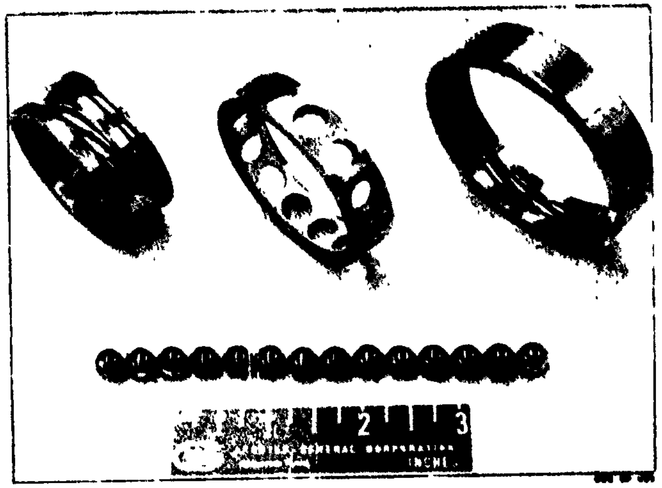

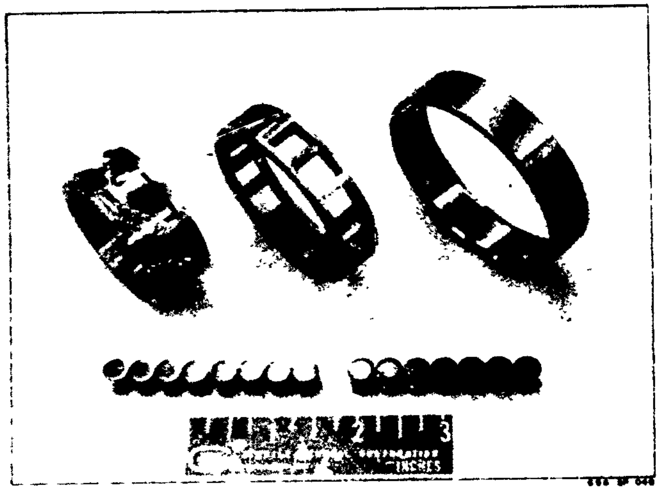

SPEED: 31,250

DURATION: 418 sec, 6 min. 58 sec.

| | LOAD | DURATION |
|---|---|---|
| AXIAL, NOMINAL: | 2890 lbs | 398 sec. |
| PEAK: | 4650 lbs | 20 sec. |
| RADIAL, NOMINAL: | 600 lbs | 403 sec. |
| PEAK: | 1115 lbs | 15 sec. |

31,250 rpm Posttest Bearings--AeroZINE 50 Lubricated

Figure IV-53

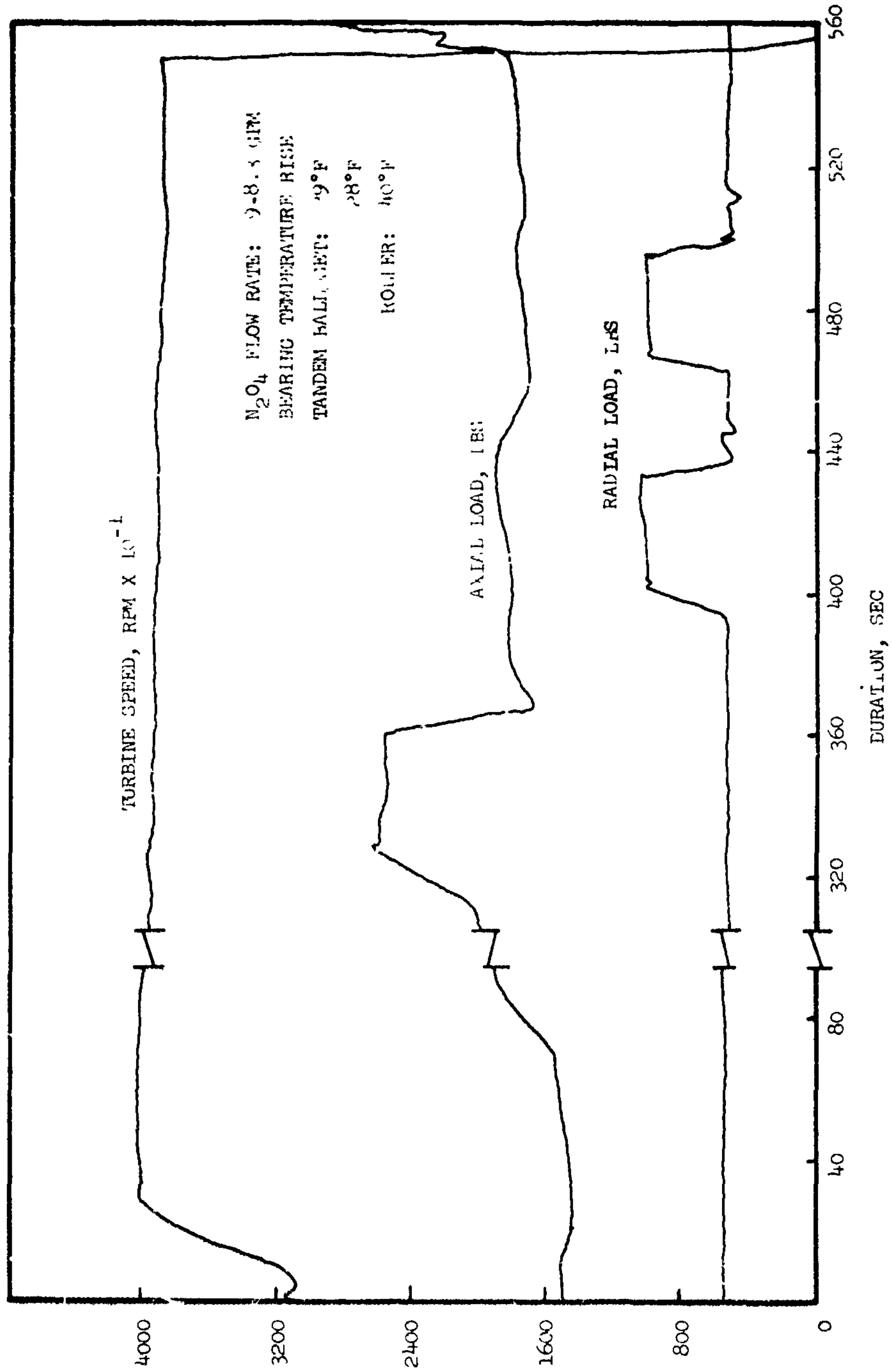

Test Data Plot--40,000 rpm $N_2O_4$ Lubricated Bearing Test 1.2-03-WAW-006B

Figure IV-54

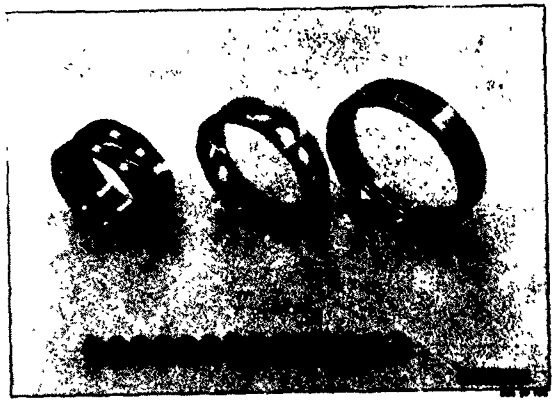

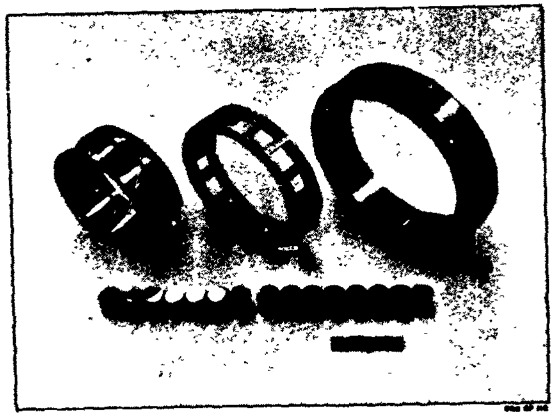

SPEED: 38,900 RPM
DURATION: 791 sec, 13 min. 11 sec.

| | LOAD | DURATION |
|---|---|---|
| AXIAL, NOMINAL: | 1500 + lbs | 739 sec. |
| PEAK. | 2500 + lbs | 52 sec. |
| RADIAL, NOMINAL: | 500 lbs | 759 sec. |
| PEAK: | 1000 lbs | 32 sec. |

40,000 rpm Posttest Bearings--$N_2O_4$ Lubricated

Figure IV-55

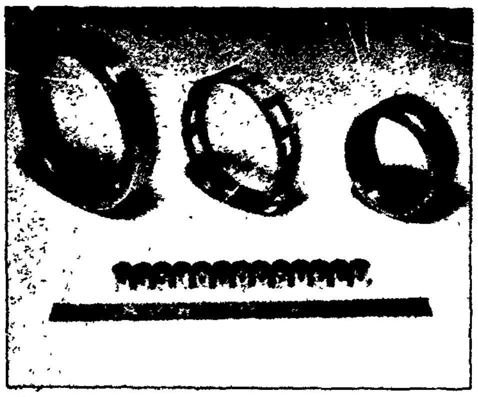

SPEED: . . . . . . . . . . . . 40,000 RPM
DURATION: . . . . 735 sec, 12 min 15 sec.

|  | LOAD | DURATION |
|---|---|---|
| RAD NOMINAL: | 550 lbs | 708 sec. |
| PEAK: | 1070 lbs | 27 sec. |

ARES ROLLER BEARING FROM A-50 TESTS
1.2-03-WAW-012,-013,-014 & -015

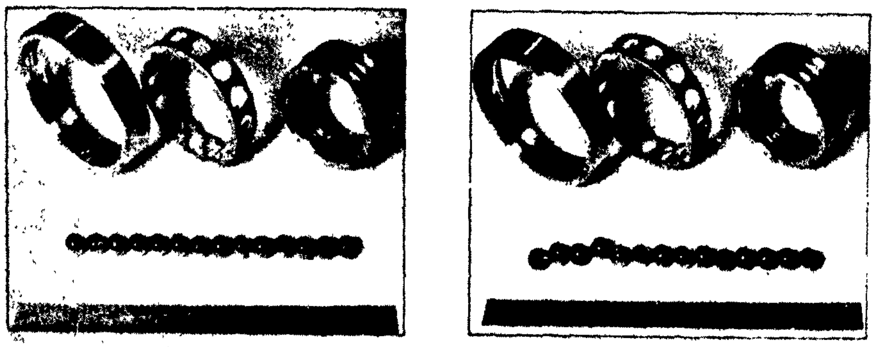

SPEED: . . . . . . . . . . . . . . . 40,000 RPM
DURATION: . . . . . . . . . 755 sec, 12 min, 35 sec

|  | LOAD | DURATION |
|---|---|---|
| AXIAL, NOMINAL: | 1700 lbs | 728 sec |
| PEAK: | 2700 lbs | 27 sec |

ARES TANDEM BALL SET FROM A-50 TEST 1.2-03-WAW-019C

40,000 rpm Posttest Bearings--AeroZINE 50 Lubricated

Figure IV-56

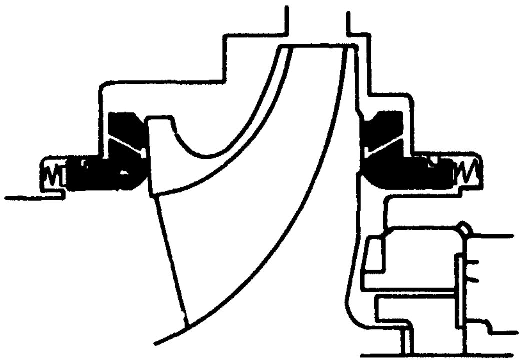

OXIDIZER IMPELLER WITH HYDROSTATIC FACE SEALS

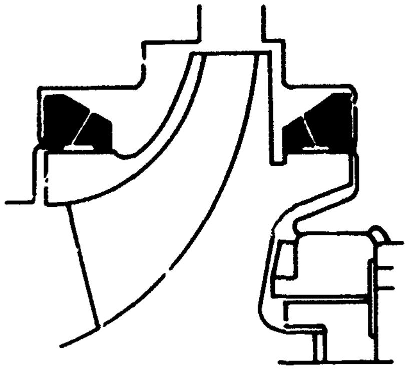

OXIDIZER IMPELLER WITH HYDROSTATIC JOURNAL SEALS

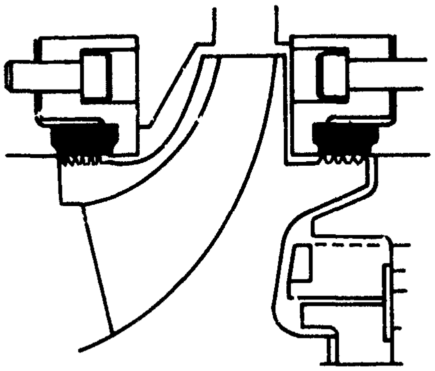

OXIDIZER PUMP WITH DOVETAIL PLASTIC INSERT LABYRINTH SEALS

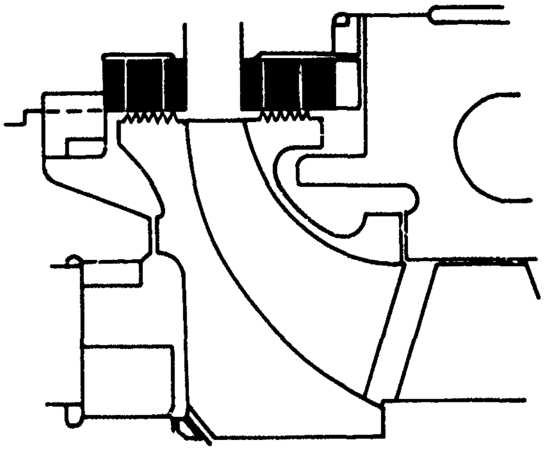

FUEL PUMP WITH PRESSURE RELIEVED PLASTIC INSERT LABYRINTH SEALS

Wear-Ring Configurations Selected for Propellant Testing

Figure IV-57

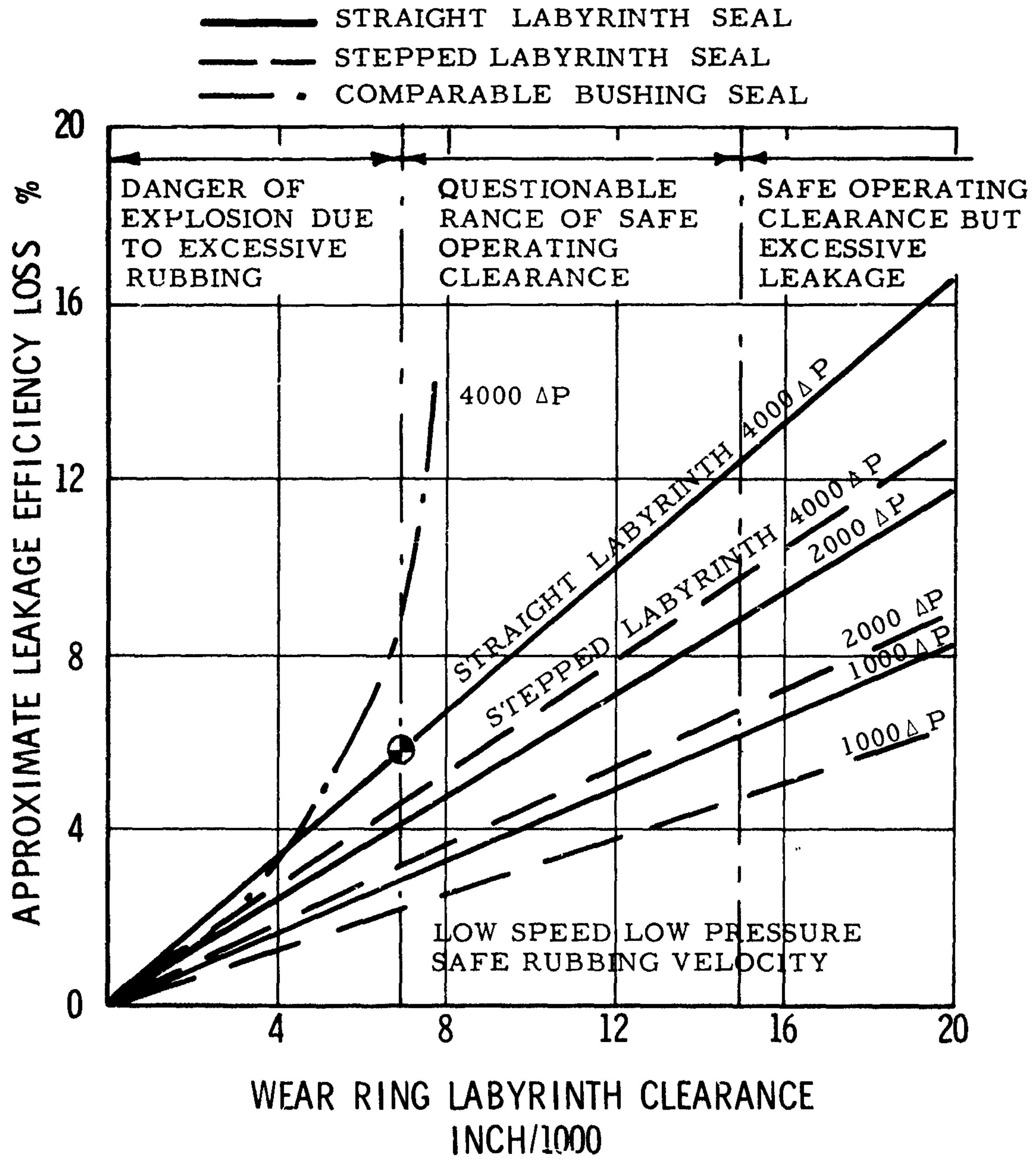

Oxidizer-Pump Efficiency Loss as a Function of Wear-Ring Radial Clearance

Figure IV-58

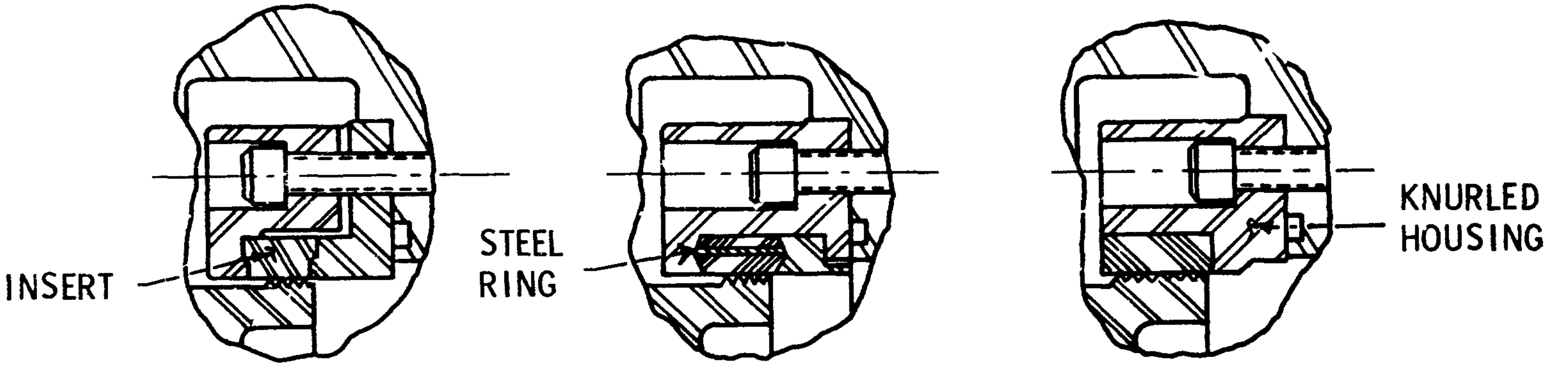
INSERT
STEEL RING
KNURLED HOUSING

DOVETAIL INSERT  REINFORCED DOVETAIL INSERT  KNURLED RETAINED

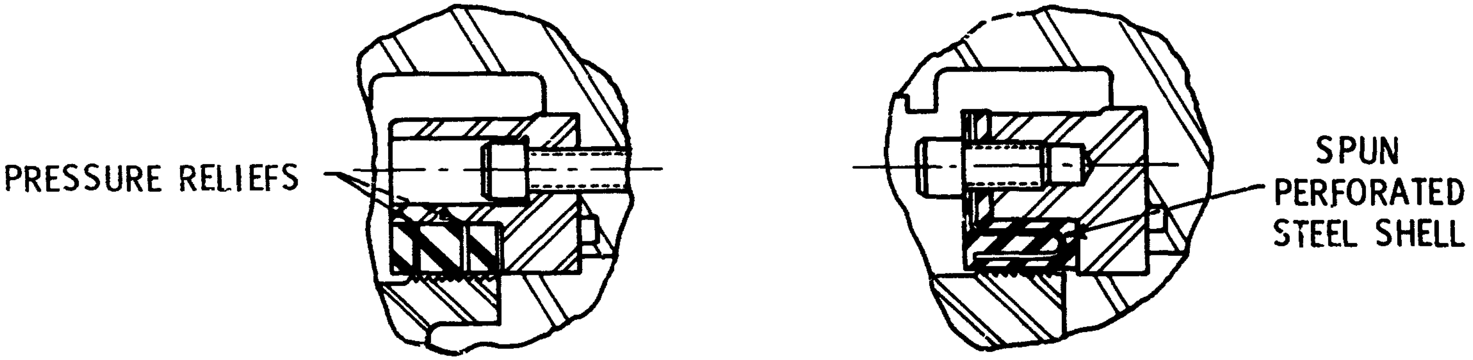
PRESSURE RELIEFS
SPUN PERFORATED STEEL SHELL

PRESSURE RELIEVED INSERT  SHELL REINFORCED INSERT

Retention Mechanisms for Straight-Labyrinth Inert Inserts

Figure IV-59

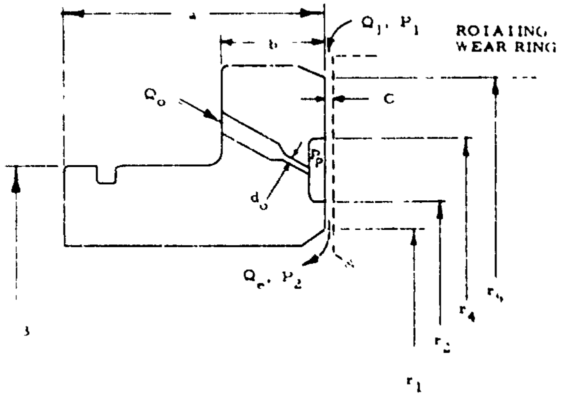

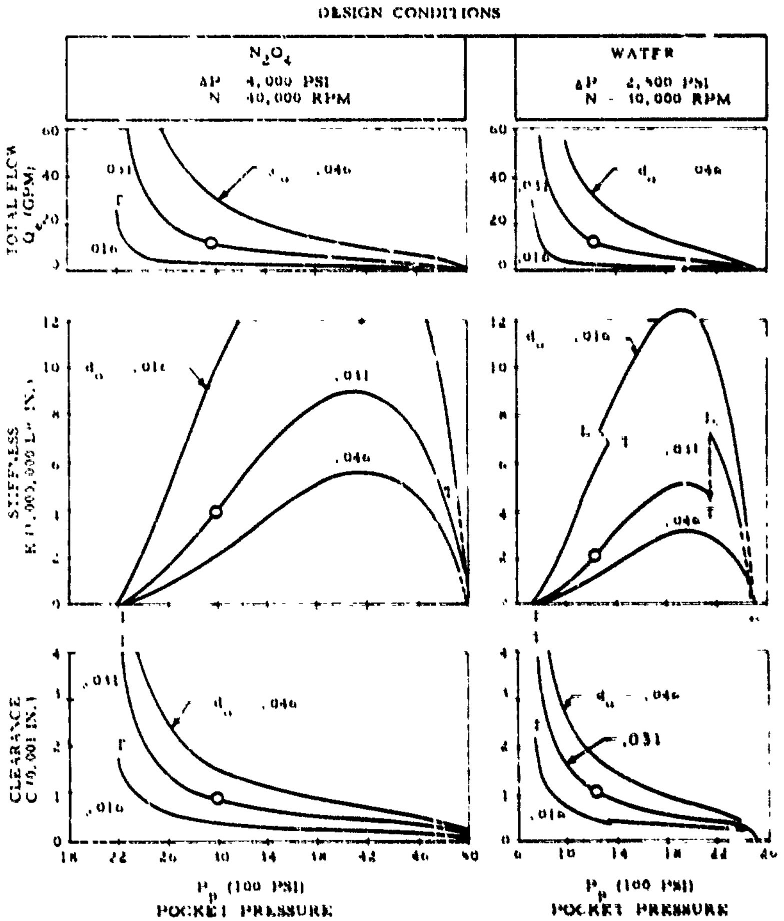

**SEAL GEOMETRY**

$r_1$ = 1.66 IN.
$r_2$ - 1.71 IN.
$r_3$ - 1.78 IN.
$r_4$ - 1.83 IN
$r_5$ - 1.96 IN.
a 0.750 IN.
b 0.300 IN.
$d_o$ 0.031 IN (DESIGN)

**NOMENCLATURE**

| | |
|---|---|
| $Q_1$ | HIGH PRESSURE LAND FLOW |
| $Q_o$ | ORIFICE FLOW |
| $Q_e$ | TOTAL SEAL FLOW |
| $P_1$ | UPSTREAM PRESSURE |
| $P_p$ | POCKET PRESSURE |
| $P_2$ | DOWNSTREAM PRESSURE |
| ΔP | $P_1 - P_2$ |
| C | OPERATING CLEARANCE |
| K | STIFFNESS |
| N | RPM |

**NOTES**

1) ◆ ON CURVE DENOTES DESIGN POINT.
2) T AND L DENOTE TURBULENT OR LAMINAR FLOW.
3) NUMBER AND $C_d$ OF ORIFICES IS 8 AND 0.82

Design Parameters of the Hydrostatic Face Wear-Ring Seal

Figure IV-60

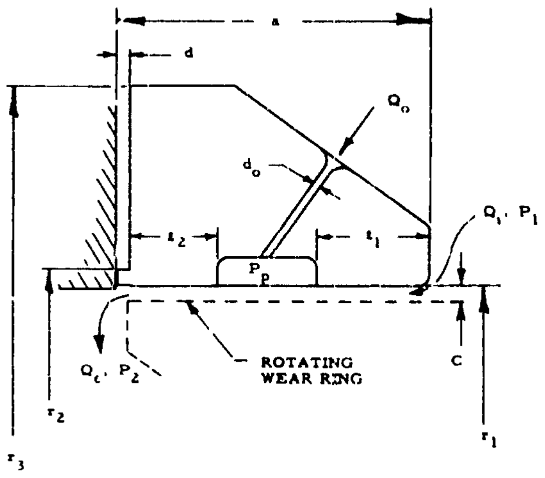

DESIGN CONDITIONS:

WATER
2500 PSI ΔP
0 AND 30,000 RPM
- - - 0 RPM
—— 30,000 RPM

NOTES:

1) SEAL HAS EIGHT ORIFICES
2) ORIFICE Cd = 0.65

SEAL GEOMETRY

$d_o$ = 0.039 IN. (EIGHT PLACES)
$r_1$ = 2.0035 IN.
$r_2$ = 2.020 IN
$r_3$ = 2.400 IN.
$t_1$ = 0.100 IN.
$t_2$ = 0.130 IN.
d = 0.010 IN.
a = 0.530 IN.

NOMENCLATURE

$Q_i$ = HIGH PRESSURE LAND FLOW
$Q_o$ = ORIFICE FLOW
$Q_e$ = TOTAL SEAL FLOW
$P_1$ = UPSTREAM PRESSURE
$P_p$ = POCKET PRESSURE
$P_2$ = DOWNSTREAM PRESSURE
ΔP = $P_1 - P_2$
C = OPERATING CLEARANCE
K = STIFFNESS
N = ROTATIONAL SPEED
ε = ECCENTRICITY RATIO
W = RESTORING FORCE

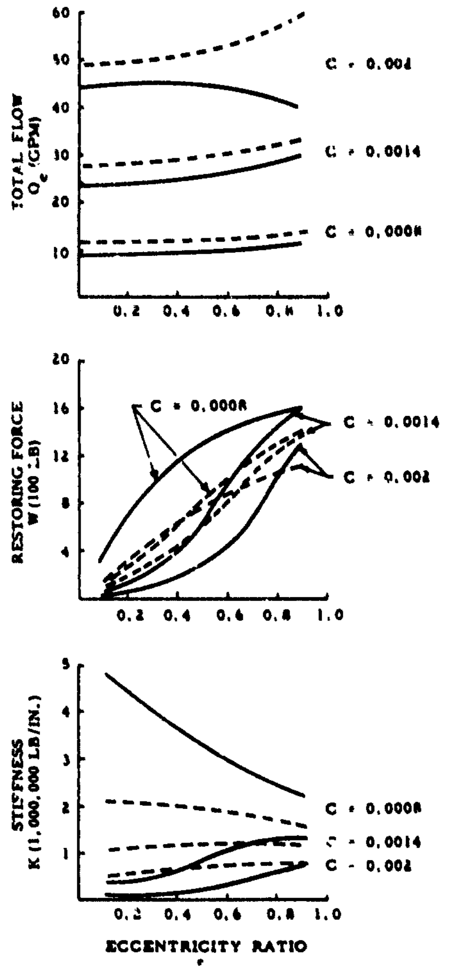

Design Parameters of the Hydrostatic Journal Wear-Ring Seal

Figure IV-61

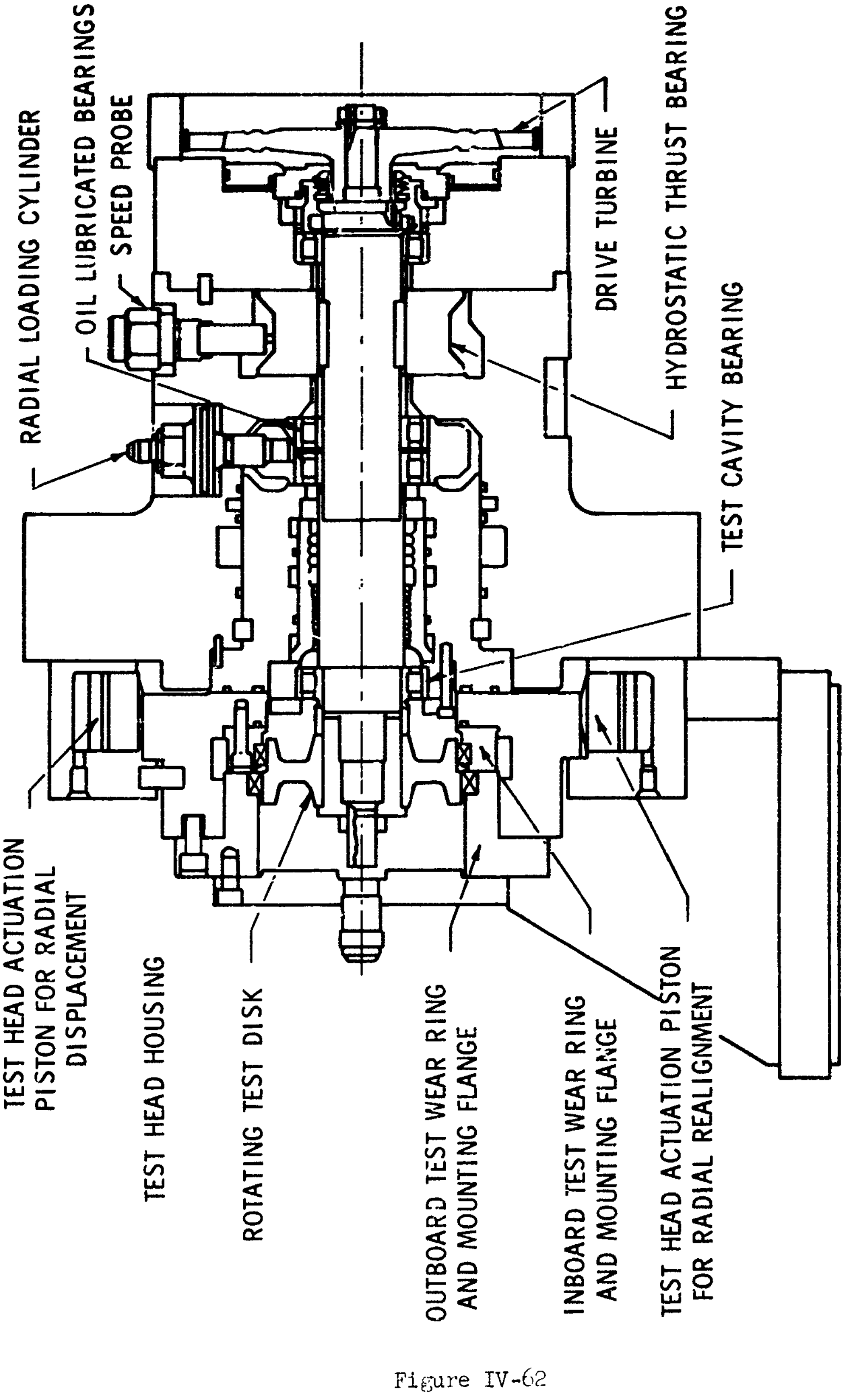
RADIAL LOADING CYLINDER
OIL LUBRICATED BEARINGS
SPEED PROBE
DRIVE TURBINE
HYDROSTATIC THRUST BEARING
TEST CAVITY BEARING
TEST HEAD ACTUATION PISTON FOR RADIAL DISPLACEMENT
TEST HEAD HOUSING
ROTATING TEST DISK
OUTBOARD TEST WEAR RING AND MOUNTING FLANGE
INBOARD TEST WEAR RING AND MOUNTING FLANGE
TEST HEAD ACTUATION PISTON FOR RADIAL REALIGNMENT

Wear-Ring Tester

Figure IV-62

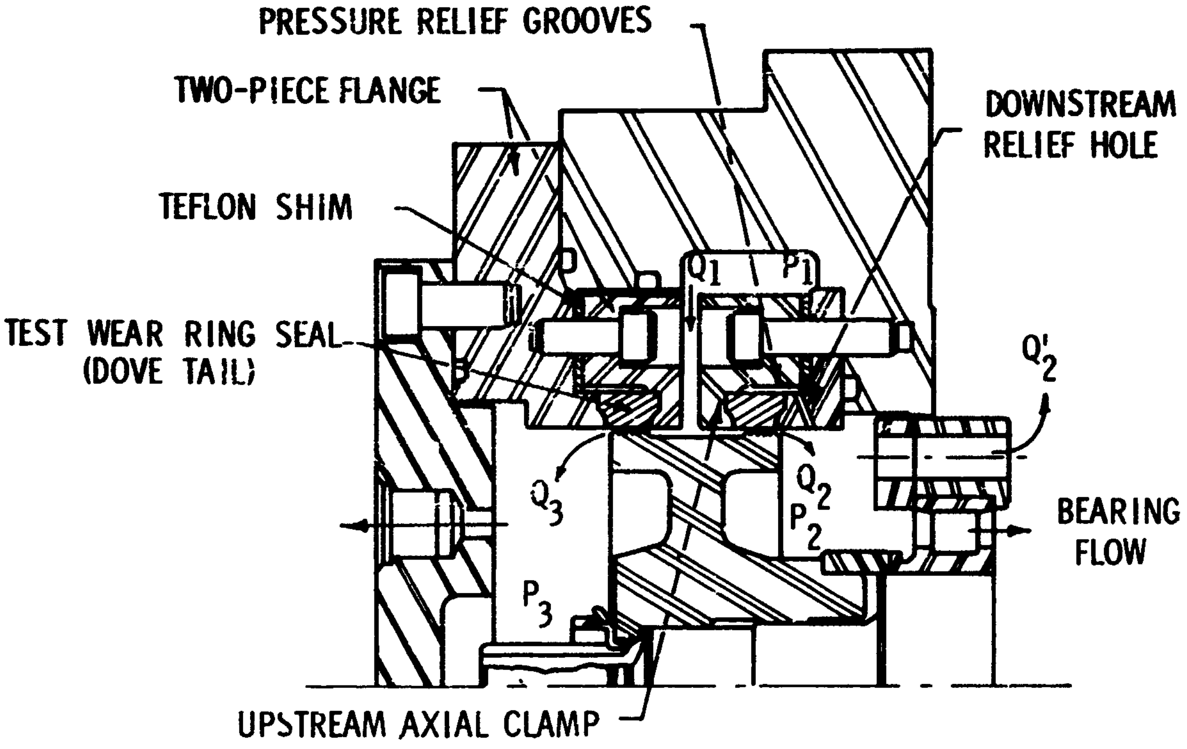
PRESSURE RELIEF GROOVES
TWO-PIECE FLANGE
DOWNSTREAM RELIEF HOLE
TEFLON SHIM
Q1
P1
TEST WEAR RING SEAL (DOVE TAIL)
Q'2
Q'3
Q2
P2
BEARING FLOW
P3
UPSTREAM AXIAL CLAMP

$Q_1$ = TOTAL INLET FLOW

$Q_2$ = INBOARD SEAL FLOW

$Q_2 - Q_2'$ = BEARING FLOW

$Q_3$ = OUTBOARD SEAL FLOW

$P_1$ = SUPPLY PRESSURE

$P_2$ = INBOARD SEAL DOWNSTREAM PRESSURE

$P_3$ = OUTBOARD SEAL DOWNSTREAM PRESSURE

Typical Wear-Ring Test Installation and Nomenclature

Figure IV-63

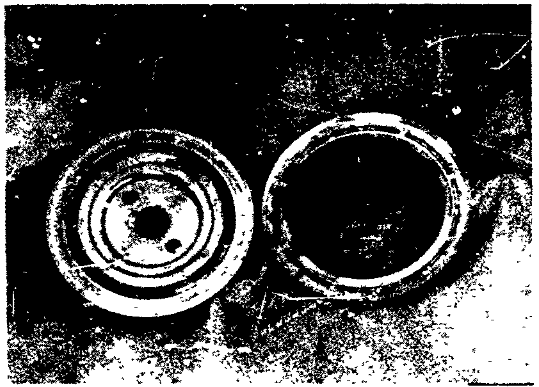

AXIAL FACE HYDROSTATIC

| | |
|---|---|
| SHAFT SPEED, RPM | 40,170 |
| WEAR RING FLOW, GPM | 19.62 |
| ΔP ACROSS SEAL, PSI | 4,072 |
| NOMINAL OPERATING CLEARANCE, IN. | .0013 |
| DEMONSTRATED AXIAL MOVEMENT, IN. | .007<br>(.002 IN. IN .2 SEC) |
| DRY RUBBING | 15,000 RPM FOR 6 SEC |

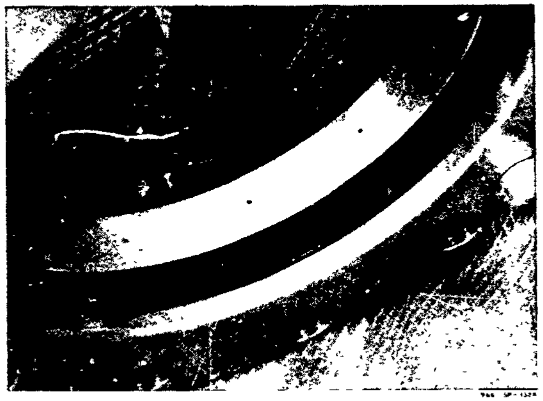

VESPEL SP-21

| | |
|---|---|
| SHAFT SPEED, RPM | 40,170 |
| WEAR RING FLOW, GPM | 38.9 |
| ΔP ACROSS SEAL, PSI | 4,072 |
| RADIAL CLEARANCE, IN. | .005 |
| AMOUNT OF RUB, IN. | .0032 |

$N_2O_4$ Wear-Ring Test Summary--Hydrostatic Face Seal and Vespel SP-21 Labyrinth Insert

Figure IV-64

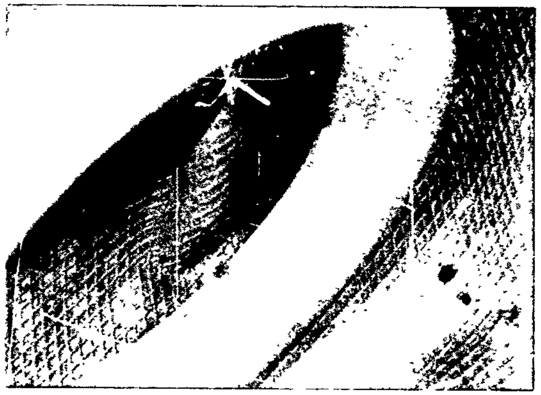

KYNAR

| | |
|---|---|
| SHAFT SPEED, RPM | 35,200 |
| WEAR RING FLOW, GPM | 34.0 |
| ΔP ACROSS SEAL, PSI | 2,264 |
| RADIAL CLEARANCE, IN. | .006 |
| AMOUNT OF RUB, IN. | .0098 |

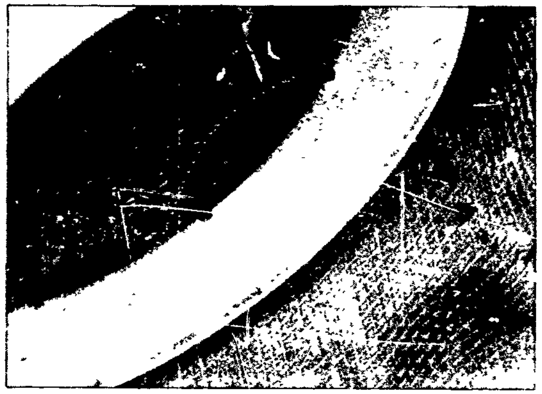

KEL-F

| | |
|---|---|
| SHAFT SPEED, RPM | 35,200 |
| WEAR RING FLOW, GPM | 32.00 |
| ΔP ACROSS SEAL, PSI | 2,258 |
| RADIAL CLEARANCE, IN. | .005 |
| AMOUNT OF RUB, IN. | .0108 |

AeroZINE 50 Wear-Ring Test Summary-Kynar and Kel-F Labyrinth Inserts

Figure IV-65

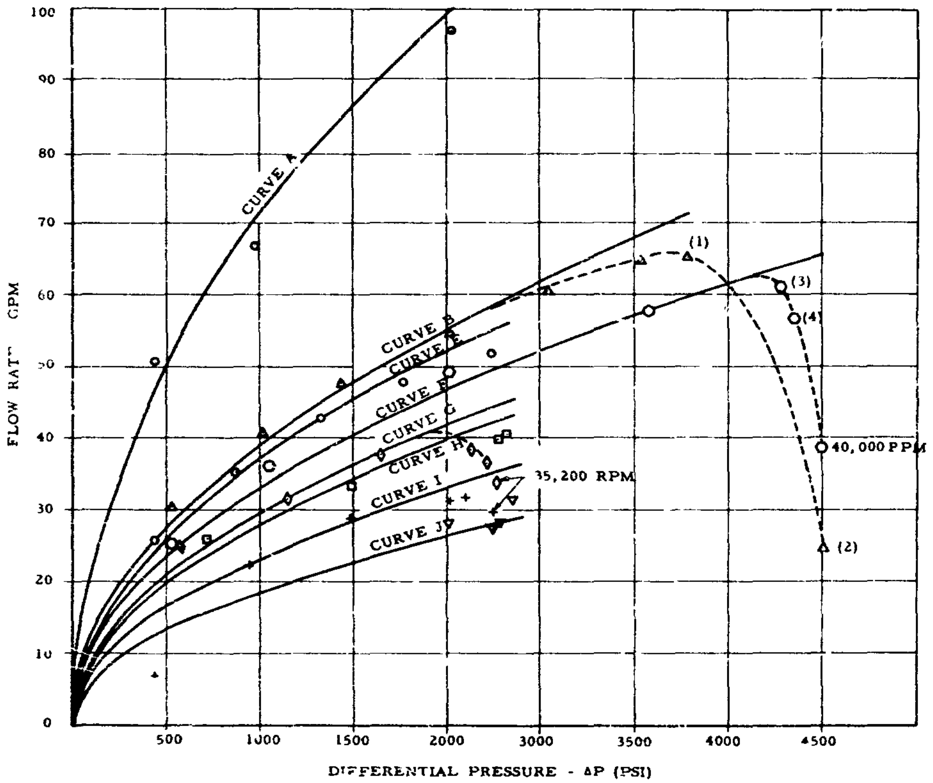

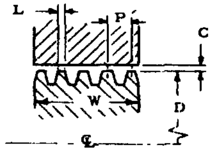

— — CALCULATED MEAN OF TEST DATA

SYMBOLS REPRESENT TEST DATA POINTS

○ METAL LABYRINTH (WATER)
△ GLASS CERAMIC FILLED TEFLON ($N_2O_4$)
□ VESPEL SP-1 (WATER)
⬡ VESPEL SP-21 ($N_2O_4$)
▽ GLASS CERAMIC FILLED TEFLON (WATER)
◇ KYNAR (A-50)
+ KEL-F (A-50)

LABYRINTH GEOMETRY

| CURVE | A | B | E | F | G | H | I | J |
|---|---|---|---|---|---|---|---|---|
| D | 3 997 | 3.580 | 3.997 | 3.580 | 3.580 | 3.580 | 3.580 | 3 580 |
| C | 0095 | 0055 | .0061 | 005 | .006 | .0046 | .005 | 0035 |
| P | .050 | 050 | 050 | .050 | .100 | 050 | .056 | 050 |
| L | 0075 | .0075 | 0075 | 0075 | .0075 | .0075 | 0075 | .0075 |
| NO. OF TEETH | 11 | 6 | 11 | 6 | 5 | 6 | 8 | 6 |
| W | .550 | .300 | 550 | 300 | .515 | 300 | .518 | .300 |
| AVG Cd | 831 | 1 08 | .864 | 996 | .664 | .755 | 662 | .547 |
| TEST FLUID | WATER | $N_2O_4$ | WATER | $N_2O_4$ | A-50 | WATER | A-50 | WATER |

(1) AFTER 5.5 SEC
(2) AFTER 8.2 SEC
(3) AFTER 2.5 SEC
(4) AFTER 17.0 SEC AND HOLDING STEADY

Water-Flow Data from Nonrotating and Rotating Straight-Labyrinth Tests

Figure IV-66

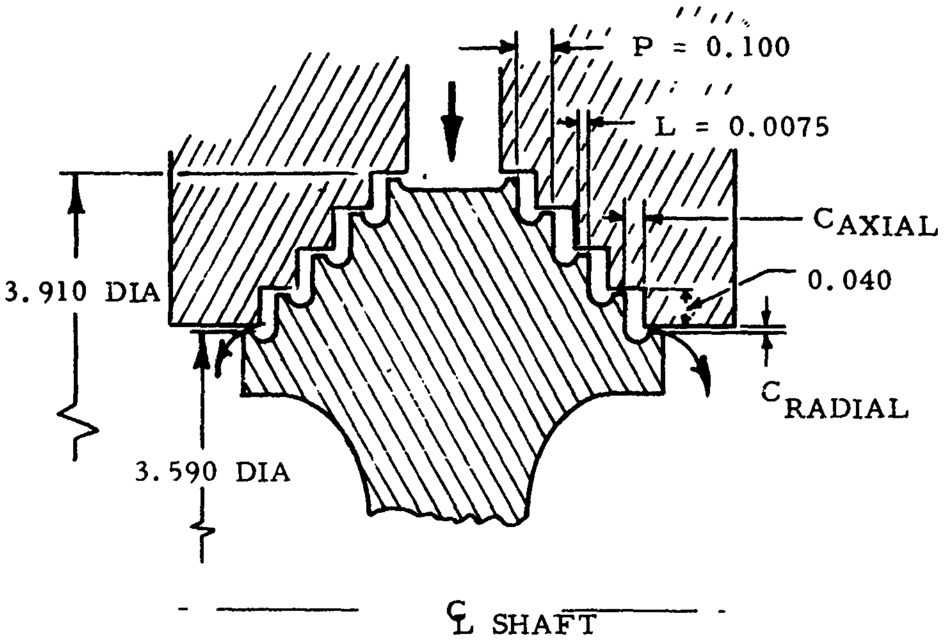
P = 0.100
L = 0.0075
C AXIAL
0.040
C RADIAL
3.910 DIA
3.590 DIA
℄ SHAFT

| TEST DATA POINT | NUMBER OF TEETH | $C_{AXIAL}$ | $C_{RADIAL}$ | ΔP (PSI) | Q (GPM) |
|---|---|---|---|---|---|
| 1 | 5 | .050 | .0055 | 1179 | 26.5 |
| 2 | 5 | .050 | .0055 | 1276 | 30.0 |
| 3 | 5 | .050 | 0055 | 2388 | 39.0 |
| 4 | 5 | .050 | .0097 | 1185 | 41.4 |
| 5 | 5 | .050 | .0097 | 1273 | 41.0 |
| 6 | 5 | .050 | .0097 | 2352 | 55.2 |
| 7 | 5 | .012 | .0055 | 2310 | 35.36 |
| 8 | 5 | .022 | .0097 | 2269 | 63.65 |

Stepped-Labyrinth Water-Flow Data

Figure IV-67

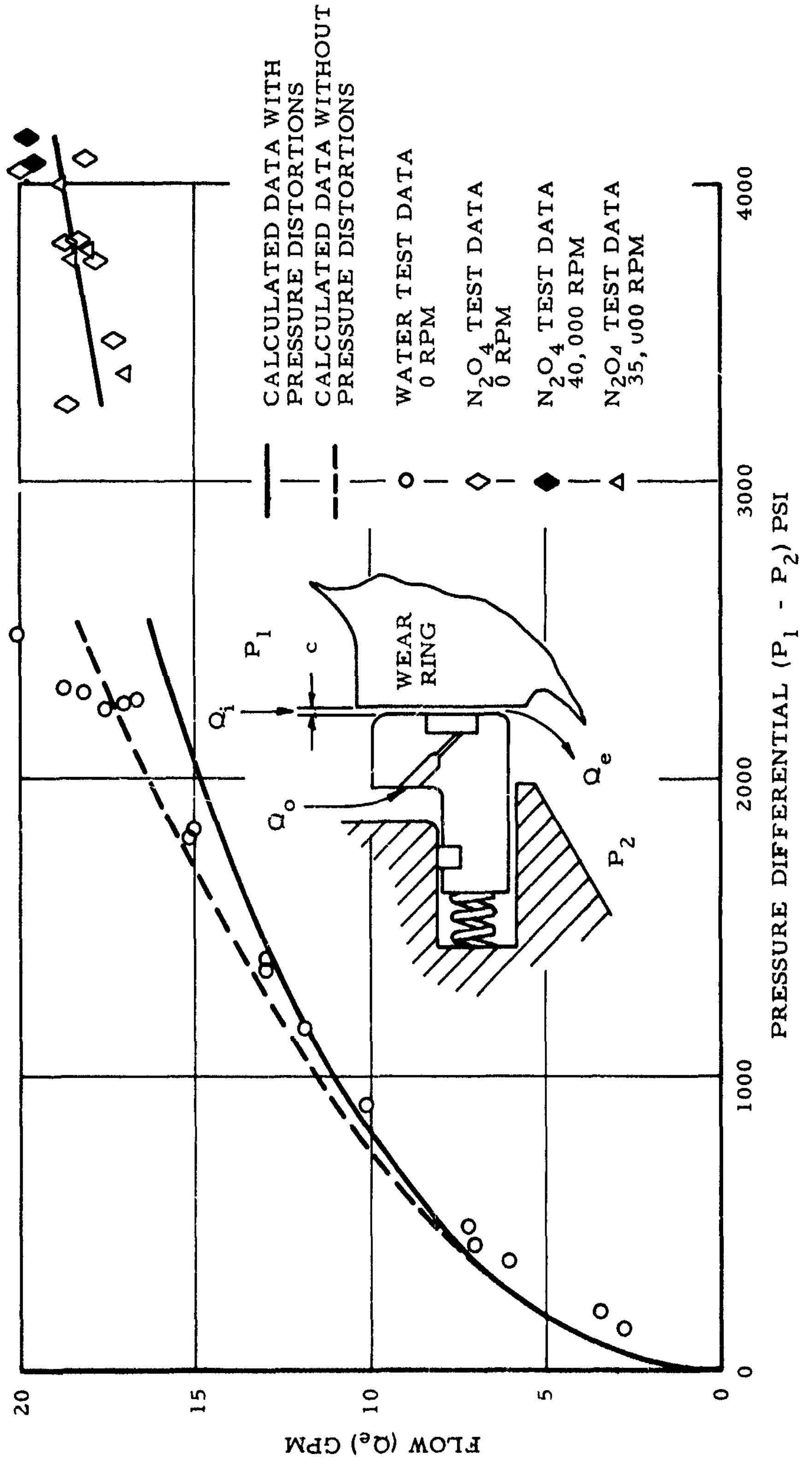

Water and $N_2O_4$ Flow Data for Hydrostatic Face Seal with Correlation with Estimated Flows

Figure IV-68

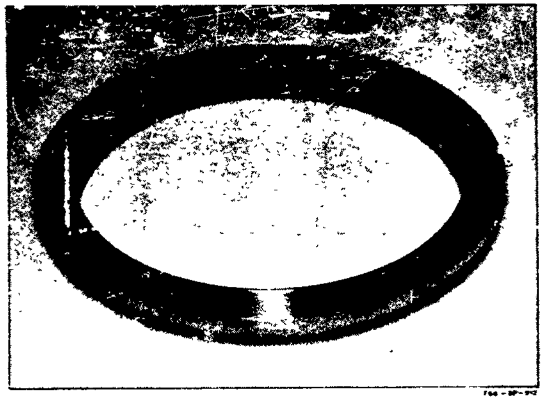

HYDROSTATIC JOURNAL SEAL

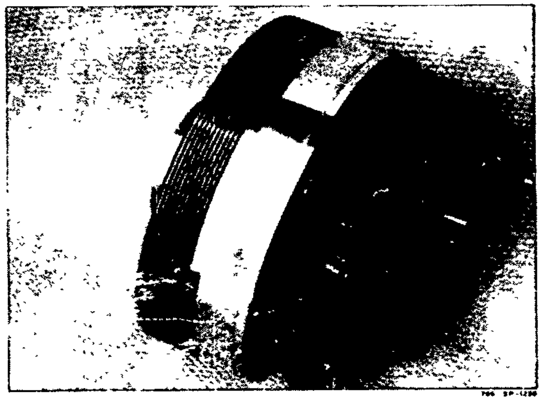

| | |
|---|---|
| SHAFT SPEED, RPM | 25,000 |
| WEAR RING FLOW, GPM | 20.10 |
| ΔP ACROSS SEAL, PSI | 2365 |
| RADIAL CLEARANCE, IN. | .0025 |
| TOTAL NUMBER OF TESTS | 10 |
| TRANSIENT TESTS | 4 |

( ROTATION TO 5000 RPM BEFORE SEAL LIFT OFF. APPROXIMATE 50 REVOLUTIONS RUBBING / TRANSIENT )

Posttest Photograph of Hydrostatic Journal Seal and Water-Test Data

Figure IV-69

HYDROSTATIC JOURNAL SEAL NONROTATING
FLOW AS A FUNCTION OF PRESSURE DIFFERENTIAL

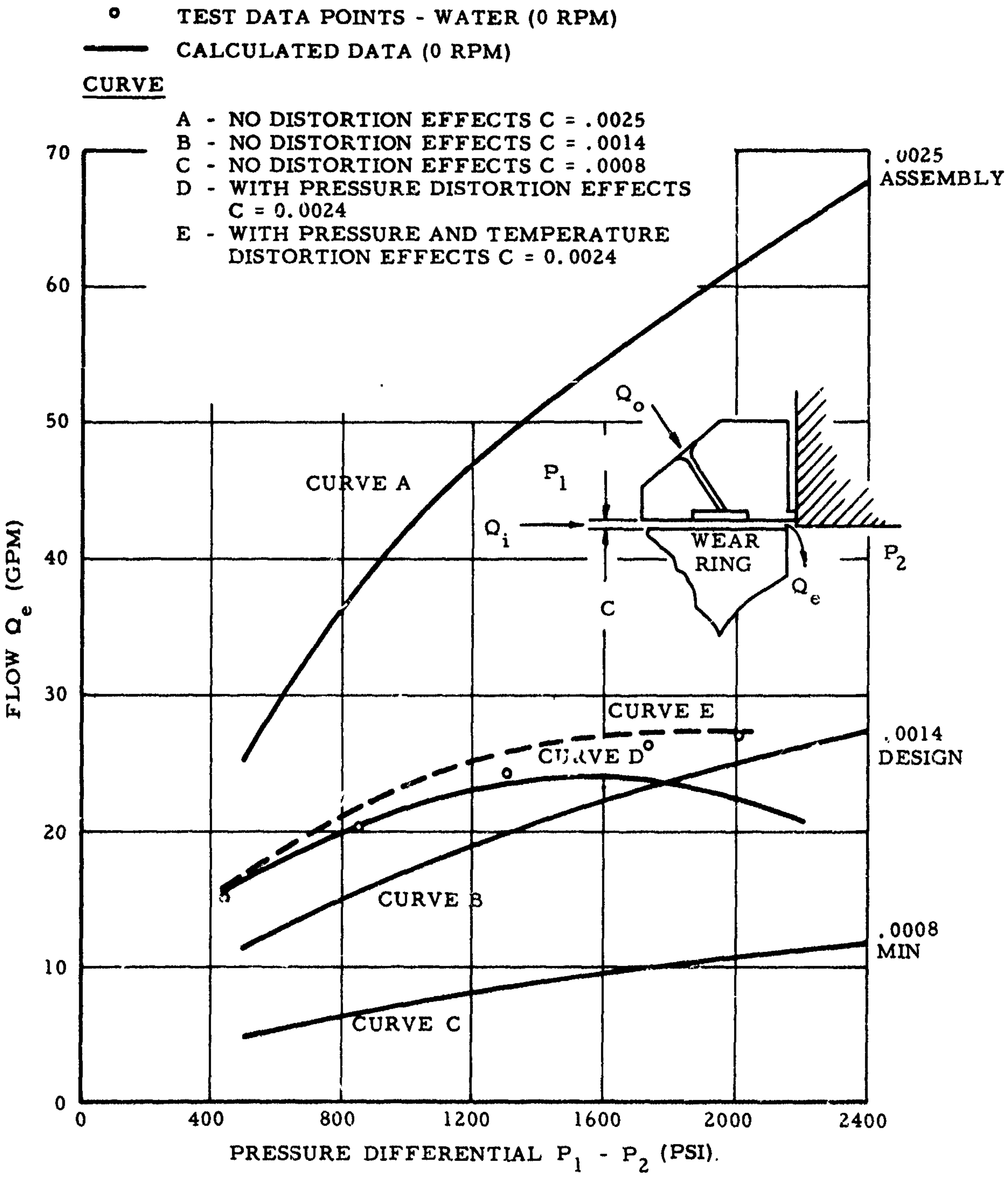

Water-Flow Data for Hydrostatic Journal Seal Correlated with Estimated Flows

Figure IV-70

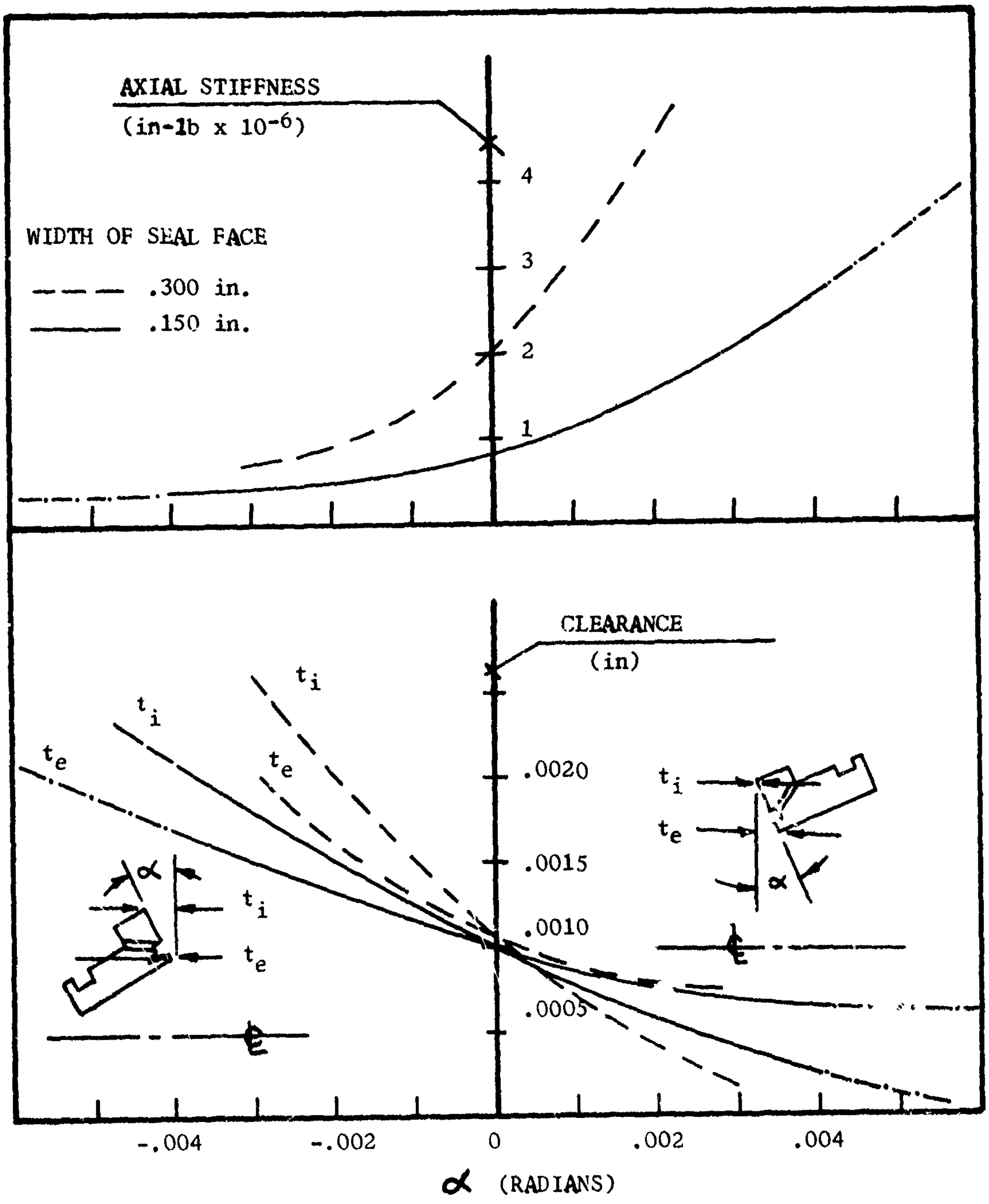

Stiffness and Clearance of Hydrostatic Face Seal
as a Function of Impeller Angular Deflections

Figure IV-71

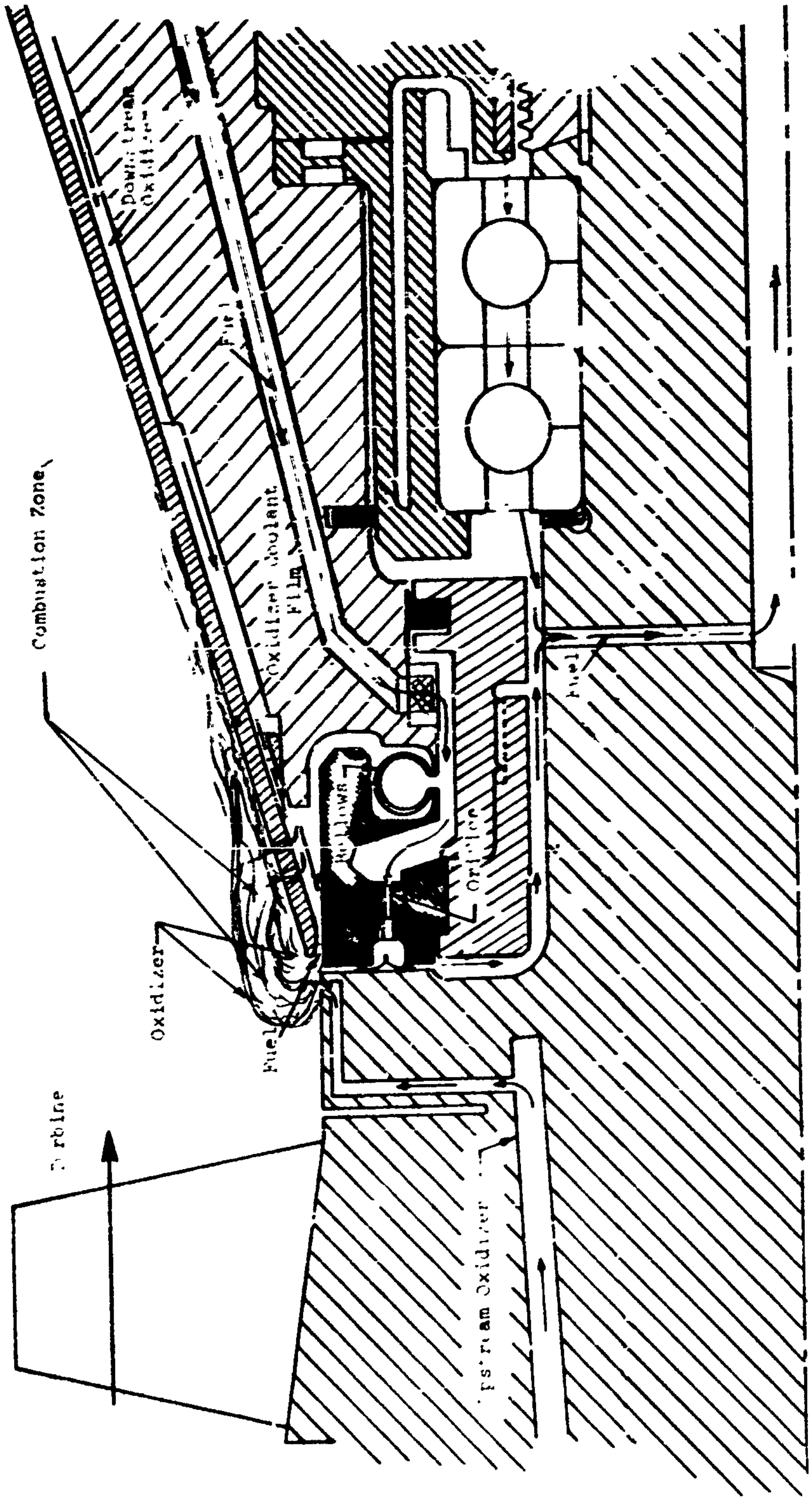
Combustion Zone
Downstream Oxidizer
Fuel
Oxidizer Coolant Film
Bellows
Orifice
Oxidizer
Fuel
Fuel
Turbine
Upstream Oxidizer

Combustion Concept of Seal (u)

Figure IV-72

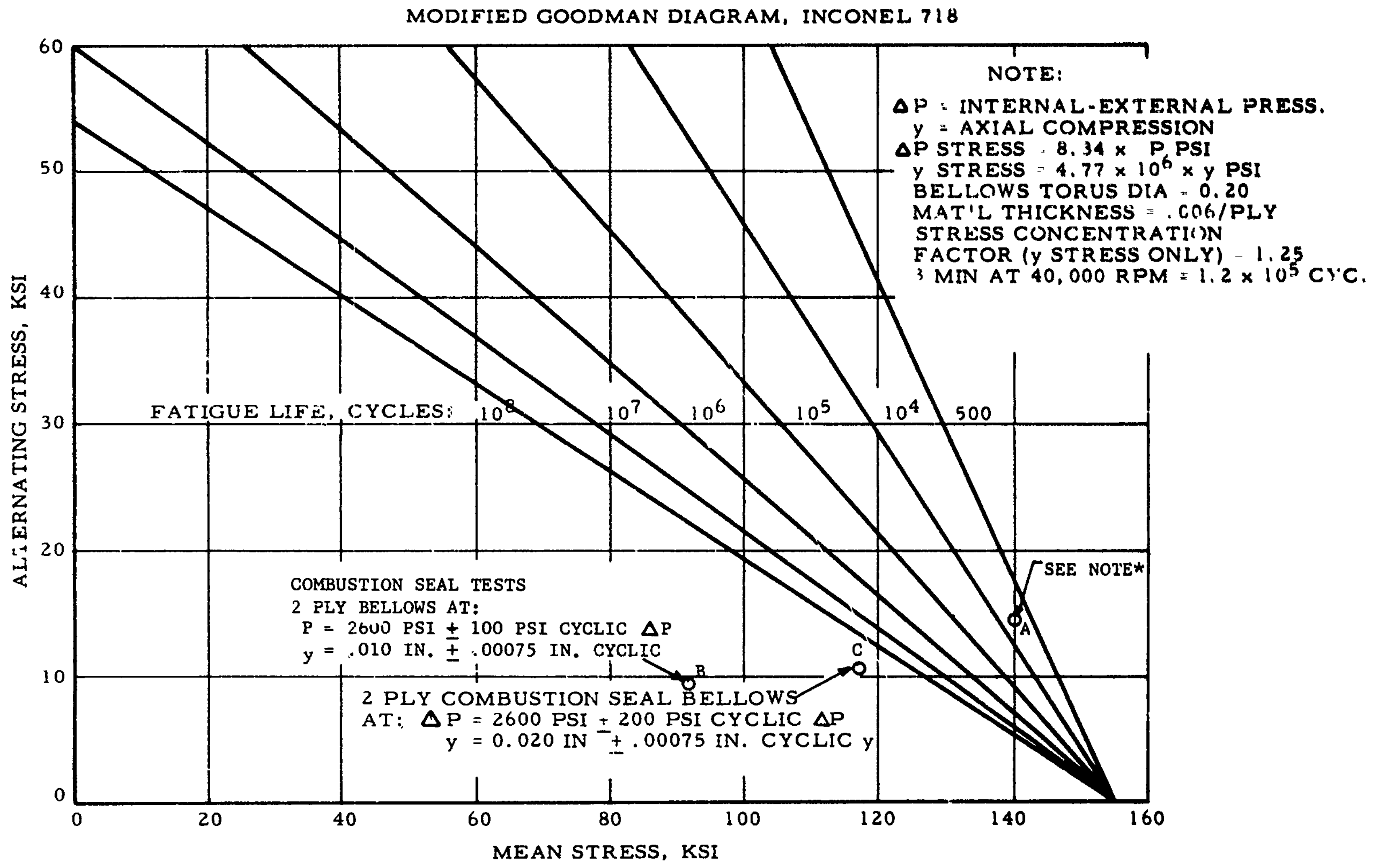

NOTE:

ΔP = INTERNAL-EXTERNAL PRESS.
y = AXIAL COMPRESSION
ΔP STRESS = 8.34 × P PSI
y STRESS = $4.77 \times 10^6 \times y$ PSI
BELLOWS TORUS DIA = 0.20
MAT'L THICKNESS = .006/PLY
STRESS CONCENTRATION FACTOR (y STRESS ONLY) = 1.25
3 MIN AT 40,000 RPM = $1.2 \times 10^5$ CYC.

COMBUSTION SEAL TESTS
2 PLY BELLOWS AT:
P = 2600 PSI ± 100 PSI CYCLIC ΔP
y = .010 IN. ± .00075 IN. CYCLIC

2 PLY COMBUSTION SEAL BELLOWS
AT: ΔP = 2600 PSI ± 200 PSI CYCLIC ΔP
y = 0.020 IN ± .00075 IN. CYCLIC y

* PROBABLE STRESS LEVEL DURING TEST 11 (SINGLE PLY BELLOWS)
CORRESPONDING CYCLIC y = ± .001", CYCLIC P = ± 100 PSI

Bellow Stresses under Operative Condition

Figure IV-73

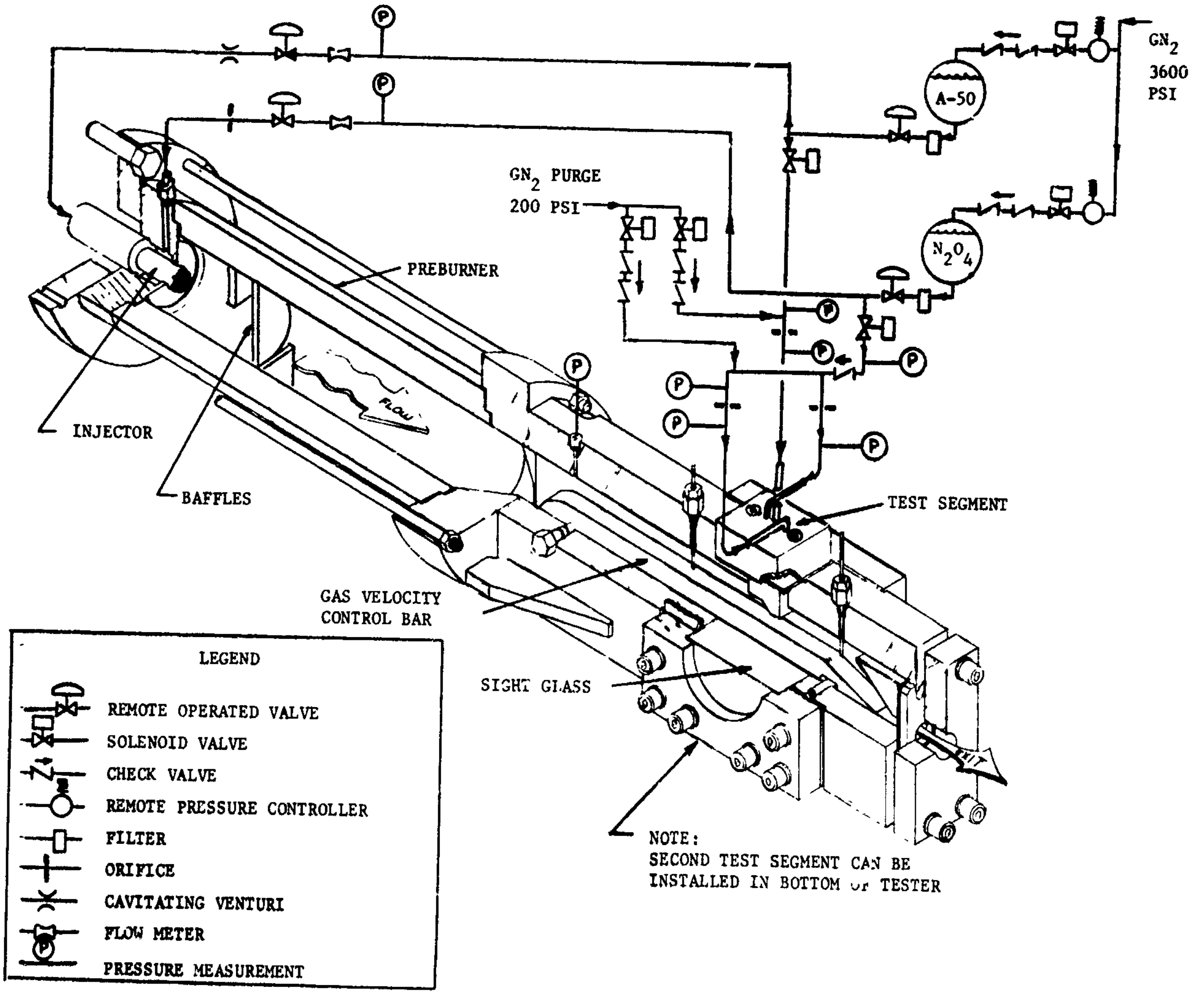
GN2
3600
PSI
A-50
GN2 PURGE
200 PSI
N2O4
PREBURNER
FLOW
INJECTOR
BAFFLES
TEST SEGMENT
GAS VELOCITY
CONTROL BAR
SIGHT GLASS
EXIT
NOTE:
SECOND TEST SEGMENT CAN BE
INSTALLED IN BOTTOM OF TESTER
LEGEND
REMOTE OPERATED VALVE
SOLENOID VALVE
CHECK VALVE
REMOTE PRESSURE CONTROLLER
FILTER
ORIFICE
CAVITATING VENTURI
FLOW METER
PRESSURE MEASUREMENT
P

2-D Seal Tester and Flow Diagram

Figure IV-74a

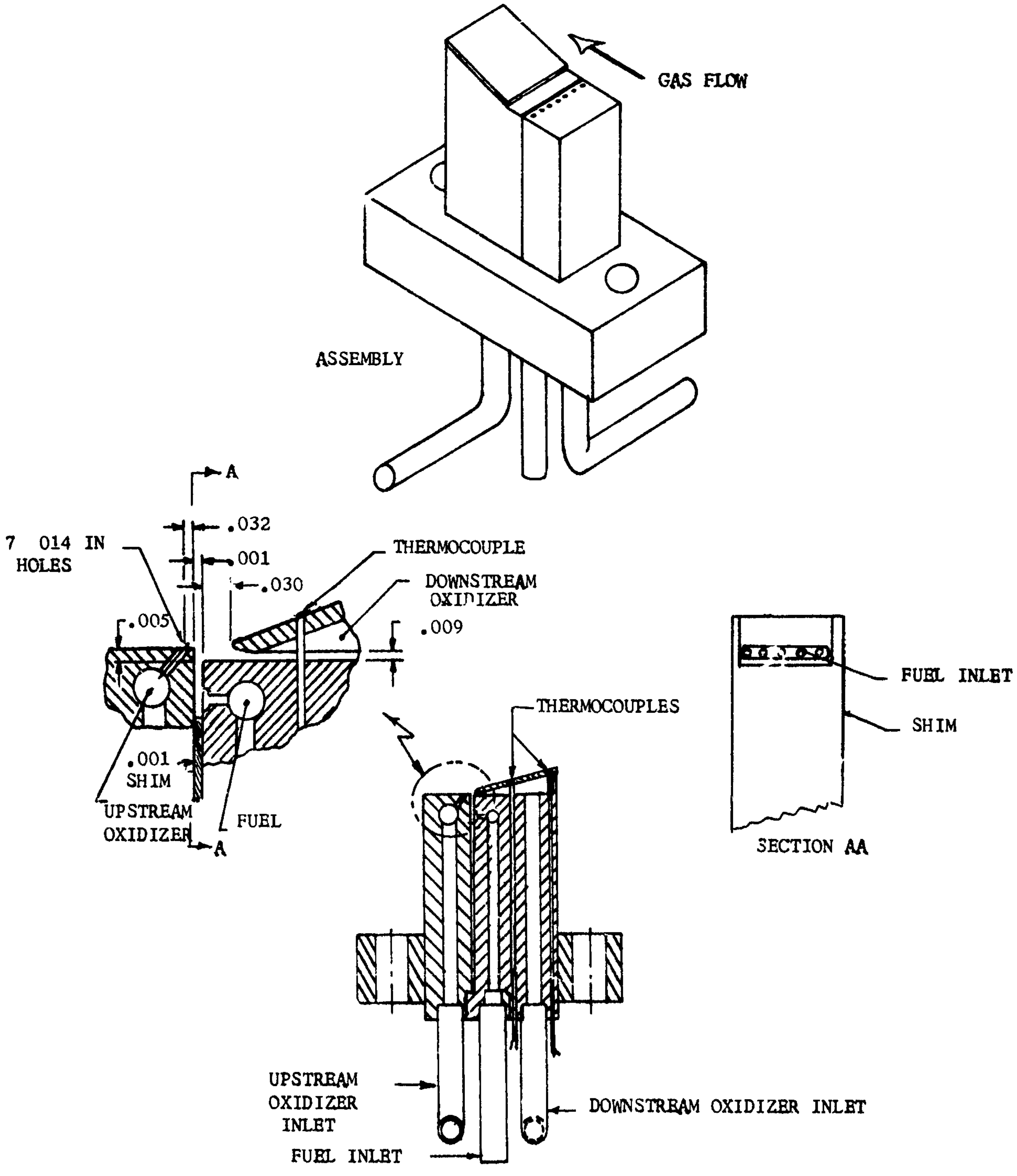
GAS FLOW
ASSEMBLY
A
.032
7 014 IN HOLES
.001
.030
THERMOCOUPLE
DOWNSTREAM OXIDIZER
.005
.009
.001 SHIM
UPSTREAM OXIDIZER
FUEL
A
THERMOCOUPLES
FUEL INLET
SHIM
SECTION AA
UPSTREAM OXIDIZER INLET
FUEL INLET
DOWNSTREAM OXIDIZER INLET
CROSS SECTION

2D Test Segment

Figure IV-74b

| Test | Seal-Segment Type and Serial No. | Propellant Flow lb/sec (Test Flows Extrapolated to Representative Full-Scale Seal Flows) | | | Segment MR | Combustion at Segment Duration Sec | 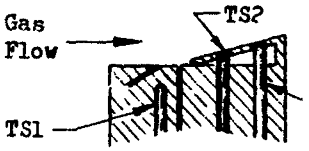<br>Seg. Temp | | |
|---|---|---|---|---|---|---|---|---|---|
| | | Fuel, A-50 | Oxidizer, $N_2O_4$ | | | | TS 1*** °F | TS 2**** °F | TS 3 °F |
| | | | Upstr. | Downstr. | | | | | |
| 24 | A-3, #1 | - | 1.75 | 3.50 | - | 1.7 | 273 | 122 | 15 |
| 25 | " | - | 0.89 | 3.71 | - | 1.6 | 220 | 121 | 15 |
| 26 | " | - | 0.93 | 2.22 | - | 1.6 | 246 | 160 | 20 |
| 27 | A-3, #1 | 0.093 | 1.82 | 2.96 | 51.5 | 3.4 | 404 | 145 | 16 |
| 28 | A-3, #3 | 0.218*<br>0.064** | 1.78 | 2.21 | 18.3*<br>62.3** | 1.5*<br>8.5** | 200 | 150 | 19 |
| 29A | A-3, #3 | 0.267*<br>0.036** | 1.82 | 2.07 | 14.6*<br>10.8** | 1.2*<br>8.8** | 220 | 145 | 19 |
| 29B | A-3, #3 | 0.268*<br>0.054** | 1.82 | 2.32 | 15.4*<br>76.6** | 1.0*<br>9.0** | 360 | 170 | 210 |
| 30 | A-3, #3 | 0.303*<br>0.089** | 1.71 | 2.32 | 13.3*<br>45.3** | 1.2*<br>8.8** | 380 | 170 | 215 |

*condition after preburner start before increase in fuel gap resistance.

**condition after fuel gap resistance adjusted to a higher stable level.

***maximum reached at end of test - thermal steady state not reached.

****maximum reached during thermal steady state.

| 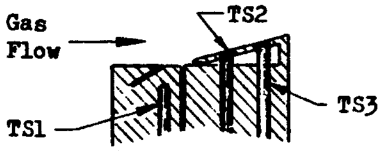 <br>Seg. Temp | | | Preburner Gas Conditions | | | Remarks |
|---|---|---|---|---|---|---|
| TS 1*** °F | TS 2**** °F | TS 3**** °F | Press., psia | Temp (Av), °F | Velocity ft/sec | |
| 273 | 122 | 152 | 1000 | 1150 | 300 | No apparent fuel flow at segment. Thermal expansion closed fuel slot. Test was terminated before all purge fluid was expelled. |
| 220 | 121 | 151 | 995 | 1150 | 300 | |
| 246 | 160 | 200 | 990 | 1150 | 300 | |
| 404 | 145 | 169 | 995 | 1150 | 300 | Intermittent fuel flow |
| 200 | 150 | 190 | 980 | 1130 | 300 | Reduction in fuel flow in all tests attributed to thermal expansion closing fuel slot. |
| 220 | 145 | 190 | 980 | 1130 | 300 | Segment fired and visually noted approx. 2.5 sec prior to preburner start. Procedure previous to these tests was to lag segment start after preburner. Fuel flow observed to decrease as soon as preburner temperature heated segment, causing slot to close. |
| 360 | 170 | 210 | 970 | 1130 | 300 | |
| 380 | 170 | 215 | 970 | 1130 | 300 | |

2-D Test Summary

Figure IV-75

2

UNCLASSIFIED

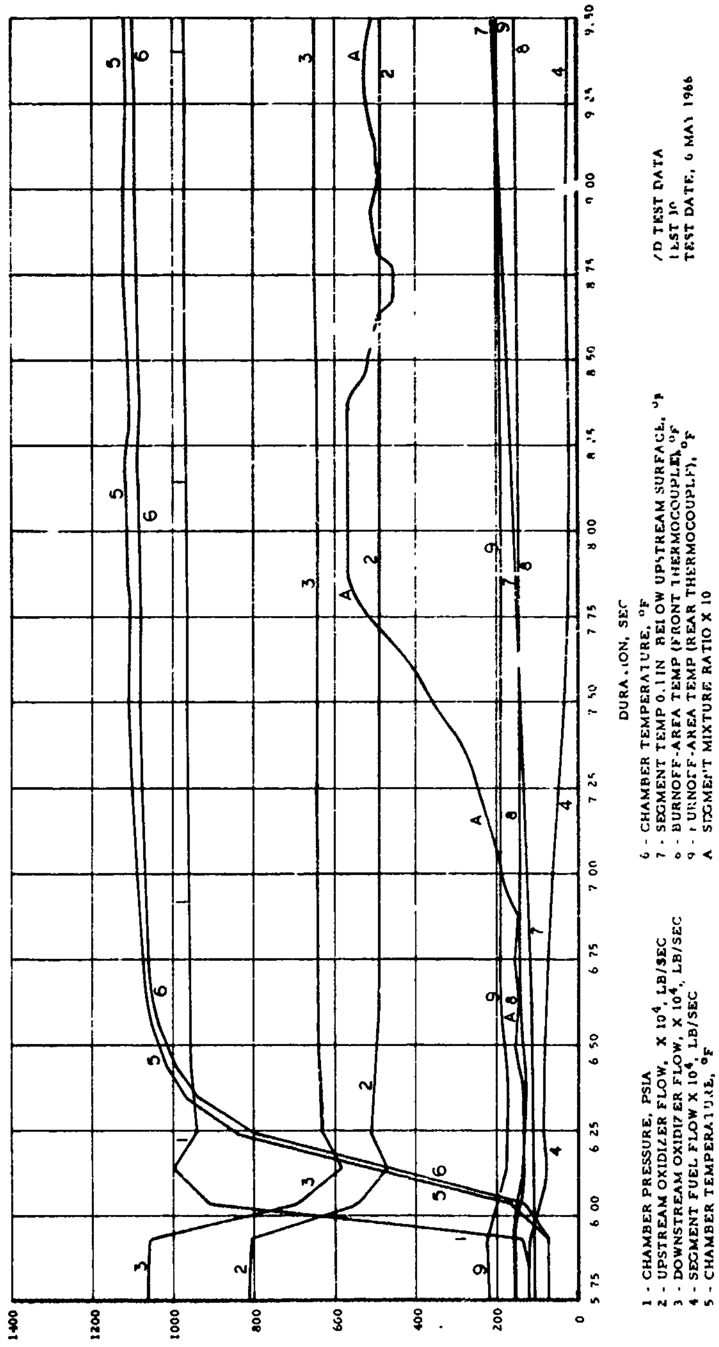

2-D Test Dat--Test 030

Figure IV-76

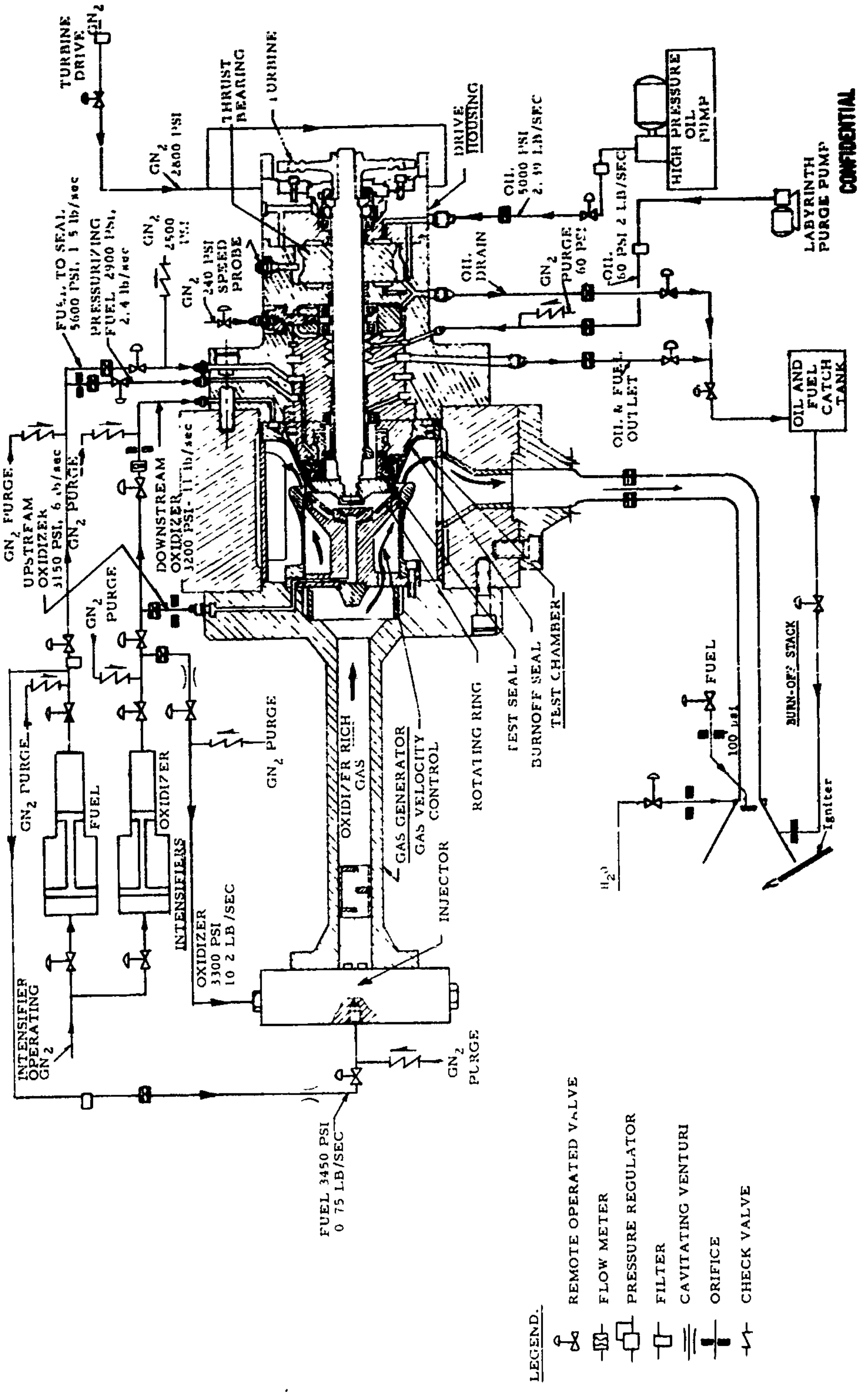
TURBINE DRIVE
$GN_2$
$GN_2$ 2800 PSI
THRUST BEARING
TURBINE
DRIVE HOUSING
OIL 5000 PSI 2.19 LB/SEC
HIGH PRESSURE OIL PUMP
CONFIDENTIAL
FUEL TO SEAL 5600 PSI, 1.5 lb/sec
PRESSURIZING FUEL 4900 PSI, 2.4 lb/sec
$GN_2$ 2500 PSI
$GN_2$ 240 PSI
SPEED PROBE
OIL DRAIN
$GN_2$ PURGE 60 PSI
OIL 60 PSI 2 LB/SEC
LABYRINTH PURGE PUMP
OIL & FUEL OUTLET
OIL AND FUEL CATCH TANK
$GN_2$ PURGE
UPSTREAM OXIDIZER 3150 PSI, 6 lb/sec
$GN_2$ PURGE
DOWNSTREAM OXIDIZER 3200 PSI - 11 lb/sec
$GN_2$ PURGE
OXIDIZER RICH GAS
GAS GENERATOR
GAS VELOCITY CONTROL
ROTATING RING
TEST SEAL
BURNOFF SEAL
TEST CHAMBER
BURN-OFF STACK
FUEL
100 psi
Igniter
$H_2O$
$GN_2$ PURGE
FUEL
OXIDIZER
$GN_2$ PURGE
INTENSIFIERS
OXIDIZER 3300 PSI 10.2 LB/SEC
INJECTOR
INTENSIFIER OPERATING $GN_2$
$GN_2$ PURGE
FUEL 3450 PSI 0.75 LB/SEC
LEGEND
REMOTE OPERATED VALVE
FLOW METER
PRESSURE REGULATOR
FILTER
CAVITATING VENTURI
ORIFICE
CHECK VALVE

Flow Diagram, Hot Tests (u)

Figure IV-77

| TEST NO. | 1966 | ROTATING TIME SECONDS | SPEED RPM | RAMP TIME SEC | CHAMBER PRESSURE PSI | SEAL FUEL FLOWS LB/SEC |  | COMMENTS |
|---|---|---|---|---|---|---|---|---|
|  |  |  |  |  |  | TOTAL | OUTFLOW |  |
| TESTS 1-6 WERE USED FOR SEQUENCE CHECKOUT AND FUEL FLOW CALIBRATION. |  |  |  |  |  |  |  | PROBLEM OF PRESSURE REVERSAL AT BELLOWS WAS CORRECTED. |
| 7 | 6-3 | 2 | 23,000 | 34 | 3100 | 0.936 | 0.225 | SPEED PROBE MALFUNCTION CAUSED OVERSPEED SHUTDOWN. |
| 8 | 6-3 | 4 | 28,000 | 24 | 3130 | 0.76 | 0.045 | FAILURE OF PRESSURIZING FULL CAUSED SEAL TO CLOSE WHILE ROTATING, WELDING FACES TOGETHER. |
| 9 | 6-10 | 0 | 0 | 24 | 3100 | 0 | 0 | FUEL VALVE FAILED TO OPEN. NO DAMAGE. VALVE WAS REBUILT. |
| 10A | 6-15 | 0 | 0 | 24 | 3100 | 1.30 | 0.17 | INTENSIFIER OVERPRESSURE INTERLOCK STOPPED TEST BEFORE ROTATION. READJUSTED SYSTEM. |
| 10B | 6-16 | 5.5 | 30,000 | 24 | 3100 | 1.24 | 0.30 | SHUTDOWN BECAUSE SPEED SIGNAL DID NOT TRANSMIT. ADDED SECOND SPEED SYSTEM. |
| 11 | 6-17 | [illegible] | 39,400 | 24 | 3200 | 1.30 | 0.27 | USED SEAL WITH 200 PSI ΔP POCKET-TO-CHAMBER. 60 SEC AT 38,000 + RPM NO FACE CONTACT. 0.0076 IN. FACE CLEARANCE. SEAL O.K. TEST SUCCESSFUL. EXCEPT SPEED SLIGHTLY LOW. RESIZED TURBINE NOZZLES. |
| 12 | 6-24 | 78 | 40,000 | 27 | 3200 | 2.14 | 0.43 | USED SEAL WITH 500 PSI ΔP POCKET-TO-CHAMBER, AND INCREASED CLEARANCE TO 0.001 IN. TO AVOID THERMAL DISTORTION EXPERIENCED IN 2D TESTS. 63 SEC AT 40,000 RPM. NO FACE CONTACT. SEAL O.K TEST COMPLETELY SUCCESSFUL. ALL OBJECTIVES REACHED. |

CONFIDENTIAL

Cold Rotating Test Summary (u)

Figure IV-78

CONFIDENTIAL

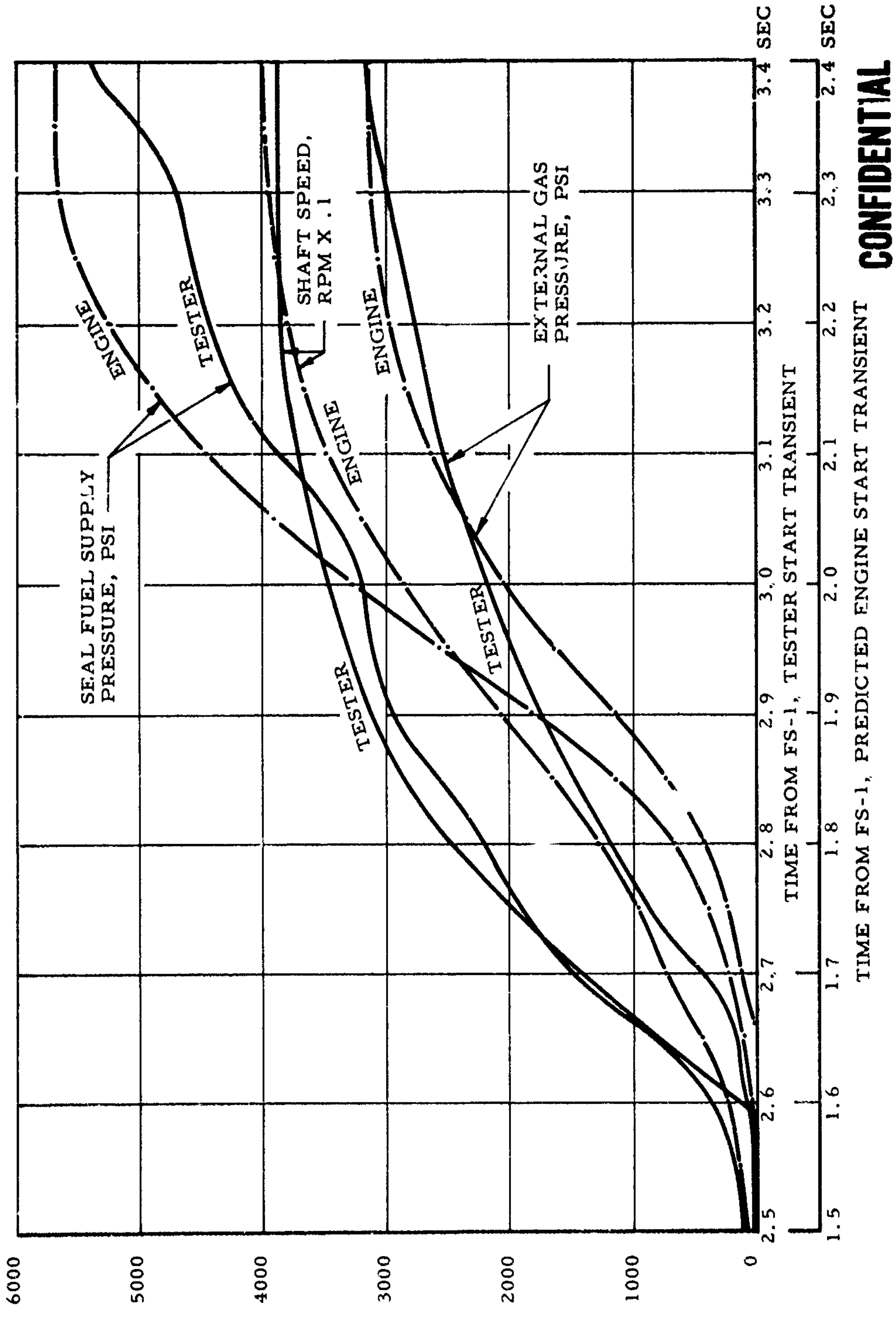

CONFIDENTIAL

Start Transient Simulation (u)

Figure IV-79

CONFIDENTIAL

# CONFIDENTIAL

Report 10830-F-1. Phase I

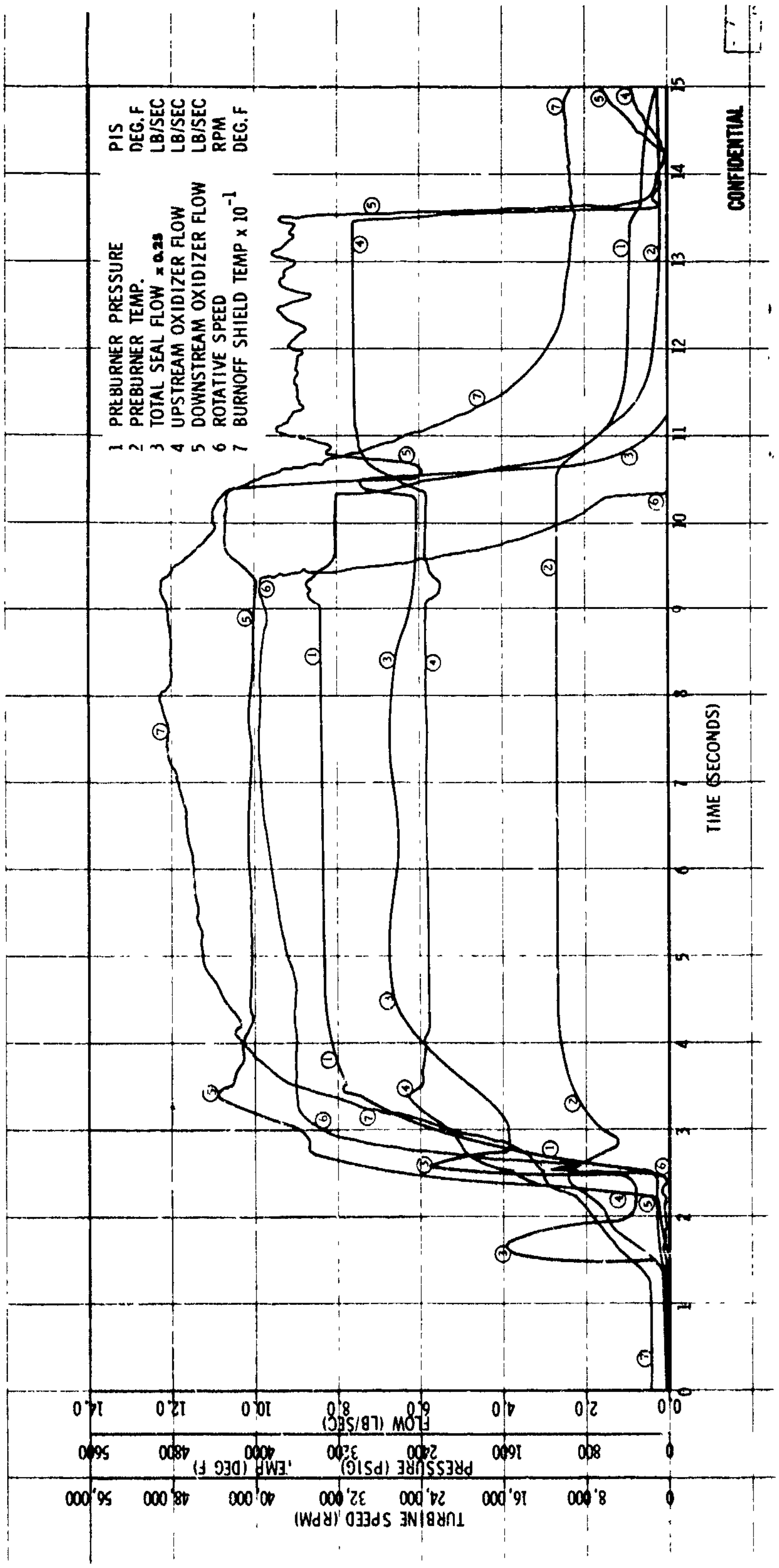

Data Plots Test 14 (u)

Figure IV-80

# CONFIDENTIAL

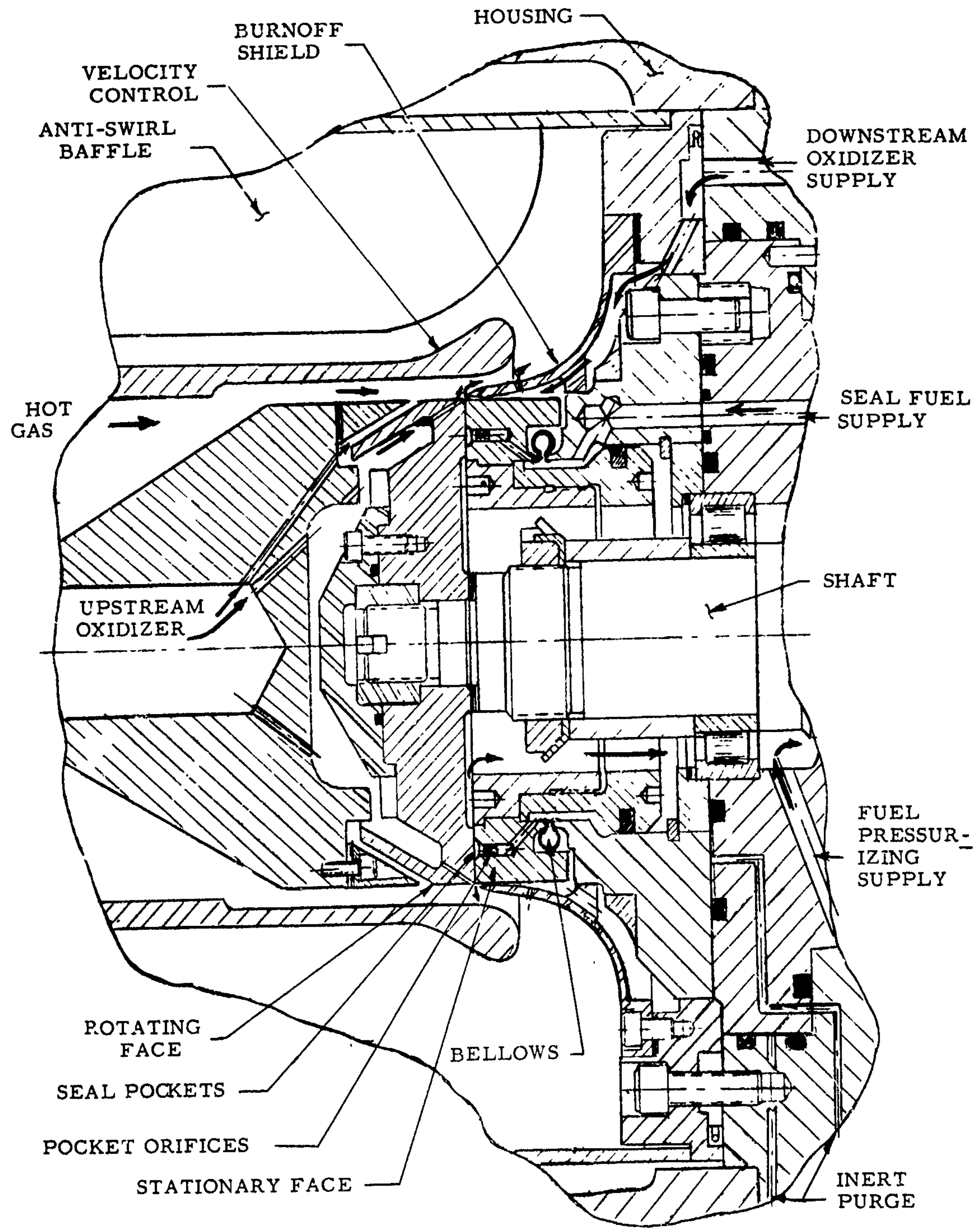
HOUSING
BURNOFF SHIELD
VELOCITY CONTROL
ANTI-SWIRL BAFFLE
DOWNSTREAM OXIDIZER SUPPLY
SEAL FUEL SUPPLY
HOT GAS
SHAFT
UPSTREAM OXIDIZER
FUEL PRESSUR-IZING SUPPLY
ROTATING FACE
BELLOWS
SEAL POCKETS
POCKET ORIFICES
STATIONARY FACE
INERT PURGE

UNCLASSIFIED

Hydrostatic Combustion Seal in Tester

Figure IV-81

| TEST NO. | DATE | DURATION, SECONDS: [illegible] | MAIN | ROTATION LIMIT AT RPM: 30,000 | 35,000 | 40,000 | PREBURNER: FLOW LB/SEC FUEL | OXID | M/R | TEMP °F | PRESS PSIA | SEALS: FLOW LB/SEC: FUEL: TOTAL FLOW | OUT FLOW | OXIDIZER: UP STREAM | DOWN STREAM | M/R | HOUSING: TEMP °F | PRESS PSIA | COMMENTS |
|---|---|---|---|---|---|---|---|---|---|---|---|---|---|---|---|---|---|---|---|
| PREBURNER CHECKOUT | | | | | | | | | | | | | | | | | | | |
| | TESTS 1, 2, 3 WERE PERFORMED TO CALIBRATE THE PREBURNER PROPELLANT VENTURIS AND TO ESTABLISH THE OPERATING CHARACTERISTICS. | | | | | | | | | | | | | | | | | | |
| 1 | -8 | 73 | [illegible] | NO SEAL USED | | | [illegible] | [illegible] | | - | - | NO SEAL USED | | | | | | | [illegible] |
| [illegible] | -8 | [illegible] | [illegible] | | | | [illegible] | | | - | | | | | | | | | [illegible] |
| 3 | -8 | 11 | [illegible] | | | | [illegible] | | - | - | - | | | | | | | | [illegible] |
| | TESTS 4, 5, 6, 7 WERE PERFORMED TO EVALUATE PREBURNER CHARACTERISTICS [illegible] | | | | | | | | | | | | | | | | | | |
| [illegible] | - | [illegible] | [illegible] | | | | [illegible] | [illegible] | [illegible] | [illegible] | [illegible] | | | | | | [illegible] | [illegible] | [illegible] |
| [illegible] | [illegible] | [illegible] | - | | | | - | - | - | - | - | | | | | | | | [illegible] |
| [illegible] | [illegible] | [illegible] | [illegible] | | | | [illegible] | [illegible] | [illegible] | [illegible] | | | | | | | | | [illegible] |
| [illegible] | [illegible] | 1 | [illegible] | | | | [illegible] | [illegible] | [illegible] | [illegible] | [illegible] | | | | | | [illegible] | [illegible] | [illegible] |
| [illegible] | | | | | | | | | | | | | | | | | | | |
| | [illegible] | | | | | | | | | | | | | | | | | | |
| [illegible] | [illegible] | [illegible] | [illegible] | [illegible] | | | [illegible] | [illegible] | [illegible] | [illegible] | [illegible] | [illegible] | | [illegible] | [illegible] | | [illegible] | [illegible] | [illegible] |
| [illegible] | - | [illegible] | | | | | [illegible] | [illegible] | [illegible] | [illegible] | [illegible] | [illegible] | | [illegible] | [illegible] | | [illegible] | | [illegible] |
| [illegible] | [illegible] | [illegible] | [illegible] | | | | [illegible] | [illegible] | [illegible] | [illegible] | [illegible] | [illegible] | [illegible] | [illegible] | [illegible] | | [illegible] | [illegible] | [illegible] |
| [illegible] | | | | | | | | | | | | | | | | | | | |
| | [illegible] | | | | | | | | | | | | | | | | | | |
| [illegible] | [illegible] | [illegible] | [illegible] | [illegible] | [illegible] | | [illegible] | [illegible] | [illegible] | [illegible] | [illegible] | [illegible] | [illegible] | [illegible] | [illegible] | [illegible] | [illegible] | [illegible] | [illegible] |
| [illegible] | [illegible] | [illegible] | [illegible] | [illegible] | | [illegible] | [illegible] | [illegible] | [illegible] | [illegible] | [illegible] | [illegible] | [illegible] | [illegible] | [illegible] | [illegible] | [illegible] | [illegible] | [illegible] |

CONFIDENTIAL

Hot Testing Test Summary (u)

Figure IV-82, Sheet 1 of 2

| TEST NO | DATE | DURATION, SECONDS |  |  |  |  |  |  |  |  |  | SEALS |  |  |  |  |  |  | COMMENTS |
|---|---|---|---|---|---|---|---|---|---|---|---|---|---|---|---|---|---|---|---|
|  |  |  |  |  |  |  |  |  |  |  |  | FLOWS LB/SEC |  |  |  |  |  |  |  |
|  |  |  |  | ROTATION TIME AT RPM |  |  | FLOW LB/SEC |  |  |  |  | FUEL |  | OXIDIZER |  |  | [illegible] |  |  |
|  |  | $FS_1$-RPM-0 | RAMP | 30,000 | 35,000 | 40,000 | FUEL | OXID | M/R | TEMP °F | PRESS PSI | TOTAL FLOW | OUT FLOW | UP STREAM | DOWN STREAM | M/R | TEMP °F | PRESS PSI |  |
| 006 | 9-1[illegible] | 6.3 | .8 | 0.1 | 0 | 0 | 0.75 | 10.[illegible] | 13.4 | 1080 | [illegible] | 1.[illegible] | 0.7[illegible] | [illegible] | 7.[illegible] | 13.7 | 70 | [illegible] | RESTART. SHUTDOWN BECAUSE OF HIGH INTERNAL PRESSURE. REPLACED FUEL PRESSURIZING ORIFICE. |
| 007 | 9-17 | 6.4 | .8 | 6.3 | 0 | 0 | 0.75 | 10.[illegible] | 13.4 | 1100 | [illegible] | [illegible] | [illegible] | [illegible] | 7.7[illegible] | 14.[illegible] | [illegible] | [illegible] | RESTART. SHUTDOWN BECAUSE OF LOW INTERNAL PRESSURE. REPLACED FUEL PRESSURIZING ORIFICE. |
| 008 | 9-17 | [illegible].5 | .8 | 9.[illegible] | 7.[illegible] | 0 | 0.75 | 10.[illegible] | 13.4 | 1100 | 3070 | [illegible] | [illegible] | [illegible] | 7.[illegible] | [illegible] | [illegible] | [illegible] | RESTART. SHUTDOWN BECAUSE OF [illegible] AREA REACTION ATTRIBUTED TO FAULTY CHAMBER LINER. [illegible] DAMAGE. ALL PARAMETERS OK. [illegible] SPEED WAS LOW. |
| 009 | 10-14 | 6.0 | .85 | .05 | 0 | 0 | 0.75 | [illegible] | 13.4 | 1100 | 3080 | 1.[illegible] | [illegible] | [illegible] | [illegible] | 14.7 | [illegible] | [illegible] | SHUTDOWN BECAUSE OF COMPUTER MALFUNCTION. VISUAL HARDWARE INSPECTION, O.K. RESET COMPUTER. |
| 010 | 10-14 | 3.0 | .85 | 0 | [illegible] | [illegible] | 0.74 | 10.[illegible] | 13.8 | 10[illegible] | [illegible] | [illegible] | [illegible] | [illegible] | [illegible] | [illegible] | [illegible] | [illegible] | RESTART. SEAL FACE SEPARATED DURING [illegible] DUE TO SURFACE CONTAMINATION. EXPLOSION DURING FILL. EXTENSIVE DAMAGE TO [illegible] AND STAND. |
| 011 | 11-12 | 10.3 | .8[illegible] | [illegible] | [illegible] | [illegible] | 0.75 | 10.1 | 13.5 | 1100 | 31[illegible]0 | 1.[illegible] | [illegible] | 1.[illegible] | [illegible].1 | [illegible] | 1000 | [illegible] | [illegible] FAILED DUE TO [illegible] VIBRATION. SEAL AND [illegible] DAMAGED. ALL ROTATING HARDWARE WAS RE-BALANCED. |
| 012 | 11-2[illegible] | [illegible] | .75 | 3.[illegible] | [illegible].1 | [illegible] | [illegible].75 | 10.0 | 13.3 | 1050 | [illegible] | 1.[illegible] | [illegible] | 0 | [illegible] | 10.[illegible] | 10[illegible] | [illegible] | ASSEMBLY [illegible] CAUSED NO [illegible]. [illegible] FAILED FROM HIGH TEMPERATURE. SEAL AND [illegible] DAMAGED. [illegible] SHIELD FAILED BECAUSE OF HIGH TEMPERATURE. |
| 013 | 12-16 | 9.2 | .90 | 3.[illegible] | 0 | [illegible] | 0.74 | 1[illegible] | 13.3 | 1080 | 3180 | [illegible] | [illegible] | [illegible] | 11.1 | [illegible] | [illegible] | [illegible] | NEW DESIGN [illegible] CRACKED AT SLOTTED TIP. NO DAMAGE. [illegible] REDESIGNED TO REPLACE SLOTS WITH RADIAL HOLES AT TIP. |
| 014 | 1-19<br>1967 | 10.3 | .95 | [illegible] | [illegible] | 0 | 0.7[illegible] | [illegible] | 13.[illegible] | 1100 | 33.0 | 1.[illegible] | 0.[illegible] | [illegible] | 10.1 | [illegible] | [illegible] | [illegible] | DOWNSTREAM VELOCITY CONTROL BOLT FAILED. [illegible] COMBUSTION DAMAGE. SEAL REUSABLE. NEW [illegible] O.K. REDESIGNED VELOCITY CONTROL TO ELIMINATE BOLTS. |

CONFIDENTIAL

Hot Testing Test Summary (u)

Figure IV-82, Sheet 2 of 2

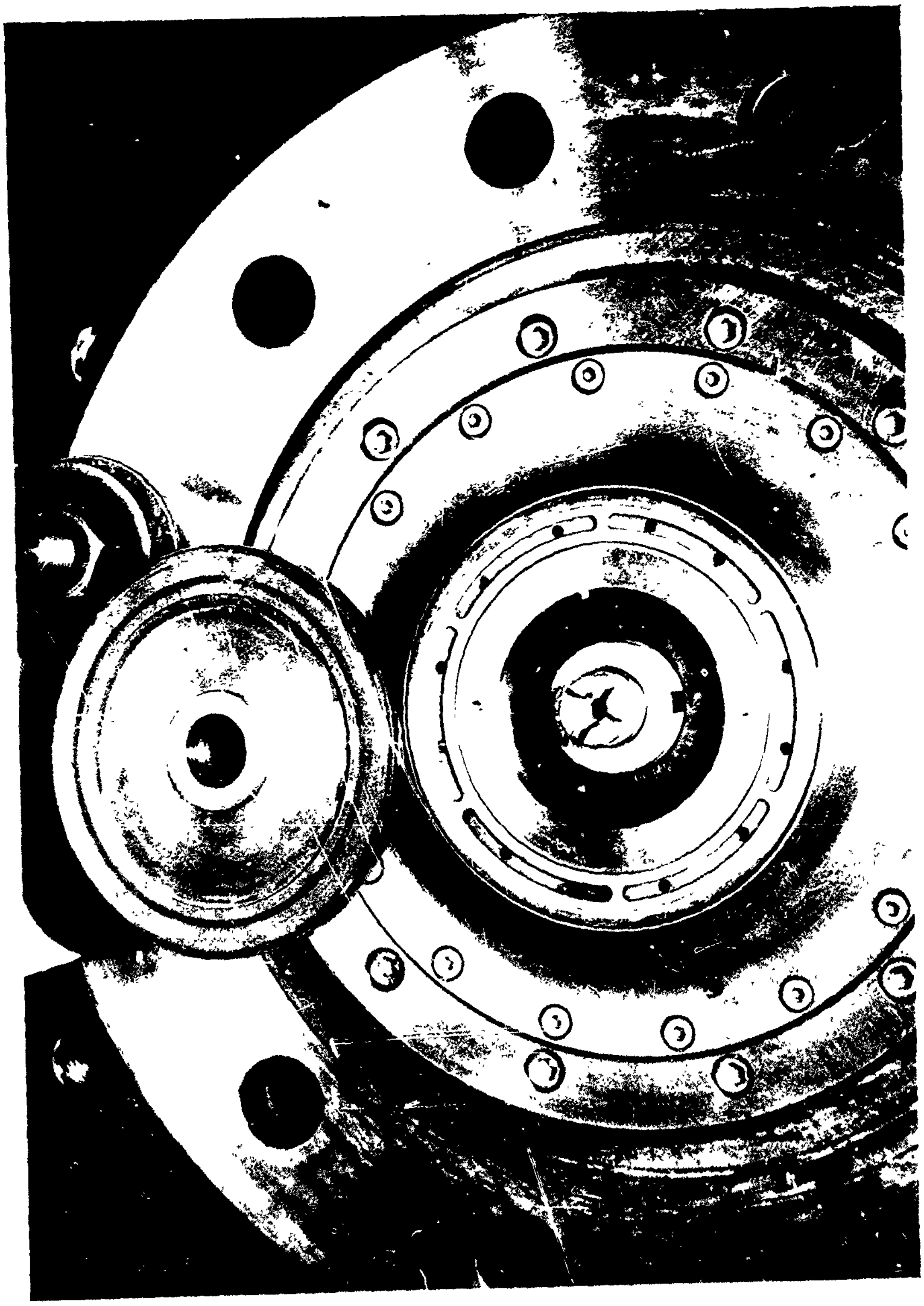

Posttest Photograph of Seal Test 14

Figure IV-83

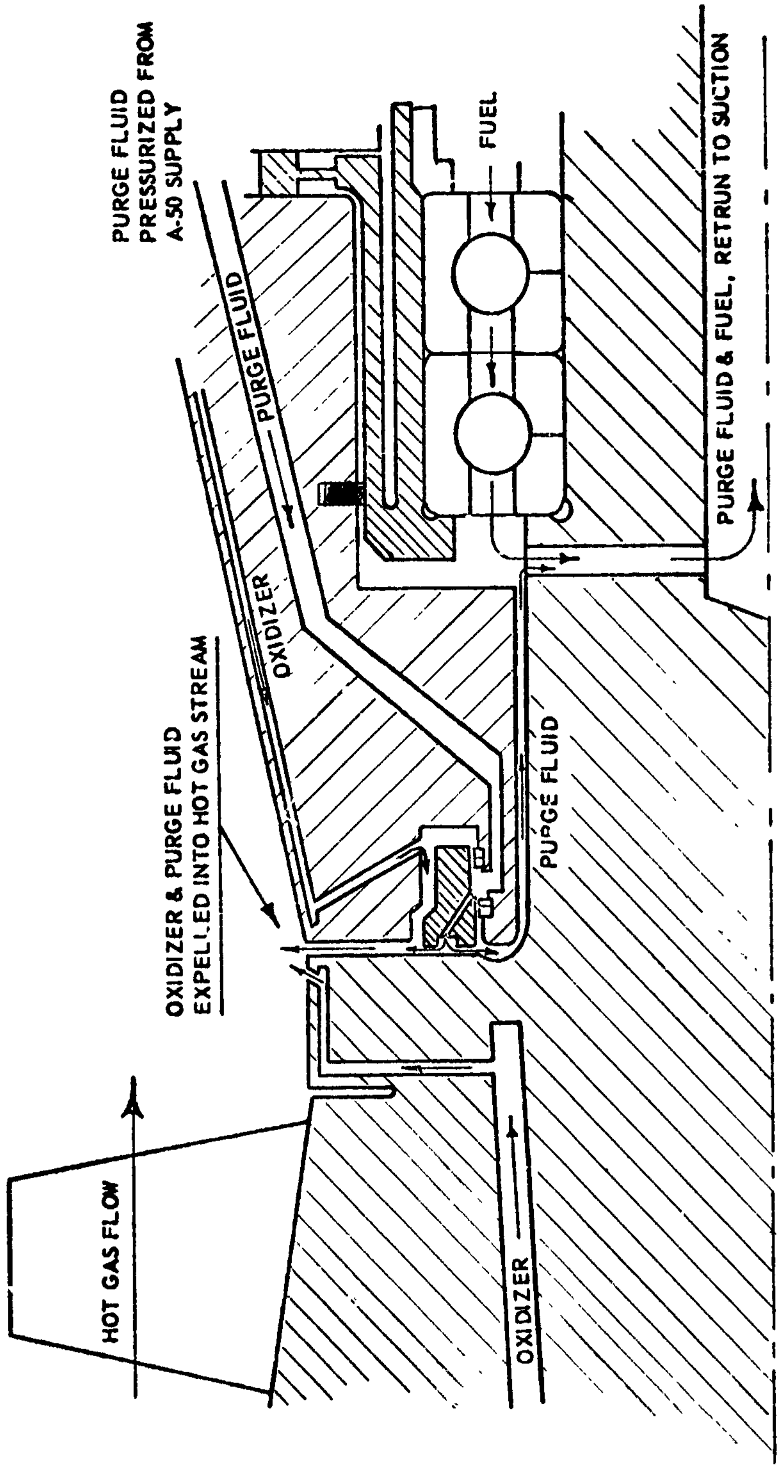
PURGE FLUID PRESSURIZED FROM A-50 SUPPLY
FUEL
PURGE FLUID & FUEL, RETRUN TO SUCTION
PURGE FLUID
OXIDIZER
OXIDIZER & PURGE FLUID EXPELLED INTO HOT GAS STREAM
PURGE FLUID
HOT GAS FLOW
OXIDIZER

Purge Seal in ARES TPA

Figure IV-84

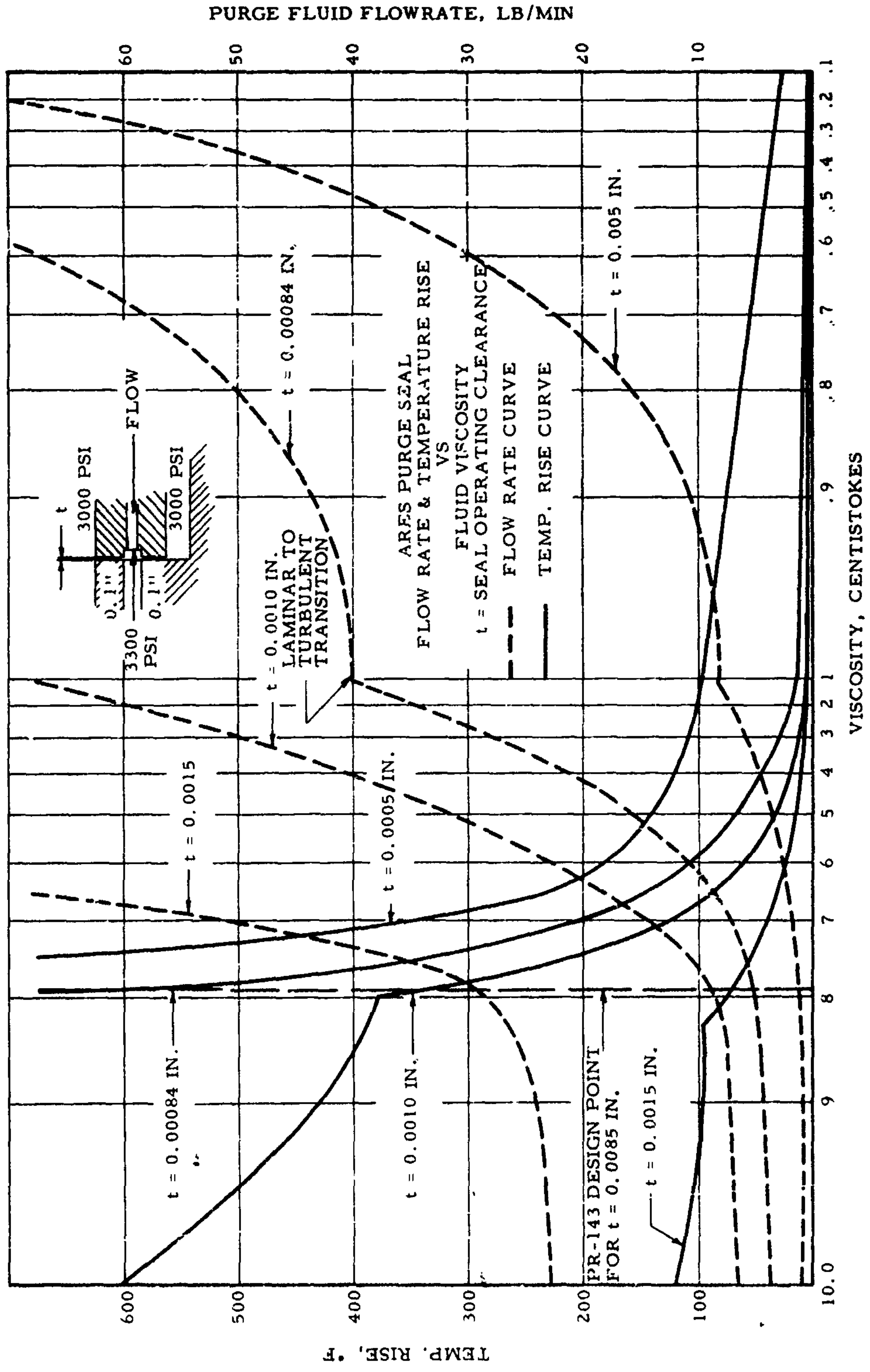

ARES Purge Seal Flowrate and Temperature Rise vs Viscosity

Figure IV-85

PURGE FLUID
(DUPONT "KRYTOX" PR 143AB)
VISCOSITY VS PRESSURE
AT 100°F

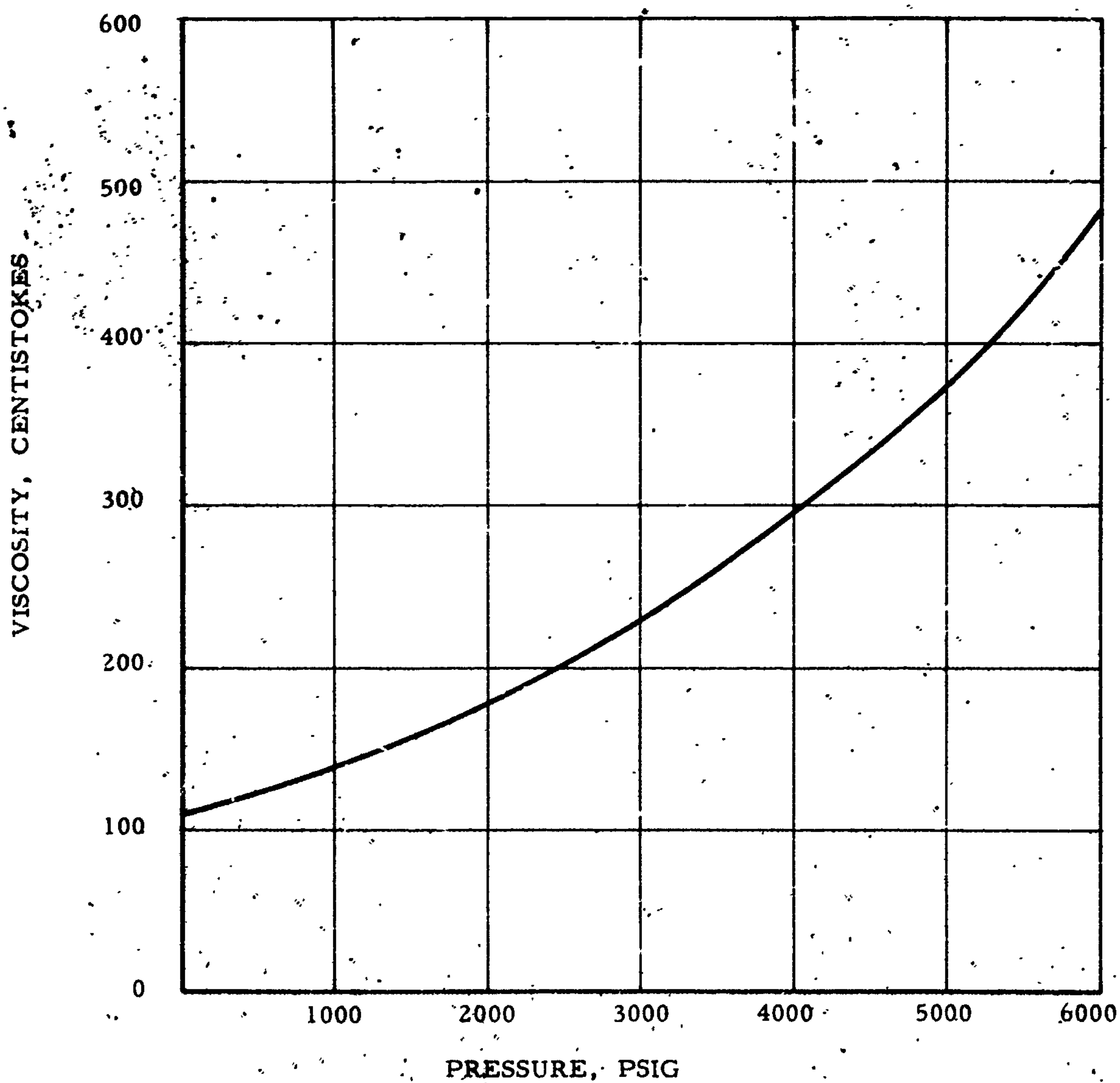

Purge Fluid Viscosity vs Pressure

Figure IV-86

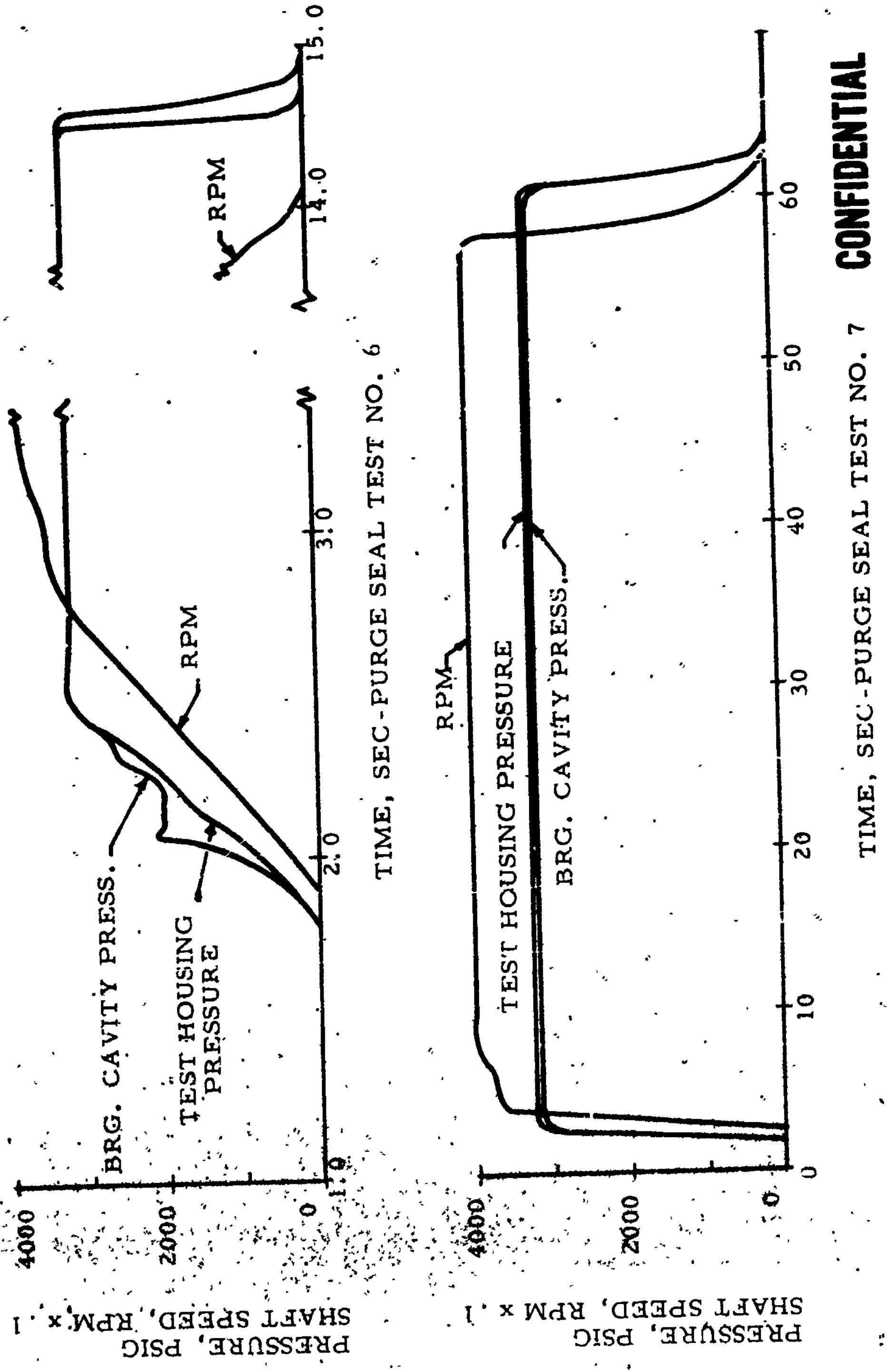

CONFIDENTIAL

Purge Seal in Tester

Figure IV-87

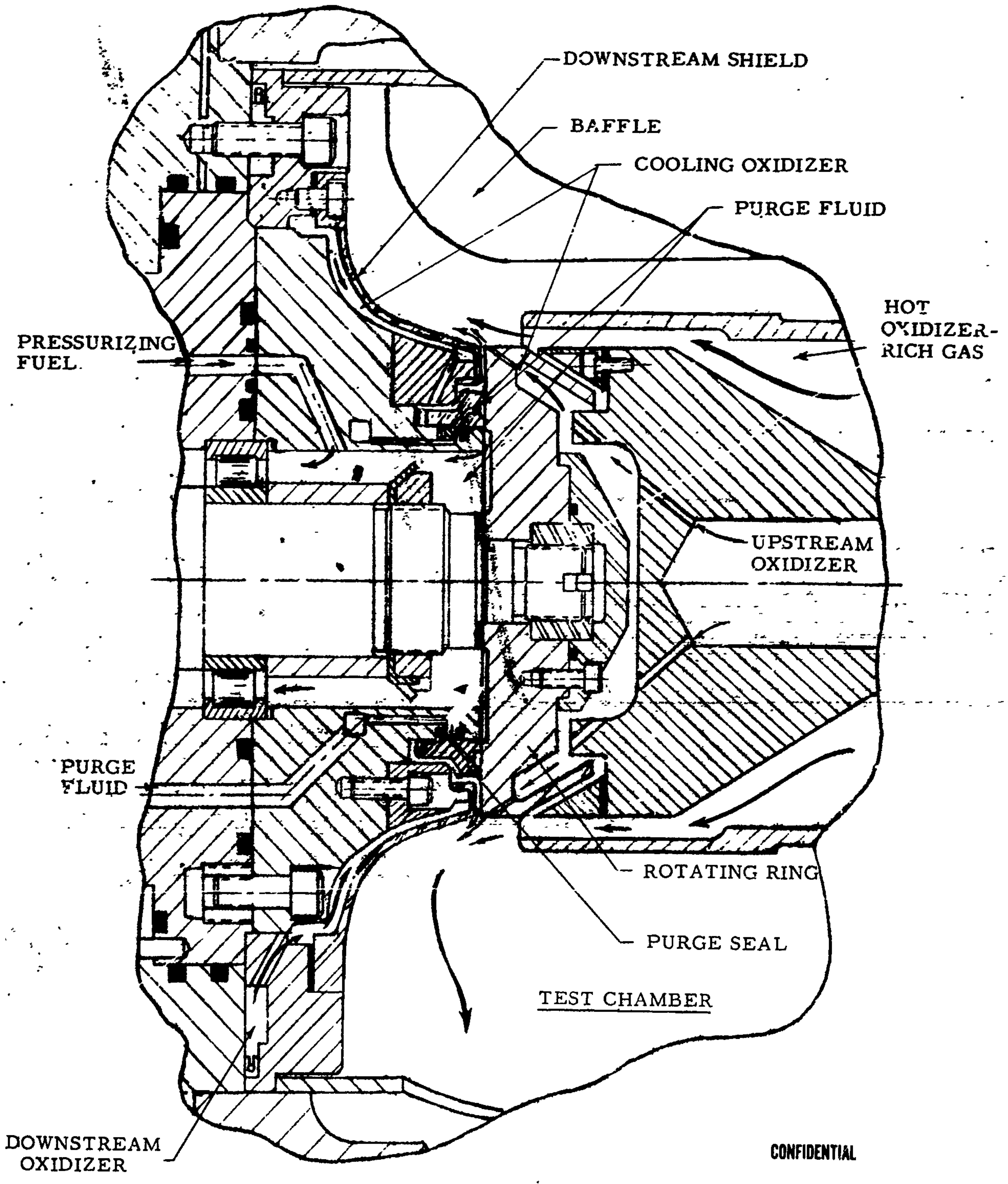
DOWNSTREAM SHIELD
BAFFLE
COOLING OXIDIZER
PURGE FLUID
HOT OXIDIZER-RICH GAS
PRESSURIZING FUEL
UPSTREAM OXIDIZER
PURGE FLUID
ROTATING RING
PURGE SEAL
TEST CHAMBER
DOWNSTREAM OXIDIZER
CONFIDENTIAL

PURGE SEAL IN TESTER

Flow Diagram (u)

Figure IV-88

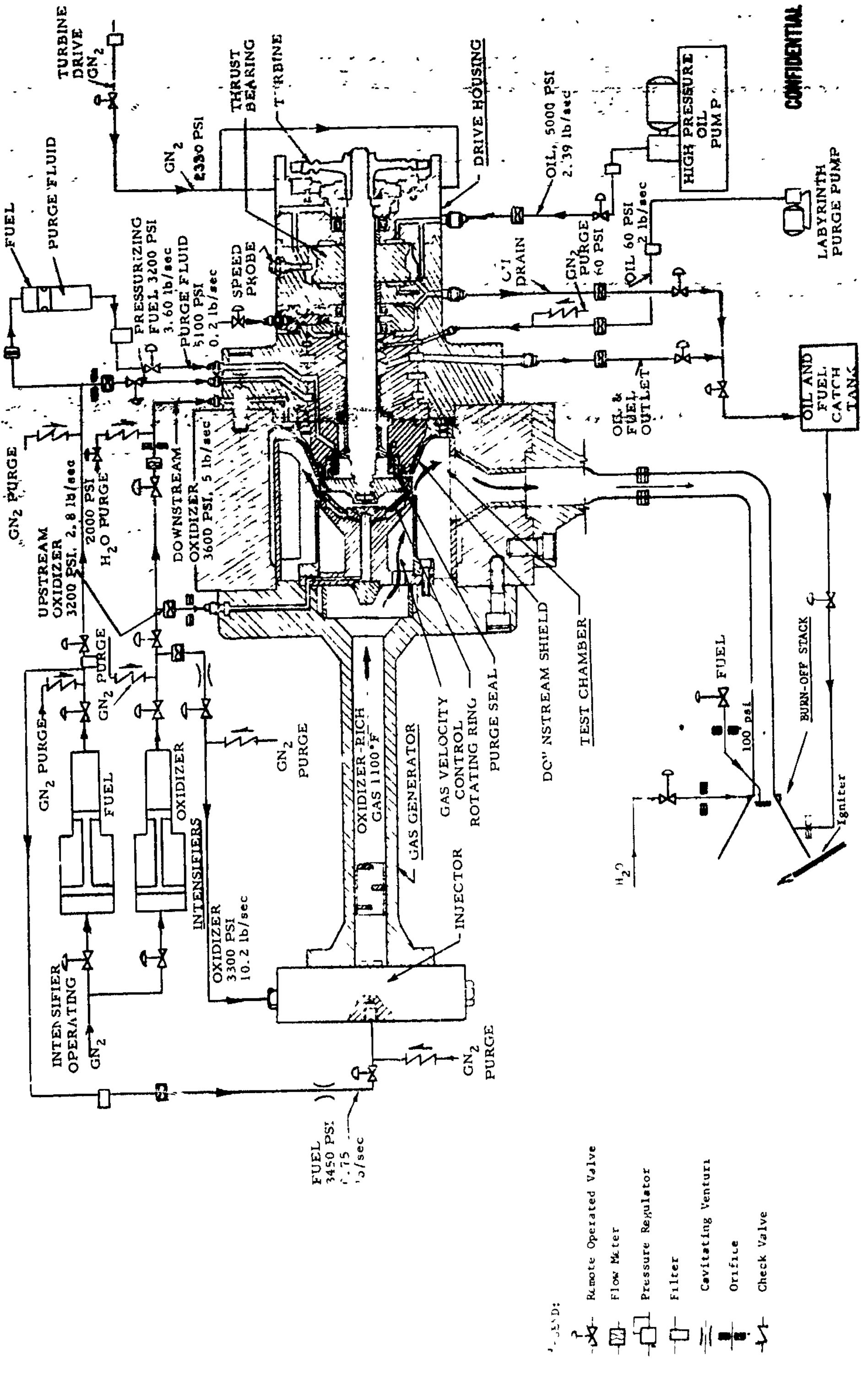
TURBINE DRIVE GN2
GN2 2330 PSI
THRUST BEARING
TURBINE
DRIVE HOUSING
OIL, 5000 PSI 2.39 lb/sec
HIGH PRESSURE OIL PUMP
CONFIDENTIAL
LABYRINTH PURGE PUMP
OIL 60 PSI .2 lb/sec
GN2 PURGE 60 PSI
OIL DRAIN
OIL & FUEL OUTLET
OIL AND FUEL CATCH TANK
FUEL
PURGE FLUID
PRESSURIZING FUEL 3200 PSI 3.60 lb/sec
PURGE FLUID 5100 PSI 0.2 lb/sec
SPEED PROBE
GN2 PURGE
UPSTREAM OXIDIZER 3200 PSI, 2.8 lb/sec
2000 PSI H2O PURGE
DOWNSTREAM OXIDIZER 3600 PSI, 5 lb/sec
GN2 PURGE
FUEL
OXIDIZER
GN2 PURGE
GN2 PURGE
INTENSIFIERS
INTENSIFIER OPERATING GN2
OXIDIZER 3300 PSI 10.2 lb/sec
OXIDIZER-RICH GAS 1100°F
GAS GENERATOR
INJECTOR
GAS VELOCITY CONTROL
ROTATING RING
PURGE SEAL
DOWNSTREAM SHIELD
TEST CHAMBER
GN2 PURGE
FUEL 3450 PSI .75 lb/sec
FUEL
100 psi
H2
BURN-OFF STACK
Igniter
LEGEND:
Remote Operated Valve
Flow Meter
Pressure Regulator
Filter
Cavitating Venturi
Orifice
Check Valve

ARES PURGE SEAL TESTER INSTALLATION FLOW DIAGRAM

Test Summary (u)

Figure IV-89

PURGE SEAL TEST SUMMARY

| TEST NO. | DATE 1966 | ROTATING TIME, SEC | SPEED, RPM | RAMP TIME, SEC | FLOWS | | | | | | MIXTURE RATIO PRE-BURNER | GAS PRESSURE, PSIG | TEMPERATURE, DEG. F | | COMMENTS |
|---|---|---|---|---|---|---|---|---|---|---|---|---|---|---|---|
| | | | | | PREBURNER LB/SEC | | SEAL | | | | | | | | |
| | | | | | | | PURGE, LB/MIN | | OXIDIZER, LB/SEC | | | | | | |
| | | | | | FUEL | OXID | TOTAL | COMB. | UP-STREAM | DOWN-STREAM | | | PRE-BURNER | CHAMBER | |
| COLD ROTATING FLOW CALIBRATION TESTS, SET UP WITH INTERMEDIATE PURGE FLUID ORIFICES (2 CU. IN./SEC) | | | | | | | | | | | | | | | |
| 1 | 9-2 | 0 | 0 | 2.5 | 0 | 0 | NO MEASURE | | 0 | 1.95 (A-50) | N/A | 3200 | AMBIENT | AMBIENT | TESTS 1 & 2 TERMINATED BECAUSE OF NO FLOW SIGNAL ON PURGE FLUID. FOUND TO BE THE RESULT OF VISCOSITY INCREASE WITH PRESSURE. FILTER & FLOW-METER REVISED TO ACCOMMODATE HIGH VISCOSITY. |
| 2 | 9-6 | 0 | 0 | 2.7 | 0 | 0 | NO MEASURE | | 0 | 1.95 (A-50) | N/A | 3200 | AMBIENT | AMBIENT | |
| 3 | 9-9 | 38 | 40,000 | 2.7 | 0 | 0 | 5.5 | 2.5 | 0 | 1.95 (A-50) | N/A | 3200 | AMBIENT | AMBIENT | 27 SECONDS AT 40,000 RPM. SLIGHT RUBBING AT SEAL FACE, ASCRIBED TO PARTIAL OBSTRUCTION IN TWO POCKET ORIFICES. HOT TESTS SET UP WITH NEXT LARGER ORIFICES. |
| HOT ROTATING PURGE SEAL TESTS, SET UP WITH PURGE FLUID ORIFICES FOR 3 CU. IN./SEC FLOW. | | | | | | | | | | | | | | | |
| 4 | 10-7 | | | | | | | | | | | | | | TESTS 4 AND 5 TERMINATED BEFORE ROTATION BECAUSE OF DIFFERENTIAL PRESSURE MALFUNCTION DUE TO HIGH VISCOSITY PURGE FLUID. |
| 5 | 10-8 | | | | | | | | | | | | | | |
| 6 | 10-10 | 11.4 | 39,000 (4 SEC) | 0.7 | 0.75 | 10.15 | 12.0 | 4.8 | 2.9 | 5.2 | 13.5 | 3350 | 1100 | 600 | SHUTDOWN BECAUSE OF DIFFERENTIAL PRESSURE UNBALANCE PRESSURE SURGE DURING STARTUP DAMAGED DOWNSTREAM SHIELD, REDUCING COOLANT TO SEAL. THIS WAS NOT DETECTED ON INSTRUMENTS AND SEAL WAS NOT INSPECTED BEFORE NEXT TEST. |
| 7 | 10-11 | 56 | 40,000+ 55.3 SEC | 0.7 | 0.75 | 10.15 | 12.0 | 4.8 | 2.8 | 4.9 | 13.5 | 3420 | 1100 | 620 | TEST WAS RUN WITH DAMAGED SHIELD. RECORDS INDICATED COMPLETE SUCCESS, BUT INSPECTION REVEALED SEAL FACE DAMAGE FROM INTER-PROPELLANT COMBUSTION DUE TO LACK OF COOLANT AND RESULTING WARPAGE. SHIELD WAS MODIFIED AND RAMP TIME INCREASED TO REDUCE SURGE AT STARTUP. |
| 8 | 10-27 | 0 | 0 | .85 | 0.75 | 10.15 | 12.0 | 4.8 | 1.9 | DROPPED TO 0 | 13.5 | 2900 | 1100 | 800 | PRESSURE SURGE CAUSED SHUTDOWN. HIGH PRESSURE IN SEAL CAVITY AND UNDER SHIELD. RAMP TIME WAS INCREASED AND SHIELD WAS MODIFIED. |
| 9 | 11-5 | 2 | 11,000 | 1.2 | 0.75 | 10.15 | 12.0 | 4.8 | 1.9 | DROPPED TO 0 | 13.5 | 2900 | 1100 | 800 | SAME AS TEST 8. AUTOMATIC SHUTDOWN DID NOT FUNCTION AND DURING MANUAL SHUTDOWN FUEL VALVE REMAINED OPEN, CAUSING EXTENSIVE DAMAGE TO SEAL AND TESTER. |

CONFIDENTIAL

Purge Seal Test Data (u)

Figure IV-90

## REFERENCES

REFERENCE

1 Hardenberg, D. E. and Zanbrich, S. Y., "Effects of External Loading on Large Outlets in a Cylindrical Vessel," Department of Engineering Mechanics, Pennsylvania State University, 15 January 1964.

2 Siebel, E. and Schwaigerer, S., "Investigations into the Strength of Contoured Branch Pipe Connections," (N65-20124). Waterloo University (Ontario) Mechanical Engineering Department, 1964.

3 Attesbury, T. J., Shipp, D. L., and McClure, G. M., "Branch Connections Data for Design," Batelle Memorial Institute to American Gas Association, 1962.

4 Hardenberg, D. E., "Stresses on Contoured Openings of Pressure Vessels," Welding Research Council Bulletin No. 51, June 1959.

5 Taylor, C. E., Line, N. C., and Schweiher, J. W., "A Three-Dimensional Photoelastic Study of Stresses Around Reinforced Outlets in Pressure Vessels," Welding Research Council Bulletin No. 51, June 1959.

6 H. Fessler and B. H. Luwin, "Stresses in Branched Pipes Under Internal Pressure," Proc. Instn. Mech. Engrs., Vol. 176, No. 29, 1962.

7 Wilson, E. L., "A Digital Computer Program for the Finite Element Analysis of Solids with Nonlinear Material Properties," Aerojet-General Corporation Technical Memorandum, 23 July 1965.

8 "The Design and Evaluation of a Low Speed Hydraulic-Driven Pump Discharge Fed Inducer Stage" Phase II, Final Report, Contract AF 04(611)-7446.

9 J. D. Chlapek, Lt., USAF, "Start-Transient Testing of a Low Speed, Hydraulic-Turbine-Driven Inducer Stage in Combination with a Rocket Engine Turbopump," Technical Report AFRPL-TR-66-124, June 1966.

10 AFRPL-TR-65-150, Integrated Components Program (u), Final Report, Contract AF 04(611)-8548, Vol. III Studies and Investigations, Section VII, Bearing Investigations, September 1965.

11 AFRPL-TR-65-191, High Chamber Pressure Rocketry Program (u), Final Report, Contract AF 04(611)-8191, Book Two, December 1965, pp. XII-14 through XII-19.

## REFERENCES (cont.)

REFERENCE

12 AFRPL-TDR-99, Integrated Components Program Phase I (u), Final Report, Contract AF 04(611)-8017; Vol. I, Technical Accomplishments, Part II, 20 January 1965, pp. IV-I-17 through IV-I-19.

13 K. J. Bell and O. P. Bergelin, "Flow Through Annular Orifices," Trans. ASME, Vol. 79, 1957, pp. 593-601.

14 G. Vermes, "A Fluid Mechanics Approach to the Labyrinth Seal Leakage Problem," Trans. ASME, Journal Eng. Power, April 1961, pp. 161-169.

15 L. N. Tao and W. F. Donovan, "Through-Flow in Concentric and Eccentric Annuli of Fine Clearances with and without Relative Motion of the Boundaries," Trans. ASME, November 1955, pp. 1291-1301.

16 Schlichting, H., Boundary Layer Theory, McGraw-Hill, New York, 1955.

17 Frankl, F., and Voishel, V., "Friction in the Turbulent Boundary Layer of a Compressible Gas at High Speeds," NACA TM-1032, 1942.

18 AFRPL-TR-65-150, Integrated Components Program Final Report, Volume III, September 1965.

19 Unpublished Aerojet-General Memorandum, A. L. Blubaugh to N. E. Van Huff.

20 Moody, L. F., "Friction Factor for Pipe Flow," Trans. ASME, November 1944.

21 Dean, L. E., and Thompson, W. R., Ignition Characteristics of Metals and Alloys, Aerojet-General Report 0-5519, October 1955.

22 Rannie, W. D., A Simplified Theory of Porous Wall Cooling, Progress Report No. 4-50-JPL-CIT.

23 Hatch, J. E., and Papell, S. S., Use of a Theoretical Flow Model to Correlate Data for Film Cooling or Heating an Adiabatic Wall by Tangential Injection of Gas of Different Fluid Properties, NASA TN D-130, November 1959.

24 Stollery, J. L., and El Ehwany, A. A. M., A Note on the Use of a Boundary-Layer Model for Correlating Film Cooling Data, Int. Journal of Heat Mass Transfer, Vol. 8, pp. 55-65, 1965.

## REFERENCES (cont.)

REFERENCE

25 J. P. Sellers, Jr., *Gaseous Film Cooling with Multiple Injection Stations*, AIAA Journal, Vol. I, No. 9, September 1963.

26 Plug Cluster Nozzle Study, Pratt and Whitney Aircraft Report PWA FR-1013, 8 September 1964 (Confidential)

27 Study for Evaluation of Plug Multichamber Configuration, Final Report for Phase I, Pratt and Whitney Aircraft Report PWA FR-1415, 29 October 1965 (Confidential)

28 Stepanoff, A. J., *Centrifugal and Axial Flow Pumps*, John Wiley & Sons, Inc., 1957.

29 Binder, R. C., *Advanced Fluid Mechanics*, Prentice Hall, 1958.

30 Daniels, F., *Outlines of Physical Chemistry*, John Wiley & Sons, 1948.

31 Memorandum #9340:6133, P. H. Raabe, to W. A. Coleal, dated 28 February 1967, Subject: "Failure Mode Analysis".

32 Memorandum #9340:6035, W. A Coleal to G. Banerian and R. Beichel, dated 25 March 1966, Subject: "ARES Controls Interlocks".

33 Memorandum #9340:6102, P. H. Raabe to W. A. Coleal, dated 14 October 1966, Subject: "ARES Maintainability".

34 Memorandum #9340:6053, R. W. Muir to W. A. Coleal, dated 8 June 1966, Subject: "Inert-Fluid Calibration and Acceptance of ARES Engines".

35 Herrmann, L. R., "A Finite Element and Analysis for Cylindrical Shells and Plates," Aerojet-General Technical Memorandum, 5 August 1966.

Report 10830-F-1, Phase I

Security Classification

## DOCUMENT CONTROL DATA - R&D

(Security classification of title, body of abstract and indexing annotation must be entered when the overall report is classified)

| | |
|---|---|
| 1 ORIGINATING ACTIVITY (Corporate author)<br>Aerojet-General Corporation<br>P.O. Box 15847, Sacramento, California | 2a REPORT SECURITY CLASSIFICATION<br>Confidential<br>2b GROUP<br>Four |
| 3 REPORT TITLE<br>ARES, Phase I Interim Final Report | |
| 4 DESCRIPTIVE NOTES (Type of report and inclusive dates)<br>Interim Final, Phase I, (1 July 1965 through 27 January 1967) | |
| 5 AUTHOR(S) (Last name, first name, initial)<br>Aerojet-General Corporation<br>Advanced Storable Rocket Engine Division | |
| 6 REPORT DATE | 7a TOTAL NO OF PAGES<br>990<br>7b NO OF REFS<br>35 |
| 8a CONTRACT OR GRANT NO<br>AF 04(611)-10830<br>b PROJECT NO<br>c<br>d | 9a ORIGINATOR'S REPORT NUMBER(S)<br>Aerojet Report 10830-F-Phase I<br>9b OTHER REPORT NO(S) (Any other numbers that may be assigned this report)<br>AFRPL-TR-[illegible]-75 |
| 10 AVAILABILITY/LIMITATION NOTICES<br>None | |
| 11 SUPPLEMENTARY NOTES | 12 SPONSORING MILITARY ACTIVITY<br>AFRPL Research and Technology Division, Edwards AFB, California |
| 13 ABSTRACT<br>See attached sheet. | |

DD FORM 1 JAN 64 1473

Security Classification

Report 10830-F-1, Phase I

Security Classification

| 14 KEY WORDS | LINK A | | LINK B | | LINK C | |
|---|---|---|---|---|---|---|
| | ROLE | WT | ROLE | WT | ROLE | WT |
| High Chamber Pressure<br>Staged Combustion<br>Storable Propellants<br>Forced Deflection Nozzle<br>Gas-Liquid Injection<br>Integrated Turbopump<br>Thrust Chamber Coatings<br>Propellant Lubricated Bearings<br>Transpiration Cooling | | | | | | |

## INSTRUCTIONS

1. ORIGINATING ACTIVITY: Enter the name and address of the contractor, subcontractor, grantee, Department of Defense activity or other organization (*corporate author*) issuing the report.

2a. REPORT SECURITY CLASSIFICATION: Enter the overall security classification of the report. Indicate whether "Restricted Data" is included. Marking is to be in accordance with appropriate security regulations.

2b. GROUP: Automatic downgrading is specified in DoD Directive 5200.10 and Armed Forces Industrial Manual. Enter the group number. Also, when applicable, show that optional markings have been used for Group 3 and Group 4 as authorized.

3. REPORT TITLE: Enter the complete report title in all capital letters. Titles in all cases should be unclassified. If a meaningful title cannot be selected without classification, show title classification in all capitals in parenthesis immediately following the title.

4. DESCRIPTIVE NOTES: If appropriate, enter the type of report, e.g., interim, progress, summary, annual, or final. Give the inclusive dates when a specific reporting period is covered.

5. AUTHOR(S): Enter the name(s) of author(s) as shown on or in the report. Enter last name, first name, middle initial. If military, show rank and branch of service. The name of the principal author is an absolute minimum requirement.

6. REPORT DATE: Enter the date of the report as day, month, year, or month, year. If more than one date appears on the report, use date of publication.

7a. TOTAL NUMBER OF PAGES: The total page count should follow normal pagination procedures, i.e., enter the number of pages containing information.

7b. NUMBER OF REFERENCES: Enter the total number of references cited in the report.

8a. CONTRACT OR GRANT NUMBER: If appropriate, enter the applicable number of the contract or grant under which the report was written.

8b, 8c, & 8d. PROJECT NUMBER: Enter the appropriate military department identification, such as project number, subproject number, system numbers, task number, etc.

9a. ORIGINATOR'S REPORT NUMBER(S): Enter the official report number by which the document will be identified and controlled by the originating activity. This number must be unique to this report.

9b. OTHER REPORT NUMBER(S): If the report has been assigned any other report numbers (*either by the originator or by the sponsor*), also enter this number(s).

10. AVAILABILITY/LIMITATION NOTICES: Enter any limitations on further dissemination of the report, other than those imposed by security classification, using standard statements such as:

(1) "Qualified requesters may obtain copies of this report from DDC."

(2) "Foreign announcement and dissemination of this report by DDC is not authorized."

(3) "U. S. Government agencies may obtain copies of this report directly from DDC. Other qualified DDC users shall request through

________________________________."

(4) "U. S. military agencies may obtain copies of this report directly from DDC. Other qualified users shall request through

________________________________."

(5) "All distribution of this report is controlled. Qualified DDC users shall request through

________________________________."

If the report has been furnished to the Office of Technical Services, Department of Commerce, for sale to the public, indicate this fact and enter the price, if known.

11. SUPPLEMENTARY NOTES: Use for additional explanatory notes.

12. SPONSORING MILITARY ACTIVITY: Enter the name of the departmental project office or laboratory sponsoring (*paying for*) the research and development. Include address.

13. ABSTRACT: Enter an abstract giving a brief and factual summary of the document indicative of the report, even though it may also appear elsewhere in the body of the technical report. If additional space is required, a continuation sheet shall be attached.

It is highly desirable that the abstract of classified reports be unclassified. Each paragraph of the abstract shall end with an indication of the military security classification of the information in the paragraph, represented as *(TS), (S), (C),* or *(U)*.

There is no limitation on the length of the abstract. However, the suggested length is from 150 to 225 words.

14. KEY WORDS: Key words are technically meaningful terms or short phrases that characterize a report and may be used as index entries for cataloging the report. Key words must be selected so that no security classification is required. Identifiers, such as equipment model designation, trade name, military project code name, geographic location, may be used as key words but will be followed by an indication of technical context. The assignment of links, rules, and weights is optional.

Security Classification

# SUPPLEMENTARY

# INFORMATION

AEROJET GENERAL TIRE GENERAL

**AEROJET - GENERAL CORPORATION**

POST OFFICE BOX 15847 • SACRAMENTO, CALIFORNIA 95813

**PROPULSION DIVISION**

pfc
17 Feb 64

AD 383737 (c)

Subject: Secrecy Order Covering Patent Application S/N 656522
"Transpiration Cooled Devices" by Robert J. Kunz et al

Gentlemen:

The United States Patent Office recently imposed a Secrecy Order upon the subject application. We have been informed that you have received information relating to the subject matter of this invention, and therefore we must advise you of your responsibilities concerning this information.

By terms of the Secrecy Order you are prohibited from disclosing or publishing the subject matter of this invention or any information relating thereto, in any way to any person not previously cognizant of the invention except by first obtaining written consent of the Commissioner of Patents. The Secrecy Order has been modified by a Permit which permits disclosure under certain conditions to Government employees, their designees, or persons employed by or working with Aerojet whose duties involve development, manufacture, or use of the subject matter of this patent application, by or for the U. S. Government, provided such persons are also advised of the Secrecy Order.

Enclosed is a copy of a United States Patent Office Secrecy Order Notice. A copy of this notice should be affixed to the cover page of Contract AF 04(611)-10830, Final Report, Phase I, in your possession which relates to the transpiration cooled devices in the subject patent application. Although there are no express handling provisions provided with regard to material under a Patent Office Secrecy Order, we ask that you safeguard it in the same manner as information classified "confidential." If you are not equipped to provide such safeguards, please return the publication to us, double-wrapped similar to classified information.

Your cooperation in fulfilling the obligation imposed by the Secrecy Order is essential. The law, 35 USC 186, provides criminal penalties for violation of a Secrecy Order up to a $10,000 fine or imprisonment for not more than two years, or both.

Very truly yours,

AEROJET-GENERAL CORPORATION

L Wing

L. Wing
Manager of Contracts
Liquid Rocket Operations

Enclosure:
(1) United States Patent Office Secrecy Order

Enclosure (1)

# United States Patent Office Secrecy Order

## NOTICE

The Aerojet-General Corporation has filed patent applications in the U. S. Patent Office to cover inventions disclosed in this publication, and the Commissioner of Patents has issued a secrecy order thereon.

Compliance with the provisions of this secrecy order requires that those who receive a disclosure of the secret subject matter be informed of the existence of the secrecy order and of the penalties for the violation thereof.

The recipient of this report is accordingly advised that this publication includes information which is now under a secrecy order. It is requested that he notify all persons who will have access to this material of the secrecy order.

Each secrecy order provides that any person who has received a disclosure of the subject matter covered by the secrecy order is

> "in nowise to publish or disclose the invention or any material information with respect thereto, including hitherto unpublished details of the subject matter of said application, in any way to any person not cognizant of the invention prior to the date of the order, including any employee of the principals, but to keep the same secret except by written permission first obtained of the Commissioner of Patents."

Although the original secrecy order forbids disclosure of the material to persons not cognizant of the invention prior to the date of the order, a supplemental permit attached to each order does permit such disclosure to:

> "(a) Any officer or employee of any department, independent agency, or bureau of the Government of the United States.
>
> "(b) Any person designated specifically by the head of any department independent agency or bureau of the Government of the United States, or by his duly authorized subordinate, as a proper individual to receive the disclosure of the above indicated application for use in the prosecution of the war.
>
> "The principals under the secrecy are further authorized to disclose the subject matter of this application to the minimum necessary number of persons of known loyalty and discretion, employed by or working with the principals or their licensees and whose duties involve cooperation in the development, manufacture or use of the subject matter by or for the Government of the United States, provided such persons are advised of the issuance of the secrecy order."

No other disclosures are authorized, without written permission from the Commissioner of Patents. Public Law No, 239, 77th Congress. provides that whoever shall "willfully publish or disclose or authorize or cause to be published or disclosed such invention, or any material information with respect thereto," which is under a secrecy order, "shall, upon conviction, be fined not more than $10,000 or imprisoned for not more than two years or both." In addition, Public Law No. 700. 76th Congress, provides that the invention in a patent may be held abandoned, if it be established that there has been a disclosure in violation of the secrecy order.

It must be understood that the requirements of the secrecy order of the Commissioner of Patents are in addition to the usual security regulations which are in force with respect to activities of the Aerojet-General Corporation. The usual security regulations must still be observed notwithstanding anything set forth in the secrecy order of the Commissioner of Patents.